Universität Rostock

HelmholtzZentrum München

JOINT MASS SPECTROMETRY CENTRE

The relationship between exposure of air pollutants and health effects

Kumulative Dissertation

zur

Erlangung des akademischen Grades

doctor rerum naturalium

(Dr. rer. nat.)

der Mathematisch-Naturwissenschaftlichen Fakultät

der Universität Rostock

Vorgelegt von

Xiao Wu

geboren am 23. Januar 1987 in Jinan, Shandong

Rostock, Mai, 2022

https://doi.org/10.18453/rosdok_id00003920

Gutachter:
Prof. Dr. Ralf Zimmermann, Universität Rostock, Institut für Chemie
Prof. Dr. Flemming Cassee, Netherlands National Institute for Public Health and the Environment

Jahr der Einreichung: 2022
Jahr der Verteidigung: 2022

Doktorandinnen/Doktoranden-Erklärung gemäß § 4 Absatz 1 Buchstaben g und h der Promotionsordnung der Mathematisch-Naturwissenschaftlichen Fakultät der Universität Rostock

Xiao Wu
Westendstraße 1
76532 Baden-Baden

Ich habe eine Dissertation zum Thema:

„The relationship between exposure of air pollutants and health effects"

an der Mathematisch-Naturwissenschaftlichen Fakultät der Universität Rostock angefertigt. Dabei wurde ich von Herrn **Professor Ralf Zimmermann** betreut.

Ich gebe folgende Erklärung ab:

a. Die Gelegenheit zum vorliegenden Promotionsvorhaben ist mir nicht kommerziell vermittelt worden. Insbesondere habe ich keine Organisation eingeschaltet, die gegen Entgelt Betreuerinnen/Betreuer für die Anfertigung von Dissertationen sucht oder die mir obliegenden Pflichten hinsichtlich der Prüfungsleistungen für mich ganz oder teilweise erledigt.

b. Ich versichere hiermit an Eides statt, dass ich die vorliegende Arbeit selbstständig angefertigt und ohne fremde Hilfe verfasst habe. Dazu habe ich keine außer den von mir angegebenen Hilfsmitteln und Quellen verwendet und die den benutzten Werken inhaltlich und wörtlich entnommenen Stellen habe ich als solche kenntlich gemacht

Baden-Baden, Mai 2022 _____

First Authorships

The following manuscripts were first-authored by Xiao Wu and published in or submitted to peer-reviewed journals. The contribution of Xiao Wu is given below.

Title: Determination of air pollution-related biomarkers of exposure in the urine of travelers between Germany and China using liquid chromatographic and liquid chromatographic-mass spectrometric methods: a pilot study.

Authors: **Xiao Wu,** Jutta Lintelmann, Sophie Klingbeil, Jie Li, Hao Wang, Evelyn Kuhn, Sebastian Ritter, Ralf Zimmermann.

Journal: Biomarkers (Impact Factor: 2.66, 2020)

Year: 2017

DOI: https://doi.org/10.1080/1354750X.2017.1306753

Contribution: Xiao Wu designed and initiated the pilot study, developed the analytical method for biomarkers, recruited the cohort, and carried out part of the sample analyses. Besides, the author carried out the data analysis, manuscript drafting, and submission.

Title: Assessment of the association of exposure to polycyclic aromatic hydrocarbons, oxidative stress, and inflammation: A cross-sectional study in Augsburg, Germany.

Authors: **Xiao Wu,** Xin Cao, Jutta Lintelmann, Annette Peters, Wolfgang Koenig, Ralf Zimmermann, Alexandra Schneider, Kathrin Wolf.

Journal: International Journal of Hygiene and Environmental Health (Impact Factor: 5.84, 2021)

Year: 2022

DOI: 10.1016/j.ijheh.2022.113993

Contribution: Xiao Wu designed the sub-cohort study in the structure of the KORA-Study. He developed HPLC (-MS/MS) based methods for OH-PAHs and biomarkers and carried out the sample analyses. Besides, the author carried out the data analysis, manuscript drafting, and submission.

Co-Authorships

The following manuscripts were co-authored by Xiao Wu and published in or submitted to peer-reviewed journals. The contribution of Xiao Wu is given below.

Title: Detection of monohydroxylated polycyclic aromatic hydrocarbons in urine and particulate matter using LC separations coupled with integrated SPE and fluorescence detection or coupled with high-resolution time-of-flight mass spectrometry

Authors: Jutta Lintelmann, **Xiao Wu**, Evelyn Kuhn, Sebastian Ritter, Claudia Schmidt, Ralf Zimmermann

Journal: Biomedical Chromatography (Impact Factor: 1.90, 2020)

Year: 2018

DOI: https://doi.org/10.1002/bmc.4183

Contribution: Xiao Wu participated in the sample analyses and manuscript drafting.

Title: Cholesterol metabolism promotes B-cell positioning during immune pathogenesis of chronic obstructive pulmonary disease.

Authors: Jie Jia, Thomas M Conlon, Rim Sj Sarker, Demet Taşdemir, Natalia F Smirnova, Barkha Srivastava, Stijn E Verleden, Gizem Güneş, **Xiao Wu**, Cornelia Prehn, Jiaqi Gao, Katharina Heinzelmann, Jutta Lintelmann, Martin Irmler, Stefan Pfeiffer, Michael Schloter, Ralf Zimmermann, Martin Hrabé de Angelis, Johannes Beckers, Jerzy Adamski, Hasan Bayram, Oliver Eickelberg, Ali Önder Yildirim.

Journal: EMBO molecular medicine (Impact Factor: 10.29, 2020)

Year: 2018

DOI: https://doi.org/10.15252/emmm.201708349

Contribution: Xiao Wu participated in the analytical method development, sample analysis, and manuscript drafting.

Acknowledgment

This work was performed and funded in the framework of the following projects:

(1) “Environmental Nanoparticles and Health: Exposure, Modeling and Epidemiology of Nanoparticles and their Composition within KORA - ULTRA III”, funded by Intramural Funding for Environmental Health Projects of Helmholtz Zentrum Muenchen;

(2) “Helmholtz Virtual Institute of Complex Molecular Systems in Environmental Health - HICE-Aerosol and Health”, funded by the Impulse and Networking Funds (INF) of the Helmholtz Association (HGF), Helmholtz Zentrum München, and University of Rostock, Germany;

(3) “New Technology of Pathogenesis, Diagnosis, and Treatment of Pneumoconiosis” project, funded by “Significant Innovation Plan of Medical and Health Science and Technology in Shandong Province”, China;

(4) The KORA study was initiated and financed by the Helmholtz Zentrum München – German Research Center for Environmental Health, which is funded by the German Federal Ministry of Education and Research (BMBF) and by the State of Bavaria. Furthermore, KORA research was supported within the Munich Center of Health Sciences (MC-Health), Ludwig- Maximilians-Universität, as part of LMUinnovativ.

Special thanks to the financial support provided by China Scholarship Council (CSC) during my PhD study.

I sincerely thank Prof. Ralf Zimmermann, Dr. Jutta Lintelmann, and Dr. Kathrin Wolf for their fully support.

I deeply thank my family for their love, comprehension, and patience.

Zusammenfassung

Hintergrund: Die Exposition gegenüber Luftschadstoffen einschließlich polyzyklischer aromatischer Kohlenwasserstoffe (PAK) wurde mit akuten und chronischen Gesundheitsschäden in Verbindung gebracht. Studien deuteten darauf hin, dass oxidativer Stress einer der wichtigsten potenziellen Pfade ist. Umfassende Beweise sind jedoch noch begrenzt. Um diese Lücke zu schließen, haben wir robuste und empfindliche Methoden der Flüssigchromatographie (-Massenspektrometrie) entwickelt, um gemeinsam das Zusammenspiel zwischen PAKs, oxidativem Stress und Gesundheitsprofilen zu untersuchen. Darüber hinaus haben wir ein Konzept zur nicht-invasiven Nutzung von Reisenden zwischen Orten mit unterschiedlichen Feinstaub-Konzentrationen als einfaches und kostengünstiges Modell vorgeschlagen, um akute gesundheitliche Auswirkungen der Exposition gegenüber Luftschadstoffen zu untersuchen.

Methoden: Wir entwickelten robuste, auf Hochleistungsflüssigkeitschromatographie und Flüssigchromatographie-Massenspektrometrie basierende Analysemethoden zur Bestimmung von Biomarkern für PAK-Exposition (hydroxylierte polyzyklische aromatische Kohlenwasserstoffe, OH-PAKs) und oxidativen Stress (Malondialdehyd, MDA; 8-Hydroxy-2'-desoxyguanosin, 8OHdG; und Vertreter der Substanzklasse der $F_{2\alpha}$-isoprostanes) im Urin von Teilnehmern einer Querschnittsstudie des zweiten Follow-up (2013/2014) der deutschen KORA Umfrage S4 und eine Pilot-Längsschnittstudie zu internationalen Reisenden. Biomarker für Entzündungen (Hochsensitives C-reaktives Protein, hs-CRP) im Serum der KORA-Kohorte wurden ebenfalls gemessen.

Ergebnisse: In beiden Kohorten waren PAK mit Biomarkern für oxidativen Stress assoziiert. In der KORA-Kohorte, die sich in einem relativ niedrigen Expositions-Setup befand, variierten die Konzentrationen von Biomarkern in verschiedenen Teilnehmergruppen nach Gesundheitsprofilen, z. Geschlecht, Alter, Rauchen oder chronische Krankheiten. Es wurden signifikante positive Assoziationen zwischen allen PH-PAKs und Biomarkern für oxidativen Stress gefunden. Darüber hinaus wurden die Assoziationen durch Entzündungen verändert. Es wurden jedoch nur bescheidene positive Assoziationen zwischen OH-PAKs und hs-CRP gefunden. Unter den Biomarkern für oxidativen Stress war nur 8OHdG signifikant positiv mit hs-CRP assoziiert (ein Anstieg von 8OHdG (log-transformiert) im Interquartilbereich war mit 13,7 % Anstieg des hs-CRP (log-transformiert) (95 %-KI: 2,2 %, 26,5 %) assoziiert.). In der Reisekohorte als hochselektiver Kohorte wurden in Proben nach der Reise im höhere mittlere Konzentrationen von Biomarkern für oxidativen Stress als in Proben vor der Ausreise aus Deutschland bemerken. Biomarker für oxidativen Stress wurden positiv mit der Exposition assoziiert. Zusätzlich wurde Oxysterol von Mäusen gemessen. Die Konzentration war bei Mäusen, die Zigarettenrauch ausgesetzt waren, signifikant höher als jenen, die gefilterter Luft ausgesetzt waren, was auf die mögliche Rolle von Oxysterol hinweist.

Schlussfolgerung: Die Ergebnisse dieser Studie legten den Zusammenhang zwischen der Exposition gegenüber PAKs, oxidativem Stress und Entzündungen nahe. Wir schlagen vor, Gesundheitsprofile und oxidativen Stress gemeinsam zu berücksichtigen, wenn die Mechanismen der gesundheitlichen Auswirkungen einer PAK-Exposition in der Zukunft untersucht werden. Darüber hinaus sind Reisende ideale Modelle für Studien zu akuten gesundheitlichen Auswirkungen durch Luftverschmutzung.

Abstract

Background: Exposure to air pollutants including polycyclic aromatic hydrocarbons (PAHs) was linked to acute and chronic health effects. Studies suggested oxidative stress as one of the key potential pathways. However, comprehensive evidence is still limited. To fill this gap, we developed robust and sensitive liquid chromatography (- mass spectrometry) methods to jointly investigate the interplay between PAHs, oxidative stress, and health profiles. Moreover, we proposed a concept of non-invasively using travelers between locations of different particulate matter (PM) concentrations as a simple and cost-effective model to investigate acute health effects from exposure to air pollutants.

Methods: We developed liquid chromatographic and liquid chromatography-mass spectrometry based analytical methods to determine biomarkers of PAH exposure (hydroxylated polycyclic aromatic hydrocarbons, OH-PAHs) and oxidative stress (Malondialdehyde, MDA; 8-hydroxy-2'-deoxyguanosine, 8OHdG; and representatives of the compound class of $F_{2\alpha}$-isoprostanes) in the urine of participants from a cross-sectional study of the second follow up (2013/2014) of the German KORA survey S4 and a pilot longitudinal study of international travelers. Biomarker of inflammation (high sensitivity C-reactive Protein, hs-CRP) in serum from the KORA cohort was also measured.

Results: In both cohorts, PAHs were associated with biomarkers of oxidative stress. In the KORA cohort, which was in a relatively low exposure setup, concentrations of biomarkers varied in different participant groups by health profiles e.g., gender, age, smoking, or chronic diseases. Significant positive associations between all OH-PAHs and oxidative stress biomarkers were found. Moreover, the associations were modified by inflammation. Yet only modest positive associations between OH-PAHs and hs-CRP were found. Among the biomarkers of oxidative stress, only 8OHdG was significantly positively associated with hs-CRP (an interquartile range increase in 8OHdG (log-transformed) was associated with a 13.7 % (95% CI: 2.2 %, 26.5 %) increase in hs-CRP (log-transformed)). In the traveler cohort, as a highly selective cohort, higher median concentrations of oxidative stress biomarkers in samples after travel were observed than in samples collected before leaving Germany. Oxidative stress biomarkers were positively associated with exposure. In addition, oxysterol from mice was determined. The concentration was significantly higher in the mice exposed to cigarette smoke than exposed to filtered air, which indicated the potential role of oxysterol.

Conclusion: The results of this study suggested the relationships between exposure to PAHs, oxidative stress, and inflammation. We suggest to consider health profiles and oxidative stress jointly when investigating mechanisms of health effects of exposure to PAHs in the future. Furthermore, our study indicated that travelers are ideal models for air pollution-induced acute health effects study.

Table of Contents

Table of Figures

Abbreviations

1-OH-Phe	1-hydroxyphenanthrene
1-OH-Pyr	1-hydroxypyrene
2-OH-Phe	2-hydroxyphenanthrene
3-OH-Phe	3-hydroxyphenanthrene
4-OH-Phe	4-hydroxyphenanthrene
7α,25-OHC	7α,25-dihydroxycholesterol
8OHdG	8-hydroxy-2'-deoxyguanosine
9-OH-Phe	9-hydroxyphenanthrene
BMI	Body Mass Index
CH25H	25-hydroxylase
COPD	Chronic obstructive pulmonary disease
CRP	C-reactive Protein
CYP	Cytochrome P450
CYP7B1	7-alpha-hydroxylase
DALYs	disability-adjusted life-years
DNA	Deoxyribonucleic acid
DNPH	2,4-dinitrophenylhydrazine
eGFR	Estimated glomerular filtration rate
GBD	Global Burden of Disease
GCV	Generalized cross-validation
HO·	Hydroxyl radicals
HR-TOF-MS	high resolution time-of-flight mass spectrometer
KORA	Cooperative Health Research in the Region of Augsburg
LC	Liquid chromatography
LC-MS	Liquid chromatography-mass spectrometry
LLE	Liquid-liquid extraction
LOQ	Limits of quantification
MDA	Malondialdehyde
NO_3·	Nitrate radicals
NO_x	Nitrogen oxides
O3	Ozone
OH-PAH	Monohydroxylated PAH
PAHs	Polycyclic aromatic hydrocarbons
PG	Prostaglandin
PM	Particulate matter
PM_{10}	Particulate matter aerodynamic diameter of 10 µm or less
$PM_{2.5}$	Particulate matter aerodynamic diameter of 2.5 µm or less
PUFA	Polyunsaturated fatty acids
QTOF-MS	Quadrupole time-of-flight mass spectrometer
ROS	Reactive oxygen species
RP	Reverse phase
SO_2	Sulfur dioxide
SOAs	Secondary organic aerosols
SPE	Solid phase extraction
TOF-MS	time-of-flight mass spectrometer
TQMS	triple quadrupole mass spectrometer
UFP	Ultrafine particles
VOCs	Volatile organic compounds
WHO	World Health Organization

1 Introduction

Individuals' continuous and ubiquitous exposure to ambient air pollution has been recognized as a global public health issue [3, 4]. According to the analysis from the Global Burden of Disease (GBD) project, between 2007 – 2017, every year more than 4 million deaths are suggested to be a result of exposure to outdoor air pollution worldwide[5], and more than 100 million disability-adjusted life-years (DALYs)[6]. In Europe, over half a million premature deaths were attributable to indoor and outdoor air pollution in 2015 [7].

1.1 Common ambient air pollutants

A large portion of the air pollutants is contributed by human activities such as biomass burning, industrial emission, transportation, construction and demolition, and agricultural activities.[8] According to the WHO, air pollutants can be classified into four major types: particulate matter (PM), nitrogen oxides (NO_x), ozone (O_3), and sulfur dioxide (SO_2) (https://www.who.int/news-room/fact-sheets/ detail/ambient-(outdoor)-air-quality-and-health).

Particulate matter is a mixture of solid particles and liquid droplets in the air. According to the diameters, they can be classified as PM_{10} (aerodynamic diameter of 10 μm or less), $PM_{2.5}$ (aerodynamic diameter of 2.5 μm or less), and ultrafine particles (UFP, aerodynamic diameter of 0.1 μm or less). Due to their small size, they can be inhaled into the lung and then cause health problems[4, 9]. It is believed that particles of smaller size can cause even greater health effects because the smaller particles are easier to deposit into the lower level of the lung and penetrate the human bloodstream. Riediker et al. reported the correlation between location and particle characteristics such as size and charge[9]. However, the toxicity of PM also depends on the source and the components[10].

Figure 1 Haze in China. Photos were taken by Xiao Wu in winter 2010

Nitrogen oxide, mostly NO and NO_2, are related to the combustion process of powerplant or transportation such as car, ship, and airplane[11, 12]. Low level nitrogen oxide can cause acute irritation to the eyes and respiratory system[13, 14]. Long-term exposure to NO_x is reported to be associated with asthma[15], reduced lung function[16], and chronic obstructive pulmonary disease (COPD)[17].

Sulfur dioxide forms in sulfur-containing biomass burning such as coal, diesel, or oil[11, 12, 18]. Similar to NO_x, SO_2 can also cause skin redness and acute irritation to the eyes and respiratory system[19]. Chronic exposure to SO_2 can cause asthma and COPD to children, and people with lung diseases or cardiovascular diseases to older people[17, 20].

The ground-level ozone is often generated as a secondary pollutant from the interaction of such chemicals with the surrounding environment and the effect of photochemical reactions in the atmosphere[12]. As a powerful oxidant with three oxygen, it has strong health effects both in long-term and short-term exposure[17, 21, 22].

Apart from these, secondary organic aerosols (SOAs) draw great attention because they can compose more than half of the total organic matter [23]. After the emission of primary volatile organic compounds (VOCs), reactions can be initiated by light, O_3, hydroxyl radicals ($HO\cdot$), and nitrate radicals ($NO_3\cdot$)[24]. These radicals can insert into a C-C double-bound or grab a hydrogen atom from organic products. For the first type, the vapor pressure will be reduced while for the second type volatility will not be impacted. Consequently, more free radicals will be formed, which will finally end up in a large amount of SOAs through complicated multi-step reactions. The formation mechanisms can be concluded as daytime atmospheric chemistry ($OH\cdot$ initiated/ O_3 initiated) and nighttime atmospheric chemistry ($OH^{\cdot}$, and NO_x initiated). A second step is the reversible distribution process of semi-volatile secondary products in the two phases of gas particles. SOA formation is also affected by other inorganic and organic components in the aerosol and many conditions such as temperature, light, and humidity. The distribution of secondary organics in the gas-particle phase determines the SOA yield. This process is controlled by the activity coefficient of the product, vapor pressure, and ambient temperature. Only when the concentration of organic matter exceeds its condensation occurs when the vapor pressure is saturated, that is, SOA is formed through the homogeneous nucleation of molecules. Even if the gas phase concentration of the substance is not saturated, it will enter the particle phase through adsorption, dissolution, or absorption. At present, there are two theories of adsorption and absorption. The adsorption theory believes that gaseous organic matter is adsorbed on the surface of particles, and the amount of adsorption is related to the specific surface area of the particles. The absorption theory believes that gaseous organic matter enters the particle phase through the process of absorption and dissolution and is in the gas-particle phase. A dynamic absorption-desorption equilibrium is maintained between the two phases, and the amount of absorption is proportional to the mass of the organic aerosol. The absorption mechanism mainly dominates the distribution of weakly polar organics such as PAHs. [25].

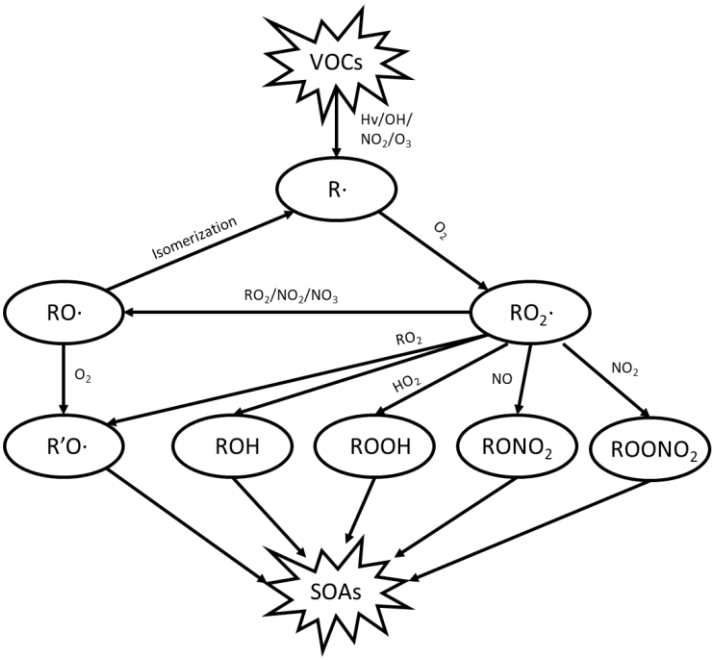

Figure 2 Simplified mechanism of the generation of SOAs through the oxidation of VOCs. In light condition, VOCs can break down to generate free radicals and trigger the subsequent reactions [1, 2].

Most anthropogenic VOCs come from motor vehicle exhausts such as benzene, phenols, and diolefins. Biologically derived VOCs are mainly terpenes. Monoterpene accounts for about 10%~15% of non-methane hydrocarbons emitted by plants [26]. Went proposed that a large amount of plant emissions terpenes react with ozone to form terpenoid particles which are removed [27]. Emissions of terpenes from plants are closely related to environmental conditions. The emission factors of terpenes tend to increase exponentially with increasing temperature. Light affects the emissions of certain substances mainly by affecting the rate of photosynthesis in plants. In addition to terpenes, plants also release many oxygen-containing organic compounds, including alcohols, ketones, organic acids, esters. Some plant oxides even emit more than monoterpenes.

Volatile aromatics are the most important anthropogenic precursors of VOCs. 50% - 70% of VOCs in the urban atmosphere come from benzene and its derivatives [28]. In North America and Europe, aromatic hydrocarbons account for the majority of urban atmospheric hydrocarbon mixtures. In North America and Europe, aromatics make up about 45% of the urban atmospheric hydrocarbon mixture. Six kinds of benzenes including toluene, (o-, m-, p-) xylene, 1,2,4-tritoluene and ethylbenzene account for 60% - 75% of aromatics. Goldan et al. research in rural areas shows that aromatics are only about 1.7% of the total VOCs concentration[29]. Motor vehicle emissions are the main source of urban aromatics. The emission characteristics vary greatly with different vehicle types, fuel, and operating conditions. Sagebiel et al. [30] studied the non-methane hydrocarbons of light and heavy vehicles in two tunnels in the United States. It is found that the proportion of aromatics in non-methane hydrocarbons is between 40% and 48% for both light-duty vehicles and heavy-duty vehicles. The 6 benzene derivatives accounted for about 60% of the aromatics, while the heavy-duty vehicle was only about 27%.

1.2 Polycyclic aromatic hydrocarbons

Among the ambient air pollutants, polycyclic aromatic hydrocarbons (PAHs) are ubiquitous, hazardous pollutants that are generated during all incomplete combustion processes of organic materials [31]. Previous studies suggested that traffic emission, domestic combustion, and industry were the main contributor to PAHs in urban areas [32]. The major intake into the organism is via dermal, respiratory, or ingestion routes [33, 34]. Eye and skin irritation, headache, nausea, and vomiting were suggested to be the short-term health effects [35, 36] while COPD, diabetes, and cardiovascular diseases were suggested to be the long-term health effects [37-39]. Previous in-vitro and in-vivo studies also suggested that oxidative stress, genotoxicity, and carcinogenicity were related to PAH exposure [40-45].

The genotoxicity of PAHs strongly depends on the structure[46]. PAHs with three or more aromatic rings have structures with “bay region” or “Fjord region”. Such region greatly enhances the bio-reactivity of the compounds to the metabolizing enzymes. The double bond can be catalyzed by the cytochrome P450 (CYP) enzyme. The produced unstable arene oxides will then be hydrolyzed to trans dihydrodiols. By the end, a vicinal diol-epoxide can be generated via CYP-catalyzed oxidation from the double bond next to the diol function. Due to the electrophiles capability, such mutagenic metabolites “bay region” or “Fjord region” can easily bind to specific sites of DNA[47]. The bulky DNA adducts could lead to replication error or removing purine base. Evidence also suggests quinones can repeatedly generate reactive oxygen species that may independently damage DNA[48].

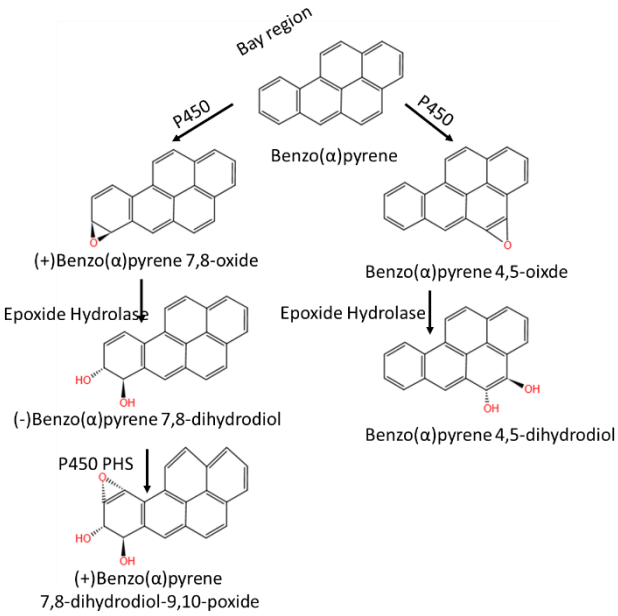

Figure 3 Typical metabolic pathways for PAHs

Exposure to PAHs can cause oxidative stress [4]. The absorbed pollutants will initiate the formation of reactive oxygen species (ROS) such as peroxides, superoxide, hydroxyl radical, and singlet oxygen [49, 50] to attack and modify adjacent macromolecules like proteins, deoxyribonucleic acid (DNA), and lipids in vivo [51]. To remove the ROS species and to maintain the oxidative stress balance, antioxidants will be generated or specific enzymatic processes will be activated. However, this balance is subtle [52]. When this balance is disturbed, oxidative stress and the resulting attack on macromolecules will finally lead to manifold acute and chronic diseases [53, 54].

It is impossible to comprehensively reflect the ways of metabolic transformation and excretion of all PAHs after their absorption into the organism because individuals are always exposed to complex mixtures of low molecular weight, medium molecular weight, and high molecular weight PAHs, and with current analytical methods. In contrast to a comprehensive picture, the use of biomarkers allows the assessment of the individual, internal PAHs burden. It turned out that the determination of monohydroxylated PAHs (OH-PAHs) in urine can be used for this purpose [55-57]. In our study, we applied the determination of 1-OH-pyrene, the main urinary metabolite of pyrene, and five urinary isomeric OH-phenanthrenes that originate from phenanthrene. Pyrene and phenanthrene are medium molecular weight PAHs, both abundant in typical environmental PAH-mixtures and further, significantly higher molecular weight PAHs. In contrast to those higher molecular weight PAHs, the OH-PAH metabolites of pyrene and phenanthrene can be reliably determined in low volume urine samples, and their concentrations – especially 1-hydroxyperene concentrations - can be used for estimating the individual exposure to PAHs [55-57].

1.3 Biomarkers of reactive oxygen species and inflammation

Estimating the burden of ROS species directly is critical to achieve due to the high reactivity. To solve this challenge, malondialdehyde (MDA), 8-hydroxy-2'-deoxyguanosine (8OHdG), and the compound class of $F_{2\alpha}$-isoprostanes were proposed as biomarkers of oxidative stress because these by-products or end-products will be excreted through feces or urine and can be well quantified. MDA, 8OHdG, and $F_{2\alpha}$-isoprostanes reflect the amounts of damaged double bonds of polyunsaturated fatty acids (PUFA) [58, 59], damaged DNA [60, 61], and damaged membrane phospholipids [62-64], respectively.

Double bonds of polyunsaturated fatty acids (PUFA) can be attacked by ROS species and result in cellular damage [65]. As a toxic secondary product of lipid peroxidation [65], MDA was suggested to be useful as a urinary biomarker for assessing the whole body burden of oxidative stress [58]. ROS species can also attack the DNA and induce G→T transversions. 8OHdG will be generated during the DNA repairing process such as base excision repair, nucleotide excision repair, and/or mismatch repair [66, 67]. After being transported outside the cells and excreted into urine[67], 8OHdG can be used as a biomarker to evaluate oxidative stress[60, 61]. Similarly, arachidonic acid in membrane phospholipids can be attacked by ROS species and produce a series of prostaglandin (PG)-like compounds[63, 68]. As a mixture of isomers that are stable, robust, and exist in all human tissues and fluids[64], studies suggested that $F_{2\alpha}$-isoprostanes were associated with many diseases and disorders such as atherosclerosis, diabetes, obesity, cigarette smoking, neurodegenerative diseases [62-64].

Such a combination greatly enhanced the reliability of the assessment of individual oxidative stress levels.

In addition to oxidative stress, inflammation has been suggested as another factor for air pollution-initiated health effects. Previous epidemiological studies reported that long-term exposure to ambient pollutants was associated with an increased serum level of C-reactive Protein (CRP), a well-known marker for inflammation [69-71]. Toxicological studies also led to similar observations: exposure to air pollution-induced inflammation responses such as increased CRP concentrations in human blood [72]. Systemic inflammation was induced by ambient air pollution via the production of cytokines such as tumor necrosis factor α and interleukin 8 [73]. Previous studies also indicated that exposure to PAHs was

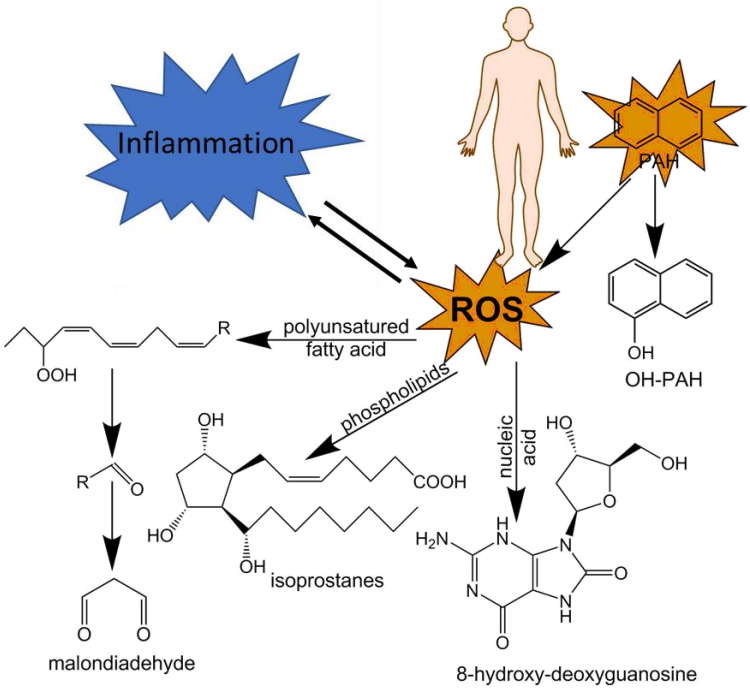

Figure 4 Simplified pathway of formation of oxidative stress biomarkers, such as lipid peroxidation product and biomarkers of exposure, such as hydroxylated polycyclic aromatic hydrocarbons.

positively associated with both, oxidative stress and inflammation [69, 74-76]. Few studies jointly considered the interplay between PAHs, oxidative stress, and health profiles.

1.4 Travelers: an ideal model

A key fact of most epidemiological studies in this field is that these studies are performed on constant cohorts to investigate air pollution-initiated health effects. However, one problem researchers often encounter is that the participants have usually been exposed to the same or similar conditions for a long period. This can conceal or change characteristics related to acute injuries. Every year, millions of people perform long-distance travel. Among the places of travel, some have relatively "clean" air while others are exposed to highly polluted air (Figure 5). Here, we followed the idea that travelers can provide an ideal model to investigate acute biological responses and health effects due to their exposure to differently polluted environments during travel.

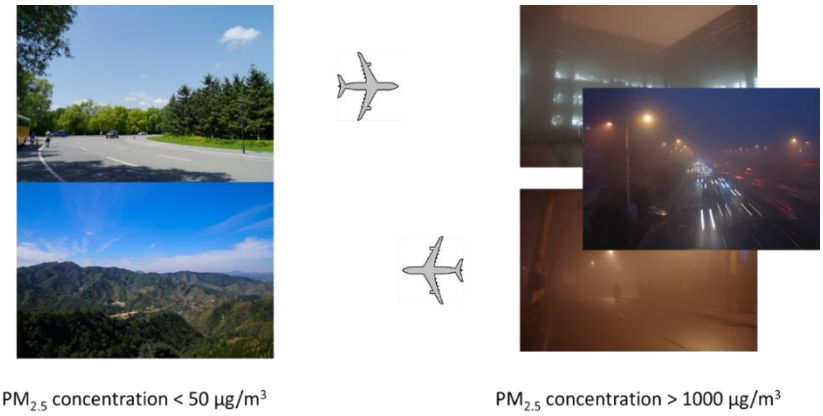

Figure 5 Photo of different air pollution levels. All photos were taken in China between 2009-2012 by Xiao.

1.5 Oxysterol in the path way of cigarette smoke induced COPD

In addition to the detection of biomarkers from human samples, molecules such as oxysterol can be detected in animal models to investigate the pathogenesis of the disease. COPD is one of the top reasons for mortality and morbidity worldwide. Yet the mechanism is not totally clear. Long-term exposure to air pollutants is supposed to be one of the key reasons, especially cigarette smoking. During chronic inflammation or infection, a teritary lymphoid organ develops which is named inducible bronchus associated lymphoid tissue [77, 78]. Emerging evidence suggests inducible bronchus associated lymphoid tissue plays an important role in the development of COPD. A previous study suggested the oxysterol metabolism of cholesterol, where 25-hydroxylase (CH25H) and 25-hydroxycholesterol 7-alpha-hydroxylase (CYP7B1) synthesize cholesterol to 7α,25-dihydroxycholesterol (7α,25-OHC), are potential pathways[79, 80]. because this oxysterol signals the migration of follicular B-cell and the production of T-cell-dependent antibody.

Therefore, to fill the gaps and to test the concept, we (1) developed robust Liquid chromatography (LC) and liquid chromatography-mass spectrometry (LC-MS) based analytical methods; (2) performed a cross-sectional cohort study in Germany to investigate the relationships; (3) carried out a pilot study among international travelers to test the novel model; (4) developed an LC-MS based analytical method

for the determination of the cholesterol to better understand the role of cholesterol in the development of COPD.

2 Methods

2.1 Study population

As a cohort study, we included a subgroup of 400 subjects without prior cardiovascular disease who participated in 2013/2014 in the second follow-up of the baseline KORA (Cooperative Health Research in the Region of Augsburg) S4 study (1999-2001, N=4,261). Participants were invited to the study center in Augsburg where they answered a computer-assisted personal interview and completed a self-administered questionnaire. All individuals were physically examined, and urine and blood samples were taken. The study design, sampling method, and data collection have been described in detail by Holle et al. [81]. All participants gave written informed consent to the study which was approved by the ethics committee of the Bavarian Medical Association.

To test the traveler model, a pilot study was performed on a small traveler cohort who traveled to China from Germany. The studied population consisted of nine non-smoking "healthy" (without doctor-diagnosed chronic diseases such as cardiovascular diseases, chronic obstructive pulmonary disease, or renal insufficiency) young male Chinese volunteers with a mean age of 29 (ranging from 26 to 34), who studied in Munich, Germany for 18 to 24 months. The volunteers subsequently traveled for a holiday to different cities of China in the time frame from December 2013 to February 2014 and returned to Germany. Information on daily $PM_{2.5}$ concentrations was collected from the official website of the China National Environmental Monitoring Centre. The main features of the travel can be described as follows: The mean travel time was 28 days (8 days– 42 days). During the whole travel time, no volunteer resided near a highway (within 100 m). Four volunteers stayed in urban areas while the other five volunteers lived in rural areas during the first week(s) of travel. During the last week of their travel, half moved to and stayed in other cities for 3-7 days. Although only non-smoking students were selected as volunteers, two were reported as severe passive smokers in the course of their trip or in Germany. The mean $PM_{2.5}$ concentration of the first week(s) of travel was 101 $\mu g/m^3$ and the mean $PM_{2.5}$ concentration of the last week of travel was 118 $\mu g/m^3$. For comparison, in Munich, during the period between December 2013 and February 2014, the mean $PM_{2.5}$ concentration was 21 $\mu g/m^3$. A sample collecting schedule was carried out for the traveler cohort. Urine samples were collected immediately upon return to Munich. Further collections were performed after one week, two weeks, and four weeks. The whole sampling cycle can be divided into five different sampling periods: one day before leaving Munich (S0); first day after return to Munich (S1); one week after return to Munich (S2); two weeks after return to Munich (S3); and four weeks after return to Munich (S4). Urine was collected in glass tubes and stored in an icebox immediately.

Anonymous self-administered questionnaires were used to collect health histories, including age, gender, respiratory diseases, and cardiovascular diseases, as well as information on travel history including the departure date, arrival date, and staying cities. Since this study is considered an observational study, no

treatment was applied (non-invasive sampling), and the signature of consent is the only risk to participants' privacy. Exception by the Ethics Committee was approved. The participants were fully informed formally. The whole study follows the principles of the Declaration of Helsinki.

2.2 Urinary sample collection and sample preparation

Spot urine sample was taken and frozen until further processing. To avoid further reactions, we thawed urine samples at 4°C and measured the samples on the same day as sample preparation.

The targeted analytes were mostly in low concentrations. Besides, samples in this study were mixtures of complex constituents that can influence the performance of the detector. Thus, various types of sample preparation were used to enrich the target analytes, remove the interfering compounds, or enhance the signal.

Solid phase extraction (SPE) is a commonly used sample pre-treatment technique in chromatography [82, 83]. By using C18, C6, or weak ion-exchange material, the cartridge can selectively enrich the targets and remove the disturbance. The whole workflow normally includes "condition" which cleans and equilibrates the cartridge with solvents and buffer, "loading" which retains target analytes, "washing" which cleans up the impurities with intermediate solvents and "eluting" which elutes out the analytes with stronger eluents. The eluted analytes can further be enriched by evaporating the solvents and re-suspending with even less volume of solvents.

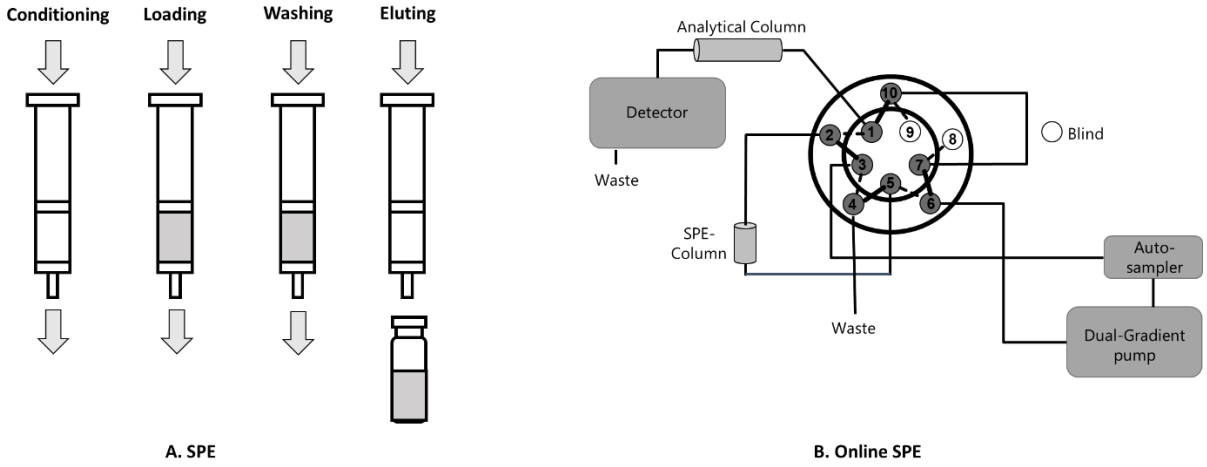

Figure 6 typical workflow of solid phase extraction and online SPE

The advantage of SPE is that it can greatly enhance the performance of the chromatographic method and reduce the matrix effects. The disadvantage of SPE is the high cost of time, manpower, and consumables. Thus, as a variant, online SPE [84, 85] was developed and used based on valve switching technique. The instrumentation of such automated solid phase extraction is normally two pumps and one or two switching valves. Similar to common SPE or so-called "off-line SPE", online SPE also includes the four steps conditioning, loading, washing, and eluting. In the conditioning step, the system equilibrates the SPE column with solvents and buffer. In the loading step, the sample will be collected from the vial with an autosampler. With the eluents, the sample will be applied to the SPE column. Then the gradient solvents will further go through the SPE column to wash it. At the last step, the value will

switch and the SPE will be connected to the analytical column. With a different gradient, the analytes will be flushed off from the SPE column and further separated with the analytical column. At last, the value will switch back again and the SPE column will be flushed and wait for the new run. Compared to the common SPE method, such an online SPE technique can greatly reduce the cost and time while improving the reproducibility by automating the whole SPE process.

Liquid-liquid extraction (LLE) is a classic extraction technique which is also known as solvent extraction[83]. It is a process of separating and extracting components in a liquid mixture with a solvent. A selected solvent that is immiscible (or slightly miscible) is added to the liquid mixture, and the different solubility of its components in the solvent is used to achieve the purpose of separation or extraction. For example, benzene is used as a solvent to separate phenol from coal tar, and isopropyl ether is used as a solvent to recover acetic acid from the dilute acetic acid solution. LLE uses a separatory funnel and other instruments in the laboratory. Industrially, it is carried out in packed towers, sieve tray towers, centrifugal extractors, spray extractors, etc. Used in organic chemistry, petroleum, food, pharmaceutical, rare elements, atomic energy, and other industries.

Extraction depends on the distribution of selected molecules from liquid bilayers or heterogeneous mixtures[86]. Liquid bilayer membranes are formed by mixing two incompatible solvents. On the other hand, a heterogeneous mixture consists of liquid and solid support materials. The target sample will interact more strongly with one solvent or phase than another. Thus, when a mixture of different phases is added, the sample will preferentially dissolve or bind to that solvent or phase. The individual phases can be separated, allowing the compounds to be purified and concentrated. There are many different variations of the extraction process. These factors vary based on factors such as selectivity, scalability, and cost. Environmental concerns may also play a role in the chosen extraction process, especially when considering industrial-scale chemical processes[87].

Derivatization: for some urinary biomarkers, the detection is often limited due to the polarity and the sensitivity. To solve such challenges, derivatizations can be used. For example, MDA is a very polar and small urinary biomarker with low detection sensitivity. The separation and detection of MDA are often difficult with LC or LC-MS). Thus 2,4-dinitrophenylhydrazine (DNPH) was used for derivatization.

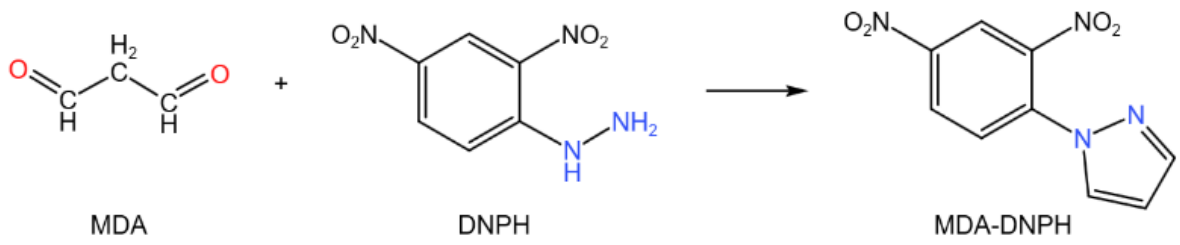

Figure 7 Derivatization of MDA with DNPH

Summary of the urinary sample preparation

MDA: 250 µL of 1mM DNPH containing 2% formic acid, 200 µL distilled water, 25 µL of 80 ng/mL d_2-MDA solution was used for the MDA-DNPH derivatization. 25 µL urine was added into the DNPH solution and vortexed with a Vortex mixer D-6012 (NeoLab, Heidelberg, Germany) for 30 seconds. Then we incubated the mixture for 70 min at 37 °C and 300 rpm in a Thermomixer comfort (Eppendorf, Hamburg, Germany). LLE was carried out with700 µL n-hexane after derivatization and well mixed by hands for 30 s. The mixture was centrifuged at 7000 rpm for 30 s in a Thermo Scientific Heraeus Pico 17 (Thermo Fisher Scientific, Darmstadt, Germany). The supernatant layer was collected. We repeated the whole LLE process once. Both portions of the collected supernatants were mixed. With a Barkey Vapotherm mobile S from Barkey GmbH (Leopoldshoehe, Germany) and a gentle nitrogen stream at room temperature, the mixture was evaporated to dryness. Fifty µL of distilled water was added to resuspend the residue for analyzing.

8OHdG: simple dilution was carried out for 8OHdG. Twenty-five micro litter urine was vortexed for 30 s and then diluted in a 1:1 proportion with 25 µL 0.1% formic acid.

$F_{2\alpha}$-isoprostanes: one milliliter of the urine sample was diluted with 2ml BIS-TRIS-HCl buffer solution (pH 6) and adjusted to pH 6 with phosphoric acid (5%) or potassium. The mixture was then applied on a polymer-based weak anion-exchange cartridge (StrataX-AW from Phenomenex, Torrance, CA) which was conditioned with MeOH/formic acid (0.1%) (98/2, v/v)

and 2ml distilled water. Then the cartridge was washed with 1ml water, 2ml MeOH/H2O (25/75, v/v), and 1ml acetonitrile. After dried with nitrogen stream for half a minute, the analytes were eluted with 3ml methanol at a speed of 30 drops/min. Nitrogen stream was used to evaporate the extract into the residue. Finally 100 µL methanol/0.1% formic acid, 50/50, v/v was used to dissolve the final residue.

OH-PAH: 5.0 mL of the urine sample was placed in a centrifuge tube. The sample was hydrolyzed with ten micro litter β-glucuronidase and 5.0 mL sodium acetate buffer solution (pH 5) overnight at 37 °C in the dark. Then the hydrolyzed urine sample was centrifuged at 1500 r/min for 10 min, and the supernatant was collected for measurement.

2.3 Instrumentation

Liquid chromatography

As one of the most important analytical techniques, LC has been widely used for more than half a century in industry and research. The liquid solvents that carry the sample mixture are pumped at high pressure through an analytical column. Different interactions between the components in the mixture and the column absorbent material can cause different retention and thus be separated when going through the columns. Such interactions are physical including hydrophobic, dipole-dipole, and ionic. As an analytical separation method, it utilizes the slight difference in the adsorption or distribution coefficients of substances in the two phases to achieve the purpose of separation. When the two phases move

relatively to each other, the measured substance is distributed between the two phases many times, so that the slight distribution difference can be greatly enhanced, and the effect of separation is achieved. The moving liquid solvents are called the "mobile phase" and the adsorbent particles in the analytical column are called the "stationary phase". [88] In the present thesis, the following types of chromatography were tested: normal phase chromatography, reverse-phase chromatography, and hydrophilic Interaction Chromatography.

Normal phase chromatography separates analytes by the affinity to the polar stationary particles [88]. A common particle material is silica. Different components engage in polar interactions with the silica surface differently. With a non-polar, non-aqueous mobile phase, components soluble in non-polar solvents can be separated. The higher polarity of the analyte, the stronger the adsorption capability is.

Partition chromatography was one of the earliest types of liquid chromatography. It separates analytes based on the polarity of analytes[89]. Hydrophilic interaction chromatography is one of such techniques. As a variant of normal phase chromatography, hydrophilic interaction chromatography uses hydrophilic stationary phases with less polar eluents such as acetonitrile while the column materials are often polar such as silica. According to the surface, it can be grouped into simple unbonded silica silanol or diol bonded phases, amino or anionic bonded phases, amide bonded phases, cationic bonded phases, and zwitterionic bonded phases.

Reverse phase (RP) chromatography is contrary to normal phase chromatography. The analytes are transported aqueous, relatively polar mobile phase [88, 90]. Then they are separated by the non-polar stationary phase. Silica particles are also common stationary phase material for reverse phase chromatography, yet a modification with C8 or C18 straight chain alkyl chain groups to the particle surface is necessary to give different retention times for polar and less polar analytes. Reverse phase chromatography is a very important analytical technique in life.

Mass spectrometry

Mass spectrometry is an analytical method for measuring ion mass-to-charge ratio. Similar to chromatography, mass spectrometry is also a very widely used analytical technique in many areas such as chemistry, environment, medicine, and life science. It can identify the analytes and provide the structure information. A mass spectrometer is generally composed of a sample input system, an ion source, a mass analyzer, a detector, and a data processing system. It can be connected with liquid chromatography, gas chromatography, and thin layer chromatography which can offer further possibilities.

The main mechanism of mass spectrometry is: (1) the components in the sample are ionized in the ion source to generate charged ions with different charge-to-mass ratios, (2) accelerate in the accelerating electric field and form an ion beam, (3) enter the mass detector. The electric and magnetic fields are used to cause opposite velocity dispersion, and they are respectively focused to obtain a mass spectrum, thereby determining their mass.

Quadrupole mass spectrometer is a mass spectrometer equipped with a quadrupole mass analyzer[91]. In the quadrupole, the four electrode rods are divided into two groups, respectively, on which a radio frequency inverse alternating voltage is applied. In such an electric field, the ions will oscillate according to the electric field. Only ions with a specific charge-to-mass ratio can pass through the electric field stably. When the voltage on the quadrupole is specified, (1) the ions with too small mass will be greatly affected by the voltage, so that they will oscillate very violently, causing the contact pole to lose its charge and be pumped out by the vacuum system; (2) the ions with too high mass cannot be pulled enough by the electric field, which eventually leads to hitting the pole or flying out of the electric field and failing to pass the mass analyzer. The ions located in this potential field, after the selected part is stabilized, can reach the detector, or enter the subsequent space for subsequent analysis.

Due to the relatively simple structure and good robustness, it is widely used especially connected with other analyzers. For example, a **triple quadrupole mass spectrometer (TQMS)** is a tandem mass spectrometer consisting of two quadrupole mass analyzers with a (non-mass-resolved) radio frequency -only quadrupole between them, acting as collision-induced dissociation collision cell, fragmenting selected precursor/precursor ions and producing fragment/product ions[91]. The triple quadrupole mass spectrometer is designed to work in 4 modes: precursor ion scan, neutral loss scan, product ion scan, and multiple reaction monitoring / selective reaction monitoring. Although TQMS is not excellent in terms of mass resolution and mass range, triple quadrupoles offer the advantages of low cost, high efficiency, and ease of operation. At the same time, MS/MS technology allows mass analysis in a spatially tandem manner. Not only can TQMS be used to explore molecular structures in fragmentation mode, but it also has excellent detection sensitivity and quantitative capabilities in selective reaction monitoring mode, especially when analyzing small molecules. triple quadrupole mass spectrometer has a wide range of applications in food and environmental analysis for additive, trace/contaminant scanning, including antibiotics and pesticides; clinical research for preclinical, endocrine, and biomarkers; toxicology for impurities, drug molecular structure elucidation, and biofluid analysis; drug discovery and development for lead compound optimization, “absorption, distribution, metabolism, and excretion”, pharmacokinetic/pharmacodynamic modeling and drug metabolite determination.

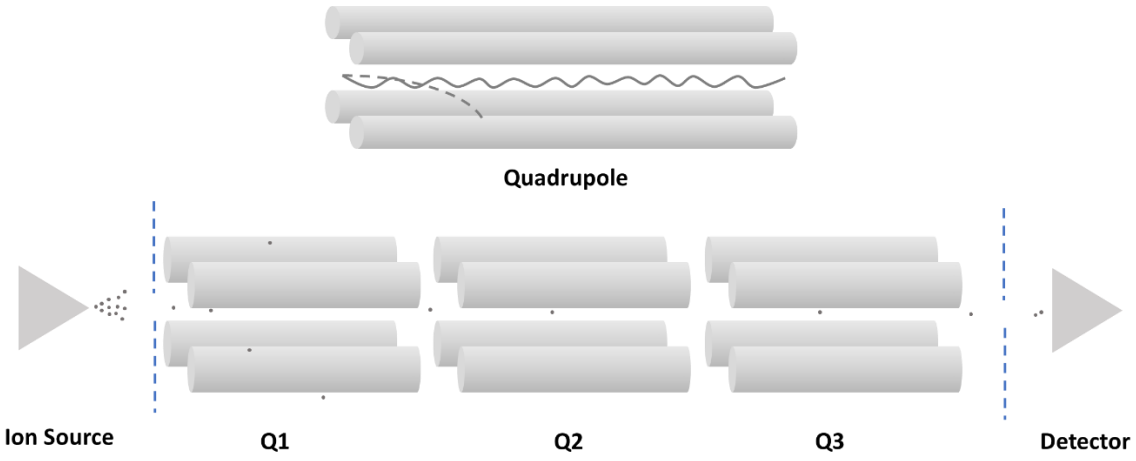

Figure 8 Quadrupole and triple Quadrupole mass spectrometer

The mass analyzer of **time-of-flight mass spectrometer (TOF-MS)** is an ion flight path[92, 93]. The ions generated by the ion source are accelerated into the fieldless flight path and fly towards the ion receiver at a constant speed. The higher the ion mass, the longer it takes to reach the receiver, the lower the ion mass, the shorter the time it takes to reach the receiver. According to this principle, ions of different masses can be separated according to the mass-to-charge ratio. The flight time of the ions is measured by fast electronics. Mass determinations are possible with an accuracy of approximately 2 ppm. Furthermore, a fairly high mass resolution can also be achieved. Time-of-flight mass spectrometry has inherent performance advantages over quadrupole mass spectrometers. It collects instantaneous full-spectrum information, greatly improving the analysis speed and sensitivity of the instrument, ensuring that any important information is not lost and allowing retrospective analysis. This makes it easier to identify unknown analytes and interpret measurement results.

High resolution time-of-flight mass spectrometer (HR-TOF-MS): The time-of-flight mass spectrometer can detect a large molecular weight range. It has a fast-scanning speed and a simple instrument structure. The main disadvantage of the early types of time-of-flight mass spectrometer is the low resolution because the initial energy of the ions when they leave the ion source is different, so the time of ions with the same mass-to-charge ratio reaching the detector has a certain distribution, resulting in a decrease in the resolving power. One of the improved methods is to add a set of electrostatic field mirrors in front of the linear detector to push back the ions in free flight. The ions with high initial energy have a long distance into the electrostatic field mirror and a long distance of return due to their fast initial velocity. The return distance of the ions with small initial energy is short so that they will be focused at a certain position on the return distance, thereby improving the resolving power of the instrument. Such time-of-flight mass spectrometers with electrostatic field mirrors are called reflectron time-of-flight mass spectrometers[94]. Moreover, the distance of the flight path can be further prolonged with the multi-reflecting techniques such as Folded Flight Path in high resolution time-of-flight mass spectrometer. In such a technique, a set of planar gridless mirrors and a set of single focusing electrostatic lenses are equipped to guide the ions through multiple lenses and reflectors [95]. The total ion path can be 20 m yet folded in a small vacuum chamber. The lens of the flight path can be doubled by reflecting the ions to send them back reversely through the path again to reach an ultra high resolution mode for FFP level resolution over 50,000. When working with a low mass resolution, isobaric compounds cannot be distinguished because isobaric compounds have the same nominal mass which only differ in elemental composition. Isobaric compounds will have different time profiles in the sample, and being able to measure and quantify them separately is important for the

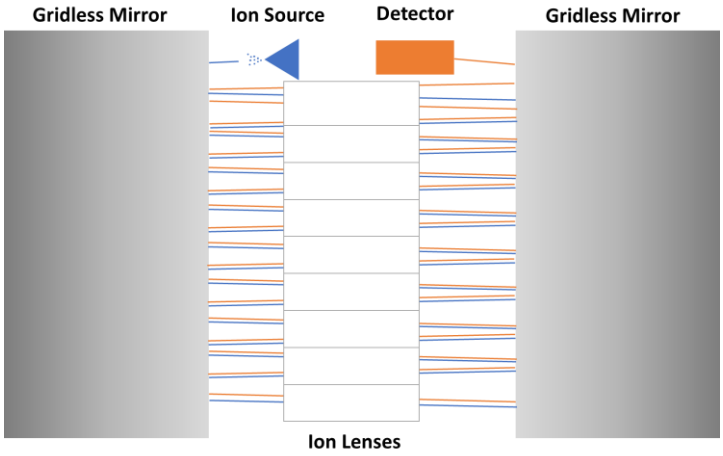

Figure 9 High resolution time-of-flight mass spectrometer

accuracy of the analytical results. Moreover, the accurate mass information provided by the mass resolution is used to determine the composition of ion peaks. This is critical for compound identification, which cannot be achieved with low resolution instruments.

Quadrupole time-of-flight mass spectrometer (QTOF-MS) combines time-of-flight and quadrupole into one instrument [96]. It uses a quadrupole, a collision cell, and the time-of-flight together thus has the advantage both of quadrupole and time-of-flight such as accurate mass measurements, high sensitivity in "full-scan", comprehensive to compound types and amount and structure information by generating product ion from the collision.

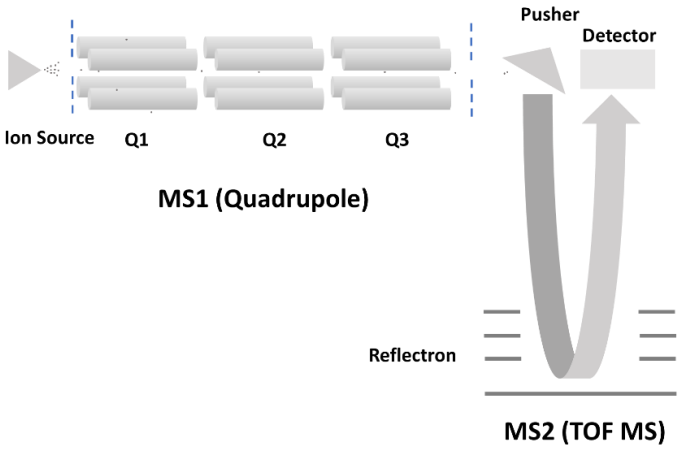

Figure 10 Quadrupole time-of-flight mass spectrometer

Ion Source

The ion source is a device that creates atomic and molecular ions. There are many different types including electron ionization, chemical ionization, photoionization, desorption ionization, spray ionization, and thermal ionization. For liquid chromatography tandem mass spectrometer, electrospray ionization, atmospheric pressure chemical ionization, atmospheric pressure photo ionization, matrix assisted laser desorption ionization, and inductively coupled plasma ionization are commonly used ion sources.

The **electron ionization** is used in mass spectrometry as a kind of "hard ionization"[97, 98]. The electron ionization source is mainly composed of an ionization chamber, a filament, an ion focusing lens, and a pair of magnetic poles. The main working principle is that the filament emits electrons with an energy of 70eV, which are focused and pass through the ionization chamber under a magnetic field to the collector. The sample molecules entering the ionization chamber are ionized with electrons at a certain energy, and ions with larger internal energy can spontaneously dissociate to generate more fragment ions when they collide with neutral molecules (such as He). All ions are focused, accelerated, and focused into an ion beam that enters the mass spectrometer.

Unlike traditional chemical ionization interfaces, **atmospheric pressure chemical ionization** technology does not use reactive gases such as methane but uses corona discharge to initiate a series of gas-phase reactions to complete the ionization process[99]. In terms of its principle, it can also be called discharge ionization or plasma ionization. The sample solution flowing out of the liquid chromatography enters a capillary tube with a nebulizing gas sleeve and is nebulized by a stream of nitrogen gas and vaporized as it passes through the heating tube. Corona discharge is carried out at the end of the heating tube. The solvent molecules are ionized as reaction gas and collide with the gaseous sample molecules. After a complex reaction process, the sample molecules generate quasi-molecular ions. They are mainly

used in compounds with strong electron affinity. Quasi-molecular ions of sample molecules pass through the screening slit and enter the mass spectrometer.

Different from chemical ionization, **atmospheric pressure photoionization ionization** is a soft ionization for MS, especially for LC-MS[100]. The vacuum ultraviolet light source ionizes molecules at atmospheric pressure. Two ways can happen in the ionization: by direct absorption followed by electron ejection or dopant, molecules can be ionized and then ionize the target analytes in a chemical ionization way.

It can analyze compounds, especially weakly polar and non-polar compounds. It can ionize polar and non-polar small molecules at the same time, which allows users to analyze more compounds at a time. Meanwhile, it greatly reduces matrix effects and related ion suppression during the assay, simplifies the sample purification process, saves sample pre-treatment time, achieves higher analyte recovery, and ensures the quality of analytical data. However, it is not as sensitive as atmospheric pressure chemical ionization. Furthermore, it is not suitable for compounds with poor thermal stability.

Electrospray ionization is currently the most commonly used interface for mass spectrometry[101]. It is a soft ionization method and can be used to study unstable and polar compounds. Electrospray ionization uses an electron field to generate charged droplets and finally generates analyte ions through a process of desolvation, which enters into mass spectrometry for analysis. This whole process includes three stages, charged droplet formation, droplet shrinkage, and generation of gas-phase ions. Electrospray ion sources can be used to study biological macromolecules such as proteins. However, the electrospray ion source requires that the sample to be tested should be able to form ions in the solution. The type and concentration of buffer in the mobile phase have a significant impact on the sensitivity. So, the selection of the mobile phase is very important. The matrix inhibition is relatively significant.

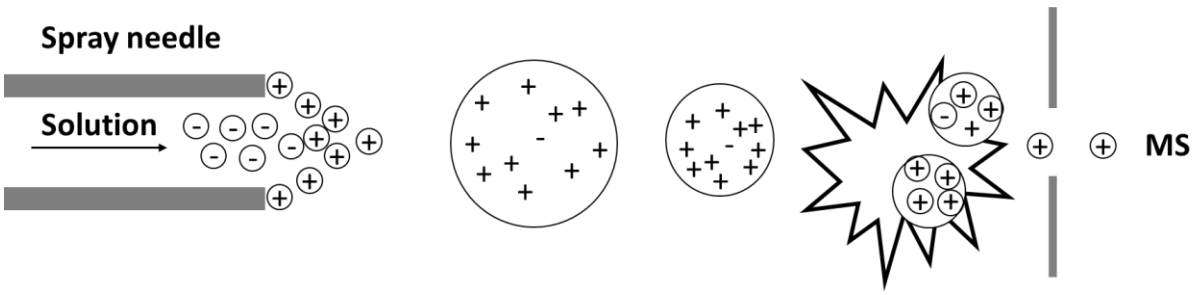

Figure 11 Electrospray ionization

Matrix-assisted laser desorption ionization is as well a soft ionization technique for mass spectrometry. It can obtain mass information of some macromolecules that are easily dissociated by conventional ionization methods to obtain molecular fragments, such as DNA, biopolymers, proteins, polypeptides, sugars as well as other large molecular weight organic molecules, such as polymers, dendrimers, and other macromolecules. The principle of this technology is the laser provides high-intensity pulsed energy to the substance to be analyzed in a tiny area and a very short time interval, so that can complete desorption and ionization instantly while does not produce thermal decomposition. It is an ionization method that directly vaporizes and ionizes non-volatile samples. Yet its ionization

mechanism is still unclear. There are two possibilities: the ions are formed in the solid state, and they are simply released when the laser is irradiated, or the molecules are ionized by laser-induced ion-molecular reactions. The desorption ionization process depends on the type of matrix, the wavelength of excitation light, and the intensity of laser irradiation. It is similar in this respect to the other soft ionization method. However, it is more likely to obtain singly charged ion peaks.

Summary of the instrumentation

MDA: 10 µL derivatized solution was injected into an LC-MS system equipped with a Kinetex RP18 endcapped column (100mm x 3mm I.D., 2.6 µm, Phenomenex, Torrance, CA) at column temperature 20 °C and a triple quadrupole mass spectrometer with electrospray ionization source. An isocratic gradient with 80% methanol and 20% H_2O (both containing 0.1% formic acid) and a flow rate of 0.2 ml/min were used in combination with a peak-cutting technique based on valve switching between 1.5 min and 2.5 min.

8OHdG: 10 µL diluted sample was injected into an LC-MS system equipped with a Gemini RP18 endcapped column (250mm x 2 mm, 5 µm, Phenomenex, Torrance, CA, protected with guard column) and a triple quadrupole mass spectrometer with electrospray ionization source. A gradient with solvent A (0.1% formic acid in water), solvent B (0.1% formic acid in methanol) and solvent C (acetonitrile) was used (Table 1). the valve switched between 3 min to 5 min to protect the detector.

$F_{2\alpha}$-isoprostanes: 20 µL extracted sample was injected into a LC-MS system equipped with a Hydro RP18 endcapped column (250mm x 2mm I.D, 4 µm, Phenomenex, Torrance, CA) and a triple quadrupole mass spectrometer with electrospray ionization source. A gradient with solvent A (0.1% formic acid in water), solvent B (0.1% formic acid in methanol) was used (Table 1). The valve switched between 3 min to 5 min to protect the detector.

Table 1 Gradient of the LC-separation of 8OHdG and $F_{2\alpha}$-isoprostanes.

	8OHdG			$F_{2\alpha}$-isoprostanes		
Time (min)	A%	B%	C%	Time (min)	A%	B%
0	80	10	10	10	50	50
5	0	100	0	20	0	100
5.5	10	90	0	30	0	100
12	10	90	0	32	50	50
13	80	10	10			
23	80	10	10			

Column temperature 20 °C, flow rate 0.2 ml/min. Solvent A is 0.1% formic acid in water, solvent B is 0.1% formic acid in methanol, solvent C is acetonitrile.

OH-PAHs: The hydrolysed sample was injected into a LC system with a fluorescence detector. A laboratory-made online SPE column (copper phthalocyaninemodified silica, 5mm x 2.1mm I.D, 45 µm – 60 µm) and a Kinetex PF analytical column (100 x 3mm I.D., 2.6 µm, Phenomenex, Aschaffenburg,

Germany) were used. The wavelength of the fluorescence detector was set at 249 nm/364nm (Ex./Em.) for OH-Phenanthrenes and 1-hydroxypyrene for 343 nm/385nm (Ex./Em.).

2.4 Individual characteristics and clinical parameters

In the KORA cohort study, fasting venous blood samples were collected during the study participants' visits. Then the samples were stored at 4 °C until further processing.

We analyzed serum Hs-CRP concentrations by latex-enhanced immunonephelometry on a BN II platform (Siemens Healthcare Diagnostics Product GmbH, Marburg, Germany) with an intra-assay coefficient of variation of 2.13 % [71]. Body Mass Index (BMI) was calculated as weight divided by height (squared). The following health status was defined: type 2 diabetes, validated by oral glucose tolerance test; pre-diabetes, impaired fasting glucose and/or impaired glucose tolerance; hypertension, either blood pressure above 140/90 mmHg or treatment of known hypertension (WHO, 1999). To evaluate the status of the kidney, the estimated glomerular filtration rate (eGFR) (mL/min per 1.73 m^2) was calculated using the 2009 CKD-EPI creatinine equation [102].

2.5 $PM_{2.5}$ index

For the pilot traveler study, we collected the daily $PM_{2.5}$ concentration data from the official website of the China National Environmental Monitoring Center. As described on the website, the monitoring activities were carried out according to the official technical regulation of China (HJ 663—2013, HJ 633—2012, HJ/T193-2005, and HJ 655-2013).

2.6 Mouse COPD models and mouse sample preparation

To investigate the role of CH25H induced inducible bronchus associated lymphoid tissue formation in vivo, B6.129S6-Ch25htm1Rus/J (Ch25h-/-) mice (Jackson Laboratory), age-matched female C57BL/6J mice (Charles River Laboratories) were used. Eight to twelve week old mice were exposed to 100% mainstream cigarette smoke (CS), which was generated from 3R4F research cigarettes (Filter removed, Tobacco Research Institute, University of Kentucky) at a particle concentration of 500 mg/m3. The exposure frequency was set for 50min twice/day, 5 days/week for 4 or 6 months. As control group, mice were exposed to filtered air. The Lungs were lavaged with 3x500ul aliquots of sterile PBS (Gibco, Life Technologies) supplemented with Complete Protease Inhibitor Cocktail tablets (Roche Diagnostics). The bronchoalveolar lavage fluid was retained for mass spectrometry analysis. All animal experiments were performed according to strict governmental and international guidelines and were approved by the local government for the administrative region of Upper Bavaria, Germany.

To analyze the 25-Hydroxycholesterol. The sample is thawed and vortexed (neolab, Munich, Germany). The whole sample is then transferred to a 2 ml Eppendorf tube and 10 µl of a 2mmol methanolic BHT solution as well as 20 µl of the diluted solution of the internal standard are added. Samples and standards are mixed with 200 µl of a KOH solution (1 M in water) and saponified at 37°C for 1 hour in an Eppendorf thermomixer comfort 5355 (Hamburg, Germany). After saponification 1 ml hexane is added and the solutions are shaken thoroughly for 5 min on a vortex. If possible, 800 µl of the hexane layer is

transferred to a 2 ml Eppendorf tube. For serum and protein samples this amount sometimes was significantly lower. Hexane is evaporated under a gentle stream of nitrogen at 45°C on a vapotherm evaporation unit from Barkey (Leopoldshöhe, Germany). As described above (see "Derivatization solution") 250 µl of the derivatization solution is added. The mixture is vortexed and incubated at 80°C for 60 min. After the derivatization step, 1 ml hexane is added, and the layers are mixed thoroughly (5 min) and centrifuged (ca. 3500 rpm, 5 min). As much hexane as possible is removed with an exact syringe and filled into an autosampler vial. Hexane is carefully evaporated with nitrogen at 45° C on the vapotherm evaporation unit. The residue is solved in 50 µl acetonitrile. After short sonication in an ultrasonic bath (Bandelin, Berlin, Germany) the solution is filled into an autosampler vial and analyzed via LC-HRTOF-MS.

2.7 Statistical Analysis - chemometrics and multivariate data analysis

Chemometrics, also known as chemical statistics, is a methodology that combines mathematics, statistics, and computer science with chemistry to solve scientific questions[103]. It includes (1) evaluating and interpreting chemical or analytical data; (2) optimizing and designing chemical or analytical processes and experiments; (3) extracting maximum chemical and analytical information from experimental data.

In chemometrics, multivariate data analysis methods are usually used including correlation analysis, regression analysis (simple regression analysis/multi linear regression analysis), analysis on variance, principal component analysis, partial least square regression, hierarchical clustering analysis, and support vector machine.

C**orrelation analysis** refers to the analysis of two or more variable elements with correlation, to measure the degree of correlation between two variable factors[104]. There should be a certain relationship or probability between the elements of the correlation before the correlation analysis can be carried out. However, it should be clarified that correlation does not equal to causation.

The Pearson correlation coefficient or also named as Pearson product-moment correlation coefficient is used to measure the correlation (linear correlation) between two variables X and Y. And an important mathematical property of correlation coefficient similarity is that changes in the position and scale of two sets of variables do not cause changes in the coefficients

$$r_{xy} = \frac{\mathrm{cov(x,y)}}{S_x S_y} = \frac{cov(x,y)}{\sqrt{cov(x,x)\,cov(y,y)}} = \frac{\sum_{i=1}^{n}(x_i-\bar{x})(y_i-\bar{y})}{\sqrt{\sum_{i=1}^{n}(x_i-\bar{x})^2\sum_{i=1}^{n}(y_i-\bar{y})^2}}$$

The value of the Pearson correlation coefficient is between -1 and 1. When 0<r<1, indicating a positive correlation; when r=0, indicating no correlation or no linear association; when -1<r<0, indicating a negative correlation.

The Spearman's rank correlation coefficient which was named after Charles Edward Spearman, is also known as the Spearman correlation coefficient. It is a nonparametric measure of the dependence of two variables. It uses a monotonic equation to evaluate the correlation of two statistical variables. If there

are no duplicate values in the data, and when the two variables are perfectly monotonically correlated, the Spearman correlation coefficient is either +1 or −1.

The Spearman correlation coefficient is defined as the Pearson correlation coefficient between the rank variables. For a sample with a sample size of n, the raw data are converted into ranking data, and the correlation coefficient ρ is

$$\rho = \frac{\sum_i (x_i - \bar{x})(y_i - \bar{y})}{\sqrt{\sum_i^n (x_i - \bar{x})^2 \sum_i^n (y_i - \bar{y})^2}}$$

Similar to the Pearson correlation coefficient, the value of the Spearman correlation coefficient is between -1 and 1. When 0<r<1, indicating a positive correlation; when r=0, indicating no correlation or no linear association; when -1<r<0, indicating a negative correlation.

T-test, analysis of variance, and Kruskal-Wallis test

The t-test which is also known as Student's t-test refers to the statistical hypothesis test of Student's t-distribution in any test statistic under the null hypothesis [105]. It is a test method in statistical inference that is used when the statistic follows a normal distribution but the variance is unknown. The premise of the t-test is that the samples follow a normal distribution or an approximately normal distribution. Otherwise, some transformations (logarithm, root, reciprocal, etc.) can be used to try to convert it into data that follows a normal distribution. To satisfy the normal distribution, only nonparametric test methods can be used.

The four most common uses of the t-test are (1) one-sample t-test, which is used to test whether the mean of a single sample is equal to the mean of a known population with unknown population variance, normally distributed data, or approximately normally distributed. (2) Independent two-sample t-test, which is used to test whether the mean values of two sets of independent normally distributed data or approximately normally distributed samples are equal. Here, it can be classified and discussed according to whether the population variance is equal or not. (3) Dependent t-test for paired samples, which is used to test whether the difference between the means of a pair of paired samples is equal to a certain value. (4) T-test for regression coefficient significance, to test whether the explanatory variables used to test the regression model have a significant effect on the explained variables.

Analysis of variance was invented by Ronald Fisher and is used to test the significance of the difference between the means of two or more samples. The core idea of variance analysis is to decompose the total variation of sample observations into two parts, random error and factor influence, and make statistical inferences with the help of F distribution.

The **Kruskal-Wallis test**[106] is a nonparametric method to test whether two or more samples come from the same probability distribution. The samples tested must be independent or uncorrelated. When considering a parametric test, this test is similar to the one-way ANOVA. However, the Kruskal-Wallis test does not assume that the samples come from a normal distribution. Its null hypothesis is that the probability distributions obeyed by each sample have the same median, and the rejection of the null

hypothesis is that the median of the probability distribution of at least one sample is different from the other samples. The test does not identify between which samples the differences occurred and the magnitude of the differences. The test statistic is calculated by:

$$H = (N-1)\frac{\sum_i^g n_i(\bar{r_i}.-\bar{r})^2}{\sum_{i=1}^g \sum_{j=1}^{n_i}\left(r_{ij}-\bar{r}\right)^2}$$

where:

N is the total number of observations across all groups, g is the number of groups, n_i is the number of observations in group i, r_{ij} is the rank (among all observations) of observation j from group i, $\bar{r_i}. = \frac{\sum_{j=1}^{n_i} r_{ij}}{n_i}$ is the average rank of all observations in group i, $\bar{r} = \frac{(N+1)}{2}$ is the average of all the r_{ij}.

Regression analysis refers to a statistical analysis method to determine the interdependent quantitative relationship between two or more variables [107]. Regression analysis can be divided into simple regression analysis and multiple regression analysis according to the number of variables involved; according to the number of dependent variables, it can be divided into simple regression analysis and multiple regression analysis; according to the type of relationship between independent variables and dependent variables, it can be divided into Linear regression analysis and nonlinear regression analysis. Multi linear regression analysis is a predictive modeling technique that studies the relationship between a dependent variable and an independent variable[108]. This technique is commonly used in predictive analytics, time series modeling, and discovering causal relationships between variables. The formula of multiple linear regression is:

$$y_i = \beta_0 + \beta_1 x_{i1} + \beta_2 x_{i2} + \cdots + \beta_p x_{ip} + \in$$

Where for $i = n\ obs$ervations: y_i is the dependent variable, x_i are explanatory variables, β_0 is y-intercept, β_p is slope coefficients for each variable, $\in$ is the model error (residuals).

In this study, Spearman correlation coefficients were calculated to explore the relationships between urinary biomarkers, individual characteristics, and clinical parameters.

Kruskal–Wallis Tests were carried out to investigate the impacts of health profiles. Potential underlying inflammation was defined as hs-CRP concentration ≥ 3 mg/L and potential renal impairment was defined as eGFR < 90 mL/min/1.73 m^2 [109].

We used multiple linear regression models to investigate the associations between i) OH-PAHs and hs-CRP, ii) OH-PAHs and oxidative stress, as well as iii) oxidative stress and hs-CRP. Log transformations were performed on the normalized concentrations of urinary biomarkers and hs-CRP to approximate normal distributions of the residuals. Based on a previous study, we created base models including age, sex, smoking, and season (spring: March to May; summer: June to August; autumn: September to November; winter: December to February) as potential confounders [110]. Also, we forced time trends into the models and optimized the smoothing parameters by optimizing the generalized cross-validation (GCV) criteria [111]. We then included respective interaction terms to investigate potential effect

modification by inflammation. Sensitivity analyses were also performed by removing season from the models to evaluate the robustness.

For the statistical analyses of the KORA study, all statistical analyses were performed with R Statistical Software (version 3.5.1, R Foundation for Statistical Computing, Vienna, Austria). All effect estimates with 95% confidence intervals are given for an interquartile range increase of the exposure concentration. For the statistical analyses of the pilot traveler study, MatLab ver. 7.11 R2010b (The MathWorks Inc., Natick, MA) was used. We considered a two-sided P value < 0.05 to be statistically significant.

3 Results

3.1 Validation of the analytical methods

Linearity, sensitivity: We set the concentration ranges between 0.2 ng/mL and 200 ng/mL linear to establish calibration curves. Linearities were good and the r^2 was higher than 0.996.

limit of quantification: Limits of quantification (LOQ) were calculated automatically for every run, using ANALYST according to the following equation.

$$\text{Limits of quantification} = \frac{10\ x\ Calculated\ Concentration}{Analyte\ Signal\ To\ Noise}$$

Instrument maintenance: Both the positive mode and negative mode of the mass spectrometer were regularly tuned and calibrated according to the handbook.

Repeatability and reproducibility: Pooled urine sample was created with six urine samples from different volunteers. Then we spiked the pooled sample to 80 ng/mL MDA, 20 ng/mL 8OHdG, or 10 ng/mL $F_{2\alpha}$-isoprostane standards and processed by the methods described previously. To investigate instrument repeatability, we injected an aliquot of the same sample 6 times. The peak areas were obtained and the coefficients of variation ranged between 1.7% and 11.6%. On 10 different days, spiked deionized water and spiked pooled urine samples were processed according to the sample preparation procedures and analyzed by LC-MS/MS as described in the previous chapter to investigate the reproducibility of the methods. To overcome instrumental fluctuation issues during the overall period of analysis, we calculated reproducibility based on concentration rather than peak area based on standard curves generated in each sequence. The coefficients of variation ranged between 6.6% and 18.3% which were good.

Recovery and matrix effects: Pooled urine samples and deionized water were spiked with standards in different levels of concentration, prepared, and analyzed according to the method described previously.

The recoveries were calculated based on the equation shown below. The recoveries ranged between 44%-120%. By back-calculations against the internal standard, the recoveries ranged between 89% and 127%.

$$\text{Recovery} = \frac{(mean\ peak\ area\ of\ spiked\ urine\ samples - mean\ peak\ area\ of\ pure\ urine\ samples)\ x\ 100}{mean\ peak\ area\ of\ methanolic\ standards}$$

3.2 Study Population of the KORA cohort

The total number of participants in the selected cohort was 400. After removing the subjects with missing values in the key outcomes, we had a final number of 392 (OH-PAHs: N = 7; MDA: N = 8; 8OHdG: N = 9; $F_{2\alpha}$-isoprostanes: N = 9; creatinine: N = 6; extremely low creatinine concentration: N = 1; hs-CRP: N = 4). The mean age of the participants was 56 years. 57 % of the participants were male. Only 37% of participants were neither smokers nor previous smokers. The mean concentration of hs-CRP was 2.4 mg/L. 21% of participants indicated potential underlying inflammation and 45% of participants were free from diagnosed diabetes or pre-diabetes (41 %).

The mean sum OH-PAHs concentration and the concentrations of 1-OH-Phe, 2-OH-Phe, 3-OH-Phe, and 1-OH-Pyr in the study participants were 0.34, 0.16, 0.08, 0.10, and 0.30 ng/mg creatinine, respectively. The mean sum $F_{2\alpha}$ -isoprostanes concentration and the concentration of 2,3-dinor-8-iso-$PGF_{2\alpha}$, 8-iso-15(R)-PG $F_{2\alpha}$, 8-iso-$PGF_{2\alpha}$, and ±5-$iPF_{2\alpha}$ in the study participants were 4.11, 2.08, 0.52, 0.27, and 1.24 ng/mg creatinine, respectively. In the Spearman correlation test between all pairwise combinations of biomarkers and clinical parameters, we observed strong correlations within the $F_{2\alpha}$-isoprostane group (0.54 – 0.88) and the OH-PAHs group (0.55 – 0.78). Thus we limited parts of the subsequent analyses to the sum of OH-PAHs concentrations and the sum of $F_{2\alpha}$-isoprostanes concentrations as indicators to reduce the number of tests and to keep the results brief. The mean concentration of MDA, 8OHdG, and creatinine in the study participants were 41.76 ng/mg creatinine, 3.35 ng/mg creatinine, and 1.34 mg/mL respectively.

Table 2 Descriptive statistics of the study population (N=400)

Characteristics	Mean or Total N	SD or (%)	Missing N
Personal Characteristics			
Age (years)	56	9.2	0
< 55	173	45%	0
≥ 55, < 65	126	33%	0
≥ 65	83	22%	0
Sex (male)	220	57%	0
Socio-economic & lifestyle characteristics			
BMI (kg/m²)	28.1	4.8	0
Obese (BMI ≥ 30 kg/m²)	116	30%	0
Smoking Status			
Non-smoker	141	37%	0
Ex-smoker	163	43%	0

Smoker	78	20%	0
Clinical Characteristics			
hs-CRP (mg/L) (N = 382)	2.39	3.36	4
Potential underlying inflammation (hs-CRP ≥ 3 mg/L)	80	21%	4
eGFR (mL/min/1.73 m^2)	89.9	9.3	7
Potential renal impairment (eGFR ≤ 90 mL/min/1.73 m^2)	179	47%	7
Diabetes Status			
No Diabetes	173	45%	0
Pre-diabetes	156	41%	0
Diabetes	53	14%	0
Hypertension Status			
Hypertension	130	34%	0
Characteristics of the day of examination			
Season			
Spring (Mar-May)	129	34%	0
Summer (Jun-Aug)	98	26%	0
Autumn (Sep-Nov)	71	18%	0
Winter (Dec-Feb)	84	22%	0
Urinary biomarkers (ng/mg Creatinine)			
OH-PAHs	0.34	0.39	0
1-OH-Phe	0.16	0.18	7
2-OH-Phe	0.08	0.12	7
3-OH-Phe	0.10	0.14	7
1-OH-Pyr	0.30	0.39	7
MDA	41.76	38.69	8
8OHdG	3.35	1.93	9
$F_{2\alpha}$-isoprostanes	4.11	2.92	9
2,3-dinor-8-iso-$PGF_{2\alpha}$	2.08	1.63	7
8-iso-15(R)-$PGF_{2\alpha}$	0.52	0.1	7
8-iso-$PGF_{2\alpha}$	0.27	0.23	9
±5-$iPF_{2\alpha}$	1.24	0.99	7
Creatinine (mg/mL)	1.34	0.81	6

SD, standard deviation; OH-PAHs, sum OH-PAHs concentration; 1-OH-Phe, 1-hydroxyphenanthrene; 2-OH-Phe, 2-hydroxyphenanthrene; 3-OH-Phe, 1-hydroxyphenanthrene; 1-OH-Pyr, 1-hydroxypyrene; MDA, malondialdehyde; 8OHdG, 8-hydroxy-2'-deoxyguanosine; $F_{2\alpha}$-isoprostanes, sum $F_{2\alpha}$-isoprostanes concentration; BMI, Body Mass Index; hs-CRP, high sensitivity C-Reactive Protein; eGFR, Estimated Glomerular Filtration Rate from Serum Creatinine and Cystatin C.

3.3 Outcomes from Kruskal–Wallis Test in KORA subcohort

We observed clearly higher MDA concentrations in participants higher than 55 years old, potential underlying inflammation, or CKD. 8OHdG concentrations were also significantly increased in participants higher than 55. Concentrations of $F_{2\alpha}$-isoprostanes were significantly higher in female participants. Participants who visited the study center in winter were detected with the highest concentrations of OH-PAHs, MDA, 8OHdG, and $F_{2\alpha}$-isoprostanes.

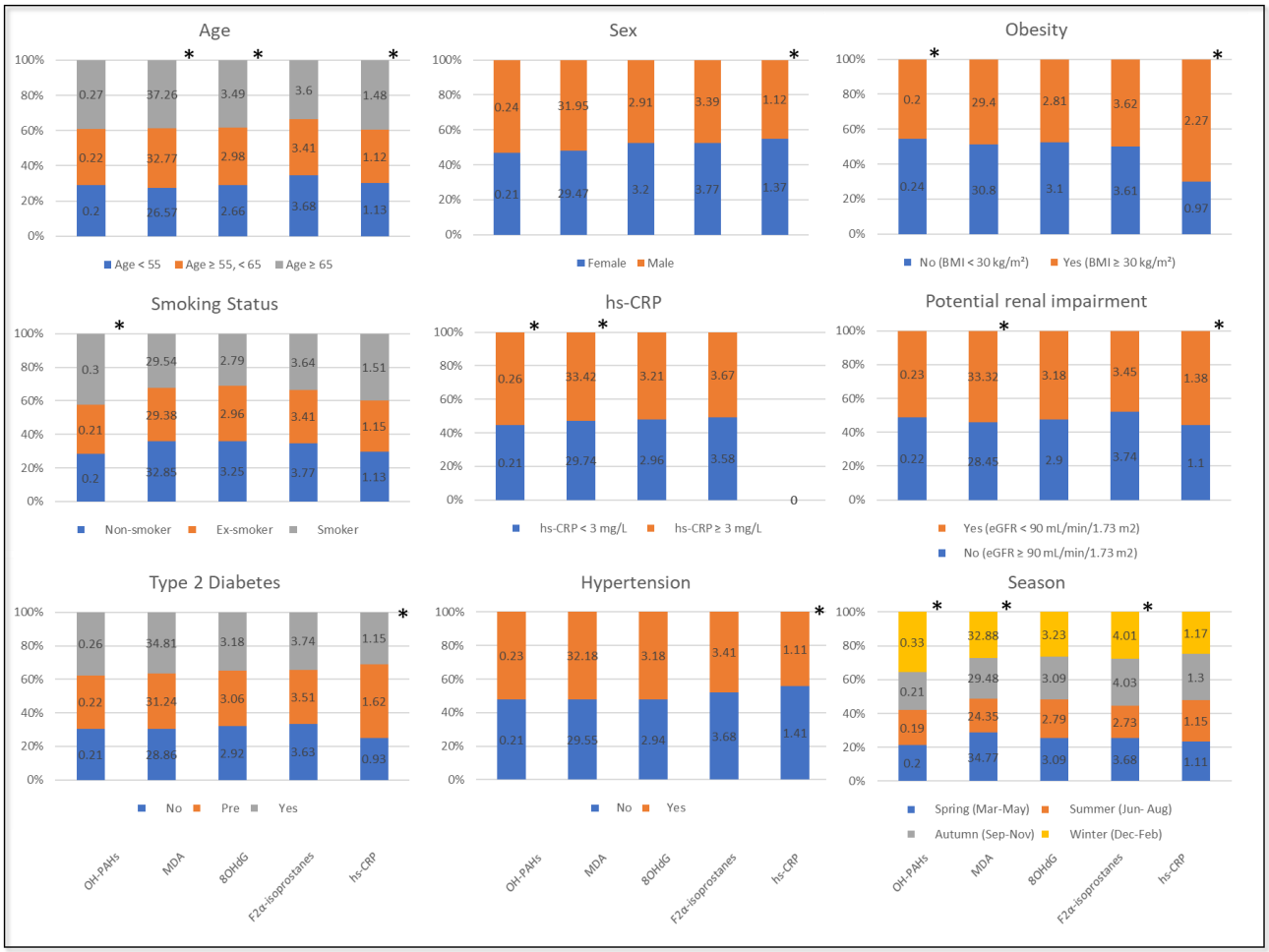

Figure 12 Kruskal–Wallis Test of OH-PAHs, oxidative stress biomarkers for different subsets of participants. (P < 0.05)*

3.4 Association between OH-PAHs, biomarkers of oxidative stress, and biomarkers of inflammation in KORA subcohort

3.4.1 Association between OH-PAHs and biomarkers of oxidative stress

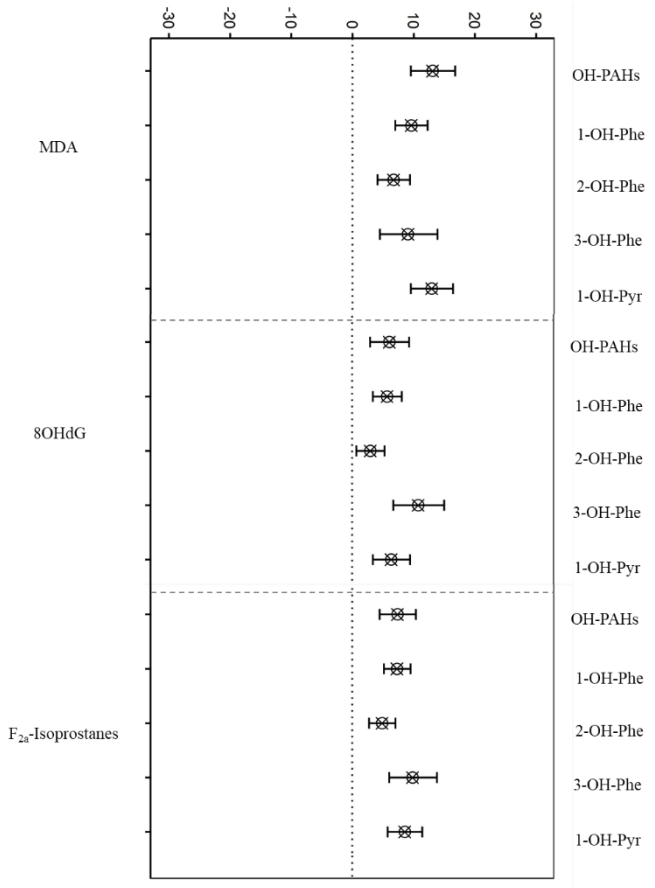

Figure 13 Percent change in biomarkers of oxidative stress (95% CI) in association with interquartile range increase of internal exposure biomarkers for the models adjusted for age, sex, smoking, trend, and season.

All OH-PAHs were significantly positively associated with oxidative stress biomarkers (Figure 13). For participants with a potential underlying state of inflammation (hs-CRP ≥ 3mg/L), we observed stronger associations between OH-PAHs and 8OHdG/$F_{2\alpha}$-isoprostanes whereas no differences were seen for MDA (figure 13).

3.4.2 Association between OH-PAHs and hs-CRP

We did not observe an association between the sum OH-PAHs or single OH-PAHs and hs-CRP (details not listed).

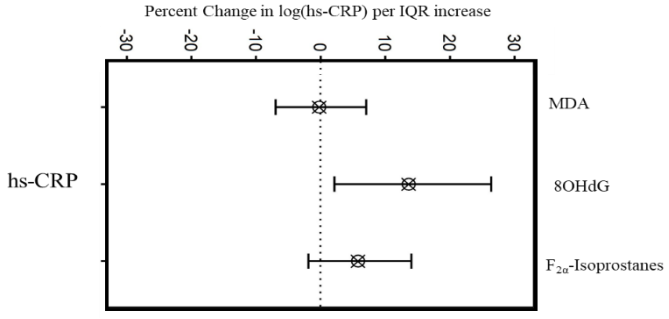

Figure 14 Percent change in hs-CRP (95% CI) in association with an interquartile range increase of oxidative stress biomarkers adjusted for age, sex, smoking, trend, and season.

3.4.3 Association between biomarkers of oxidative stress and hs-CRP

The three types of markers of oxidative stress showed quite different associations with hs-CRP. MDA was not associated at all, while 8OHdG was significantly positively associated, and $F_{2\alpha}$-isoprostanes indicated only a slight positive association.

3.5 Results of the pilot traveler study

Altogether nine volunteers who traveled to China for vacation were investigated. Samples were collected before and after the trip (S0, S1, S2, S3, and S4). Based on the outcome of the KORA cohort study, we consider $PM_{2.5}$ exposure, cigarette smoking, age, gender, and health status to be the most important factors affecting the acute oxidative stress response. Thus, all these volunteers were young, relatively "healthy", non-smoking males. For $PM_{2.5}$, the mean values of the concentrations 7 days before each sample collection were used. In most cases, Δ $PM_{2.5}$ between S0/S1 and Δ $PM_{2.5}$ between S1/S2 were mostly higher than 50 $\mu g/m^3$, which indicates that most of the volunteers were exposed to much worse air conditions during the trip. An exception was volunteer A09, for whom the difference during the trip was relatively low. Furthermore, it was recognized that volunteers A01 and A06 were exposed to severe passive cigarette smoking during the trips. In former studies, significant smoking and passive smoking were related to increased levels of MDA, 8OHdG, and $F_{2\alpha}$-isoprostane, as reported by Solak et al. [112], Yao et al. [113], and Ahmadzadehfar et al. [114]. Finally, the travel duration of volunteer A08 was much shorter than the other volunteers. Thus, the cohort for the final analysis was further refined to volunteers who 1) traveled more than 3 weeks and 2) had Δ $PM_{2.5}$ higher than 50 $\mu g/m^3$ during the last 7 days of their journey, and 3) were not exposed to cigarette smoke for further investigation (A02, A03, A04, A05, and A07).

The time trends of median values of the target substances observed from this refined cohort are shown in Figure 15**Error! Reference source not found.**. The concentration of $PM_{2.5}$ shows nearly constant and low values in the measurements after returning from their trip. The highest median concentrations of the oxidative stress biomarkers MDA (Figure 15 B), the oxidative DNA damage biomarker 8OHdG (Figure 15 C), and the polycyclic aromatic hydrocarbon exposure biomarker OH-PAHs (Figure 15 E) are found directly after returning from China (S3 samples). In contrast, for the $F_{2\alpha}$-isoprostanes (arachidonic acid oxidation biomarkers, Figure 15 D), no direct correlation is observed. This indicates that there are time-lags for $F_{2\alpha}$-isoprostanes formation or excretion, as the maximum concentrations are observed in S1, S2, or even S3.

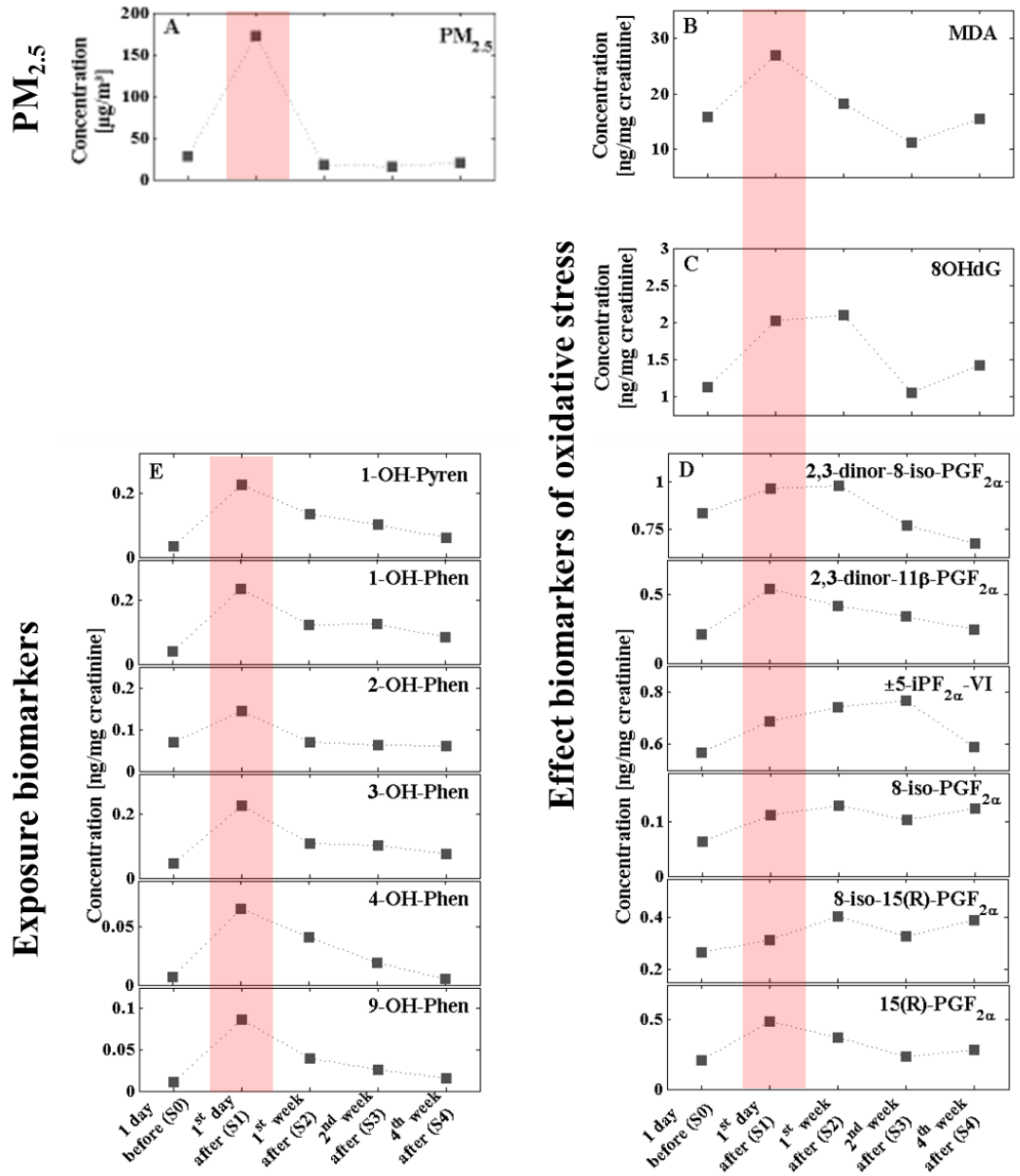

Figure 15 Time trend curves for the median values of:

A) $PM_{2.5}$-concentration;

B) Concentration of malondialdehyde, a biomarker of lipid peroxidation (oxidative stress);

C) Concentration of 8-Hydroxy-2'-deoxyguanosine, a biomarker of oxidative DNA damage (oxidative stress);

D) Concentration of $F_{2\alpha}$-isoprostanes, biomarkers of arachidonic acid oxidations (oxidative stress);

E) Concentration of hydroxylated PAHs, biomarkers of polycyclic aromatic hydrocarbon exposure in the urine of the travelers (valid cases A02, A03, A04, A05, A07) starting with before travel (S0), directly after travel (S1) and the 4 weeks after return (S2, S3, S4).

Based on the time trends of the medians, correlation coefficients were calculated and are shown in a heatmap in Figure 16. OH-PAHs are mostly associated with $F_{2\alpha}$-isoprostanes and 8OHdG.

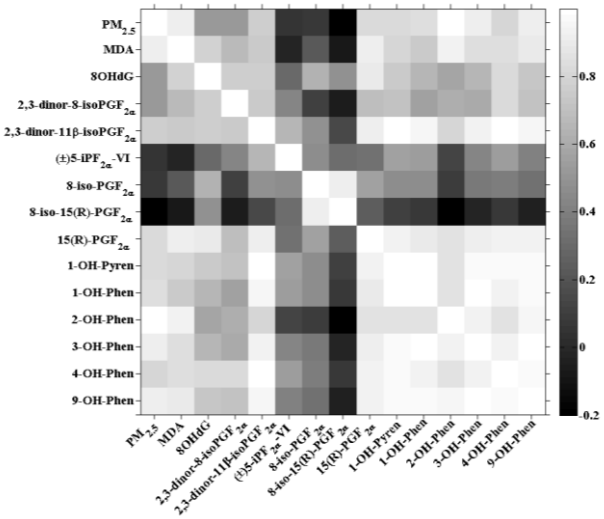

Figure 16 Heatmap of the correlation coefficient for median values of the $PM_{2.5}$-concentrations, the concentration of malondialdehyde (MDA), the concentration of 8-Hydroxy-2'-deoxyguanosine (8OHdG), the concentration of $F_{2\alpha}$-isoprostanes, and the concentration of hydroxy-polycyclic aromatic hydrocarbon (OH-PAH).

3.6 Oxysterol in B-cell positioning drives COPD

After the exposure to cigarette smoke generated from 3R4F research cigarettes at a particle concentration of 500 mg/m³ for at least 16 months, the concentration of CH25H in the bronchoalveolar lavage fluid from the female C57BL/6J mice was significantly higher than in the bronchoalveolar lavage fluid from the female C57BL/6J mice exposed to filtered air. This result indicated that cigarette smoke activated CH25H signaling in the airway epithelium may confer inducible bronchus associated lymphoid tissue formation.

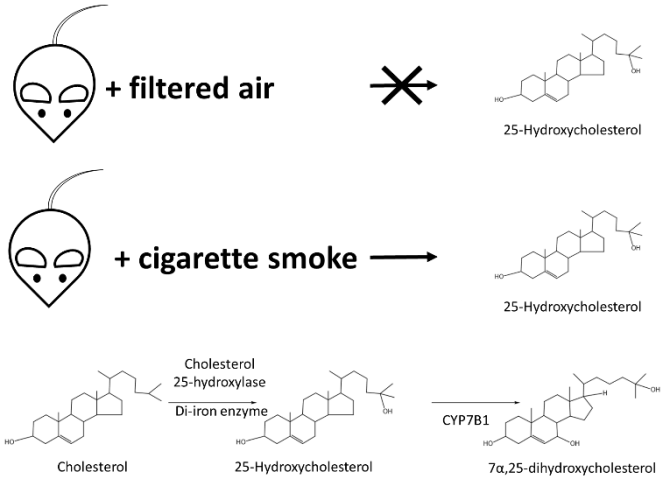

Figure 17 The role of oxysterol in B-cell positioning drives COPD

4 Discussion

Matrix effects from the constituents of the urine can strongly influence sample processing and the electrospray ionization in the way of precision, accuracy, and recovery of the method [115, 116]. The addition of isotopically labeled internal standards is necessary to overcome matrix effects and to increase reliability [117]. Individual detection methods and sample processing methods had to be developed for each compound or compound class due to the very low concentrations of the biomarkers and their different challenges. For the determination of MDA, chemical derivatization with DNPH was applied, followed by a liquid-liquid extraction to remove excessive DNPH [118]. For 8OHdG, strong matrix effects due to interfering components were observed. However, strategies such as SPE could neither improve recovery nor significantly reduce components from the interfering matrix. We thus direct

injected the diluted urine sample, in combination with the peak cutting technique. For $F_{2\alpha}$-isoprostanes, we employed an SPE technique for selective enrichment and clean-up of the substances. Method development and optimization led to three analytical methods allowing practicable, sensitive, and reliable quantification of the selected markers of oxidative stress in sample volumes below or equal to 1 mL. For serum and plasma, the challenges are even greater. The detection limits that could be reached by applying derivatization and LC-HRTOF-MS analysis were in a range between 0.05 ng and 0.2 ng on the column. Especially the concentrations levels of bronchoalveolar lavage fluid samples often were found in this range, rendering reliable quantification difficult. Although the concentrations in serum and plasma samples are higher, their sample processing revealed other problems. The protein content led to an additional, disturbing layer between hexane and the aqueous part after the saponification step. Therefore sometimes only a small part of the hexane could be used. More and over the chromatographic system as well as the electrospray source of the LC-HRTOF-MS showed fast contamination indicated by increased pressure and decreased sensitivity. Three strategies were followed to degrade the problems: Time and temperature of the saponification and denaturation steps were increased, the volume of KOH-solution was increased from 200 µl to 400 µl per sample, and the extraction volume (hexane) was increased three- and six-fold. None of these actions solved the problem meaning that the results for the protein samples must be considered carefully.

Different **instrumentations** were selected for the detection of the targeted analytes: for OH-PAHs, due to the structure of the rings, OH-PAHs have very characteristic UV absorbance spectra The absorbance bands are unique for each ring structure. For example, a set of isomers can present different UV absorbance spectrums. With such characteristic UV absorbance spectra, the detection can be easily done with a UV detector. Meanwhile, a large amount of OH-PAHs is also fluorescent. When they are excited, they can emit light with characteristic wavelengths. Thus, the detection of OH-PAHs is mostly done with a UV or fluorescence detector. For the detection of oxidative stress biomarkers, because the size of the cohort can be large including hundreds or even thousands of participants. Moreover, the concentrations of the targeted analytes are normally at a very low level even after sample enrichment. Therefore, very robust instrumentations are highly demanded. The triple quadrupole mass spectrometer has a relatively simple structure and is very robust. With the collision of parent ion and selection of the fragmented production ion, the TQMS is thus robust, sensitive, and high specificity. So, we used TQMS for the analysis of low concentrated oxidative stress biomarkers in a high sample number. The detection of cholesterols requires both high sensitivity and high resolution. For example, 25-Hydroxycholesterol and its internal standard 25-hydroxycholesterol-d_6 are large molecules showing slightly different retention times of ca. 740 s and 730 s, respectively. The high resolution of the TOF-MS allows for highly reliable identification of the target substance in real samples. However, with increasing mass resolution the application of signal-to-noise ratios for the calculation of instrument detection limits loses its validity. The insufficient sensitivity of the high resolution TOF-MS also encountered many difficulties

due to the low concentration levels of targeted analytes. The detection limits that could be reached by applying derivatization and LC-HRTOF-MS analysis were in a range between 0.05 ng and 0.2 ng on column. Especially the concentrations levels of bronchoalveolar lavage fluid samples often were found in this range, rendering reliable quantification difficult. Although the concentrations in serum and plasma samples are higher, their sample processing revealed other problems. The protein content led to an additional, disturbing layer between hexane and the aqueous part after the saponification step. Therefore sometimes only a small part of the hexane could be used. More and over the chromatographic system as well as the electrospray source of the LC-HRTOF-MS showed fast contamination indicated by increased pressure and decreased sensitivity. Three strategies were followed to degrade the problems: Time and temperature of the saponification and denaturation steps were increased, the volume of KOH-solution was increased from 200 µl to 400 µl per sample, and the extraction volume (hexane) was increased three- and six-fold. None of these actions solved the problem meaning that the results for the protein samples must be considered carefully.

In both cohorts, spot urine (KORA) samples or first void urine (traveler) samples were collected. Because the excretion ratio of creatinine is relatively constant [119], the concentration of creatinine was used in previous studies as an indicator of kidney filtration to normalize the concentration of other urinary biomarkers [68, 120, 121]. However, it should be noted that Stiegel et al. investigated 280 urine samples from 29 healthy adults and found that creatinine level is inversely related to urinary excretion rate (r^2=0.6858). But more than 30% of creatinine variance is from sources beyond dilution/hydration [122]. In future studies, cautious consideration should be taken when using creatinine correction. A 24-h complete urine collection will be a more accurate solution with more reliable information. In this study, spot sample collection was nevertheless employed because it is less time-consuming and more convenient for volunteers.

In the cross-sectional KORA cohort, biomarkers of PAHs exposure, oxidative stress, and inflammation were determined to investigate the interplay in between. The concentrations of OH-PAHs were comparatively low in our study. A study carried out among 300 participants from 7 Asian countries reported the mean concentrations of 2-OH-Phe, 3-OH-Phe, and 1-OH-Pyr ranged between 0.07 – 0.58 ng/mL, 0.10 – 0.71 ng/mL, and 0.17 – 0.67 ng/mL respectively [123] while in our study, the mean concentrations were 0.09, 0.11, and 0.35 ng/mL respectively (before normalized by urinary creatinine).

The concentrations of the biomarkers of oxidative stress and inflammation were higher in older participants (MDA, 8OHdG, and hs-CRP), obesity (hs-CRP), potential underlying inflammation (MDA), potential renal impairment (MDA and hs-CRP), as well as in participants with diagnosed diseases like type 2 diabetes (hs-CRP) or hypertension (hs-CRP), or for participants who had their clinical visit in autumn and winter (MDA and 8OHdG).

4.1 Health profiles

Sex: We observed lower concentrations of $F_{2\alpha}$-isoprostanes in men than in women. Similarly, a study from the U.S examining 65 participants (19 male, 46 female; 38.6 ± 11.1 years old) found higher concentrations of $F_{2\alpha}$-isoprostanes in females [124]. Such different concentration levels in males and females may be caused by the different content of lean body mass, and bone mineral content in male and female participants [124].

Age: Many studies suggest that free radicals play an important role in aging [125-127]. In our study, biomarkers of ROS damage were MDA and 8OHdG. Their concentrations were also higher in the older groups (between 55 to 65 and older than 65 years). The reason could be that organism aging accumulates oxidative damage generated by ROS.

Smoking: Huge amounts of PAHs are content in cigarette smoke [128]. After intake of such a high abundance of PAHs, the group of smokers showed the highest level of PAHs metabolites in urine. Similarly, a cohort study among 388 participants (288 non-smokers and 100 smokers) found highly significant differences between these two groups of participants and dose-response relationships concerning cigarettes smoked per day for 2-, 3- and 4-OH-Phe and 1-OH-Pyr [129]. Moreover, researchers found significant correlations between urinary OH-PAH levels and cigarette smoking among 4092 participants in China [130].

Obesity and chronic diseases: Higher concentrations of hs-CRP were observed in participants with obesity, CKD, diabetes, and hypertension indicating an underlying inflammatory state. Two studies compared patients with different stages of CKD with control groups and found higher oxidative stress levels and inflammation in CKD patients [131, 132]. Similarly, we observed higher concentrations of MDA, 8OHdG, and hs-CRP in participants with CKD as well as an indication for $F_{2\alpha}$-isoprostanes. A study across 80 participants reported that hypertension may increase the level of hs-CRP [133] which matches our observation. Two studies among a cohort of North Indians and a cohort of African Americans both found that higher concentrations of hs-CRP were associated with diabetes or, to a lesser degree, insulin resistance [134, 135].

Season: Significantly higher OH-PAHs levels were observed in urine samples collected during the heating seasons. Studies carried out in Europe and China in recent years monitored the atmospheric PAHs and reported similar seasonal variations. Different source contributions between the heating season and the non-heating season were suggested to be the main reason [136, 137]. Moreover, Li et al. monitored the atmospheric PAHs in the Augsburg region (Germany) between 2014 – 2015 and suggested that biomass burning for domestic heating during autumn and winter was the major contributor [138]. This observation matched our results of the seasonal OH-PAHs changes 1) indicating that ambient PAHs might be an important source of PAHs intake; 2) suggesting the levels of oxidative stress markers (MDA and $F_{2\alpha}$-isoprostanes) were significantly higher in samples taken in the heating

season, which may also be related to increased ambient PAHs pollution. Both short- and long-term studies suggested higher concentrations of OH-PAHs, and increased oxidative stress biomarkers could be detected after exposure to ambient pollutants [139-141].

4.2 Associations

Two studies from the USA and Japan investigated the association between selected oxidative stress markers (MDA, 8OHdG, and $F_{2\alpha}$-isoprostanes) and OH-PAHs among two smaller cohorts [76, 141]. Ferguson et al. reported that some PAHs metabolites showed consistent positive associations with the urinary oxidative stress markers (8OHdG and 8-isoprostane) after investigating urine samples from 200 pregnant women in the United States. Bortey-Sam et al. analyzed the urine samples collected from 202 residents in Kumasi, Japan, and found significant positive correlations between the sum OH-PAHs, 2-OH-Nap, 2-3-OH-fluorenes, and MDA and a positive correlation between 4-OH-Phe and 8OHdG. These findings matched our study, in which all examined oxidative stress markers showed positive associations with OH-PAHs.

In our study, more pronounced associations were found in participants with potential underlying systematic inflammation between OH-PAHs and 8OHdG as well as $F_{2\alpha}$-isoprostanes, whereas no difference was seen for MDA. This finding indicates that oxidative stress is deteriorated, or is promoted by systematic inflammation. Biswas et al. found that the inflammation process not only can produce reactive species, but also exaggerate the generation of reactive species [142]. Similarly, other underlying long-term risk factor profiles associated with obesity, diabetes, or CKD, may be responsible for increased levels of oxidative stress, as suggested by our data.

Positive associations between urinary OH-PAHs concentrations and hs-CRP were also observed in the same study by Ferguson et al. [76]. A study carried out among 999 participants of the National Health and Nutrition Examination Survey (NHANES) in 2003-2004 also found positive associations in groups with medium (concentrations of 2-PH-Phe between low and high) and high levels of 2-OH-Phe and 9-hydroxyfluorene. No association could be observed in the group with lower levels of 2-OH-Phe, and 9-hydroxyfluorene [69]. In our study, we observed no or only slight indications for an association between OH-PAHs and hs-CRP. Compared to the study carried out in 7 Asian countries [123], the KORA cohort was exposed to relatively low levels of PAHs exposure. Thus, we can conclude that acute low-level PAHs exposure was associated with only limited increase in hs-CRP. For long-term exposure, however, we observed significant positive associations between long-term exposure to ambient air pollution and hs-CRP in our previous KORA FF4 study across the full sample of 2252 participants [71].

It has been shown that ROS plays an important role in the signaling of inflammatory responses [4]. In our study with comparable low OH-PAHs concentrations, 8OHdG was still significantly positively associated with hs-CRP while MDA and $F_{2\alpha}$-isoprostanes showed no or only a slight positive association. From non-enzymatic and free radical-mediated oxidations MDA[59] and $F_{2\alpha}$-isoprostanes

[62, 63] are generated. Yet the generation of 8OHdG is enzymatical during DNA impairment and repairing [60]. In the continuum of oxidative stress and antioxidation described by Peters et al. [4], MDA and $F_{2\alpha}$-isoprostanes could be generated through all phases, while 8OHdG is mostly generated in the later phases of e.g. inflammation and cell death when ROS exceeds antioxidation.

However, there were some limitations of this KORA cohort: First, it was a cross-sectional cohort study and the samples were collected only at one single time point through 2013 – 2014; second, the cohort was exposed to relatively low concentrations of air pollutants for a long period. Thus, we proposed a concept that uses traveler models for longitudinal PM pollution-induced acute health effects study and carried out the pilot study. In the pilot study, we observed decreasing trends of biomarkers and high levels of associations. Similar to our observations from the KORA cohort, associations between exposure ($PM_{2.5}$ or PAHs), $F_{2\alpha}$-isoprostanes, and MDA were found. It took 2-4 weeks for most of the biomarkers to clear the decreasing trends while the downtrends of OH-PAHs lasted for only 1-2 weeks till achieving pre-travel values. Similar trends of urinary OH-PAH concentrations were also observed by Lin et al. after investigating 10 students who traveled between China and the USA [143] and by Thai et al. after analyzing urine samples of a family which traveled between Vietnam and Australia [144]. This indicates, as reported [145], a faster removal pathway from the organism, for PAH. The differences in the $PM_{2.5}$ concentrations between China and Germany match the overall increasing (S0 and S1) and decreasing (S1 to S4) trends of oxidative stress biomarkers and PAH metabolites although the patterns of $F_{2\alpha}$-isoprostanes and 8OHdG varied. Such findings match the outcome from the KORA cohort: The pathways and excretions varied between the three types of biomarkers of oxidative. Allen et al. exposed 10 volunteers to air with a high $PM_{2.5}$ concentration ($205.3\pm6.2\ \mu g/m^3$) for 2 hours, and no significant variations of $F_{2\alpha}$-isoprostanes or 8OHdG concentrations were observed in the next 1.5h, 3 h, 6 h, 12 h, and 22 h after exposure [146]. We suppose that there is a lag between the exposure and the yield of $F_{2\alpha}$-isoprostanes/ 8OHdG, which can be even one or two weeks long, due to the differences in pathways while MDA was generated much faster after the exposure. This is also supported by the results of Lin et al.: before and during the 2008 Beijing Olympic Games, associations between air pollutants and 8OHdG/ MDA were investigated. Their results showed the fast response of pollutants/ MDA while lags were found between pollutants and 8OHdG [147].

5 Conclusion

As one of the top reasons for worldwide mortality, ambient air pollution is an issue for global public health. It is important to monitor the exposure and investigate the health effects. However, the great diversity in combinations of source, composition, and metabolic pathways makes direct evaluation of exposure burden very critical to achieve.

Therefore, the strategy biomarker monitoring was used: (1) OH-PAHs, biomarkers of PAHs, were selected as indexes for the individual external exposure levels. (2) MDA, a by-product from the attack

of the ROS species to PUFA. 8OHdG, a product during ROS caused DNA damage and repairing and $F_{2\alpha}$-isoprostanes, a series of compounds produced when ROS attacking membrane phospholipids were selected as urinary biomarkers for oxidative stress. (3) Hs-CRP was selected to monitor the potential systematic inflammation. In addition, cholesterols were determined from biological samples in mice to better understand the pathway of cigarette smoke induced COPD.

Different LC-MS instrumentations were established to analyze all these analytes. For example, due to the very low concertation levels of oxidative stress biomarkers and the very high total number of samples, a triple quadrupole mass spectrometer was used which benefits from the simple structure, robustness, and high sensitivity. Due to the low concentration and special features of isotopically labeled standards of oxysterols, the ultra high resolution time of flight mass spectrometer was used for the measurement of cholesterols because the flight path of the ions can be very long in such mass spectrometer which provides the extremely high resolution for both large and small molecules.

A cohort in the Augsburg region was selected to investigate the health effects caused by exposing to external air pollution. Associations between concentrations of OH-PAHs and oxidative stress were observed. Higher concentrations of oxidative stress biomarkers were found in participants with health profiles such as higher age, smoking habits, obesity, and chronic diseases. Also, we found the concentration of hs-CRP was positively associated with the concentration of 8OHdG. The results of the KORA cross-sectional cohort study suggested relationships between exposure to PAHs, oxidative stress, and health profiles. To compensate for the setup of this cohort, we proposed to use travellers as models to investigate the acute health effects which related to air pollution. The results from the pilot study proved the concept that travellers are ideal for studying the acute exposure induced health effects.

In addition to human studies, animal models are important for investigating the pathological development of air pollution exposure induced diseases and for understanding the pathways. The very high resolution mass spectrometer is proven to be a very powerful tool for determining targeted large metabolites for example the oxysterols in present work.

Overall, our study investigated the air pollution induced health effects in a comprehensive way which provides both ideal tools and information for future studies.

6 Reference

1. Xu, J., et al., Photochemical impacts on the toxicity of PM2.5. Critical Reviews in Environmental Science and Technology, 2022. 52(1): p. 130-156.

2. Kroll, J.H. and J.H. Seinfeld, Chemistry of secondary organic aerosol: Formation and evolution of low-volatility organics in the atmosphere. Atmospheric Environment, 2008. 42(16): p. 3593-3624.

3. Health-Effects-Institute, State of Global Air 2017. Special Report, 2017.

4. Peters, A., T.S. Nawrot, and A.A. Baccarelli, Hallmarks of environmental insults. Cell, 2021. 184(6): p. 1455-1468.

5. Cohen, A.J., et al., Estimates and 25-year trends of the global burden of disease attributable to ambient air pollution: an analysis of data from the Global Burden of Diseases Study 2015. The Lancet, 2017. 389(10082): p. 1907-1918.

6. Cohen, A.J., et al., Estimates and 25-year trends of the global burden of disease attributable to ambient air pollution: an analysis of data from the Global Burden of Diseases Study 2015. Lancet, 2017. 389(10082): p. 1907-1918.

7. European-Environment-Agency, Air quality in Europe 2018 report. European Environment Agency, 2018.

8. Manisalidis, I., et al., Environmental and Health Impacts of Air Pollution: A Review. 2020. 8.

9. Riediker, M., et al., Particle toxicology and health - where are we? Particle and Fibre Toxicology, 2019. 16(1): p. 19.

10. Kelly, F.J. and J.C. Fussell, Size, source and chemical composition as determinants of toxicity attributable to ambient particulate matter. Atmospheric Environment, 2012. 60: p. 504-526.

11. Ohara, T., et al., An Asian emission inventory of anthropogenic emission sources for the period 1980-2020. Atmospheric Chemistry and Physics, 2007. 7(16): p. 4419-4444.

12. Liu, X., et al., Air pollution in Germany: Spatio-temporal variations and their driving factors based on continuous data from 2008 to 2018. Environmental Pollution, 2021. 276: p. 116732.

13. Schwartz, J. and S. Zeger, Passive smoking, air pollution, and acute respiratory symptoms in a diary study of student nurses. Am Rev Respir Dis, 1990. 141(1): p. 62-7.

14. Norback, D., et al., Volatile organic compounds (VOC), formaldehyde and nitrogen dioxide (NO2) in schools in Johor Bahru, Malaysia: Associations with rhinitis, ocular, throat and dermal symptoms, headache and fatigue. Sci Total Environ, 2017. 592: p. 153-160.

15. Gauderman, W.J., et al., Childhood asthma and exposure to traffic and nitrogen dioxide. Epidemiology, 2005. 16(6): p. 737-43.

16. Gehring, U., et al., Air pollution exposure and lung function in children: the ESCAPE project. Environ Health Perspect, 2013. 121(11-12): p. 1357-64.

17. Ghanbari Ghozikali, M., et al., Evaluation of Chronic Obstructive Pulmonary Disease (COPD) attributed to atmospheric O3, NO2, and SO2 using Air Q Model (2011-2012 year). Environmental Research, 2016. 144: p. 99-105.

18. Lu, Z., Q. Zhang, and D.G. Streets, Sulfur dioxide and primary carbonaceous aerosol emissions in China and India, 1996-2010. Atmospheric Chemistry and Physics, 2011. 11(18): p. 9839-9864.

19. Iwasawa, S., et al., Effects of SO2 on respiratory system of adult Miyakejima resident 2 years after returning to the island. J Occup Health, 2009. 51(1): p. 38-47.

20. Rosser, F., et al., Annual SO2 exposure, asthma, atopy, and lung function in Puerto Rican children. Pediatr Pulmonol, 2020. 55(2): p. 330-337.

21. Faridi, S., et al., Long-term trends and health impact of PM2.5 and O3 in Tehran, Iran, 2006–2015. Environment International, 2018. 114: p. 37-49.

22. Sicard, P., et al., Effect of O3, PM10 and PM2.5 on cardiovascular and respiratory diseases in cities of France, Iran and Italy. Environmental Science and Pollution Research, 2019. 26(31): p. 32645-32665.

23. Huang, R.-J., et al., High secondary aerosol contribution to particulate pollution during haze events in China. Nature, 2014. 514(7521): p. 218-222.

24. Xu, L., et al., Anthropogenic Effects on Biogenic Secondary Organic Aerosol Formation. Advances in Atmospheric Sciences, 2021. 38(7): p. 1053-1084.

25. Mahilang, M., M.K. Deb, and S. Pervez, Biogenic secondary organic aerosols: A review on formation mechanism, analytical challenges and environmental impacts. Chemosphere, 2021. 262: p. 127771.

26. Kesselmeier, J. and M.J.J.o.A.C. Staudt, Biogenic Volatile Organic Compounds (VOC): An Overview on Emission, Physiology and Ecology. 1999. 33: p. 23-88.

27. Went, F.W., Blue Hazes in the Atmosphere. Nature, 1960. 187(4738): p. 641-643.

28. Odum, J.R., et al., Aromatics, Reformulated Gasoline, and Atmospheric Organic Aerosol Formation. Environmental Science & Technology, 1997. 31(7): p. 1890-1897.

29. Goldan, P.D., et al., Hydrocarbon measurements in the southeastern United States: The Rural Oxidants in the Southern Environment (ROSE) Program 1990. 1995. 100: p. 25945-25963.

30. Sagebiel, J.C., et al., Real-world emissions and calculated reactivities of organic species from motor vehicles. Atmospheric Environment, 1996. 30(12): p. 2287-2296.

31. Keyte, I.J., R.M. Harrison, and G. Lammel, Chemical reactivity and long-range transport potential of polycyclic aromatic hydrocarbons--a review. Chem Soc Rev, 2013. 42(24): p. 9333-91.

32. Kamal, A., et al., PAH exposure and oxidative stress indicators of human cohorts exposed to traffic pollution in Lahore city (Pakistan). Chemosphere, 2015. 120: p. 59-67.

33. VanRooij, J.G., et al., Absorption of polycyclic aromatic hydrocarbons through human skin: differences between anatomical sites and individuals. J Toxicol Environ Health, 1993. 38(4): p. 355-68.

34. Andersen, M.H.G., et al., Assessment of polycyclic aromatic hydrocarbon exposure, lung function, systemic inflammation, and genotoxicity in peripheral blood mononuclear cells from firefighters before and after a work shift. Environmental and Molecular Mutagenesis, 2018. 59(6): p. 539-548.

35. Kouassi, Y.M., et al., Acute exposure to creosote vapors in a company of the electricity sector in Abidjan. Archives Des Maladies Professionnelles Et De L Environnement, 2016. 77(2): p. 186-191.

36. Al-Delaimy, W.K., C.W. Larsen, and K. Pezzoli, Differences in Health Symptoms among Residents Living Near Illegal Dump Sites in Los Laureles Canyon, Tijuana, Mexico: A Cross Sectional Survey. International Journal of Environmental Research and Public Health, 2014. 11(9): p. 9532-9552.

37. Yang, L., et al., Polycyclic aromatic hydrocarbons are associated with increased risk of chronic obstructive pulmonary disease during haze events in China. Sci Total Environ, 2017. 574: p. 1649-1658.

38. Cao, L., et al., Polycyclic aromatic hydrocarbon exposure and atherosclerotic cardiovascular disease risk in urban adults: The mediating role of oxidatively damaged DNA. Environ Pollut, 2020. 265(Pt A): p. 114860.

39. Alshaarawy, O., H.A. Elbaz, and M.E. Andrew, The association of urinary polycyclic aromatic hydrocarbon biomarkers and cardiovascular disease in the US population. Environ Int, 2016. 89-90: p. 174-8.

40. Kubo, T., et al., Seasonal Fluctuation of Polycyclic Aromatic Hydrocarbons and Aerosol Genotoxicity in Long-Range Transported Air Mass Observed at the Western End of Japan. International Journal of Environmental Research and Public Health, 2020. 17(4): p. 15.

41. McCarrick, S., et al., In vitro and in vivo genotoxicity of oxygenated polycyclic aromatic hydrocarbons. Environmental Pollution, 2019. 246: p. 678-687.

42. Kumar, A., et al., Characteristics, toxicity, source identification and seasonal variation of atmospheric polycyclic aromatic hydrocarbons over East India. Environmental Science and Pollution Research, 2020. 27(1): p. 678-690.

43. Danielsen, P.H., et al., Oxidative Stress, DNA Damage, and Inflammation Induced by Ambient Air and Wood Smoke Particulate Matter in Human A549 and THP-1 Cell Lines. Chemical Research in Toxicology, 2011. 24(2): p. 168-184.

44. Lan, Q., et al., Oxidative damage-related genes AKR1C3 and OGG1 modulate risks for lung cancer due to exposure to PAH-rich coal combustion emissions. Carcinogenesis, 2004. 25(11): p. 2177-2181.

45. Lu, S.Y., et al., Associations between polycyclic aromatic hydrocarbon (PAH) exposure and oxidative stress in people living near e-waste recycling facilities in China. Environment International, 2016. 94: p. 161-169.

46. Xue, W. and D. Warshawsky, Metabolic activation of polycyclic and heterocyclic aromatic hydrocarbons and DNA damage: a review. Toxicol Appl Pharmacol, 2005. 206(1): p. 73-93.

47. Ewa, B. and M. Danuta, Polycyclic aromatic hydrocarbons and PAH-related DNA adducts. J Appl Genet, 2017. 58(3): p. 321-330.

48. Guengerich, F.P., Cytochrome p450 and chemical toxicology. Chem Res Toxicol, 2008. 21(1): p. 70-83.

49. Apel, K. and H. Hirt, REACTIVE OXYGEN SPECIES: Metabolism, Oxidative Stress, and Signal Transduction. Annual Review of Plant Biology, 2004. 55(1): p. 373-399.

50. Tao, F., B. Gonzalez-Flecha, and L. Kobzik, Reactive oxygen species in pulmonary inflammation by ambient particulates. Free Radical Biology and Medicine, 2003. 35(4): p. 327-340.

51. Risom, L., P. Moller, and S. Loft, Oxidative stress-induced DNA damage by particulate air pollution. Mutat Res, 2005. 592(1-2): p. 119-37.

52. Droge, W., Free radicals in the physiological control of cell function. Physiol Rev, 2002. 82(1): p. 47-95.

53. Taverne, Y.J., et al., Reactive oxygen species and the cardiovascular system. Oxid Med Cell Longev, 2013. 2013: p. 862423.

54. McCord, J.M., Human disease, free radicals, and the oxidant/antioxidant balance. Clinical Biochemistry, 1993. 26(5): p. 351-357.

55. Mesquita, S.R., et al., Toxic assessment of urban atmospheric particle-bound PAHs: relevance of composition and particle size in Barcelona (Spain). Environ Pollut, 2014. 184: p. 555-62.

56. Aquilina, N.J., et al., Environmental and biological monitoring of exposures to PAHs and ETS in the general population. Environ Int, 2010. 36(7): p. 763-71.

57. Urbancova, K., et al., Evaluation of 11 polycyclic aromatic hydrocarbon metabolites in urine of Czech mothers and newborns. Science of The Total Environment, 2017. 577: p. 212-219.

58. Chen, J.L., et al., Determination of urinary malondialdehyde by isotope dilution LC-MS/MS with automated solid-phase extraction: a cautionary note on derivatization optimization. Free Radic Biol Med, 2011. 51(9): p. 1823-9.

59. Ayala, A., M.F. Muñoz, and S. Argüelles, Lipid Peroxidation: Production, Metabolism, and Signaling Mechanisms of Malondialdehyde and 4-Hydroxy-2-Nonenal. Oxidative Medicine and Cellular Longevity, 2014. 2014: p. 360438.

60. Evans, M.D., M. Saparbaev, and M.S. Cooke, DNA repair and the origins of urinary oxidized 2'-deoxyribonucleosides. Mutagenesis, 2010. 25(5): p. 433-42.

61. Valavanidis, A., T. Vlachogianni, and C. Fiotakis, 8-hydroxy-2' -deoxyguanosine (8-OHdG): A Critical Biomarker of Oxidative Stress and Carcinogenesis. Journal of Environmental Science and Health Part C-Environmental Carcinogenesis & Ecotoxicology Reviews, 2009. 27(2): p. 120-139.

62. Morrow, J.D. and L.J. Roberts, The isoprostanes - Current knowledge and directions for future research. Biochemical Pharmacology, 1996. 51(1): p. 1-9.

63. Milne, G.L., H.Y. Yin, and J.D. Morrow, Human biochemistry of the isoprostane pathway. Journal of Biological Chemistry, 2008. 283(23): p. 15533-15537.

64. Galano, J.M., et al., Isoprostanes, neuroprostanes and phytoprostanes: An overview of 25 years of research in chemistry and biology. Progress in Lipid Research, 2017. 68: p. 83-108.

65. Ayala, A., M.F. Munoz, and S. Arguelles, Lipid peroxidation: production, metabolism, and signaling mechanisms of malondialdehyde and 4-hydroxy-2-nonenal. Oxid Med Cell Longev, 2014. 2014: p. 360438.

66. Klein, J.C., et al., REPAIR AND REPLICATION OF PLASMIDS WITH SITE-SPECIFIC 8-OXODG AND 8-AAFDG RESIDUES IN NORMAL AND REPAIR-DEFICIENT HUMAN-CELLS. Nucleic Acids Research, 1992. 20(17): p. 4437-4443.

67. Dizdaroglu, M., Oxidatively induced DNA damage: Mechanisms, repair and disease. Cancer Letters, 2012. 327(1-2): p. 26-47.

68. Morrow, J.D., et al., A series of prostaglandin F2-like compounds are produced in vivo in humans by a non-cyclooxygenase, free radical-catalyzed mechanism. Proc Natl Acad Sci U S A, 1990. 87(23): p. 9383-7.

69. Everett, C.J., et al., Association of urinary polycyclic aromatic hydrocarbons and serum C-reactive protein. Environmental Research, 2010. 110(1): p. 79-82.

70. Hennig, F., et al., Association between Source-Specific Particulate Matter Air Pollution and hs-CRP: Local Traffic and Industrial Emissions. Environmental Health Perspectives, 2014. 122(7): p. 703-710.

71. Pilz, V., et al., C-reactive protein (CRP) and long-term air pollution with a focus on ultrafine particles. Int J Hyg Environ Health, 2018. 221(3): p. 510-518.

72. Chuang, K.-J., et al., The Effect of Urban Air Pollution on Inflammation, Oxidative Stress, Coagulation, and Autonomic Dysfunction in Young Adults. American Journal of Respiratory and Critical Care Medicine, 2007. 176(4): p. 370-376.

73. Pope, C.A., 3rd, et al., Exposure to Fine Particulate Air Pollution Is Associated With Endothelial Injury and Systemic Inflammation. Circ Res, 2016. 119(11): p. 1204-1214.

74. Farzan, S.F., et al., Urinary polycyclic aromatic hydrocarbons and measures of oxidative stress, inflammation and renal function in adolescents: NHANES 2003-2008. Environmental Research, 2016. 144: p. 149-157.

75. Clark, J.D., et al., Exposure to polycyclic aromatic hydrocarbons and serum inflammatory markers of cardiovascular disease. Environmental Research, 2012. 117: p. 132-137.

76. Ferguson, K.K., et al., Urinary Polycyclic Aromatic Hydrocarbon Metabolite Associations with Biomarkers of Inflammation, Angiogenesis, and Oxidative Stress in Pregnant Women. Environmental Science & Technology, 2017. 51(8): p. 4652-4660.

77. Moyron-Quiroz, J.E., et al., Role of inducible bronchus associated lymphoid tissue (iBALT) in respiratory immunity. Nature Medicine, 2004. 10(9): p. 927-934.

78. Hwang, J.Y., T.D. Randall, and A. Silva-Sanchez, Inducible bronchus-associated lymphoid tissue: Taming inflammation in the lung. Frontiers in Immunology, 2016. 7(JUN).

79. Hannedouche, S., et al., Oxysterols direct immune cell migration via EBI2. Nature, 2011. 475(7357): p. 524-7.

80. Li, J., et al., EBI2 augments Tfh cell fate by promoting interaction with IL-2-quenching dendritic cells. Nature, 2016. 533(7601): p. 110-114.

81. Holle, R., et al., KORA--a research platform for population based health research. Gesundheitswesen, 2005. 67 Suppl 1: p. S19-25.

82. Liška, I., J. Krupčíik, and P.A. Leclercq, The use of solid sorbents for direct accumulation of organic compounds from water matrices–a review of solid-phase extraction techniques. Journal of High Resolution Chromatography, 1989. 12(9): p. 577-590.

83. Kanu, A.B., Recent developments in sample preparation techniques combined with high-performance liquid chromatography: A critical review. Journal of Chromatography A, 2021. 1654.

84. Kuklenyik, Z., et al., Automated solid-phase extraction approaches for large scale biomonitoring studies. Journal of Chromatographic Science, 2009. 47(1): p. 12-18.

85. Boos, K.S., J. Lintelmann, and A. Kettrup, Coupled-column high-performance liquid chromatographic method for the determination of 1-hydroxypyrene in urine of subjects exposed to polycyclic aromatic hydrocarbons. Journal of Chromatography A, 1992. 600(2): p. 189-194.

86. Alberti, S., A. Gladfelter, and T. Mittag, Considerations and Challenges in Studying Liquid-Liquid Phase Separation and Biomolecular Condensates. Cell, 2019. 176(3): p. 419-434.

87. Chemat, F., M.A. Vian, and G. Cravotto, Green extraction of natural products: Concept and principles. International Journal of Molecular Sciences, 2012. 13(7): p. 8615-8627.

88. Nesterenko, P.N. and M.D. Palamareva, Liquid chromatography | Overview, in Encyclopedia of Analytical Science. 2019. p. 174-181.

89. Buszewski, B. and S. Noga, Hydrophilic interaction liquid chromatography (HILIC)--a powerful separation technique. Analytical and bioanalytical chemistry, 2012. 402(1): p. 231-247.

90. Lawrence, J.F., Determination of environmental contaminants in foods by liquid chromatography - an overview. International Journal of Environmental Analytical Chemistry, 1992. 49(1-2): p. 15-29.

91. Yost, R.A. and C.G. Enke, Selected Ion Fragmentation with a Tandem Quadrupole Mass Spectrometer. Journal of the American Chemical Society, 1978. 100(7): p. 2274-2275.

92. Agüera, A., M.d.M.G. Ramos, and A.R. Fernández-Alba, Chapter 2 - Chemical Evaluation of Water Treatment Processes by LC–(Q)TOF-MS: Identification of Transformation Products, in Comprehensive Analytical Chemistry, A.R. Fernandez-Alba, Editor. 2012, Elsevier. p. 61-109.

93. Wiley, W.C. and I.H. McLaren, Time-of-flight mass spectrometer with improved resolution. Review of Scientific Instruments, 1955. 26(12): p. 1150-1157.

94. Cornett, D.S., et al., Reflectron time-of-flight mass spectrometer for laser photodissociation. Review of Scientific Instruments, 1992. 63(4): p. 2177-2186.

95. Willis, P., J. Jaloszynski, and V. Artaev, Improving duty cycle in the Folded Flight Path high-resolution time-of-flight mass spectrometer. International Journal of Mass Spectrometry, 2021. 459.

96. Borchers, C., et al. Preliminary comparison of precursor scans and liquid chromatography-tandem mass spectrometry on a hybrid quadrupole time-of-flight mass spectrometer. in Journal of Chromatography A. 1999.

97. Mühlberger, F., et al., Comprehensive on-line characterization of complex gas mixtures by quasi-simultaneous resonance-enhanced multiphoton ionization, vacuum-UV single-photon ionization, and electron impact ionization in a time-of-flight mass spectrometer: Setup and instrument characterization. Analytical Chemistry, 2004. 76(22): p. 6753-6764.

98. Aiken, A.C., P.F. DeCarlo, and J.L. Jimenez, Elemental analysis of organic species with electron ionization high-resolution mass spectrometry. Analytical Chemistry, 2007. 79(21): p. 8350-8358.

99. Andrade, F.J., et al., Atmospheric pressure chemical ionization source. 1. Ionization of compounds in the gas phase. Analytical Chemistry, 2008. 80(8): p. 2646-2653.

100. Robb, D.B., T.R. Covey, and A.P. Bruins, Atmospheric pressure photoionization: An ionization method for liquid chromatography-mass spectrometry. Analytical Chemistry, 2000. 72(15): p. 3653-3659.

101. Fenn, J.B., et al., Electrospray ionization–principles and practice. Mass Spectrometry Reviews, 1990. 9(1): p. 37-70.

102. Levey, A.S., et al., A new equation to estimate glomerular filtration rate. Ann Intern Med, 2009. 150(9): p. 604-12.

103. Kumar, N., et al., Chemometrics tools used in analytical chemistry: An overview. Talanta, 2014. 123: p. 186-199.

104. Schober, P. and L.A. Schwarte, Correlation coefficients: Appropriate use and interpretation. Anesthesia and Analgesia, 2018. 126(5): p. 1763-1768.

105. Rice, J.A., Mathematical Statistics and Data Analysis, Third Edition. 2005.

106. Chan, Y. and R.P. Walmsley, Learning and understanding the Kruskal-Wallis one-way analysis-of- variance-by-ranks test for differences among three or more independent groups. Physical Therapy, 1997. 77(12): p. 1755-1762.

107. Draper, N.R. and H. Smith, Applied regression analysis. Applied Regression Analysis. 2014. 1-716.

108. Wu, J., Study applicable for multi-linear regression analysis and logistic regression analysis. Open Electrical and Electronic Engineering Journal, 2014. 8: p. 782-786.

109. Inker, L.A., et al., Estimating glomerular filtration rate from serum creatinine and cystatin C. N Engl J Med, 2012. 367(1): p. 20-9.

110. Yang, Q., et al., Polycyclic aromatic hydrocarbon (PAH) exposure and oxidative stress for a rural population from the North China Plain. Environ Sci Pollut Res Int, 2015. 22(3): p. 1760-9.

111. Wood, S.N., Low-rank scale-invariant tensor product smooths for generalized additive mixed models. Biometrics, 2006. 62(4): p. 1025-36.

112. Solak, Z.A., et al., Effect of different levels of cigarette smoking on lipid peroxidation, glutathione enzymes and paraoxonase 1 activity in healthy people. Clinical and Experimental Medicine, 2005. 5(3): p. 99-105.

113. Yao, Q.H., et al., Determination of urinary oxidative DNA damage marker 8-hydroxy-2 '-deoxyguanosine and the association with cigarette smoking. Talanta, 2004. 63(3): p. 617-623.

114. Ahmadzadehfar, H., et al., Passive cigarette smoking increases isoprostane formation. Life Sciences, 2006. 78(8): p. 894-897.

115. Taylor, P.J., Matrix effects: The Achilles heel of quantitative high-performance liquid chromatography-electrospray-tandem mass spectrometry. Clinical Biochemistry, 2005. 38(4): p. 328-334.

116. Dams, R., et al., Matrix effect in bio-analysis of illicit drugs with LC-MS/MS: Influence of ionization type, sample preparation, and biofluid. Journal of the American Society for Mass Spectrometry, 2003. 14(11): p. 1290-1294.

117. Hsu, J.L., et al., Stable-isotope dimethyl labeling for quantitative proteomics. Analytical Chemistry, 2003. 75(24): p. 6843-6852.

118. Czauderna, M., J. Kowalczyk, and M. Marounek, The simple and sensitive measurement of malondialdehyde in selected specimens of biological origin and some feed by reversed phase high performance liquid chromatography. Journal of Chromatography B-Analytical Technologies in the Biomedical and Life Sciences, 2011. 879(23): p. 2251-2258.

119. Bowers, L.D. and E.T. Wong, Kinetic serum creatinine assays. II. A critical evaluation and review. Clinical chemistry, 1980. 26(5): p. 555-61.

120. Renner, T., T. Fechner, and G. Scherer, Fast quantification of the urinary marker of oxidative stress 8-hydroxy-2 '-deoxyguanosine using solid-phase extraction and high-performance liquid chromatography with triple-stage quadrupole mass detection. Journal of Chromatography B, 2000. 738(2): p. 311-317.

121. Waikar, S.S., V.S. Sabbisetti, and J.V. Bonventre, Normalization of urinary biomarkers to creatinine during changes in glomerular filtration rate. Kidney international, 2010. 78(5): p. 486-94.

122. Stiegel, M.A., et al., Kidney injury biomarkers and urinary creatinine variability in nominally healthy adults. Biomarkers, 2015. 20(6-7): p. 436-52.

123. Guo, Y., et al., Concentrations and Profiles of Urinary Polycyclic Aromatic Hydrocarbon Metabolites (OH-PAHs) in Several Asian Countries. Environmental Science & Technology, 2013. 47(6): p. 2932-2938.

124. Ma, E., et al., F2-Isoprostanes Reflect Oxidative Stress Correlated With Lean Mass and Bone Density but Not Insulin Resistance. Journal of the Endocrine Society, 2017. 1(5): p. 436-448.

125. Finkel, T. and N.J. Holbrook, Oxidants, oxidative stress and the biology of ageing. Nature, 2000. 408(6809): p. 239-47.

126. Harman, D., Aging: a theory based on free radical and radiation chemistry. J Gerontol, 1956. 11(3): p. 298-300.

127. Guyton, K.Z., et al., Age-related changes in activation of mitogen-activated protein kinase cascades by oxidative stress. J Investig Dermatol Symp Proc, 1998. 3(1): p. 23-7.

128. Vu, A.T., et al., Polycyclic Aromatic Hydrocarbons in the Mainstream Smoke of Popular U.S. Cigarettes. Chemical research in toxicology, 2015. 28(8): p. 1616-1626.

129. Heudorf, U. and J. Angerer, Urinary monohydroxylated phenanthrenes and hydroxypyrene – the effects of smoking habits and changes induced by smoking on monooxygenase-mediated metabolism. International Archives of Occupational and Environmental Health, 2001. 74(3): p. 177-183.

130. Cao, L., et al., Effects of environmental and lifestyle exposures on urinary levels of polycyclic aromatic hydrocarbon metabolites: A cross-sectional study of urban adults in China. Chemosphere, 2020. 240: p. 124898.

131. Oberg, B.P., et al., Increased prevalence of oxidant stress and inflammation in patients with moderate to severe chronic kidney disease. Kidney Int, 2004. 65(3): p. 1009-16.

132. Karamouzis, I., et al., Increase in oxidative stress but not in antioxidant capacity with advancing stages of chronic kidney disease. Am J Nephrol, 2008. 28(3): p. 397-404.

133. Abd El Aziz, W., et al., A comparative analysis of the level of high-sensitivity C-reactive protein in individuals with and without hypertension. Menoufia Medical Journal, 2019. 32(1): p. 187-193.

134. Mahajan, A., et al., High-Sensitivity C-Reactive Protein Levels and Type 2 Diabetes in Urban North Indians. The Journal of Clinical Endocrinology & Metabolism, 2009. 94(6): p. 2123-2127.

135. Effoe, V.S., et al., High-Sensitivity C-Reactive Protein Is Associated With Incident Type 2 Diabetes Among African Americans: The Jackson Heart Study. Diabetes care, 2015. 38(9): p. 1694-1700.

136. Albuquerque, M., M. Coutinho, and C. Borrego, Long-term monitoring and seasonal analysis of polycyclic aromatic hydrocarbons (PAHs) measured over a decade in the ambient air of Porto, Portugal. Science of The Total Environment, 2016. 543: p. 439-448.

137. Schnelle-Kreis, J., et al., Semi volatile organic compounds in ambient PM2.5. Seasonal trends and daily resolved source contributions. Environ Sci Technol, 2007. 41(11): p. 3821-8.

138. Li, F., et al., Spatial and temporal variation of sources contributing to quasi-ultrafine particulate matter PM(0.36) in Augsburg, Germany. Sci Total Environ, 2018. 631-632: p. 191-200.

139. Motorykin, O., et al., Metabolism and excretion rates of parent and hydroxy-PAHs in urine collected after consumption of traditionally smoked salmon for Native American volunteers. The Science of the total environment, 2015. 514: p. 170-177.

140. Li, Z., et al., Excretion profiles and half-lives of ten urinary polycyclic aromatic hydrocarbon metabolites after dietary exposure. Chemical research in toxicology, 2012. 25(7): p. 1452-1461.

141. Bortey-Sam, N., et al., Oxidative stress and respiratory symptoms due to human exposure to polycyclic aromatic hydrocarbons (PAHs) in Kumasi, Ghana. Environmental Pollution, 2017. 228: p. 311-320.

142. Biswas, S.K., Does the Interdependence between Oxidative Stress and Inflammation Explain the Antioxidant Paradox? Oxid Med Cell Longev, 2016. 2016: p. 5698931.

143. Lin, Y., et al., Urinary Metabolites of Polycyclic Aromatic Hydrocarbons and the Association with Lipid Peroxidation: A Biomarker-Based Study between Los Angeles and Beijing. Environmental Science & Technology, 2016. 50(7): p. 3738-3745.

144. Thai, P.K., et al., Biomonitoring of polycyclic aromatic hydrocarbons exposure in small groups of residents in Brisbane, Australia and Hanoi, Vietnam, and those travelling between the two cities. Chemosphere, 2015. 139: p. 358-364.

145. Wu, M.T., et al., Cytochrome P450 1A1 MspI polymorphism and urinary 1-hydroxypyrene concentrations in coke-oven workers. Cancer Epidemiol Biomarkers Prev, 1998. 7(9): p. 823-9.

146. Allen, J., et al., Effect of diesel exhaust inhalation on antioxidant and oxidative stress responses in adults with metabolic syndrome. Inhal Toxicol, 2009. 21(13): p. 1061-7.

147. Lin, W., et al., Association between changes in exposure to air pollution and biomarkers of oxidative stress in children before and during the Beijing Olympics. American journal of epidemiology, 2015. 181(8): p. 575-83.

Appendix

Curriculum Vitae

Name	Xiao Wu
Date and place of birth	23.01.1987 Shandong, China

Education

09.2012 - present	PhD Student, University of Rostock and Comprehensive Molecular Analysis (CMA) group of Helmholtz Zentrum Muenchen
09.2009 - 06.2012	Master of Environmental and Occupational Health, Shandong University, China
09.2005 - 06.2009	Bachelor of Biology, Shandong Normal University, China

Publication 1

Determination of air pollution-related biomarkers of exposure in urine of travelers between Germany and China using liquid chromatographic and liquid chromatographic-mass spectrometric methods: a pilot study. **Xiao Wu,** Jutta Lintelmann, Sophie Klingbeil, Jie Li, Hao Wang, Evelyn Kuhn, Sebastian Ritter, Ralf Zimmermann, Biomarkers, 2017, DOI: https://doi.org/10.1080/1354750X.2017.1306753.

Publication 2

Assessment of the association of exposure to polycyclic aromatic hydrocarbons, oxidative stress, and inflammation: A cross-sectional study in Augsburg, Germany. **Xiao Wu,** Xin Cao, Jutta Lintelmann, Annette Peters, Wolfgang Koenig, Ralf Zimmermann, Alexandra Schneider, Kathrin Wolf, International Journal of Hygiene and Environmental Health,2022, DOI: 10.1016/j.ijheh.2022.113993

Publication 3

Detection of monohydroxylated polycyclic aromatic hydrocarbons in urine and particulate matter using LC separations coupled with integrated SPE and fluorescence detection or coupled with high-resolution time-of-flight mass spectrometry. Jutta Lintelmann, **Xiao Wu**, Evelyn Kuhn, Sebastian Ritter, Claudia Schmidt, Ralf Zimmermann, Biomedical Chromatography, 2018, DOI: https://doi.org/10.1002/bmc.4183.

Publication 4

Cholesterol metabolism promotes B-cell positioning during immune pathogenesis of chronic obstructive pulmonary disease. Jie Jia, Thomas M Conlon, Rim Sj Sarker, Demet Taşdemir, Natalia F Smirnova, Barkha Srivastava, Stijn E Verleden, Gizem Güneş, **Xiao Wu**, Cornelia Prehn, Jiaqi Gao, Katharina Heinzelmann, Jutta Lintelmann, Martin Irmler, Stefan Pfeiffer, Michael Schloter, Ralf Zimmermann, Martin Hrabé de Angelis, Johannes Beckers, Jerzy Adamski, Hasan Bayram, Oliver Eickelberg, Ali Önder Yildirim, EMBO molecular medicine, 2018, DOI: https://doi.org/10.15252/emmm.201708349.

Conference

(1) Determination of biomarkers of oxidative stress basing in urine using on LC and LC-MS/MS methods (Poster). Xiao Wu, Jutta Lintelmann, Evelyn Kuhn, Sebastian Ritter, Ralf Zimmermann. International Symposium on High Performance Liquid Phase Separations & Related Techniques (HPLC) 2015.

(2) Detection of air pollution-related biomarkers of exposure and harm in urine of travellers between Germany and China. Xiao Wu, Jutta Lintelmann, Sophie Klingbeil, Jie Li, Ralf Zimmermann. European aerosol conference (EAC) 2017.

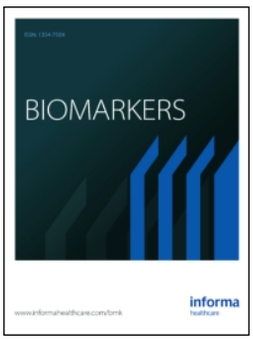

Biomarkers

ISSN: 1354-750X (Print) 1366-5804 (Online) Journal homepage: http://www.tandfonline.com/loi/ibmk20

Determination of air pollution-related biomarkers of exposure in urine of travellers between Germany and China using liquid chromatographic and liquid chromatographic-mass spectrometric methods: a pilot study

Xiao Wu, Jutta Lintelmann, Sophie Klingbeil, Jie Li, Hao Wang, Evelyn Kuhn, Sebastian Ritter & Ralf Zimmermann

To cite this article: Xiao Wu, Jutta Lintelmann, Sophie Klingbeil, Jie Li, Hao Wang, Evelyn Kuhn, Sebastian Ritter & Ralf Zimmermann (2017): Determination of air pollution-related biomarkers of exposure in urine of travellers between Germany and China using liquid chromatographic and liquid chromatographic-mass spectrometric methods: a pilot study, Biomarkers, DOI: 10.1080/1354750X.2017.1306753

To link to this article: http://dx.doi.org/10.1080/1354750X.2017.1306753

BIOMARKERS, 2017
http://dx.doi.org/10.1080/1354750X.2017.1306753

Taylor & Francis
Taylor & Francis Group

RESEARCH ARTICLE

Determination of air pollution-related biomarkers of exposure in urine of travellers between Germany and China using liquid chromatographic and liquid chromatographic-mass spectrometric methods: a pilot study

Xiao Wu[a,b,c]#, Jutta Lintelmann[a,b], Sophie Klingbeil[c]#, Jie Li[d], Hao Wang[e]#, Evelyn Kuhn[a], Sebastian Ritter[a] and Ralf Zimmermann[a,b,c]

[a]Cooperation Group Comprehensive Molecular Analytics, Helmholtz Zentrum Muenchen – German Research Centre for Environmental Health GmbH, Neuherberg, Germany; [b]HICE – Helmholtz Virtual Institute of Complex Molecular Systems in Environmental Health: Aerosol and Health, Neuherberg, Germany; [c]Department of Analytical Chemistry, Institute of Chemistry, University of Rostock, Rostock, Germany; [d]Department of Environmental Health, Shandong University, Jinan, China; [e]Department of Emergency, Qilu Hospital of Shandong University, Jinan, China

ABSTRACT

Objective: The influence of different exposures to $PM_{2.5}$ (particulate matter with an aerodynamic diameter below 2.5 μm) on the concentrations of biomarkers of exposure and oxidative stress should be investigated. For this purpose, urine samples from individuals travelling from Germany to China were collected and analysed.

Materials: Robust LC and LC-MS/MS methods were established for the determination of biomarkers including 8-hydroxy-2′-deoxyguanosine, malondialdehyde, $F_{2\alpha}$-isoprostanes and hydroxylated polycyclic aromatic hydrocarbons. As a pilot study, nine volunteers travelled from Germany (mean daily concentration of $PM_{2.5}$: 21 μg/m^3) to China (mean daily concentration of $PM_{2.5}$: 108 μg/m^3). Urine samples were collected before and after the trip.

Results: In samples collected after return to Germany, the median concentrations of oxidative stress biomarkers were observed to be higher than in samples collected before leaving Germany. Decreasing trends were observed in the sequences of samples collected after return in the following weeks. Correlations were found between exposure and oxidative stress biomarkers.

Conclusion: Travellers are ideal models for PM pollution-induced acute health effects study. Exposure to PM pollution can cause oxidative stress and damage.

ARTICLE HISTORY
Received 11 September 2016
Revised 9 February 2017
Accepted 10 March 2017

KEYWORDS
Air pollution; oxidative stress; PAH; 8-hydroxy-2′-deoxyguanosine; malondialdehyde; $F_{2\alpha}$-isoprostanes

Introduction

Over the last few decades, China had notable success in terms of economic growth, as well as booming transportation and industry. However, these changes are accompanied by worse air quality, which is caused by fossil fuel and biomass combustion (Boffetta *et al.* 1997, Bostrom *et al.* 2002, Chan and Yao 2008). Particularly in winter, heavy hazes often cover huge areas of north China, which has become a global concern. One of the major components of haze is particulate matter (PM) consisting of suspended solid or liquid particles. They can be inhaled and accumulated in the bronchus and pulmonary alveolar surfaces, inducing the formation of reactive oxygen species (ROS) such as peroxides, superoxide, hydroxyl radical and singlet oxygen. These species disturb the natural oxidative stress balance by attacking macromolecules, such as phospholipids, proteins and DNA. Furthermore, they can induce cell apoptosis. Their reactivity can be blocked by antioxidants or internal enzymatic processes of the cell. Particles with diameter <2.5 μm ($PM_{2.5}$) have been proven to be more harmful because they can be inhaled into the deeper lung regions and can penetrate into cell membranes. In China, the daily $PM_{2.5}$ concentrations in some cities even exceeded 1000 μg/m^3 in the winter of 2015, although as described in the national ambient air quality regulations in China (GB 3095-2012), the threshold for annual average $PM_{2.5}$ mass concentration levels is 35 μg/m^3. Exposure to such high levels of $PM_{2.5}$ is linked to short-term, as well as long-term diseases, such as respiratory infections, asthma, airway irritation, reduced lung function, cardiovascular diseases and cardiopulmonary diseases (Risom *et al.* 2005, de Kok *et al.* 2006, Dumax-Vorzet *et al.* 2015, Jaligama *et al.* 2015, Kumarathasan *et al.* 2015, Pardo *et al.* 2015, Sijan *et al.* 2015). It is of great importance to investigate the health effects caused by exposure to $PM_{2.5}$. During various phases of oxidative stress, biomolecules, including phospholipids, proteins and DNA, are oxidatively attacked. These biochemical processes, on the one hand, can induce further development of diseases such as cancer. On the other hand, the formed oxidation products

CONTACT Ralf Zimmermann ralf.zimmermann@uni-rostock.de Cooperation Group Comprehensive Molecular Analytics, Helmholtz Zentrum Muenchen - German Research Centre for Environmental Health GmbH, Ingolstaedter Landstr. 1, D-85764 Neuherberg, Germany
#Xiao Wu and Hao Wang are responsible for statistical design and Sophie Klingbeil is responsible for statistical analysis. xiao.wu@helmholtz-muenchen.de (X. Wu); hktk_sd2007@163.com (H. Wang); sophie.klingbeil2@uni-rostock.de (S. Klingbeil).

Supplemental data for this article can be accessed here.

and metabolites can be used as indicators of air pollution exposure and harm. One strategy is to determine the biomarkers in urine samples, such as malondialdehyde (MDA) (Czauderna *et al.* 2011), $F_{2\alpha}$-isoprostanes (Milne *et al.* 2008) and 8-hydroxy-2'-deoxyguanosine (8OHdG) (Valavanidis *et al.* 2009). Due to the non-invasive character of urine sampling, such methods are also appropriate for studies of large populations.

DNA damage biomarker: 8-hydroxy-2′-deoxyguanosine

8-Hydroxy-2′-deoxyguanosine is generated during DNA repair pathways and can be excreted into urine due to its water-solubility (Klein *et al.* 1992, Dizdaroglu 2012). Oxidative stress is suggested to be one of the reasons of DNA damage. Also, 8OHdG is considered to be an ideal biomarker of oxidative stress due to the following reasons: (1) 8OHdG is not involved in further reactions; (2) cell death and diet would not increase the urinal 8OHdG levels (Evans *et al.* 2004, 2010, Halliwell 2007, Valavanidis *et al.* 2009).

Lipid peroxidation biomarker: malondialdehyde

Malondialdehyde is an important secondary product of lipid peroxidation, generated when oxidative species react with double bonds of polyunsaturated fatty acids (PUFAs) (McCord 1993). Previous studies have shown the relation between MDA and oxidative stress by analysing bio-matrices with liquid chromatographic (LC) or gas chromatographic (GC) methods (Giera *et al.* 2012). Due to its very high reactivity, MDA can disturb many normal reactions. Thus, it is a highly toxic molecule both inside and outside of cells. Furthermore, MDA is a very important target biomarker to indicate the level of oxidative stress (Czauderna *et al.* 2011).

Arachidonic acid oxidation biomarker: $F_{2\alpha}$-isoprostanes

$F_{2\alpha}$-isoprostanes are a series of prostaglandin (PG)-like compounds that are generated by non-enzymatic, free radical-mediated oxidation of arachidonic acid. Due to the non-enzymatic reaction, numerous isomers are formed, some of which are cytotoxic (Morrow *et al.* 1990, Milne *et al.* 2008). However, they are also potential *in vivo* biomarkers of oxidative stress. They are stable, robust, and exist in all human tissues and fluids. Their occurrence may be related to a diverse array of human disorders, such as atherosclerosis, diabetes, obesity, cigarette smoking, neurodegenerative diseases and many others (Milne *et al.* 2008). Previous studies were mostly based on GC or GC-mass spectrometric (GC-MS) techniques (Mori *et al.* 2000, Walter *et al.* 2000, Dreissigacker *et al.* 2010).

Polycyclic aromatic hydrocarbon exposure biomarker: hydroxylated polycyclic aromatic hydrocarbons

Polycyclic aromatic hydrocarbons belong to a class of substances containing fused aromatic rings. They are mostly generated during the combustion of biomass and coal. Traffic and industry are considered to be the main sources of emissions in urban areas (Bressi *et al.* 2013). PAH has been the subject of many studies due to its ubiquitous distribution, long-time persistence in environmental compartments, and numerous health effects. Among these are chronic effects, such as carcinogenicity, and acute effects, such as the induction of inflammation processes. After entering the human body through inhalation, ingestion or skin permeation, the PAH are spread and located in specific lipid-rich tissues or transported into the liver and kidney. Metabolic degradation partly converts PAH into electrophilic metabolites that can finally produce reactive oxidative reagents (Franco *et al.* 2008). One important metabolic pathway in mammalians requires the contribution of cytochrome P450 enzymes and microsomal epoxide hydrolase. This oxidative metabolism results in the formation of dihydrodiols, tetrahydrotetrols, monohydroxy-PAH (OH-PAH) and DNA-adducts. Products with five or more rings are mostly excreted into faeces, while most of the lower-molecular-weight products with two to four rings are excreted into urine, and the determination of OH-PAH in urine is a helpful tool to assess the individual internal burden of PAH (Wu *et al.* 1998).

Concept of exposure assessment

In environmental health studies and epidemiological studies, one problem researchers often encounter is that the subjects under study have usually been exposed to the same or similar conditions for a long period. This can conceal or change characteristics related to acute injuries. Every year, millions of people perform long-distance travels. Among the places of travel, some have relatively "clean" air while others are exposed to highly polluted air. Here, we follow the idea that travellers can provide an ideal model to investigate acute biological responses and health effects due to their exposure to differently polluted environments during travel. Similar study designs were reported by Thai *et al.* (2015), Lin *et al.* (2016) and Rossnerova *et al.* (2011). Thai and coworkers collected urine samples from one family who travelled between Australia and Vietnam and found that OH-PAH concentrations in urine samples were higher during the stay in Vietnam. Lin *et al.* (2016) investigated OH-PAH and MDA in urine samples, which were collected from students who travelled from Los Angeles to Beijing. The OH-PAH and MDA concentrations showed significant changes related to the respective location. Both studies are mainly focussed on PAH-exposure-related biomarker levels in urine. Values for external, ambient pollutants like $PM_{2.5}$ or PAH were not determined and considered. In a sub-study by Rossnerova *et al.* (2011), air pollution-related effects were examined by evaluating frequencies of micronuclei of four travellers between Prague and the Ostrava region, Czech Republic. Biomarkers of oxidative stress or OH-PAH were not determined. To the best of our knowledge, our study is the first that considered and analysed biomarkers for lipid peroxidation, arachidonic oxidation, DNA damage, PAH exposure and ambient $PM_{2.5}$ data as well.

Since 2012, our research group has been involved in joint environmental health projects of the Helmholtz Zentrum München in which – among others – the relation between

exposure to $PM_{2.5}$, ultrafine particulate matter ($PM_{0.1}$) and diseases are investigated in the framework of the "Cooperative Health Research in the Augsburg Region – KORA" and "Helmholtz Virtual Institute of Complex Molecular Systems in Environmental Health – HICE". For the project discussed in this study, LC- and LC-MS-based methods for the determination of OH-PAH, MDA, 8OHdG and $F_{2\alpha}$-isoprostanes in urine were required. For the determination of OH-PAH we had recourse to an established method. However, for the other analytes, we had to develop a sensitive, robust, and low sample-consuming method allowing reliable quantification in sample volumes below one millilitre. For this purpose, LC mass spectrometric (LC-MS) methods were optimized and validated. The methods consisted of sample processing, chromatographic separation and tandem mass spectrometric detection. The applicability of the methods should be demonstrated by conducting a smaller study in which a group of volunteers undergoing periodic exposure to high levels of particulate matter are investigated by collecting and analysing urine samples at defined points of time.

Clinical significance

The clinical significance in the presented study is summarized below:

- We proposed non-invasive, reliable and applicable LC-based methods, which are suitable for routine analyses. Valuable information can be obtained to monitor oxidative stress and to investigate the health risks, which are induced by air pollution exposure and other hazards.
- Short-term air pollution exposure induced acute effects should get more attention. More investigations should be performed especially for exposure to critical air pollutions.

Methods

Study population

To investigate the applicability of the analytical method and to examine the influence of ambient air on urinary concentrations of the biomarkers of interest, a pilot study was performed by focussing specially on individuals travelling to China from Germany. The studied population consisted of nine non-smoking "healthy" (without doctor-diagnosed chronic diseases such as cardiovascular diseases, chronic obstructive pulmonary disease or renal insufficiency) young male Chinese volunteers with a mean age of 29 (ranging 26–34), who studied in Munich, Germany for 18 to 24 months. The volunteers subsequently travelled for a holiday to different cities of China in the time frame from December 2013 to February 2014 and returned to Germany. Information on daily $PM_{2.5}$ concentrations *i* was collected from the official website of the China National Environmental Monitoring Centre. The main features of the travel can be described as follows: The mean travel time was 28 days (8 days– 42 days). During the whole travel time, no volunteer resided near a highway (within 100 m). Four volunteers stayed in urban areas while the other five volunteers lived in rural areas during the first week(s) of travel. During the last week of their travel, half moved to and stayed in other cities for 3–7 days. Although only non-smoking students were selected as volunteers, two were reported as severe passive smokers in the course of their trip or in Germany. The mean $PM_{2.5}$ concentration of the first week(s) of travel was 101 $\mu g/m^3$ and the mean $PM_{2.5}$ concentration of the last week of travel was 118 $\mu g/m^3$. For comparison, in Munich, during the period between December, 2013 and February, 2014, the mean $PM_{2.5}$ concentration was 21 $\mu g/m^3$. Anonymous self-administered questionnaires were used to collect health histories, including age, gender, respiratory diseases, cardiovascular diseases, as well as information of travel history including the departure date, arrival date and staying cities. Since this study is considered as an observational study, no treatment was applied (non-invasive sampling), and signature of consent is the only risk for participants' privacy. Exception by the Ethics Committee was approved. The participants were fully informed formally. The whole study follows the principles of the Declaration of Helsinki.

Sample collection and sampling schedule

First void urine samples were collected. Midstream specimens of the first void urine were collected one day before departure. Then, urine samples were collected immediately upon return to Munich. Further collections were performed after one week, two weeks and four weeks. The whole sampling cycle can be divided into five different sampling periods: one day before leaving Munich (S0); first day after return to Munich (S1); one week after return to Munich (S2); two weeks after return to Munich (S3); and four weeks after return to Munich (S4) (Figure 1). Urine was collected in glass tubes and stored in an ice box immediately. The samples were then stored at –20 °C in the laboratory until sample preparation.

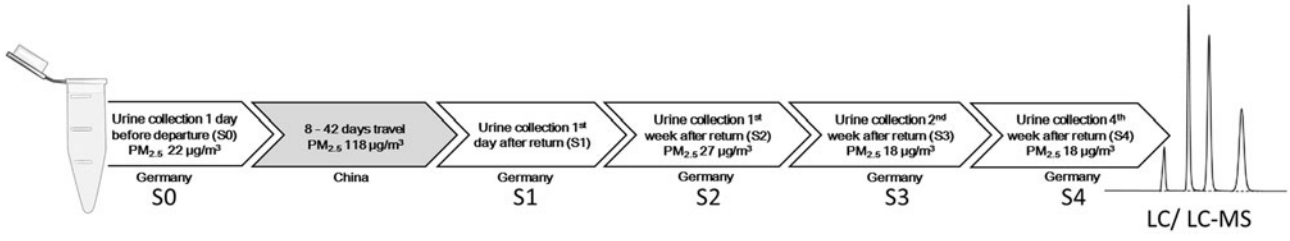

Figure 1. Schedule for urine sampling.

Materials

LC/MS grade methanol, water, acetonitrile, dichloromethane and sodium acetate were purchased from VWR International (Darmstadt, Germany). LC-grade methanol, *n*-hexane and acetonitrile were obtained from Merck (Darmstadt, Germany). LC/MS-grade acetic acid and formic acid were from Fisher Scientific (Geel, Belgium). To prepare LC-grade water, a Milli-Q Ultra Plus Water System (Millipore, Schwabach, Germany) was employed. β-Glucuronidase/Arylsulfatase (from Helix pomatia) solution was from Roche Diagnostics (Mannheim, Germany). SPE-cartridges Focus (60 mg/3 ml) and Strata X-AW 33 u Polymeric weak Anion (60 mg/3 ml) were from Agilent Technologies (Santa Clara, CA) and Phenomenex (Torrance, CA). Nitrogen was provided by a central gas supply by a liquid nitrogen tank or from gas bottles (5.0 purity) (Linde, Germany). 2,4-Dinitrophenylhydrazine was obtained from Sigma-Aldrich (St. Louis, MO). Standard compounds were purchased from different companies and institutes. 8-OHdG and MDA were from Sigma-Aldrich (St. Louis, MO). $^{15}N_5$-8OHdG and 1,1,3,3-tetraethoxypropane (d_2-TEP) were purchased from Cambridge Isotope Laboratories (Andover, MA). 2,3-dinor-8-iso Prostaglandin $F_{2\alpha}$ (2,3-dinor-8-iso$PGF_{2\alpha}$), 2,3-dinor-11β-Prostaglandin $F_{2\alpha}$ (2,3-dinor-11β-$PGF_{2\alpha}$), 8-iso-15(R)-Prostaglandin $F_{2\alpha}$ (8-iso-15(R)-$PGF_{2\alpha}$), 8-iso-Prostaglandin $F_{2\alpha}$ (8-iso-$PGF_{2\alpha}$), ±5-iso-Prostaglandin $F_{2\alpha}$-VI (±5-i$PF_{2\alpha}$-VI), 15(R)-Prostaglandin $F_{2\alpha}$ (15(R)-$PGF_{2\alpha}$) and ±5-iso-Prostaglandin $F_{2\alpha}$-VI-d11 (±5iPF2α-VI-d11) were obtained from Cayman Chemical (Ann Arbor, MI). Creatinine was from Acros Organics (Morris Plains, NJ). 1-Hydroxyphenanthrene and 9-hydroxyphenanthrene were from Santa Cruz Biotechnology, Inc. (Santa Cruz, CA). 2-Hydroxyphenanthrene, 3-hydroxyphenanthrene, 4-hydroxyphenanthrene and 1-hydroxypyrene were purchased from the PAH Research Institute Dr. Schmidt (Greifenberg, Germany).

Standard and isotopically labelled standard

Isotopically labelled standards, including $^{15}N_5$-8OHdG, d_2-MDA and ±5iPF2α-VI-d11, were used as internal standards to obtain the actual recovery of each sample and each target compound. Back-calculation based on internal standards was used to prevent deviations generated by matrix effects. 8-OHdG and $^{15}N_5$-8OHdG standards were prepared by diluting 1 mg of the standard in 1 ml distilled water to obtain stock solutions with a final concentration of 1 mg/ml. The MDA standard was obtained by diluting 1 mg standard into 100 ml acetonitrile to obtain a final concentration of 10 μg/ml for the stock solution. D_2-MDA was prepared hydrolysing 1 mg/ml d_2-TEP at room temperature for 2 h with 0.02 N HCL (Chen *et al.* 2011). The resulting solution of d_2-MDA was observed to be stable for at least 3 months at −20 °C. This solution was used for all experiments in this study. Stock solutions of $F_{2\alpha}$-isoprostanes were prepared with methanol to obtain the following final concentrations: 2,3-dinor-8-iso$PGF_{2\alpha}$ 100 ng/ml, 2,3-dinor-11β-$PGF_{2\alpha}$ 100 ng/ml, i$PF_{2\alpha}$-IV 100 ng/ml, 8-iso-15(R)-$PGF_{2\alpha}$ 50 ng/ml, 8-iso-$PGF_{2\alpha}$ 50 ng/ml, ±5-i$PF_{2\alpha}$-VI 100 ng/ml, 15(R)-$PGF_{2\alpha}$ 100 ng/ml. Stock solution of ±5i$PF_{2\alpha}$-VI-d11 was prepared with methanol to obtain a final concentration of 10 ng/ml. Stock solutions were stored at −20 °C. The stock solution of creatinine was prepared by diluting 1.0 mg creatinine in a 10-ml volumetric flask, which was subsequently filled to the mark with methanol and stored at −20 °C. Standard solutions were obtained by diluting the stock solutions into distilled water/methanol (MDA, 8OHdG/OH-PAHs, $F_{2\alpha}$-isoprostanes and creatinine). The solutions were placed into the autosampler directly after preparation and before the sequence was started.

Sample preparation and instrumentation

Urine samples were thawed at 4 °C to avoid further reactions. All prepared samples were measured on the same day as sample preparation, except for the MDA-DNPH products and extracts of solid-phase extraction, which were frozen at –20 °C before measurement.

Analyses of MDA, 8OHdG and $F_{2\alpha}$-isoprostanes

Analyses were carried out with a triple quadrupole mass spectrometer, API-3000 (AB Sciex, Darmstadt, Germany) equipped with an electrospray ion source (ESI), coupled to an HPLC system HP1100 including a pump, degasser, autosampler and column oven with a six-port switching valve (Agilent Technologies, Waldbronn, Germany). Different analytical columns were applied for the respective LC-separations. All analyses were performed in the multi-reaction monitoring (MRM) mode. All of the target analytes were tuned by continuously infusing 1 μg/ml standard solutions into mass spectrometer with a syringe pump at a flow of 0.2 ml/min. Instrument control and data processing were performed with Analyst software, version 1.6.2 (AB Sciex).

MDA: To prepare the MDA-DNPH derivatized solution, 250 μl of 1 mM DNPH containing 2% formic acid was mixed with 200 μl distilled water and 25 μl of 80 ng/ml d_2-MDA solution. After 30 s vortex with a Vortex mixer D-6012 (NeoLab, Heidelberg, Germany), 25 μl urine was added into the DNPH solution. The mixture was incubated for 70 min at 37 °C and 300 rpm in a Thermomixer comfort (Eppendorf, Hamburg, Germany). After derivatization, 700 μl *n*-hexane was added, mixed well by hands for 30 s, and centrifuged at 7000 rpm for 30 s in a Thermo Scientific Heraeus Pico 17 (Thermo Fisher Scientific, Darmstadt, Germany). The hexane supernatant was collected. This step was repeated once. Following this, the collected supernatants were combined and evaporated to dryness in a Barkey Vapotherm mobile S from Barkey GmbH (Leopoldshöhe, Germany) under a gentle stream of nitrogen at room temperature. The residue was re-suspended in 50 μl distilled water. The products were kept away from light in order to avoid suspected light-induced decomposition (Pilz *et al.* 2000). 10 μl of the solution containing the derivatization products was injected on a Kinetex® RP18 endcapped column (100 mm × 3 mm I.D., 2.6 μm, Phenomenex, Torrance, CA). An isocratic separation was carried out with 80% methanol and 20% H_2O (both containing 0.1% formic acid). A peak-cutting technique was adopted. The valve was switched on at 1.5 min and switched off at

2.5 min to reduce the amount of residual DNPH entering the mass spectrometer. The column temperature was 20 °C and the flow rate was 0.2 ml/min.

8OHdG: For the measurement of 8OHdG, 25 µl urine was vortexed for 30 s and then diluted in a 1:1 proportion with 25 µl 0.1% formic acid. 10 µl of the diluted sample was directly injected onto a Gemini® RP18 endcapped column (250 mm × 2 mm, 5 µm, Phenomenex, Torrance, CA) with a guard column of the same material (Phenomenex, Torrance, CA). The mobile phase consisted of solvent A (0.1% formic acid in water), solvent B (0.1% formic acid in methanol) and solvent C (acetonitrile). The gradient applied is shown in Table 1. To protect the mass spectrometer, the peak-cutting technique was also employed. During the elution of analytes and internal standard, the switching valve connected the mass spectrometer to the analytical column for 2 min (from 3 min to 5 min).

$F_{2\alpha}$-isoprostanes: For $F_{2\alpha}$-isoprostanes, a polymer-based weak anion-exchange cartridge (StrataX-AW from Phenomenex, Torrance, CA) was used for solid-phase extraction (SPE), following the extraction method described in the literature (Medina *et al.* 2012). 1 ml of the urine sample was diluted with 2 ml BIS-TRIS-HCl buffer solution (pH 6) and adjusted to pH 6 with phosphoric acid (5%) or potassium hydroxide solution (10%). The optimised method involved conditioning with 2 ml MeOH/formic acid (0.1%) (98/2, v/v) and 2 ml distilled water. 3 ml of the buffered sample was applied on the SPE-column. The washing step was performed with 1 ml water, 2 ml MeOH/H_2O (25/75, v/v), and 1 ml acetonitrile. The column was dried under a gentle nitrogen stream for 30 s. 3 ml methanol was used for the elution step, with a flow rate of ca. 30 drops per minute. The extracts were evaporated at 30 °C with nitrogen in the Barkey Vapotherm. The residue was dissolved in 100 µl methanol/0.1% formic acid, 50/50, v/v and filled in an autosampler vial. 20 µl of the extract was applied on a Hydro® RP18 endcapped column (250 mm × 2 mm I.D, 4 µm, Phenomenex, Torrance, CA). A gradient of solvent A (0.1% formic acid in water) and solvent B (methanol) was applied for the separation of the isomeric $F_{2\alpha}$-isoprostanes (Taylor and Traber 2010). The parameters of the mass spectrometer are listed in Table 2. Six-point linear calibration curves were established separately over ranges of 0.1–100 ng/ml. The results were back-calculated based on the internal standards.

Table 1. Gradient of the LC-separation of 8OHdG and $F_{2\alpha}$-isoprostanes.

8OHdG				$F_{2\alpha}$-isoprostanes		
Time (min)	A (%)	B (%)	C (%)	Time (min)	A (%)	B (%)
0	80	10	10	10	50	50
5	0	100	0	20	0	100
5.5	10	90	0	30	0	100
12	10	90	0	32	50	50
13	80	10	10	42	50	50
23	80	10	10			

Column temperature 20 °C, flow rate 0.2 ml/min. Solvent A is 0.1% formic acid in water, solvent B is 0.1% formic acid in methanol, solvent C is acetonitrile.

OH-PAH

The LC method for measuring OH-PAH was modified basing on a former work (Lintelmann *et al.* 1994). Briefly, the urine samples were enzymatically treated with β-glucuronidase/arylsulfatase to hydrolyse conjugates among the analytes, glucuronic acid and sulphate. After centrifugation, the sample was directly injected into an LC-system with integrated SPE and fluorescence detection. The determination of OH-PAH was carried out on an Ultimate 3000 HPLC system (Thermo Scientific, Dreieich, Germany) consisting of a dual-gradient pump DGP 3600 M, an autosampler WPS-3000 TSL and a column compartment TCC-3200 equipped with two 10-port switching valves from Valco, a PDA 3000 photo diode array detector and a RF 2000 fluorescence detector. A laboratory-made solid-phase extraction column (copper phthalocyanine-modified silica, 45 µm – 60 µm, 5 mm × 2.1 mm I.D) and an analytical column from Phenomenex (Kinetex PFP, 2.6 µm 100 × 3 mm I.D., with SecurityGuardTM PFP, 2.1 mm I.D.; Phenomenex, Aschaffenburg, Germany) were used for online extraction and subsequent separation. Time-programmed fluorescence detection was applied. OH-Phenanthrenes were quantified at 249 nm/364 nm (Ex./Em.) and 1-hydroxypyrene was detected at 343 nm/385 nm (Ex./Em.).

Table 2. Optimized LC-MS/MS conditions for all biomarkers.

Analytes	8OHdG	MDA	2,3-dinor -8-iso-$PGF_{2\alpha}$	2,3-dinor -11β-$PGF_{2\alpha}$	8-iso -15(R)-$PGF_{2\alpha}$	8-iso -$PGF_{2\alpha}$	±5-i$PF_{2\alpha}$ -VI	15(R) -$PGF_{2\alpha}$
Nebulizer gas*	6	6	12	12	12	12	12	12
Curtain gas*	8	8	8	8	8	8	8	8
Collision gas*	6	6	8	8	8	8	8	8
IonSpray voltage	5000	5000	−4400	−4400	−4400	−4400	−4400	−4400
Temperature	500	500	500	500	500	500	500	500
Declustering potential	24	45	−28	−28	−58	−58	−52	−58
Focusing potential	60	95	−70	−70	−128	−128	−115	−128
Entrance potential	5	9	−7	−7	−7	−7	−7	−7
Collision energy	44	23	−18	−23	−35	−35	−34	−35
Collision cell potential	10	10	−4	−6	−3	−3	−7	−3
Transitions	284→168	235→159	353→237	353→145	353→193	353→193	353→115	353→193
Internal/reference Std.	289→145	237→161	364.5→115					

*Arbitrary units used in the instrument.

Creatinine

Creatinine concentrations were used to normalize the concentrations of target compounds. A fast HPLC method was developed for the determination of creatinine. On a Phenomenex Luna NH_2-column (3 µm, 150 mm × 2 mm I.D.), creatinine was separated from the matrix components using acetonitrile/water, 80/20, v/v at 0.55 ml/min and 15 °C. Detection and quantification were carried out at 235 nm. To verify the identification, UV-spectra were regularly recorded and compared with the standard spectrum. 10 µl of a diluted and vortexed urine sample (1:20 with water, 0.5 min on a vortex from Neolab, Heidelberg, Germany) were injected. The analysis was carried out on an HP 1100 system from Agilent (St. Clara, CA).

$PM_{2.5}$ index

The daily $PM_{2.5}$ concentration data were collected from the official website of the China National Environmental Monitoring Centre. All monitoring activities and methods were carried out according to the official technical regulation of China (HJ 663-2013, HJ 633-2012, HJ/T193-2005 and HJ 655-2013).

Statistical analysis

All statistical analyses were conducted with MatLab ver. 7.11 R2010b (The MathWorks Inc., Natick, MA).

Results

Validation of the analytical methods

Linearity, sensitivity and limit of quantification: Linear calibration curves were established in concentration range between 0.2 ng/ml and 200 ng/ml. Linearities of calibration functions were good, with $r^2 > 0.996$. Limits of quantification (LOQ) were calculated automatically for every run, using ANALYST according to the following equation. The detailed results are shown in Table 3.

$$\text{Limits of quantification} = \frac{10 \times \textit{Calculated Concentration}}{\textit{Analyte Signal To Noise}}$$

Instrument tuning and calibration: The mass spectrometer was regularly tuned and calibrated in the positive and negative modes with PPG tuning solutions (low/high concentration polypropylene glycols, AB Sciex, Darmstadt, Germany), according to the handbook.

Repeatability and reproducibility: Six urine samples from different volunteers were pooled together and spiked with 80 ng/ml MDA, 20 ng/ml 8OHdG, or 10 ng/ml $F_{2\alpha}$-isoprostane standards and processed by the methods described in 2.4. The instrument repeatability was investigated by injecting an aliquot of the same sample six times. The peak areas were obtained and the coefficients of variation were between 1.7 and 11.6%. To investigate the reproducibility of the methods, on 10 different days, deionized water was spiked with 40 ng/ml MDA or 10 ng/ml 5-iP$F_{2\alpha}$-VI-d11, and pooled urine was spiked with 5 ng/ml 8OHdG or 10 ng/ml $F_{2\alpha}$-Isoprostanes (except ±5iPF2α-VI-d11). The spiked samples were processed according to the sample preparation procedures described in Section 'Sample preparation and instrumentation' and analysed by LC-MS/MS. During the overall period of analysis, there was slight instrumental fluctuation. To overcome this issue, the reproducibility was obtained based on the calculated concentration instead of the peak area. New standard curves were generated in every sequence. The coefficients of variation of the calculated concentrations were good, with values between 6.6 and 18.3%. Results are shown in Table 4.

Recovery and matrix effects: Six urine samples from different volunteers were pooled together. The urine mixture and pure deionized water were spiked with different standard concentrations. Then, the spiked urine, non-spiked urine and spiked deionized water were analysed. For MDA and d_2-MDA, urine mixtures or deionized water were spiked with 25 µl of 40 ng/ml, 80 ng/ml, 120 ng/ml and 160 ng/ml MDA standards each, and derivatized with DNPH according to the method described previously. All the derivatization products were analysed with LC-MS/MS. For 8OHdG and $^{15}N_5$-8OHdG, the urine mixtures and deionized water were mixed with equal amounts of 10 ng/ml, 20 ng/ml, 40 ng/ml, 60 ng/ml and 100 ng/ml standards, or deionized water. The spiked and non-spiked samples were injected directly into the LC-MS/MS. For $F_{2\alpha}$-isoprostanes, the urine mixtures and deionized water were spiked with standards and IP$F_{2\alpha}$-IV to obtain 10 ng/ml spiked samples. The spiked samples and the pure urine samples were processed with SPE and analysed with the LC-MS/MS method described previously. The recoveries were calculated based on the equation shown below. The results are shown in Table 5. Recoveries between 44 and 120% were obtained. Recoveries based on back-calculations

Table 3. Linearity, sensitivity and limit of quantification for the target analytes.

Analytes (ng/ml)	8OHdG	$^{15}N_5$- 8OHdG	MDA	d_2 -MDA	2,3-dinor -8-iso -$PGF_{2\alpha}$	2,3-dinor -11β -$PGF_{2\alpha}$	8-iso -15(R) -$PGF_{2\alpha}$	8-iso -$PGF_{2\alpha}$	±5-iP$F_{2\alpha}$ -VI	15(R) -$PGF_{2\alpha}$
Calibration function	$Y = 4.32 e+003x - 162$	$Y = 716x + 61.1$	$Y = 4.12 e+003x + 1.63 e+004$	$Y = 1.73 e+004x - 3.29 e+004$	$Y = 67.6x + 0.00243$	$Y = 48.7x - 0.0628$	$Y = 27.8x + 0.00828$	$Y = 58.6x + 0.155$	$Y = 0.462x + 0.00112$	$Y = 0.355x + 0.00361$
Range	0.1–40	0.1–40	5–200	5–200	1–50	1–50	0.5–25	0.5–25	1–50	1–50
Number of calibration levels number	8	6	7	7	5	5	5	5	5	5
r^2	0.997	0.997	0.998	0.997	0.997	0.996	0.995	0.996	0.999	0.999
LOQ	0.58	2.73	2.00	1.22	0.03	0.08	0.08	0.03	0.04	0.05

against the internal standard resulted in values between 89 and 127%.

$$\text{Recovery} = \frac{\left(\begin{array}{l}\textit{mean peak area of spiked urine samples}\\ -\textit{mean peak area of pure urine samples}\end{array}\right)\times 100}{\textit{mean peak area of methanolic standards}}$$

Urine samples

Altogether nine volunteers who travelled to China for vacation were investigated. Samples were collected before and after the trip (S0, S1, S2, S3 and S4). Details can be found in Section 'Sample collection and sampling schedule' and Figure 1). Time trends of target substances of each volunteer are shown in Supplementary Figure 1 in the course of time before and after return to Munich (S0, S1, S2, S3 and S4). Previous studies have reported the health-relevant effects of $PM_{2.5}$, including chronic and acute damage to the respiratory system, cardiovascular system and more (Kampa and Castanas 2008). Additionally, researchers have noted the harm and effect of both cigarette smoking and passive-smoking on biomarker excretion (Yao *et al.* 2004, Ahmadzadehfar *et al.* 2006). Thus, we consider $PM_{2.5}$ and cigarette smoking to be the most important factors affecting the acute oxidative stress response when these volunteers were in China. The overview of the main influencing factors is shown in Table 6. For $PM_{2.5}$, the mean values of the concentrations 7 days before each sample collection were used. In most cases, large differences in the air pollution between Germany and China were observed: $\Delta PM_{2.5}$ between S0/S1 and $\Delta PM_{2.5}$ between S1/S2 were mostly higher than 50 $\mu g/m^3$, which indicates that most of the volunteers were exposed to much worse air conditions in China than in Germany. An exception was volunteer A09, for whom the difference between air pollution in China and Germany was relatively low. Furthermore, it was recognized that volunteers A01 and A06 were exposed to severe passive cigarette smoking. In former studies, significant smoking and passive smoking were related to increased levels of MDA, 8OHdG and $F_{2\alpha}$-isoprostane, as reported by Solak *et al.* (2005), Yao *et al.* (2004) and Ahmadzadehfar *et al.* (2006). Finally, the travel duration of volunteer A08 was much shorter than the other volunteers. Thus, the cohort for the final analysis was further refined: volunteers who (1) travelled more than 3 weeks and (2) had $\Delta PM_{2.5}$ higher than 50 $\mu g/m^3$ during the last 7 days of their journey and (3) were not exposed to cigarette smoke were selected for detailed data analysis (A02, A03, A04, A05 and A07).

The course of the concentration of the target substances observed from this refined cohort is depicted in a Boxplot graph representation (shown in Supplementary Figure 2). The time trends of median values from the Boxplot are shown in Figure 2. The concentration of $PM_{2.5}$ shows nearly constant and low values in the measurements after returning from China. The highest median concentrations of the oxidative stress biomarkers MDA (Figure 2(B)), the oxidative DNA damage biomarker 8OHdG (Figure 2(C)), and the polycyclic aromatic hydrocarbon exposure biomarker OH-PAHs (Figure 2(E)) are found directly after returning from China (S1 samples). In contrast, for the $F_{2\alpha}$-isoprostanes (arachidonic acid oxidation biomarkers, Figure 2(D)), no direct correlation is observed. This indicates that there are time-lags for $F_{2\alpha}$-isoprostanes formation or excretion, as the maximum concentrations are observed in S1, S2 or even S3. Basing on the time trends of the medians, correlation coefficients were calculated and are shown in a heatmap in Figure 3. During exposure of $PM_{2.5}$, reactive oxygen species are generated which can attack various targets, including fatty acids, arachidonic acids and DNA. As shown in Figure 3, strong correlations were found between $PM_{2.5}$/MDA. In Figure 2, notably broad and high concentration(s) were seen after travel (S1, S2 or S3), implying a connection between $PM_{2.5}$ and $F_{2\alpha}$-isoprostanes. These patterns varied from the pattern of $PM_{2.5}$, and the correlation coefficient values were between –0.2 and 0.7. Similar as $F_{2\alpha}$-isoprostanes, the highest median concentrations of 8OHdG were found in S1 and S2, which were two times higher than the others.

Discussion

Constituents of the urine matrix influence sample processing and in particular, influence the signal intensity during electrospray ionization. This observation is well known and can significantly impact the precision, accuracy and recovery of the method (Wampler *et al.* 1993, Dams *et al.* 2003, Taylor 2005). To overcome these problems, the addition of isotopically

Table 4. Repeatability and reproducibility.

Analytes (%)	8OHdG	$^{15}N_5$-8OHdG	MDA	d_2-MDA	2,3-dinor -8-iso -$PGF_{2\alpha}$	2,3-dinor -11β -$PGF_{2\alpha}$	8-iso -15(R) -$PGF_{2\alpha}$	8-iso -$PGF_{2\alpha}$	±5 -$iPF_{2\alpha}$ -VI	15(R) -$PGF_{2\alpha}$
Repeatability ($n = 6$)	1.7	3.2	6.1	5.3	3.3	4.7	7.7	7.4	11.6	6.6
Reproducibility ($n = 10$)	7.0	9.6	12.3	12.2	14.9	15.0	18.3	14.8	17.3	6.6

Table 5. Recovery of target analytes.

Analytes (%) (n =12)	8OHdG	$^{15}N_5$-8OHdG*	MDA	d_2-MDA*	2,3-dinor -8-iso$PGF_{2\alpha}$	2,3-dinor -11β-$PGF_{2\alpha}$	8-iso-15(R) -$PGF_{2\alpha}$	8-iso -$PGF_{2\alpha}$	±5-$iPF_{2\alpha}$-VI	15(R) -$PGF_{2\alpha}$	±5iP $F_{2\alpha}$VI-d11*
Recovery	44	47	86	97	63	120	79	72	68	75	64
Recovery based on ISTD	94		89		97	99	127	119	103	94	

*Internal standard.

labelled internal standards was necessary and led to increased reliabilities of all methods (Hsu *et al.* 2003). For each compound or compound class investigated, characteristic problems emerged during method development. Due to these obstacles, individual methods and sample processing methods had to be developed. For the determination of MDA, chemical derivatization with DNPH was applied, followed by a liquid–liquid extraction to remove excessive DNPH (Czauderna *et al.* 2011). For 8OHdG, strong matrix effects due to interfering components were observed. Strategies such as SPE could neither improve recovery nor significantly reduce components from the interfering matrix. Direct injection of the diluted urine sample, in combination with peak cutting showed the best results. For $F_{2\alpha}$-isoprostanes, an SPE step was needed for selective enrichment and clean-up of the substances. Method development and optimization led to three analytical methods allowing practicable, sensitive and reliable quantification of the selected markers of oxidative stress in sample volumes below or equal to 1 ml.

In this study, first void urine samples were collected. Results before and after creatinine correction are summarized and shown in Supplemental Table 1. Because the excretion ratio of creatinine is relatively constant (Bowers and Wong 1980), the concentration of creatinine was used in previous studies as an indicator of kidney filtration to normalize the concentration of other urinary biomarkers (Morrow *et al.* 1990, Renner *et al.* 2000, Waikar *et al.* 2010, Lam *et al.* 2012).

Table 6. Overview of main influencing factors of travel period.

	7 days mean concentration of $PM_{2.5}$ levels before measurement ($\mu g/m^3$)										
Volunteer	S0* (Munich)	S1 (China)	S2 (Munich)	S3 Munich)	S4 (Munich)	$\Delta PM_{2.5}$ (S0, S1)	$\Delta PM_{2.5}$ (S1, S2)	Severe Passive-Smoking	Travel duration (days)	Taken for further considerations	Remark
A01	24	83	29	12	16	58	53	Yes	24	No	A**
A02	24	83	31	10	16	58	52	No	24	Yes	
A03	28	172	18	15	20	144	154	No	29	Yes	
A04	28	105	37	19	20	77	68	No	40	Yes	
A05	16	179	18	15	20	163	161	No	26	Yes	
A06	13	86	32	23	20	73	54	Yes	38	No	A
A07	32	208	18	15	20	176	190	No	27	Yes	
A08	19	113	28	27	16	94	85	No	8	No	B
A09	13	31	30	24	15	18	1	No	26	No	

*S0, S1, S2, S3 and S4 Sampling cycle: S0, one day before leaving Munich; S1, first day after return to Munich; S2, one week after return to Munich; S3, two weeks after return to Munich; S4, four weeks after return to Munich.
**A: Severe passive smoking; B: Short travel duration.

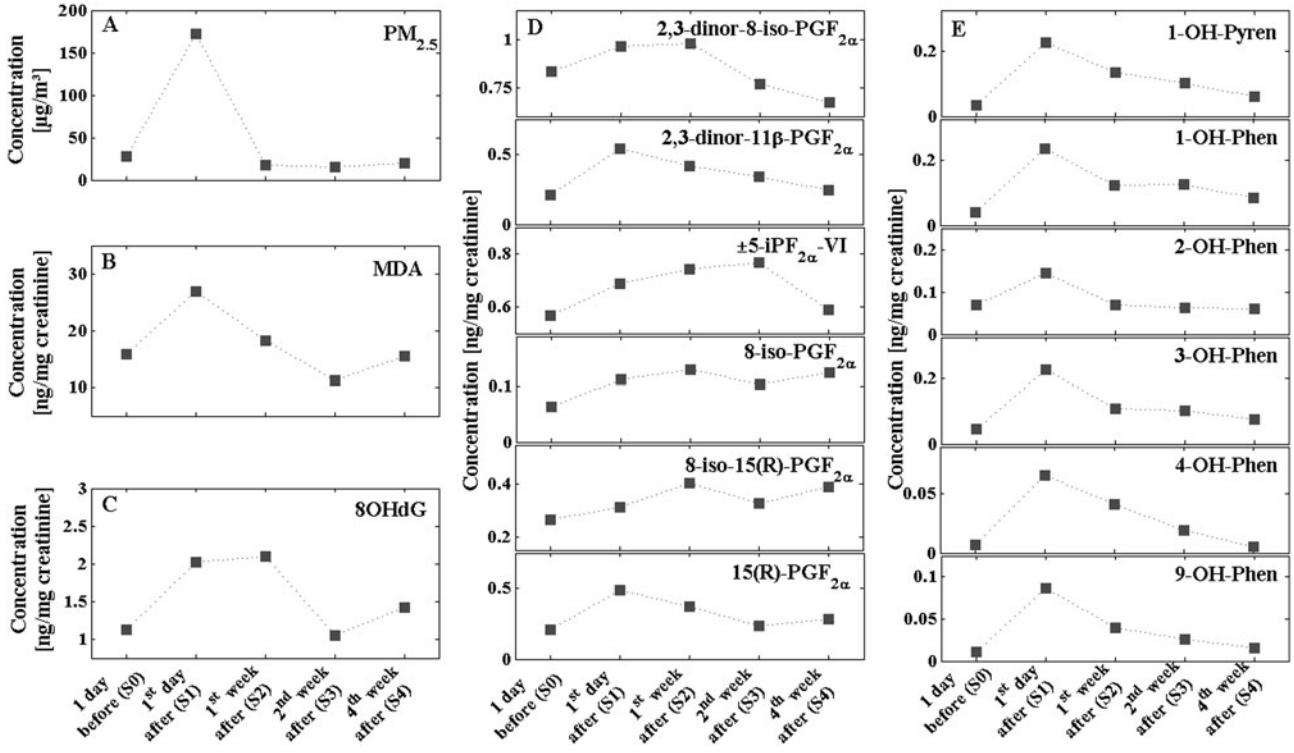

Figure 2. Time trend curves for the median values of: (A) $PM_{2.5}$-concentration; (B) Concentration of malondialdehyde, a biomarker of lipid peroxidation (oxidative stress); (C) Concentration of 8-Hydroxy-2'-deoxyguanosine, a biomarker of oxidative DNA damage (oxidative stress); (D) Concentration of isoprostanes, biomarkers of arachidonic acid oxidations (oxidative stress); (E) Concentration of hydroxylated PAHs, biomarkers of polycyclic aromatic hydrocarbon exposure in the urine of the travellers (valid cases A02, A03, A04, A05, A07) starting with before travel (S0), directly after travel (S1) and the 4 weeks after return (S2, S3, S4).

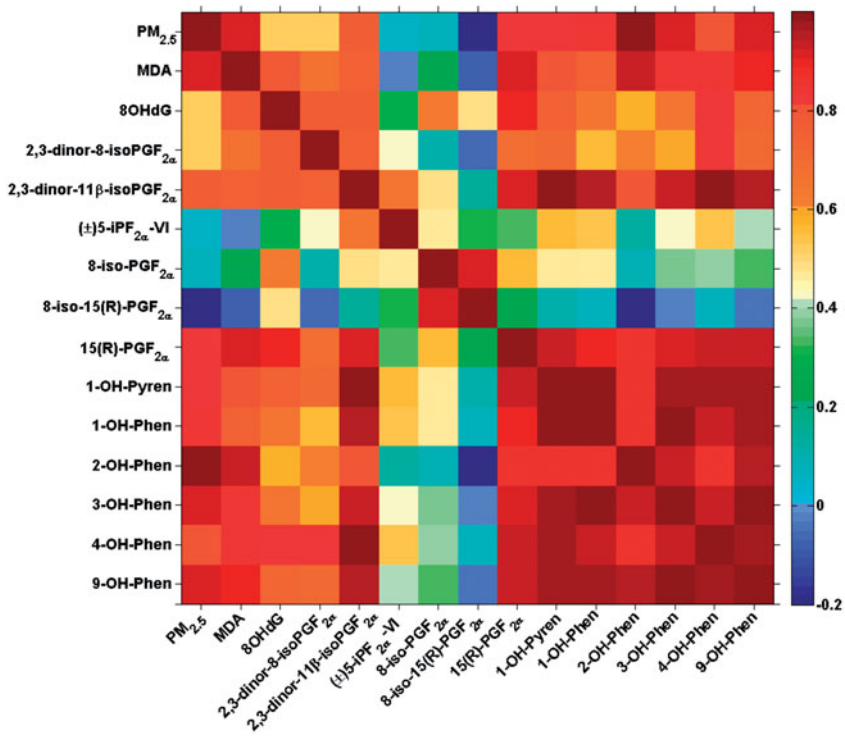

Figure 3. Heatmap of the correlation coefficient for median values of the $PM_{2.5}$-concentrations, the concentration of malondialdehyde (MDA), the concentration of 8-Hydroxy-2'-deoxyguanosine (8OHdG), the concentration of isoprostanes, and the concentration of hydroxylated PAHs. It can be seen that very high correlations are observed between $PM_{2.5}$ exposure MDA (lipid peroxidation) and the PAH exposure biomarker. The isoprostanes are less well correlated, probably due to a longer excretion time constant.

However, it should be noted that Stiegel *et al.* (2015) investigated 280 urine samples from 29 healthy adults and found that creatinine level is inversely related to urinary excretion rate (r^2=0.6858). But more than 30% of creatinine variance is from sources beyond dilution/hydration (Stiegel *et al.* 2015). In future studies, cautious consideration should be taken when using creatinine correction. Besides, a 24-h complete urine collection is more accurate with more reliable information. In this study, spot sample collection was nevertheless employed because it is less time consuming and more convenient for volunteers.

In the refined cohort, decreasing trends of biomarkers and high correlation coefficients were found. Syslova *et al.* (2009) also reported the associations between oxidative stress, $F_{2\alpha}$-isoprostanes and MDA. Pope *et al.* (2002) investigated a cohort consisting of 1.2 million citizens and found associations between daily air pollution and increased risk of various health effects. The decreasing trends lasted for 2–4 weeks for most of the biomarkers while the downtrends of OH-PAHs lasted for only 1–2 weeks till pre-travel values were achieved. Similar trends of urinary OH-PAH concentrations were also observed by Lin *et al.* (2016) after investigating 10 students who travelled between China and the USA and by Thai *et al.* (2015) after analysing urine samples of a family which travelled between Vietnam and Australia. This indicates, in accordance with the literature (Wu *et al.* 1998), a faster removal pathway from the organism, for PAH. The differences in the $PM_{2.5}$ concentrations between China and Germany match the overall increasing (S0 and S1) and decreasing (S1 to S4) trends of oxidative stress biomarkers and PAH metabolites although the patterns of $F_{2\alpha}$-isoprostanes and 8OHdG varied. Allen *et al.* (2009) exposed 10 volunteers to air with a high $PM_{2.5}$ concentration ($205.3 \pm 6.2\ \mu g/m^3$) for 2 h, and no significant variations of $F_{2\alpha}$-isoprostanes or 8OHdG concentrations were observed in the next 90 min, 3 h, 6 h, 12 h and 22 h after exposure. We suppose that there is a lag between the exposure and the yield of $F_{2\alpha}$-isoprostanes/8OHdG, which can be even one or two weeks long, due to the differences in pathways while MDA was generated much faster after the exposure. This is also supported by the results of Lin *et al.* (2015): before and during the 2008 Beijing Olympic Games, associations between air pollutants and 8OHdG/MDA were investigated. Their results showed fast response of pollutants/MDA while lags were found between pollutants and 8OHdG. Associations were also observed within the group of OH-PAHs, and between OH-PAHs/MDA and OH-PAHs/$PM_{2.5}$. As one of the most important $PM_{2.5}$ pollutants, recent studies underline the associations between OH-PAHs and oxidative stress biomarkers of exposure to PAH (Grimmer *et al.* 1997, Strickland and Kang 1999, Motorykin *et al.* 2015). Long-term effects were studied: Wang *et al.* (2015) and Guo *et al.* (2014) reported the increase of 8OHdG and 8-iso-$PGF_{2\alpha}$ upon occupational exposure to coke ovens. Noh *et al.* (2015) reported a positive correlation between MDA, 8-OHdG and OH-PAH in long-term participants in clean-up work after the Hebei Spirit oil spill. Yang *et al.* (2015), who investigated a rural population in the North China Plain, found a correlation between PAH exposure and MDA, while no statistically significant association was found between PAH exposure and 8OHdG. This may also be due to the lag between exposure and 8OHdG production. Overall, our study matches these previous studies, and the hypothesis that travellers who were

exposed to worse air conditions during travel showed rapid health responses was supported. It seems that different oxidative stress biomarkers are generated through different pathways at different rates, which should be considered in further studies of acute effects related to air pollution.

Conclusions

The results of the present study are as follows:

- The optimized methods show high practicability and reliability. Thus, they can be used for routine analyses in future studies.
- The investigated volunteers who were exposed to high levels of $PM_{2.5}$ conditions showed increased concentrations of biomarkers for PAH exposure.
- High oxidative stress and oxidative DNA damages evolved fast and significantly.
- The concept of using air-travellers as model is feasible and worth to be further explored within a larger cohort.

To the best of our knowledge, this study is the first of using travellers to study rapid health responses taking into consideration biomarkers of exposure, biomarkers of oxidative stress and environmental $PM_{2.5}$ exposure as well. We propose the concept of non-invasive urine sampling and biomarker analysis before and after travel between locations with different $PM_{2.5}$ concentrations as a simple and cost-effective method for further studies on the biological and health effects of human exposure to air pollution, including fundamental and applied public health and epidemiological studies.

Since this cohort is a pilot study with a limited number of volunteers, we are not able to prove if the flight period is another key impactor of oxidative stress. However, former studies on occupational exposure of cabin crew members and pilots indicate that flights which forbid in-cabin smoking are not likely to induce air pollution-caused oxidative stress due to the high air exchange rate and efficient air filtration (Lindgren and Norback 2002).

We believe that further studies based on the concept of biomarker monitoring in air travellers using larger number of volunteers and different travel routes and time can provide valuable information on the health risks of air pollution. In particular, the recruitment of organized travel groups, where large number of people undergo similar exposure histories, could be advantageous. Additionally, adjunct exposure monitoring, e.g. by a mini-aethalometer for measuring black carbon (soot) concentrations and collecting filters for analysis of the polycyclic aromatic hydrocarbons, might be applied (Schnelle-Kreis *et al.* 2011).

Acknowledgments

We thank all the people who offered their kind help and efforts during the whole project, and in particular, the people who were involved as volunteers during the months of sampling and our colleagues for their inputs.

Disclosure statement

There are no conflicts of interest and the manuscript was conducted by the highest principles of human subject and animal welfare.

Funding

This work was performed and funded in the framework of the following projects: a) "Environmental Nanoparticles and Health: Exposure, Modeling and Epidemiology of Nanoparticles and their Composition within KORA - ULTRA III", funded by Intramural Funding for Environmental Health Projects of Helmholtz Zentrum München; b) "Helmholtz Virtual Institute of Complex Molecular Systems in Environmental Health - HICE-Aerosol and Health", funded by the Impulse and Networking Funds (INF) of the Helmholtz Association (HGF), Germany; c) "New Technology of Pathogenesis, Diagnosis and Treatment of Pneumoconiosis" project, funded by "Significant Innovation Plan of Medical and Health Science and Technology in Shandong Province", China.

References

Ahmadzadehfar, H., *et al*., 2006. Passive cigarette smoking increases isoprostane formation. *Life sciences*, 78, 894–897.

Allen, J., *et al*., 2009. Effect of diesel exhaust inhalation on antioxidant and oxidative stress responses in adults with metabolic syndrome. *Inhalation Toxicology*, 21, 1061–1067.

Boffetta, P., Jourenkova, N., and Gustavsson, P. 1997. Cancer risk from occupational and environmental exposure to polycyclic aromatic hydrocarbons. *Cancer Causes Control*, 8, 444–472.

Bostrom, C.E., *et al*., 2002. Cancer risk assessment, indicators, and guidelines for polycyclic aromatic hydrocarbons in the ambient air. *Environmental Health Perspectives*, 110(Suppl 3), 451–488.

Bowers, L.D., and Wong, E.T. 1980. Kinetic serum creatinine assays. II. A critical evaluation and review. *Clinical Chemistry*, 26, 555–561.

Bressi, M., *et al*., 2013. A one-year comprehensive chemical characterisation of fine aerosol (PM2.5) at urban, suburban and rural background sites in the region of Paris (France). *Atmospheric Chemistry and Physics*, 13, 7825–7844.

Chan, C.K., and Yao, X. 2008. Air pollution in mega cities in China. *Atmospheric Environment*, 42, 1–42.

Chen, J.L., *et al*., 2011. Determination of urinary malondialdehyde by isotope dilution LC-MS/MS with automated solid-phase extraction: a cautionary note on derivatization optimization. *Free Radical Biology and Medicine* 51, 1823–1829.

Czauderna, M., Kowalczyk, J., and Marounek, M. 2011. The simple and sensitive measurement of malondialdehyde in selected specimens of biological origin and some feed by reversed phase high performance liquid chromatography. *Journal of Chromatography B-Analytical Technologies in the Biomedical and Life Sciences*, 879, 2251–2258.

Dams, R., *et al*., 2003. Matrix effect in bio-analysis of illicit drugs with LC-MS/MS: influence of ionization type, sample preparation, and biofluid. *Journal of the American Society for Mass Spectrometry*, 14, 1290–1294.

de Kok, T.M., *et al*., 2006. Toxicological assessment of ambient and traffic-related particulate matter: a review of recent studies. *Mutation Research*, 613, 103–122.

Dizdaroglu, M. 2012. Oxidatively induced DNA damage: mechanisms, repair and disease. *Cancer Letters*, 327, 26–47.

Dreissigacker, U., *et al*., 2010. Human plasma concentrations of malondialdehyde (MDA) and the F-2-isoprostane 15(S)-8-iso-PGF(2 alpha) may be markedly compromised by hemolysis: evidence by GC-MS/MS and potential analytical and biological ramifications. *Clinical Biochemistry*, 43, 159–167.

Dumax-Vorzet, A.F., *et al*., 2015. Cytotoxicity and genotoxicity of urban particulate matter in mammalian cells. *Mutagenesis*, 30, 621–633.

Evans, M.D., Dizdaroglu, M., and Cooke, M.S. 2004. Oxidative DNA damage and disease: induction, repair and significance. *Mutation Research – Reviews in Mutation Research*, 567, 1–61.

Evans, M.D., Saparbaev, M., and Cooke, M.S. 2010. DNA repair and the origins of urinary oxidized 2'-deoxyribonucleosides. *Mutagenesis*, 25, 433–442.

Franco, S.S., Nardocci, A.C., and Gunther, W.M. 2008. PAH biomarkers for human health risk assessment: a review of the state-of-the-art. *Cadernos de Saude Publica*, 24(Suppl 4), s569–s580.

Giera, M., Lingeman, H., and Niessen, W.M. 2012. Recent advancements in the LC- and GC-based analysis of malondialdehyde (MDA): a brief overview. *Chromatographia*, 75, 433–440.

Grimmer, G., *et al*., 1997. Determination of urinary metabolites of polycyclic aromatic: hydrocarbons (PAH) for the risk assessment of PAH-exposed workers. *International Archives of Occupational and Environmental Health*, 69, 231–239.

Guo, H., *et al*., 2014. Women are more susceptible than men to oxidative stress and chromosome damage caused by polycyclic aromatic hydrocarbons exposure. *Environmental and Molecular Mutagenesis*, 55(6), 472–481.

Halliwell, B. 2007. Oxidative stress and cancer: have we moved forward? *Biochemical Journal*, 401, 1–11.

Hsu, J.L., *et al*., 2003. Stable-isotope dimethyl labeling for quantitative proteomics. *Analytical Chemistry*, 75, 6843–6852.

Jaligama, S., *et al*., 2015. Exposure to deepwater horizon crude oil burn-off particulate matter induces pulmonary inflammation and alters adaptive immune response. *Environmental Science & Technology*, 49, 8769–8776.

Kampa, M., and Castanas, E. 2008. Human health effects of air pollution. *Environmental Pollution*, 151, 362–367.

Klein, J.C., *et al*., 1992. Repair and replication of plasmids with site-specific 8-oxodG and 8-AAFdG residues in normal and repair-deficient human cells. *Nucleic Acids Research*, 20, 4437–4443.

Kumarathasan, P., *et al*., 2015. Nitrative stress, oxidative stress and plasma endothelin levels after inhalation of particulate matter and ozone. *Particle and Fibre Toxicology*, 12, 28.

Lam, P.M.W., *et al*., 2012. Rapid measurement of 8-oxo-7,8-dihydro-2′-deoxyguanosine in human biological matrices using ultra-high-performance liquid chromatography-tandem mass spectrometry. *Free Radical Biology and Medicine*, 52, 2057–2063.

Lin, W., *et al*., 2015. Association between changes in exposure to air pollution and biomarkers of oxidative stress in children before and during the Beijing Olympics. *American Journal of Epidemiology*, 181, 575–583.

Lin, Y., *et al*., 2016. Urinary metabolites of polycyclic aromatic hydrocarbons and the association with lipid peroxidation: a biomarker-based study between Los Angeles and Beijing. *Environmental Science & Technology*, 50, 3738–3745.

Lindgren, T., and Norback, D. 2002. Cabin air quality: indoor pollutants and climate during intercontinental flights with and without tobacco smoking. *Indoor Air*, 12, 263–272.

Lintelmann, J., Hellemann, C., and Kettrup, A. 1994. Coupled-column high-performance liquid chromatographic method for the determination of four metabolites of polycyclic aromatic hydrocarbons, 1-, 4- and 9-hydroxyphenanthrene and 1-hydroxypyrene, in urine. *Journal of Chromatography B, Biomedical Applications*, 660, 67–73.

McCord, J.M. 1993. Human disease, free radicals, and the oxidant/antioxidant balance. *Clinical Biochemistry*, 26, 351–357.

Medina, S., *et al*., 2012. A ultra-pressure liquid chromatography/triple quadrupole tandem mass spectrometry method for the analysis of 13 eicosanoids in human urine and quantitative 24 hour values in healthy volunteers in a controlled constant diet. *Rapid Communications in Mass Spectrometry*, 26, 1249–1257.

Milne, G.L., Yin, H., and Morrow, J.D. 2008. Human biochemistry of the isoprostane pathway. *Journal of Biological Chemistry*, 283, 15533–15537.

Mori, T.A., *et al*., 2000. Effect of omega 3 fatty acids on oxidative stress in humans: GC-MS measurement of urinary F-2-isoprostane excretion. *Redox Report*, 5, 45–46.

Morrow, J.D., *et al*., 1990. A series of prostaglandin F2-like compounds are produced in vivo in humans by a non-cyclooxygenase, free radical-catalyzed mechanism. *Proceedings of the National Academy of Sciences USA*, 87, 9383–9387.

Motorykin, O., *et al*., 2015. Determination of parent and hydroxy PAHs in personal PM(2).(5) and urine samples collected during Native American fish smoking activities. *Science of the Total Environment*, 505, 694–703.

Noh, S.R., *et al*., 2015. Oxidative stress biomarkers in long-term participants in clean-up work after the Hebei Spirit oil spill. *Science of the Total Environment*, 515, 207–214.

Pardo, M., *et al*., 2015. Single exposure to near roadway particulate matter leads to confined inflammatory and defense responses: possible role of metals. *Environmental Science & Technology*, 49, 8777–8785.

Pilz, J., Meineke, I., and Gleiter, C.H. 2000. Measurement of free and bound malondialdehyde in plasma by high-performance liquid chromatography as the 2,4-dinitrophenylhydrazine derivative. *Journal of chromatography. B, Biomedical Sciences and Applications* 742, 315–325.

Pope 3rd, C. A., *et al*., 2002. Lung cancer, cardiopulmonary mortality, and long-term exposure to fine particulate air pollution. *Journal of the American Medical Association*, 287, 1132–1141.

Renner, T., Fechner, T., and Scherer, G. 2000. Fast quantification of the urinary marker of oxidative stress 8-hydroxy-2 '-deoxyguanosine using solid-phase extraction and high-performance liquid chromatography with triple-stage quadrupole mass detection. *Journal of Chromatography B*, 738, 311–317.

Risom, L., Moller, P., and Loft, S. 2005. Oxidative stress-induced DNA damage by particulate air pollution. *Mutation Research*, 592, 119–137.

Rossnerova, A., *et al*., 2011. Automated scoring of lymphocyte micronuclei by the MetaSystems Metafer image cytometry system and its application in studies of human mutagen sensitivity and biodosimetry of genotoxin exposure. *Mutagenesis*, 26, 169–175.

Schnelle-Kreis, J., *et al*., 2011. Application of direct thermal desorption gas chromatography time-of-flight mass spectrometry for determination of nonpolar organics in low-volume samples from ambient particulate matter and personal samplers. *Analytical and Bioanalytical Chemistry*, 401, 3083–3094.

Sijan, Z., *et al*., 2015. An in vitro alveolar macrophage assay for the assessment of inflammatory cytokine expression induced by atmospheric particulate matter. *Environmental Toxicology*, 30, 836–851.

Solak, Z.A., *et al*., 2005. Effect of different levels of cigarette smoking on lipid peroxidation, glutathione enzymes and paraoxonase 1 activity in healthy people. *Clinical and Experimental Medicine*, 5, 99–105.

Stiegel, M.A., *et al*., 2015. Kidney injury biomarkers and urinary creatinine variability in nominally healthy adults. *Biomarkers*, 20, 436–452.

Strickland, P., and Kang, D. 1999. Urinary 1-hydroxypyrene and other PAH metabolites as biomarkers of exposure to environmental PAH in air particulate matter. *Toxicology Letters*, 108, 191–199.

Syslova, K., *et al*., 2009. Rapid and easy method for monitoring oxidative stress markers in body fluids of patients with asbestos or silica-induced lung diseases. *Journal of Chromatography B, Analytical Technologies in the Biomedical and Life Sciences*, 877, 2477–2486.

Taylor, A.W., and Traber, M.G. 2010. Quantitation of plasma total 15-series F-2-isoprostanes by sequential solid phase and liquid-liquid extraction. *Analytical Biochemistry*, 396, 319–321.

Taylor, P.J. 2005. Matrix effects: the Achilles heel of quantitative high-performance liquid chromatography-electrospray-tandem mass spectrometry. *Clinical Biochemistry*, 38, 328–334.

Thai, P.K., *et al*., 2015. Biomonitoring of polycyclic aromatic hydrocarbons exposure in small groups of residents in Brisbane, Australia and Hanoi, Vietnam, and those travelling between the two cities. *Chemosphere*, 139, 358–364.

Valavanidis, A., Vlachogianni, T., and Fiotakis, C. 2009. 8-hydroxy-2′ -deoxyguanosine (8-OHdG): a critical biomarker of oxidative stress and carcinogenesis. *Journal of Environmental Science and Health*

Part C – Environmental Carcinogenesis & Ecotoxicology Reviews, 27, 120–139.

Waikar, S.S., Sabbisetti, V.S., and Bonventre, J.V. 2010. Normalization of urinary biomarkers to creatinine during changes in glomerular filtration rate. *Kidney International*, 78, 486–494.

Walter, M.F., *et al*., 2000. Streamlined F-2-isoprostane analysis in plasma and urine with high-performance liquid chromatography and gas chromatography/mass spectroscopy. *Analytical Biochemistry*, 280, 73–79.

Wampler, F.M., Blades, A.T., and Kebarle, P. 1993. Negative ion electrospray mass spectrometry of nucleotides: ionization from water solution with SF6 discharge suppression. *Journal of the American Society for Mass Spectrometry*, 4, 289–295.

Wang, T., *et al*., 2015. The effects of heavy metals and their interactions with polycyclic aromatic hydrocarbons on the oxidative stress among coke-oven workers. *Environmental Research*, 140, 405–413.

Wu, M.T., *et al*., 1998. Cytochrome P450 1A1 MspI polymorphism and urinary 1-hydroxypyrene concentrations in coke-oven workers. *Cancer Epidemiology, Biomarkers & Prevention*, 7, 823–829.

Yang, Q.Y., *et al*., 2015. Polycyclic aromatic hydrocarbon (PAH) exposure and oxidative stress for a rural population from the North China Plain. *Environmental Science and Pollution Research*, 22, 1760–1769.

Yao, Q.H., *et al*., 2004. Determination of urinary oxidative DNA damage marker 8-hydroxy-2'-deoxyguanosine and the association with cigarette smoking . *Talanta*, 63, 617–623.

International Journal of Hygiene and Environmental Health 244 (2022) 113993

Contents lists available at ScienceDirect

International Journal of Hygiene and Environmental Health

journal homepage: www.elsevier.com/locate/ijheh

Assessment of the association of exposure to polycyclic aromatic hydrocarbons, oxidative stress, and inflammation: A cross-sectional study in Augsburg, Germany

Xiao Wu [a,b], Xin Cao [a,b], Jutta Lintelmann [c], Annette Peters [d,e,f], Wolfgang Koenig [g,h,i], Ralf Zimmermann [a,b], Alexandra Schneider [d,1], Kathrin Wolf [d,1,*], for the KORA-Study group [2]

[a] Division of Analytical and Technical Chemistry, Institute of Chemistry, University of Rostock, Rostock, Germany
[b] Cooperation Group of Comprehensive Molecular Analytics, Helmholtz Zentrum München, Neuherberg, Germany
[c] Metabolomics and Proteomics Core, Helmholtz Zentrum München, Neuherberg, Germany
[d] Institute of Epidemiology, Helmholtz Zentrum München, Neuherberg, Germany
[e] German Center for Diabetes Research, Munich, Germany
[f] Institute for Medical Information Processing, Biometry and Epidemiology, Medical Faculty, Ludwig Maximilian University of Munich, Munich, Germany
[g] German Heart Centre Munich, Technical University of Munich, Munich, Germany
[h] DZHK, German Centre for Cardiovascular Research, Partner Site Munich, Munich, Germany
[i] Institute of Epidemiology and Medical Biometry, University of Ulm, Ulm, Germany

ARTICLE INFO

Keywords:
PAH
Oxidative stress
Inflammation
Biomarker
Air pollution

ABSTRACT

Background: Exposure to polycyclic aromatic hydrocarbons (PAHs) has been linked to acute and chronic health effects through the suggested pathways of oxidative stress and inflammation. However, evidence is still limited. We aimed to investigate jointly the relationship of PAHs, oxidative stress, and inflammation.

Methods: We measured 13 biomarkers of PAH exposure (n = 6: hydroxylated polycyclic aromatic hydrocarbons, [OH-PAHs]), oxidative stress (n = 6: malondialdehyde (MDA); 8-hydroxy-2′-deoxyguanosine (8-OHdG); and 4 representatives of the compound class of $F_{2\alpha}$-isoprostanes) in urine, and inflammation (n = 1: high-sensitivity C-reactive protein, [hs-CRP]) in serum from 400 participants at the second follow-up (2013/2014) of the German KORA survey S4. Multiple linear regression models were applied to investigate the interplay between biomarkers.

Results: Concentrations of biomarkers varied according to sex, age, smoking status, season, and a history of obesity, diabetes, or chronic kidney disease. All OH-PAHs were significantly and positively associated with oxidative stress biomarkers. An interquartile range (IQR) increase in sum OH-PAHs was associated with a 13.3% (95% CI: 9.9%, 16.9%) increase in MDA, a 6.5% (95% CI: 3.5%, 9.6%) increase in 8-OHdG, and an 8.4% (95% CI: 6.6%, 11.3%) increase in sum $F_{2\alpha}$-isoprostanes. Associations were more pronounced between OH-PAHs and $F_{2\alpha}$-isoprostanes but also between OH-PAHs and 8-OHdG for participants with potential underlying systemic inflammation (hs-CRP $\geq$ 3 mg/L). We observed no association between OH-PAHs and hs-CRP levels. While 8-OHdG was significantly positively associated with hs-CRP (13.7% [95% CI: 2.2%, 26.5%] per IQR increase in 8-OHdG), $F_{2\alpha}$-isoprostanes and MDA indicated only a positive or null association, respectively.

Conclusion: The results of this cross-sectional study suggest, at a population level, that exposure to PAHs is associated with oxidative stress even in a low exposure setting. Oxidative stress markers, but not PAHs, were associated with inflammation. Individual risk factors were important contributors to these processes and should be considered in future studies. Further longitudinal studies are necessary to investigate the causal chain of the associations.

* Corresponding author. Institute of Epidemiology, Helmholtz Zentrum München, Ingolstaedter Landstr. 1, 85764, Neuherberg, Germany.
E-mail address: kathrin.wolf@helmholtz-muenchen.de (K. Wolf).

[1] Shared last authorship.

[2] The KORA-Study Group consists of A. Peters (speaker), L. Schwettmann, R. Leidl, M. Heier, B. Linkohr, H. Grallert, C. Gieger, J. Linseisen and their co-workers, who are responsible for the design and conduct of the KORA studies.

https://doi.org/10.1016/j.ijheh.2022.113993
Received 8 January 2022; Received in revised form 18 May 2022; Accepted 5 June 2022
Available online 28 June 2022

1. Introduction

Polycyclic aromatic hydrocarbons (PAHs) are non-polar, semi-volatile, organic pollutants composed of several aromatic rings (Keyte et al., 2013). They are ubiquitous and hazardous pollutants which are generated during incomplete combustion of organic materials. Traffic emissions, domestic combustion, and industry practices are suggested to be the main anthropogenic sources of PAHs in urban areas (Kamal et al., 2015).

A large proportion of anthropogenically and naturally generated PAHs is occurring and transported in the air, and here – depending on physico-chemical parameters – bound to particles or in the gas phase (Kraus et al., 2011; Li et al., 2021; Liu et al., 2019). Worldwide, strong efforts are performed to control and decrease the ambient PAH-concentrations by creating limiting regulations and applying new technologies for anthropogenic processes such as heating, industrial processes and traffic. This is on the one hand reflected by relatively low PAH concentrations in our study region as previously reported (Li et al., 2018). On the other hand, depending on the current meteorological conditions (season in general but also specific events), PAHs levels can be significantly increased, either nationwide or only at specific sites (Fuchte et al., 2022). Additionally, it is expected that climate change has an impact on PAH-levels (Garrido et al., 2014) which is not yet fully understood. PAHs are one of the major groups of ambient pollutants that cause severe health effects and have been investigated for decades. Lipophilic PAHs can be absorbed via dermal, respiratory, or ingestion routes (Andersen et al., 2018; VanRooij et al., 1993). Short-term exposure to PAHs can cause acute health effects such as eye and skin irritation, headache, nausea, and vomiting. They can also induce inflammatory processes (Al-Delaimy et al., 2014). Long-term exposure to PAHs can lead to chronic health issues, such as chronic obstructive pulmonary disease, diabetes, and cardiovascular diseases (Alshaarawy et al., 2016; Cao et al., 2020; Yang et al., 2017). PAHs were also related to oxidative stress, genotoxicity, and carcinogenicity in both in vitro and in vivo studies (Danielsen et al., 2011; Kumar et al., 2020; Lan et al., 2004; Lu et al., 2016; McCarrick et al., 2019).

Individuals are always exposed to complex mixtures of low molecular weight, medium molecular weight and high molecular weight PAHs, and with current analytical methods it is impossible to comprehensively reflect the ways of metabolic transformation and excretion of all PAHs after their absorption in the organism. The use of biomarkers allows the assessment of the individual, internal PAH burden, and the determination of monohydroxylated PAHs (OH-PAHs) in urine have been previously used for this purpose (Aquilina et al., 2010; Ifegwu and Anyakora, 2016; Mesquita et al., 2014; Urbancova et al., 2016). In this study, we determined 1-OH-pyrene, the main urinary metabolite of pyrene, and five urinary isomeric OH-phenanthrenes originating from phenanthrene. Pyrene and phenanthrene are medium molecular weight PAHs, which are both abundant in typical environmental PAH-mixtures together with further, especially higher molecular weight PAHs. In contrast to those higher molecular weight PAHs, the OH-PAH metabolites of pyrene and phenanthrene can be reliably determined in low volume urine samples, and their concentrations – especially 1-hydroxypyrene concentrations - can be used for estimating the individual exposure to PAHs.

Oxidative stress is an important pathway linking exposure to ambient pollution and acute and chronic diseases (Peters et al., 2021). The induction of a disease process begins with the generation of oxidative stress in the organism. Once the pollutants are absorbed, the formation of reactive oxygen species (ROS) such as peroxides, superoxides, hydroxyl radicals, and singlet oxygen can be initiated (Apel and Hirt, 2004; Tao et al., 2003). These species can attack and modify adjacent macromolecules such as proteins, DNA, and lipids in vivo (Risom et al., 2005). Humans have protective mechanisms against ROS, such as antioxidants, or the activation of specific enzymatic processes to remove ROS species and maintain the oxidative stress balance. If this subtle balance is disturbed (Droge, 2002), oxidative stress and the resulting attack on macromolecules can lead to acute and chronic diseases of the respiratory, cardiovascular, or immunological systems (McCord, 1993; Michael et al., 2013; Miller, 2020; Taverne et al., 2013).

Due to the high reactivity of ROS species, direct quantification is critical. Some by-products or end products of oxidative stress that are excreted through faeces or urine can be quantified. We selected the established biomarkers malondialdehyde (MDA), 8-hydroxy-2′-deoxyguanosine (8-OHdG), and the compound class of $F_{2\alpha}$-isoprostanes. MDA, 8-OHdG, and $F_{2\alpha}$-isoprostanes reflect the amount of damaged double bonds of polyunsaturated fatty acids (PUFAs) (Ayala et al., 2014; Yoon et al., 2012), damaged DNA (Evans et al., 2010; Valavanidis et al., 2009), and damaged membrane phospholipids (Galano et al., 2017; Milne et al., 2008; Morrow and Roberts, 1996), respectively. Using a combination of oxidative stress biomarkers increases reliability when assessing individual oxidative stress levels (Zhu et al., 2021).

Inflammation is another possible pathway for air pollution-initiated health effects. Previous epidemiological studies have reported that long-term exposure to ambient pollutants is associated with increased serum levels of C-reactive protein (CRP), a well-known marker for inflammation (Everett et al., 2010; Hennig et al., 2014; Ostro et al., 2014; Pilz et al., 2018). Toxicological studies have led to similar observations—exposure to air pollution induces inflammatory responses such as increased CRP concentrations in human blood (Chuang et al., 2007). Systemic inflammation is induced by ambient air pollution via the production of cytokines such as tumor necrosis factor-α and interleukin-8 (Pope et al., 2016). Previous studies also indicated that PAH exposure is positively associated with oxidative stress and inflammation (Clark et al., 2012; Everett et al., 2010; Farzan et al., 2016; Ferguson et al., 2017; Gerlofs-Nijland et al., 2009; Lu et al., 2016; Vattanasit et al., 2014).

Although many studies have investigated the associations between OH-PAHs and oxidative stress or between OH-PAHs and inflammation or OH-PAHs and lifestyle factors and health characteristics, only two epidemiological studies have jointly considered the interplay, however both being limited by small and/or highly selected populations (Ferguson et al., 2017; Zhang et al., 2020). To fill this gap, we conducted this cross-sectional study among the general adult population and examined if (1) the concentration of OH-PAHs, oxidative stress markers, and high-sensitivity CRP (hs-CRP) varied among subgroups; (2) OH-PAHs were associated with oxidative stress, including potential effect modification by underlying systemic inflammation because large amount of ROS could be generated during the inflammatory process and disturb the balance (Fialkow et al., 2007); (3) OH-PAHs were associated with hs-CRP and (4) the selected oxidative stress markers were similarly associated with hs-CRP.

2. Methods

2.1. Study population

We included a selected subgroup of 400 subjects at different stages of impaired glucose metabolism without prior cardiovascular disease who participated in 2013/2014 in the second follow-up (FF4) of the baseline KORA (Cooperative Health Research in the region of Augsburg) S4 study (1999–2001, N = 4261) (Bamberg et al., 2017). Participants were invited to the study center in Augsburg, where they answered a computer-assisted personal interview and completed a self-administered questionnaire. All individuals were physically examined, and urine and blood samples were collected. The general KORA study design, sampling method, and data collection have been described in detail by Holle et al. (2005). All participants provided written informed consent to participate in the study which was approved by the ethics committee of the Bavarian Medical Association.

2.2. Urinary biomarker measurements

For each participant, a spot urine sample was collected. For further processing, the samples were stored at −80 °C in a central storage unit. All urinary biomarkers were analysed in our lab in 2015/16 using previously established liquid chromatography (LC)- based methods. OH-PAHs (1-OH-Phe, 1-hydroxyphenanthrene; 2-OH-Phe, 2-hydroxyphenanthrene; 3-OH-Phe, 3-hydroxyphenanthrene; 4-OH-Phe, 4-hydroxyphenanthrene; 9-OH-Phe, 9-hydroxyphenanthrene; 1-OH-Pyr, 1-hydroxypyrene) were measured on an Ultimate 3000 HPLC system with an RF 2000 fluorescence detector (Thermo Scientific, Dreieich, Germany) (Lintelmann et al., 2018). MDA, 8-OHdG, and $F_{2\alpha}$-isoprostanes (2,3-dinor-8-iso-$PGF_{2\alpha}$, 8-iso-15(R)-$PGF_{2\alpha}$, 8-iso-$PGF_{2\alpha}$, and ±5-$iPF_{2\alpha}$) were determined with LC-mass spectrometry, using a triple quadrupole mass spectrometer API-4000 (AB Sciex, Darmstadt, Germany) equipped with an electrospray ion source (ESI) (Wu et al., 2017). The sum concentrations of OH-PAHs (1-OH-Phe, 2-OH-Phe, and 3-OH-Phe) (Hou et al., 2019; Lu et al., 2016) and the sum concentration of $F_{2\alpha}$ -isoprostanes (Montuschi et al., 2004) were calculated. OH-PAHs, biomarkers of oxidative stress, and creatinine concentrations which were below the limit of detection (LOD) were set to half of the concentration of the LOD ($N_{1\text{–OH-Phe}} = 8$, $N_{2\text{–OH-Phe}} = 19$, $N_{3\text{–OH-Phe}} = 10$, $N_{4\text{–OH-phe}} = 152$, $N_{9\text{–OH-Phe}} = 260$, $N_{1\text{–OH-Pyr}} = 14$, $N_{MDA} = 0$, $N_{8\text{-OHdG}} = 0$, $N_{2,3\text{-dinor-8-iso-PGF2}\alpha} = 2$, $N_{8\text{-iso-15(R)-PGF2}\alpha} = 4$, $N_{8\text{-iso-PGF2}\alpha} = 6$, $N_{\pm5\text{-iPF2}\alpha} = 1$, $N_{creatinine} = 0$). Since more than 20% of 4-OH-Phe concentrations and 9-OH-Phe concentrations were below the LOD, we did not consider 4-OH-Phe and 9-OH-Phe in later data analysis. Creatinine was quantified on an HP 1100 LC system with an ultraviolet detector (Agilent, St. Clara, CA, USA) (Wu et al., 2017). The concentrations of urinary biomarkers were normalised to creatinine concentrations.

2.3. Individual characteristics and clinical parameters

Fasting venous blood samples were collected during the study participants' visits and stored at 4 °C until further processing. Hs-CRP concentrations in serum samples were assayed by latex-enhanced immunonephelometry on a BN II platform (Siemens Healthcare Diagnostics Product GmbH, Marburg, Germany) with an intra-assay coefficient variation of 2.13% (Pilz et al., 2018). Serum creatinine concentrations were determined using an automated Jaffé method (Technicon, SMAC autoanalyzer; Tarrytown, New York, USA) (Aumann et al., 2015). As a marker for kidney disease, we calculated the estimated glomerular filtration rate (eGFR) (mL/min per 1.73 m^2) using the 2009 CKD-EPI creatinine equation (Levey et al., 2009). Body mass index (BMI) was calculated as the weight divided by height (squared). Type 2 diabetes was validated either by an oral glucose tolerance test, a previous diagnosis, or a current intake of glucose-lowering agents. Pre-diabetes was defined as impaired fasting glucose and/or impaired glucose tolerance. Hypertension was defined as blood pressure >140/90 mmHg or treatment of known hypertension (WHO, 1999).

2.4. Ambient air pollution

Long-term ambient air pollution exposure was estimated using land use regression models for all KORA participants' residential addresses (Wolf et al., 2017). Ambient concentrations of particulate matter smaller than 2.5 μm in aerodynamic diameter ($PM_{2.5}$) and nitrogen dioxide (NO_2) were measured at 20 and 40 sites, respectively, between March 2014 and April 2015, and temporally adjusted for discontinuous site measurements. The annual average concentrations were then modelled using linear regression incorporating predictors such as traffic, land use, population, and building density. Details of the estimation can be found in our previous publication (Wolf et al., 2017).

2.5. Statistical analysis

Spearman correlation coefficients were calculated to explore the relationships of urinary biomarkers, individual characteristics, and clinical parameters.

We performed Kruskal-Wallis tests to compare biomarker concentrations across the subgroups. Obesity was defined as BMI ≥30 kg/m^2, potential underlying inflammation was defined by the hs-CRP concentration ≥3 mg/L, and potential renal impairment as eGFR <90 mL/min/1.73 m^2 (Inker et al., 2012). Seasons were defined as: spring: March to May; summer: June to August; autumn: September to November; winter: December to February.

We used multiple linear regression models to investigate the associations between i) OH-PAHs and oxidative stress, ii) OH-PAHs and hs-CRP, and iii) oxidative stress and hs-CRP. The normalised concentrations of urinary biomarkers and the concentration of hs-CRP were log-transformed to approximate normal distribution of the residuals and to stabilise the variance. In the base model, we included age, sex, smoking, and season as potential confounders, as suggested in a previous study (Yang et al., 2015). The time trend was included to adjust for potential fluctuations during the study period. The smoothing parameter for the trend was chosen by optimising the generalised cross-validation criteria (Wood, 2006). In an extended model, we additionally adjusted for obesity, diabetes, and potential renal impairment. We further included an interaction term to investigate the potential effect modification by underlying systemic inflammation. To evaluate the robustness of our results, we altered our base model adjustment by (1) removing season or (2) additionally adjusting for annual mean concentrations of ambient $PM_{2.5}$ and NO_2 exposure (Spearman correlation 0.71). All statistical analyses were performed using the R Statistical Software (version 3.5.1, R Foundation for Statistical Computing, Vienna, Austria). A two-sided P value < 0.05 was considered to be statistically significant. All effect estimates are presented as percent change of the geometric mean of the biomarkers with corresponding 95% confidence intervals for an interquartile range increase in exposure concentration.

3. Results

3.1. Study population

From the original group of 400 participants, 18 subjects were excluded due to missing values in the main outcomes (OH-PAHs: N = 7; MDA: N = 8; 8-OHdG: N = 9; $F_{2\alpha}$-isoprostanes: N = 9; creatinine: N = 6; extremely low creatinine concentration: N = 1; hs-CRP: N = 4). The mean age of the participants was 56 years (Table 1). Overall, 220 (57%) participants were male, 78 (20%) were smokers, and 163 (43%) reported a smoking history. The geometric mean concentration of hs-CRP was 1.31 mg/L. In total, 80 participants (21%) showed potential underlying inflammation (hs-CRP ≥ 3 mg/L). Overall, 53 participants were diagnosed with diabetes (14%), and 156 participants were diagnosed with pre-diabetes (41%).

The geometric means of the sum OH-PAHs concentration and the concentrations of 1-OH-Phe, 2-OH-Phe, 3-OH-Phe, and 1-OH-Pyr were 0.24, 0.11, 0.05, 0.06, and 0.16 ng/mg creatinine, respectively. The geometric means of the sum of $F_{2\alpha}$-isoprostanes concentration and the concentration of 2,3-dinor-8-iso-$PGF_{2\alpha}$ 8-iso-15(R)-$PGF_{2\alpha}$, 8-iso-$PGF_{2\alpha}$, and ±5-$iPF_{2\alpha}$ were 3.56, 1.71, 0.44, 0.22, and 1.06 ng/mg creatinine, respectively. The geometric mean concentrations of MDA, 8-OHdG, and creatinine in the study participants were 33.77 ng/mg creatinine, 2.94 ng/mg creatinine and 1.08 mg/mL, respectively. The annual means of individual ambient exposure of $PM_{2.5}$ and NO_2 were 11.72 μg/m^3 and 13.62 μg/m^3, respectively. Supplemental Fig. 1 shows the Spearman correlation coefficients between all pairwise combinations of biomarkers and clinical parameters. Strong correlations were observed within the $F_{2\alpha}$-isoprostane group (0.54–0.90) and the OH-PAH group (0.78–0.93). Therefore, we limited parts of the subsequent analyses to

Table 1
Descriptive statistics of the study population (N = 400).

Characteristics	Mean ± SD or Total N (%)	Missing N
Personal Characteristics		
Age (years)	56 ± 9.2	
<55	173 (45%)	
≥55, <65	126 (33%)	
≥65	83 (22%)	
Sex (male)	220 (57%)	
Socio-economic & lifestyle characteristics		
BMI (kg/m^2)	28.1 ± 4.8	
Obese (BMI ≥30 kg/m^2)	116 (30.4%)	
Smoking Status		
Non-smoker	141 (37%)	
Ex-smoker	163 (43%)	
Smoker	78 (20%)	
Clinical Characteristics		
hs-CRP (mg/L) (N = 382)	2.39 ± 3.36	4
Potential underlying inflammation (hs-CRP ≥ 3 mg/L)	80 (21%)	4
eGFR (mL/min/1.73 m^2)	89.9 ± 9.3	7
Potential renal impairment (eGFR <90 mL/min/1.73 m^2)	179 (47%)	7
Diabetes Status		
No Diabetes	173 (45%)	
Pre-diabetes	156 (41%)	
Diabetes	53 (14%)	
Hypertension Status		
Hypertension	130 (34%)	
Characteristics of the day of examination		
Season		
Spring (Mar–May)	129 (34%)	
Summer (Jun–Aug)	98 (26%)	
Autumn (Sep–Nov)	71 (18%)	
Winter (Dec–Feb)	84 (22%)	
Urinary biomarkers (ng/mg Creatinine)		
OH-PAHs	0.34 ± 0.39	7
1-OH-Phe	0.16 ± 0.18	7
2-OH-Phe	0.08 ± 0.12	7
3-OH-Phe	0.10 ± 0.14	7
1-OH-Pyr	0.30 ± 0.39	7
MDA	41.76 ± 38.69	8
8-OHdG	3.35 ± 1.93	9
$F_{2\alpha}$-isoprostanes	4.11 ± 2.92	9
2,3-dinor-8-iso-$PGF_{2\alpha}$	2.08 ± 1.63	7
8-iso-15(R)-$PGF_{2\alpha}$	0.52 ± 0.1	7
8-iso-$PGF_{2\alpha}$	0.27 ± 0.23	9
±5-$iPF_{2\alpha}$	1.24 ± 0.99	7
Creatinine (mg/mL)	1.34 ± 0.81	6
Annual mean of individual ambient exposure (μg/m^3)		
$PM_{2.5}$	11.72 ± 1.01	
NO_2	13.62 ± 4.35	

SD, standard deviation; OH-PAHs, sum OH-PAHs concentration; 1-OH-Phe, 1-hydroxyphenanthrene; 2-OH-Phe, 2-hydroxyphenanthrene; 3-OH-Phe, 1-hydroxyphenanthrene; 1-OH-Pyr, 1-hydroxypyrene; MDA, malondialdehyde; 8-OHdG, 8-hydroxy-2′-deoxyguanosine; $F_{2\alpha}$-isoprostanes, sum $F_{2\alpha}$-isoprostanes concentration; BMI, Body Mass Index; hs-CRP, high sensitivity C-Reactive Protein; eGFR, Estimated Glomerular Filtration Rate from Serum Creatinine and Cystatin C; $PM_{2.5}$, particulate matter smaller than 2.5 μm in aerodynamic diameter; NO_2, nitrogen dioxide.

the sum of OH-PAH concentrations and the sum of $F_{2\alpha}$-isoprostanes concentrations as indicators to reduce the number of tests.

3.2. Distribution of biomarker levels across different subgroups

Table 2 shows the median concentrations of biomarkers in the selected subgroups. MDA concentrations were significantly higher in participants with higher age (≥55 years), potential underlying inflammation, potential renal impairment, or in participants who had their examinations in spring/winter. 8-OHdG concentrations were significantly higher in older participants (age ≥55 years). Concentrations of $F_{2\alpha}$-isoprostanes were significantly higher in female participants or participants who visited the study center in autumn/winter. Hs-CRP concentrations were significantly higher in older participants (≥65 years), potential renal impairment, diabetes, obesity, or hypertension.

3.3. Association between OH-PAHs and biomarkers of oxidative stress

All OH-PAHs were significantly positively associated with oxidative stress biomarkers (Fig. 1). For participants with a potential underlying state of inflammation (hs-CRP ≥ 3 mg/L), we observed stronger associations between OH-PAHs and $F_{2\alpha}$-isoprostanes and between OH-PAHs and 8-OHdG, whereas no differences were observed for MDA (Fig. 2). Additional adjustment for obesity, diabetes, and potential renal impairment did not considerably change the estimates.

3.4. Association between OH-PAHs and hs-CRP

We did not observe an association between the sum of OH-PAHs or single OH-PAHs and hs-CRP for both model adjustment sets, although the estimates tended to be slightly higher in the extended covariate model (Fig. 3).

3.5. Association between biomarkers of oxidative stress and hs-CRP

The effect estimates of the three biomarkers of oxidative stress indicated different patterns of association with hs-CRP (Fig. 4). In the base covariate model, MDA was not associated with hs-CRP, $F_{2\alpha}$-isoprostanes indicated a positive association, and 8-OHdG was significantly positively associated. When additionally adjusting for obesity, diabetes, and potential renal impairment, the positive association between $F_{2\alpha}$-isoprostanes and hs-CRP turned significant.

3.6. Robustness of multiple linear regression models

All effect estimates remained robust when excluding season from the regression models (Supplemental Tables 1–3) or when additionally adjusting for annual mean concentrations of ambient $PM_{2.5}$ and NO_2.

4. Discussion

4.1. Summary

In this cross-sectional study of 400 residents of the Augsburg region (Germany) conducted in 2013/2014, we determined biomarkers of PAH exposure, oxidative stress, and inflammation to investigate the interplay between these three groups of biomarkers. (1) The concentrations of OH-PAHs were comparably lower in our study than in other studies. For example, a study carried out among 300 participants from 7 Asian countries reported that the mean concentrations of 2-OH-Phe, 3-OH-Phe, and 1-OH-Pyr ranged between 0.072–0.58 ng/mL, 0.101–0.714 ng/mL, and 0.167–0.667 ng/mL, respectively (Guo et al., 2013) while in our study, the mean concentrations were 0.09, 0.11, and 0.35 ng/ml, respectively (before normalisation by urinary creatinine). The concentrations of the biomarkers of oxidative stress and inflammation were significantly higher in older (MDA, 8-OHdG, and hs-CRP) and obese (hs-CRP) participants, participants with potential underlying inflammation (MDA) and potential renal impairment (MDA, 8-OHdG and hs-CRP), as well as in participants with diagnosed diseases like type 2 diabetes (hs-CRP) or hypertension (hs-CRP), or for participants who had their clinical visit in spring/winter (MDA) or autumn/winter ($F_{2\alpha}$-isoprostanes) compared to their respective counterparts. (2) Positive associations were found between OH-PAHs and biomarkers of oxidative stress, and were more pronounced in participants with potential underlying inflammation. (3) However, no association was observed between OH-PAH and hs-CRP concentrations. (4) Among the three oxidative stress markers, only 8-OHdG was significantly positively associated with hs-CRP, whereas $F_{2\alpha}$-isoprostanes only indicated a positive association, and

Table 2
Kruskal-Wallis Test of OH-PAHs, oxidative stress, and inflammation biomarkers for different subsets of participants.

	N	OH-PAHs (ng/mg Creatinine)		MDA (ng/mg Creatinine)		8-OHdG (ng/mg Creatinine)		$F_{2\alpha}$-isoprostanes (ng/mg Creatinine)		hs-CRP (mg/L)	
		Median	p	Median	p	Median	p	Median	p	Median	p
Age											
Age <55	173	0.20	0.11	26.57	<0.01	2.66	<0.01	3.68	0.64	1.13	0.04
Age ≥55, <65	126	0.22		32.77		2.98		3.41		1.12	
Age ≥65	83	0.27		37.26		3.49		3.60		1.48	
Sex											
Female	162	0.21	0.16	29.47	0.19	3.20	0.17	3.77	0.01	1.37	0.08
Male	220	0.24		31.95		2.91		3.39		1.12	
Obesity											
No (BMI <30 kg/m^2)	266	0.24	0.01	30.80	0.69	3.10	0.12	3.61	0.57	0.97	<0.01
Yes (BMI ≥30 kg/m^2)	116	0.20		29.40		2.81		3.62		2.27	
Smoking Status											
Non-smoker	141	0.20	<0.01	32.85	0.20	3.25	0.50	3.77	0.08	1.13	0.50
Ex-smoker	163	0.21		29.38		2.96		3.41		1.15	
Smoker	78	0.30		29.54		2.79		3.64		1.51	
Potential underlying systemic inflammation											
No (hs-CRP < 3 mg/L)	302	0.21	0.04	29.74	0.03	2.96	0.08	3.58	0.55	–	–
Yes (hs-CRP ≥ 3 mg/L)	80	0.26		33.42		3.21		3.67		–	
Potential renal impairment											
No (eGFR ≥90 mL/min/1.73 m^2)	199	0.22	0.72	28.45	0.01	2.90	0.04	3.74	0.08	1.10	0.02
Yes (eGFR <90 mL/min/1.73 m^2)	179	0.23		33.32		3.18		3.45		1.38	
Type 2 Diabetes											
No	173	0.21	0.46	28.86	0.09	2.92	0.19	3.63	0.58	0.93	<0.01
Pre	156	0.22		31.24		3.06		3.51		1.62	
Yes	53	0.26		34.81		3.18		3.74		1.15	
Hypertension											
No	253	0.21	0.97	29.55	0.30	2.94	0.08	3.68	0.29	1.11	<0.01
Yes	139	0.23		32.18		3.18		3.41		1.41	
Season											
Spring (Mar–May)	129	0.20	<0.01	34.77	<0.01	3.09	0.24	3.68	<0.01	1.11	0.77
Summer (Jun–Aug)	98	0.19		24.35		2.79		2.73		1.15	
Autumn (Sep–Nov)	71	0.21		29.48		3.09		4.03		1.30	
Winter (Dec–Feb)	84	0.33		32.88		3.23		4.01		1.17	

hs-CRP, high sensitivity C-Reactive Protein; eGFR, Estimated Glomerular Filtration Rate from Serum Creatinine and Cystatin C, OH-PAHs, sum OH-PAHs concentration; 1-OH-Phe, 1-hydroxyphenanthrene; 2-OH-Phe, 2-hydroxyphenanthrene; 3-OH-Phe, 1-hydroxyphenanthrene; 1-OH-Pyr, 1-hydroxypyrene; MDA, malondialdehyde; 8-OHdG, 8-hydroxy-2′-deoxyguanosine; $F_{2\alpha}$-isoprostanes, sum $F_{2\alpha}$-isoprostanes concentration; BMI, Body Mass Index; potential renal impairment, chronic kidney disease.

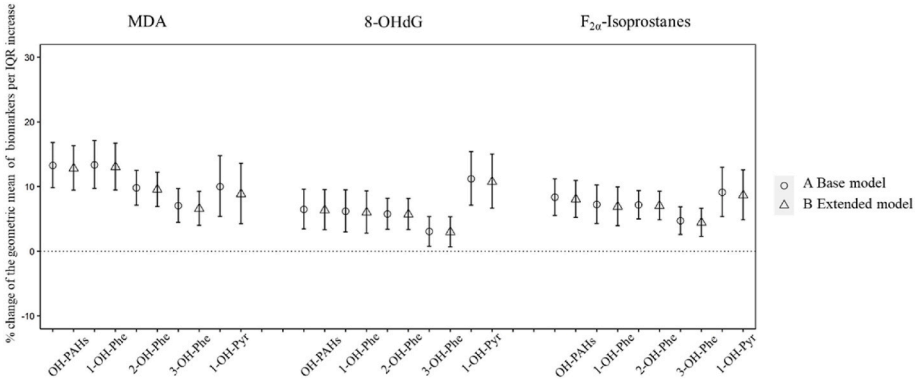

Fig. 1. Percent change in biomarkers of oxidative stress (95% CI) in association with an interquartile range increase in internal exposure biomarkers adjusted for age, sex, smoking, trend, and season (A Base model) and additionally adjusted for obesity, diabetes and potential renal impairment (B Extended model).

MDA was not associated at all. When additionally adjusting for obesity, diabetes, and potential renal impairment, the positive association between $F_{2\alpha}$-isoprostanes and hs-CRP turned significant.

4.2. Biomarkers varied across different subgroups

Sex: We observed higher concentrations of $F_{2\alpha}$-isoprostanes in women than in men. A similar study from the U.S. examining 65 participants (19 male, 46 female; 38.6 ± 11.1 years old) also found higher concentration of $F_{2\alpha}$-isoprostanes in females (Ma et al., 2017). Such different concentration levels in males and females may be caused by a decrease in oestrogen levels, which reduces the antioxidative capability in the postmenopausal period (Zaja-Milatovic et al., 2009), or due to the different ratios in content of lean body mass and bone mineral in male and female participants (Ma et al., 2017).

Age: Many studies have reported an association between aging and ROS, suggesting that free radicals play an important role in aging (Finkel and Holbrook, 2000; Guyton et al., 1998; Harman, 1956). In the present study, the biomarkers of ROS damage, MDA and 8-OHdG, showed higher concentrations in the older groups (between 55 and 65 years and

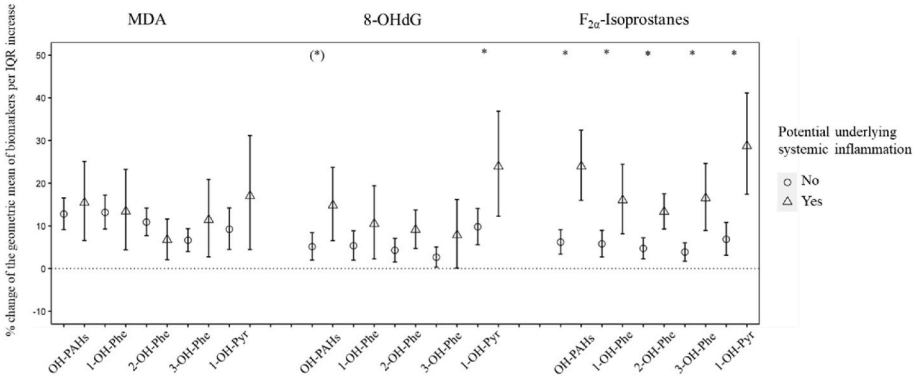

Fig. 2. Effect modification by potential underlying systemic inflammation (hs-CRP ≥ 3 mg/L vs. hs-CRP < 3 mg/L) of the association between OH-PAHs and oxidative stress biomarkers adjusted for age, sex, smoking, trend, and season (Base model). (* p-value of interaction <0.05, (*) p-value of interaction <0.1).

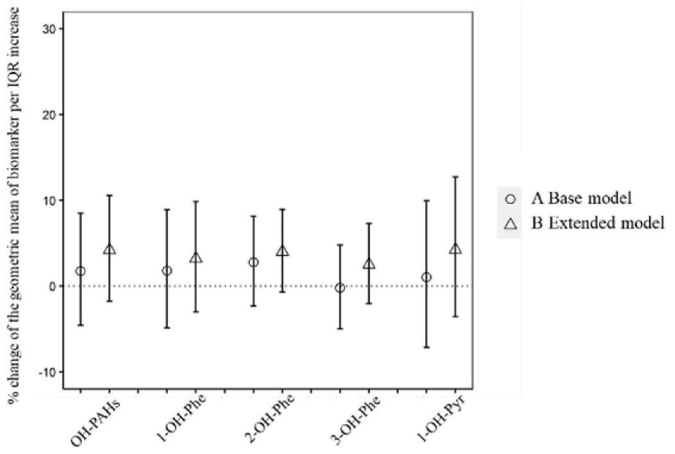

Fig. 3. Percent change in hs-CRP (95% CI) in association with an interquartile range increase in OH-PAHs adjusted for age, sex, smoking, trend, and season (A Base model) and additionally adjusted for obesity, diabetes and potential renal impairment (B Extended model).

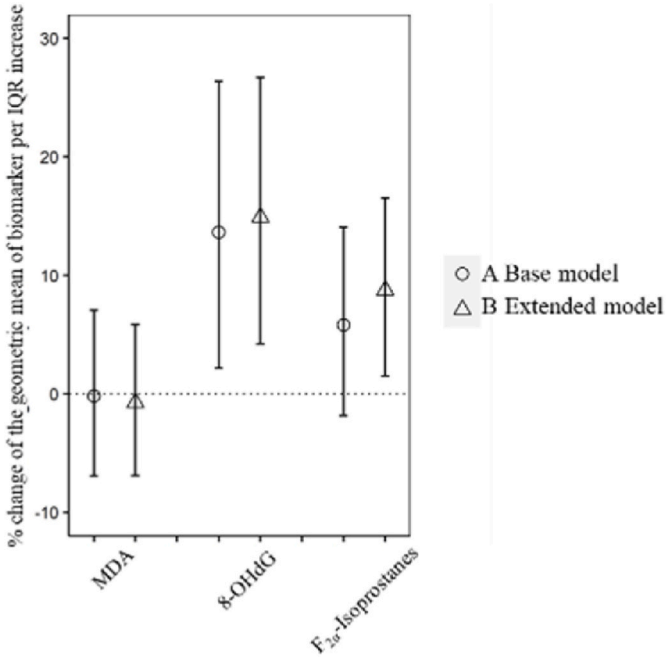

Fig. 4. Percent change in hs-CRP (95% CI) in association with an interquartile range increase in oxidative stress biomarkers adjusted for age, sex, smoking, trend, and season (A Base model) and additionally adjusted for obesity, diabetes and potential renal impairment (B Extended model).

older than 65 years) which is consistent with the theory that organisms age because they accumulate oxidative damage generated by ROS.

Smoking: Cigarette smoke contains large amounts of PAHs (Vu et al., 2015), and the group of smokers showed the highest level of PAH metabolites in urine. Similarly, a cohort study among 288 non-smokers and 100 smokers found highly significant differences and dose-response relationships with regard to cigarettes smoked per day for 2- OH-Phe, 3-OH-Phe, 4-OH-Phe, and 1-OH-Pyr (Heudorf and Angerer, 2001). In addition, a cross-sectional study among 4092 participants in China found significant correlations between urinary OH-PAH levels and cigarette smoking (Cao et al., 2020a).

Obesity and chronic diseases: Participants with obesity, potential renal impairment, diabetes, and hypertension showed higher concentrations of hs-CRP, indicating an underlying inflammatory state in these participants. Two studies compared patients at different stages of chronic kidney disease (CKD) with a control group and found higher oxidative stress levels and inflammation in patients with CKD (Karamouzis et al., 2008; Oberg et al., 2004). Accordingly, we observed higher concentrations of MDA, 8-OHdG, and hs-CRP in participants with potential renal impairment, as well as an indication for $F_{2\alpha}$-isoprostanes. Two studies among a cohort of North Indians and a cohort of African Americans found that higher concentrations of hs-CRP were associated with diabetes or, to a lesser degree, insulin resistance (Effoe et al., 2015; Mahajan et al., 2009). A study from Egypt, including 80 participants, reported that hypertension may increase the level of hs-CRP (Abd El Aziz et al., 2019), which matches our observations.

Season: We found significantly higher OH-PAH levels in urine samples collected during winter. We assume that a large part of the internal PAH burden is caused by exposure to PAH-polluted ambient air. Several studies have monitored atmospheric PAHs in Europe and China in recent years and reported similar seasonal variations due to different source contributions between autumn-winter and spring-summer (Albuquerque et al., 2016; Dvorská et al., 2011; Liu et al., 2014; Schnelle-Kreis et al., 2007). Moreover, Li et al. suggested that biomass burning for domestic heating during the heating season (October to March) was the major contributor to atmospheric PAHs in the Augsburg region (Germany) between 2014 and 2015 (Li et al., 2018). This observation was consistent with our results of seasonal variations in OH-PAHs, indicating that ambient PAHs might be an important source of PAH intake. In addition, the levels of oxidative stress markers (MDA and $F_{2\alpha}$-isoprostanes) were significantly higher in samples taken in spring/winter or autumn/winter, which may also be related to increased ambient PAHs pollution. Both short- and long-term studies suggest that higher concentrations of OH-PAHs and increased levels of oxidative

stress biomarkers can be detected after exposure to ambient pollutants (Bortey-Sam et al., 2017; Li et al., 2012; Lu et al., 2016; Moller and Loft, 2010; Motorykin et al., 2015; Suzuki et al., 1995).

4.3. Associations between OH-PAHs and oxidative stress and the role of inflammation

Two smaller cohort studies investigated the association between selected oxidative stress markers (MDA, 8-OHdG, and $F_{2\alpha}$-isoprostanes) and OH-PAHs in Japan and the United States (Bortey-Sam et al., 2017; Ferguson et al., 2017). Bortey-Sam et al. found significantly positive correlations between the sum of OH-PAHs, 2-OH-naphthalene, 2-3-OH-fluorenes, and MDA, and a positive correlation between 4-OH-Phe and 8-OHdG in urine samples collected from 202 residents of Kumasi, Japan. Ferguson et al. investigated urine samples of 200 pregnant women in the United States and reported that some PAH metabolites were consistently positively associated with urinary oxidative stress markers (8-OHdG and 8-isoprostane) (Ferguson et al., 2017). These findings were confirmed by our study, in which all examined oxidative stress markers showed positive associations with OH-PAHs. It should be mentioned that Ferguson et al. used specific gravity-corrected urinary concentrations in their study. Recent investigations showed that both, creatinine and specific gravity can be used as tools for normalisation or correction and no significant differences considering the results are expected in generally healthy individuals (Sallsten and Barregard, 2021). Although Kuiper et al. recently recommended the specific gravity method (Kuiper et al., 2021), at the time our samples were analysed (2015/16), most other studies were also based on creatinine normalised values.

In our study, the associations between OH-PAHs, 8-OHdG and $F_{2\alpha}$-isoprostanes were more pronounced in participants with potential underlying systemic inflammation, whereas no difference was observed for MDA. This finding indicates that oxidative stress is deteriorated, or is promoted by systemic inflammation. In a review article, Biswas et al. pointed out that inflammation processes can produce reactive species, and an inflammatory status may exaggerate the generation of reactive species (Biswas, 2016). Similarly, other underlying long-term risk factor profiles associated with obesity, diabetes, or CKD, may be responsible for increased levels of oxidative stress, as suggested by our data.

4.4. Associations between OH-PAHs and hs-CRP

A cohort study by Clark et al. using data of 3219 participants aged 20 years and older from the U.S National Health and Nutrition Examination Survey (NHANES) 2001–2004 investigated the relationship between OH-PAHs and inflammatory markers (homocysteine, fibrinogen, white blood cell count), but found no significant differences between high and low levels (75th vs. 25th percentiles) of all PAH metabolites in non-smoking participants (Clark et al., 2012). The study by Ferguson et al. observed positive associations between urinary OH-PAH concentrations and hs-CRP, but not with inflammatory cytokines (IL-1β, IL-6, IL-10, and TNF-α). In this analysis, we observed only slight indications for a positive association between OH-PAHs and hs-CRP levels. Clark et al. did not specify whether they used spot urine or 24 h urine, thus the comparability is limited.

In our previous KORA FF4 study across the full sample of 2252 participants, we observed significant positive associations between long-term exposure to ambient air pollution and hs-CRP (Pilz et al., 2018). In summary, our findings in this relatively low-exposure setting point to only weak associations between OH-PAHs and inflammation.

4.5. Association between oxidative stress and hs-CRP varied for different biomarkers

It has been shown that ROS play an important role in the signalling of inflammatory responses (Peters et al., 2021). In this analysis, 8-OHdG was significantly positively associated with hs-CRP, while MDA showed no association. When additionally adjusting for obesity, diabetes and potential renal impairment, the positive association between $F_{2\alpha}$-isoprostanes and hs-CRP turned significant. Although MDA, $F_{2\alpha}$-isoprostanes, and 8-OHdG are all indicators of ROS levels, they are generated from different pathways. While MDA (Ayala et al., 2014; Chen et al., 2011) and $F_{2\alpha}$-isoprostanes (Galano et al., 2017; Milne et al., 2008; Morrow and Roberts, 1996) are generated from non-enzymatic and free radical-mediated oxidation, 8-OHdG is formed enzymatically during DNA impairment and repair (Evans et al., 2010; Valavanidis et al., 2009). Different phases of oxidative stress from tolerance, adaptation, inflammation, and cell death were described by Peters et al. as a continuum (Peters et al., 2021). Therefore, MDA and $F_{2\alpha}$-isoprostanes can be generated through all phases of the continuum, while 8-OHdG is only generated in the later phases, for example, inflammation and cell death when ROS exceed antioxidation (Asanka Sanjeewa et al., 2021; Janovits et al., 2021; Luan et al., 2022; Trettin et al., 2014). Moreover, MDA is highly reactive and very polar. It is generated in the early phase of the exposure but gets cleared very fast (Siu and Draper, 1982; Traverso et al., 2004) whereas $F_{2\alpha}$-isoprostanes are relatively stable (Milne et al., 2008). This might be one explanation why we observed no association between hs-CRP and MDA but an indication for $F_{2\alpha}$-isoprostanes.

4.6. Strengths and limitations

One strength of this study is the selection of various biomarkers of oxidative stress, which were measured in our laboratory using established high-performance analytical methods. Each marker or each group of markers reflects characteristic damage to cellular macromolecules, namely the double bonds of PUFA, DNA, and membrane phospholipids. This allows the investigation of their interplay with respect to the internal PAH burden, which was also determined in our lab, along with the inflammation marker hs-CRP. Another strength of our study is the high number and diversity of individual participants' data available for the sub-cohort of the KORA study. The combination of lab-generated data with comprehensive information of the participants allowed us to perform more comprehensive investigations and better control of confounders than in previous studies.

There were several limitations to this study. First, our study was a cross-sectional study, and each participant was sampled only at a single time point from 2013 to 2014. Second, as a selected subset of participants was included in this analysis, our findings might not be representative for the general population. Third, OH-PAHs and biomarkers of oxidative stress were analysed from urine samples, while hs-CRP was analysed from serum samples. Metabolites in urine are considered as end products (Ayala et al., 2014; Evans et al., 2010; Morrow and Roberts, 1996) whereas metabolites in serum can function and participate in metabolic processes (Gewurz et al., 1982). However, this could also be considered an opportunity to observe and interpret the data within a larger frame. Fourth, the half-lives of the biomarkers might differ which could be one of the reasons why we did not observe an association between OH-PAHs and hs-CRP (Li et al., 2012; Pepys and Hirschfield, 2003). Finally, only spot urine samples were collected and analysed. However, we applied creatinine normalisation, an effective normalisation method to minimise the differences between the concentrations of OH-PAHs in spot, first-morning, and 24-h urine samples (Li et al., 2010).

5. Conclusion

In this cross-sectional study, we observed associations between exposure to PAHs, oxidative stress, and inflammation, even in a low exposure setting. We found positive associations between OH-PAHs and oxidative stress that were more pronounced in participants with an underlying inflammatory state. Additionally, hs-CRP was positively associated with increased markers of oxidative stress but not directly

with PAHs. Individual risk factors were important contributors to these processes and should be considered as potential confounders in future studies. Further longitudinal studies are necessary to investigate the causal chain of the associations.

Declaration of interest

All authors declare that no conflict of interest exists.

Acknowledgement

The KORA study was initiated and financed by the Helmholtz Zentrum München – German Research Center for Environmental Health, which is funded by the German Federal Ministry of Education and Research (BMBF) and by the State of Bavaria. Furthermore, KORA research was supported within the Munich Center of Health Sciences (MC-Health), Ludwig- Maximilians-Universität, as part of LMUinnovativ.

Mr. Xiao Wu holds a China Scholarship Council Studentship with the University of Rostock and Helmholtz Zentrum München.

Appendix A. Supplementary data

Supplementary data to this article can be found online at https://doi.org/10.1016/j.ijheh.2022.113993.

References

Abd El Aziz, W., Abou Elnour, E., Mena, M., El-brol, R., 2019. A comparative analysis of the level of high-sensitivity C-reactive protein in individuals with and without hypertension. Menoufia Medical Journal 32, 187–193.

Al-Delaimy, W.K., Larsen, C.W., Pezzoli, K., 2014. Differences in health symptoms among residents living near illegal dump sites in Los Laureles Canyon, Tijuana, Mexico: a cross sectional survey. Int. J. Environ. Res. Publ. Health 11, 9532–9552.

Albuquerque, M., Coutinho, M., Borrego, C., 2016. Long-term monitoring and seasonal analysis of polycyclic aromatic hydrocarbons (PAHs) measured over a decade in the ambient air of Porto. Portugal. Sci Total Environ 543, 439–448.

Alshaarawy, O., Elbaz, H.A., Andrew, M.E., 2016. The association of urinary polycyclic aromatic hydrocarbon biomarkers and cardiovascular disease in the US population. Environ. Int. 89–90, 174–178.

Andersen, M.H.G., Saber, A.T., Pedersen, J.E., Pedersen, P.B., Clausen, P.A., Lohr, M., Kermanizadeh, A., Loft, S., Ebbehoj, N.E., Hansen, A.M., Kalevi Koponen, I., Norskov, E.C., Vogel, U., Moller, P., 2018. Assessment of polycyclic aromatic hydrocarbon exposure, lung function, systemic inflammation, and genotoxicity in peripheral blood mononuclear cells from firefighters before and after a work shift. Environ. Mol. Mutagen. 59, 539–548.

Apel, K., Hirt, H., 2004. Reactive oxygen species: metabolism, oxidative stress, and signal transduction. Annu. Rev. Plant Biol. 55, 373–399.

Aquilina, N.J., Delgado-Saborit, J.M., Meddings, C., Baker, S., Harrison, R.M., Jacob 3rd, P., Wilson, M., Yu, L., Duan, M., Benowitz, N.L., 2010. Environmental and biological monitoring of exposures to PAHs and ETS in the general population. Environ. Int. 36, 763–771.

Asanka Sanjeewa, K.K., Herath, K.H.I.N.M., Yang, H.W., Choi, C.S., Jeon, Y.J., 2021. Anti-inflammatory mechanisms of fucoidans to treat inflammatory diseases: a review. Mar. Drugs 19.

Aumann, N., Baumeister, S.E., Rettig, R., Lieb, W., Werner, A., Doring, A., Peters, A., Koenig, W., Hannemann, A., Wallaschofski, H., Nauck, M., Stracke, S., Volzke, H., Meisinger, C., 2015. Regional Variation of Chronic Kidney Disease in Germany: Results from Two Population-Based Surveys, vol. 40. Kidney Blood Press Res, pp. 231–243.

Ayala, A., Munoz, M.F., Arguelles, S., 2014. Lipid peroxidation: production, metabolism, and signaling mechanisms of malondialdehyde and 4-hydroxy-2-nonenal. Oxid. Med. Cell. Longev. 2014, 360438.

Bamberg, F., Hetterich, H., Rospleszcz, S., Lorbeer, R., Auweter, S.D., Schlett, C.L., Schafnitzel, A., Bayerl, C., Schindler, A., Saam, T., Müller-Peltzer, K., Sommer, W., Zitzelsberger, T., Machann, J., Ingrisch, M., Selder, S., Rathmann, W., Heier, M., Linkohr, B., Meisinger, C., Weber, C., Ertl-Wagner, B., Massberg, S., Reiser, M.F., Peters, A., 2017. Subclinical disease burden as assessed by whole-body MRI in subjects with prediabetes, subjects with diabetes, and normal control subjects from the general population: the KORA-MRI study. Diabetes 66, 158–169.

Biswas, S.K., 2016. Does the interdependence between oxidative stress and inflammation explain the antioxidant paradox? Oxid. Med. Cell. Longev. 2016, 5698931.

Bortey-Sam, N., Ikenaka, Y., Akoto, O., Nakayama, S.M.M., Asante, K.A., Baidoo, E., Obirikorang, C., Saengtienchai, A., Isoda, N., Nimako, C., Mizukawa, H., Ishizuka, M., 2017. Oxidative stress and respiratory symptoms due to human exposure to polycyclic aromatic hydrocarbons (PAHs) in Kumasi, Ghana. Environ. Pollut. 228, 311–320.

Cao, L., Wang, D., Zhu, C., Wang, B., Cen, X., Chen, A., Zhou, H., Ye, Z., Tan, Q., Nie, X., Feng, X., Xie, Y., Yuan, J., Chen, W., 2020. Polycyclic aromatic hydrocarbon exposure and atherosclerotic cardiovascular disease risk in urban adults: the mediating role of oxidatively damaged DNA. Environ. Pollut. 265, 114860.

Chen, J.L., Huang, Y.J., Pan, C.H., Hu, C.W., Chao, M.R., 2011. Determination of urinary malondialdehyde by isotope dilution LC-MS/MS with automated solid-phase extraction: a cautionary note on derivatization optimization. Free Radic. Biol. Med. 51, 1823–1829.

Chuang, K.J., Chan, C.C., Su, T.C., Lee, C.T., Tang, C.S., 2007. The effect of urban air pollution on inflammation, oxidative stress, coagulation, and autonomic dysfunction in young adults. Am. J. Respir. Crit. Care Med. 176, 370–376.

Clark 3rd, J.D., Serdar, B., Lee, D.J., Arheart, K., Wilkinson, J.D., Fleming, L.E., 2012. Exposure to polycyclic aromatic hydrocarbons and serum inflammatory markers of cardiovascular disease. Environ. Res. 117, 132–137.

Danielsen, P.H., Moller, P., Jensen, K.A., Sharma, A.K., Wallin, H., Bossi, R., Autrup, H., Molhave, L., Ravanat, J.L., Briede, J.J., de Kok, T.M., Loft, S., 2011. Oxidative stress, DNA damage, and inflammation induced by ambient air and wood smoke particulate matter in human A549 and THP-1 cell lines. Chem. Res. Toxicol. 24, 168–184.

Droge, W., 2002. Free radicals in the physiological control of cell function. Physiol. Rev. 82, 47–95.

Dvorská, A., Lammel, G., Klánová, J., 2011. Use of diagnostic ratios for studying source apportionment and reactivity of ambient polycyclic aromatic hydrocarbons over Central Europe. Atmos. Environ. 45, 420–427.

Effoe, V.S., Correa, A., Chen, H., Lacy, M.E., Bertoni, A.G., 2015. High-sensitivity C-reactive protein is associated with incident type 2 diabetes among African Americans: the Jackson heart study. Diabetes Care 38, 1694–1700.

Evans, M.D., Saparbaev, M., Cooke, M.S., 2010. DNA repair and the origins of urinary oxidized 2'-deoxyribonucleosides. Mutagenesis 25, 433–442.

Everett, C.J., King, D.E., Player, M.S., Matheson, E.M., Post, R.E., Mainous 3rd, A.G., 2010. Association of urinary polycyclic aromatic hydrocarbons and serum C-reactive protein. Environ. Res. 110, 79–82.

Farzan, S.F., Chen, Y., Trachtman, H., Trasande, L., 2016. Urinary polycyclic aromatic hydrocarbons and measures of oxidative stress, inflammation and renal function in adolescents: NHANES 2003-2008. Environ. Res. 144, 149–157.

Ferguson, K.K., McElrath, T.F., Pace, G.G., Weller, D., Zeng, L., Pennathur, S., Cantonwine, D.E., Meeker, J.D., 2017. Urinary polycyclic aromatic hydrocarbon metabolite associations with biomarkers of inflammation, angiogenesis, and oxidative stress in pregnant women. Environ. Sci. Technol. 51, 4652–4660.

Fialkow, L., Wang, Y., Downey, G.P., 2007. Reactive oxygen and nitrogen species as signaling molecules regulating neutrophil function. Free Radic. Biol. Med. 42, 153–164.

Finkel, T., Holbrook, N.J., 2000. Oxidants, oxidative stress and the biology of ageing. Nature 408, 239–247.

Fuchte, H.E., Paas, B., Auer, F., Bayer, V.J., Achten, C., Schäffer, A., Smith, K.E.C., 2022. Identification of sites with elevated PM levels along an urban cycle path using a mobile platform and the analysis of 48 particle bound PAH. Atmos. Environ. 271, 118912.

Galano, J.M., Lee, Y.Y., Oger, C., Vigor, C., Vercauteren, J., Durand, T., Giera, M., Lee, J. C., 2017. Isoprostanes, neuroprostanes and phytoprostanes: an overview of 25years of research in chemistry and biology. Prog. Lipid Res. 68, 83–108.

Garrido, A., Jiménez-Guerrero, P., Ratola, N., 2014. Levels, trends and health concerns of atmospheric PAHs in Europe. Atmos. Environ. 99, 474–484.

Gerlofs-Nijland, M.E., Rummelhard, M., Boere, A.J., Leseman, D.L., Duffin, R., Schins, R. P., Borm, P.J., Sillanpaa, M., Salonen, R.O., Cassee, F.R., 2009. Particle induced toxicity in relation to transition metal and polycyclic aromatic hydrocarbon contents. Environ. Sci. Technol. 43, 4729–4736.

Guyton, K.Z., Gorospe, M., Wang, X., Mock, Y.D., Kokkonen, G.C., Liu, Y., Roth, G.S., Holbrook, N.J., 1998. Age-related changes in activation of mitogen-activated protein kinase cascades by oxidative stress. J. Invest. Dermatol. Symp. Proc. 3, 23–27.

Harman, D., 1956. Aging: a theory based on free radical and radiation chemistry. J. Gerontol. 11, 298–300.

Hennig, F., Fuks, K., Moebus, S., Weinmayr, G., Memmesheimer, M., Jakobs, H., Brocker-Preuss, M., Fuhrer-Sakel, D., Mohlenkamp, S., Erbel, R., Jockel, K.H., Hoffmann, B., Heinz Nixdorf Recall Study Investigative, G, 2014. Association between source-specific particulate matter air pollution and hs-CRP: local traffic and industrial emissions. Environ. Health Perspect. 122, 703–710.

Holle, R., Happich, M., Lowel, H., Wichmann, H.E., Group, M.K.S., 2005. KORA–a research platform for population based health research. Gesundheitswesen 67 (Suppl. 1), S19–S25.

Hou, J., Yin, W., Li, P., Huang, Y., Wan, Y., Hu, C., Xu, T., Cheng, J., Wang, L., Yu, Z., Yuan, J., 2019. Effect of exposure to phthalates on association of polycyclic aromatic hydrocarbons with 8-hydroxy-2'-deoxyguanosine. Sci. Total Environ. 691, 378–392.

Ifegwu, O.C., Anyakora, C., 2016. Chapter six - polycyclic aromatic hydrocarbons: Part II, urine markers. In: Makowski, G.S. (Ed.), Advances in Clinical Chemistry. Elsevier, pp. 159–183.

Inker, L.A., Schmid, C.H., Tighiouart, H., Eckfeldt, J.H., Feldman, H.I., Greene, T., Kusek, J.W., Manzi, J., Van Lente, F., Zhang, Y.L., Coresh, J., Levey, A.S., Investigators, C.-E., 2012. Estimating glomerular filtration rate from serum creatinine and cystatin C. N. Engl. J. Med. 367, 20–29.

Janovits, P.M., Leiguez, E., Portas, V., Teixeira, C., 2021. A metalloproteinase induces an inflammatory response in preadipocytes with the activation of cox signalling pathways and participation of endogenous phospholipases a2. Biomolecules 11.

Kamal, A., Qamar, K., Gulfraz, M., Anwar, M.A., Malik, R.N., 2015. PAH exposure and oxidative stress indicators of human cohorts exposed to traffic pollution in Lahore city (Pakistan). Chemosphere 120, 59–67.

Karamouzis, I., Sarafidis, P.A., Karamouzis, M., Iliadis, S., Haidich, A.B., Sioulis, A., Triantos, A., Vavatsi-Christaki, N., Grekas, D.M., 2008. Increase in oxidative stress but not in antioxidant capacity with advancing stages of chronic kidney disease. Am. J. Nephrol. 28, 397–404.
Keyte, I.J., Harrison, R.M., Lammel, G., 2013. Chemical reactivity and long-range transport potential of polycyclic aromatic hydrocarbons–a review. Chem. Soc. Rev. 42, 9333–9391.
Kraus, U., Breitner, S., Schnelle-Kreis, J., Cyrys, J., Lanki, T., Rückerl, R., Schneider, A., Brüske, I., Gu, J., Devlin, R., Wichmann, H.E., Zimmermann, R., Peters, A., 2011. Particle-associated organic compounds and symptoms in myocardial infarction survivors. Inhal. Toxicol. 23, 431–447.
Kuiper, J.R., O'Brien, K.M., Ferguson, K.K., Buckley, J.P., 2021. Urinary specific gravity measures in the U.S. population: implications for the adjustment of non-persistent chemical urinary biomarker data. Environ. Int. 156, 106656.
Kumar, A., Sankar, T.K., Sethi, S.S., Ambade, B., 2020. Characteristics, toxicity, source identification and seasonal variation of atmospheric polycyclic aromatic hydrocarbons over East India. Environ. Sci. Pollut. Res. Int. 27, 678–690.
Lan, Q., Mumford, J.L., Shen, M., Demarini, D.M., Bonner, M.R., He, X., Yeager, M., Welch, R., Chanock, S., Tian, L., Chapman, R.S., Zheng, T., Keohavong, P., Caporaso, N., Rothman, N., 2004. Oxidative damage-related genes AKR1C3 and OGG1 modulate risks for lung cancer due to exposure to PAH-rich coal combustion emissions. Carcinogenesis 25, 2177–2181.
Levey, A.S., Stevens, L.A., Schmid, C.H., Zhang, Y.L., Castro 3rd, A.F., Feldman, H.I., Kusek, J.W., Eggers, P., Van Lente, F., Greene, T., Coresh, J., Ckd, E.P.I., 2009. A new equation to estimate glomerular filtration rate. Ann. Intern. Med. 150, 604–612.
Li, F., Gu, J., Xin, J., Schnelle-Kreis, J., Wang, Y., Liu, Z., Shen, R., Michalke, B., Abbaszade, G., Zimmermann, R., 2021. Characteristics of chemical profile, sources and PAH toxicity of PM(2.5) in beijing in autumn-winter transit season with regard to domestic heating, pollution control measures and meteorology. Chemosphere 276, 130143.
Li, Z., Romanoff, L.C., Lewin, M.D., Porter, E.N., Trinidad, D.A., Needham, L.L., Patterson Jr., D.G., Sjodin, A., 2010. Variability of urinary concentrations of polycyclic aromatichydrocarbon metabolite in general population and comparison of spot, first-morning, and24-h void sampling. J. Expo Sci. Environ. Epidemiol. 20, 526–535.
Li, F., Schnelle-Kreis, J., Cyrys, J., Wolf, K., Karg, E., Gu, J., Orasche, J., Abbaszade, G., Peters, A., Zimmermann, R., 2018. Spatial and temporal variation of sources contributing to quasi-ultrafine particulate matter PM0.36 in Augsburg, Germany. Sci. Total Environ. 631–632, 191–200.
Li, Z., Romanoff, L., Bartell, S., Pittman, E.N., Trinidad, D.A., McClean, M., Webster, T.F., Sjodin, A., 2012. Excretion profiles and half-lives of ten urinary polycyclic aromatic hydrocarbon metabolites after dietary exposure. Chem. Res. Toxicol. 25, 1452–1461.
Lintelmann, J., Wu, X., Kuhn, E., Ritter, S., Schmidt, C., Zimmermann, R., 2018. Detection of monohydroxylated polycyclic aromatic hydrocarbons in urine and particulate matter using LC separations coupled with integrated SPE and fluorescence detection or coupled with high-resolution time-of-flight mass spectrometry. Biomed. Chromatogr. : BMC (Biomed. Chromatogr.) 32, e4183.
Liu, D., Xu, Y., Chaemfa, C., Tian, C., Li, J., Luo, C., Zhang, G., 2014. Concentrations, seasonal variations, and outflow of atmospheric polycyclic aromatic hydrocarbons (PAHs) at Ningbo site, Eastern China. Atmos. Pollut. Res. 5, 203–209.
Liu, X., Schnelle-Kreis, J., Schloter-Hai, B., Ma, L., Tai, P., Cao, X., Yu, C., Adam, T., Zimmermann, R., 2019. Analysis of PAHs associated with PM10 and PM2.5 from different districts in Nanjing. Aerosol Air Qual. Res. 19, 2294–2307.
Lu, S.Y., Li, Y.X., Zhang, J.Q., Zhang, T., Liu, G.H., Huang, M.Z., Li, X., Ruan, J.J., Kannan, K., Qiu, R.L., 2016. Associations between polycyclic aromatic hydrocarbon (PAH) exposure and oxidative stress in people living near e-waste recycling facilities in China. Environ. Int. 94, 161–169.
Luan, M., Wang, H., Wang, J., Zhang, X., Zhao, F., Liu, Z., Meng, Q., 2022. Advances in anti-inflammatory activity, mechanism and therapeutic application of ursolic acid. Mini-Rev. Med. Chem. 22, 422–436.
Mahajan, A., Tabassum, R., Chavali, S., Dwivedi, O.P., Bharadwaj, M., Tandon, N., Bharadwaj, D., 2009. High-sensitivity C-reactive protein levels and type 2 diabetes in urban North Indians. J. Clin. Endocrinol. Metab. 94, 2123–2127.
McCarrick, S., Cunha, V., Zapletal, O., Vondracek, J., Dreij, K., 2019. In vitro and in vivo genotoxicity of oxygenated polycyclic aromatic hydrocarbons. Environ. Pollut. 246, 678–687.
McCord, J.M., 1993. Human disease, free radicals, and the oxidant/antioxidant balance. Clin. Biochem. 26, 351–357.
Mesquita, S.R., van Drooge, B.L., Reche, C., Guimaraes, L., Grimalt, J.O., Barata, C., Pina, B., 2014. Toxic assessment of urban atmospheric particle-bound PAHs: relevance of composition and particle size in Barcelona (Spain). Environ. Pollut. 184, 555–562.
Michael, S., Montag, M., Dott, W., 2013. Pro-inflammatory effects and oxidative stress in lung macrophages and epithelial cells induced by ambient particulate matter. Environ. Pollut. 183, 19–29.
Miller, M.R., 2020. Oxidative stress and the cardiovascular effects of air pollution. Free Radic. Biol. Med. 151, 69–87.
Milne, G.L., Yin, H., Morrow, J.D., 2008. Human biochemistry of the isoprostane pathway. J. Biol. Chem. 283, 15533–15537.
Moller, P., Loft, S., 2010. Oxidative damage to DNA and lipids as biomarkers of exposure to air pollution. Environ. Health Perspect. 118, 1126–1136.
Montuschi, P., Barnes, P.J., Roberts 2nd, L.J., 2004. Isoprostanes: markers and mediators of oxidative stress. FASEB J 18, 1791–1800.
Morrow, J.D., Roberts 2nd, L.J., 1996. The isoprostanes. Current knowledge and directions for future research. Biochem. Pharmacol. 51, 1–9.
Motorykin, O., Santiago-Delgado, L., Rohlman, D., Schrlau, J.E., Harper, B., Harris, S., Harding, A., Kile, M.L., Massey Simonich, S.L., 2015. Metabolism and excretion rates of parent and hydroxy-PAHs in urine collected after consumption of traditionally smoked salmon for Native American volunteers. Sci. Total Environ. 514, 170–177.
Oberg, B.P., McMenamin, E., Lucas, F.L., McMonagle, E., Morrow, J., Ikizler, T.A., Himmelfarb, J., 2004. Increased prevalence of oxidant stress and inflammation in patients with moderate to severe chronic kidney disease. Kidney Int. 65, 1009–1016.
Ostro, B., Malig, B., Broadwin, R., Basu, R., Gold, E.B., Bromberger, J.T., Derby, C., Feinstein, S., Greendale, G.A., Jackson, E.A., Kravitz, H.M., Matthews, K.A., Sternfeld, B., Tomey, K., Green, R.R., Green, R., 2014. Chronic PM2.5 exposure and inflammation: determining sensitive subgroups in mid-life women. Environ. Res. 132, 168–175.
Pepys, M.B., Hirschfield, G.M., 2003. C-reactive protein: a critical update. J. Clin. Invest. 111, 1805–1812.
Peters, A., Nawrot, T.S., Baccarelli, A.A., 2021. Hallmarks of environmental insults. Cell 184, 1455–1468.
Pilz, V., Wolf, K., Breitner, S., Ruckerl, R., Koenig, W., Rathmann, W., Cyrys, J., Peters, A., Schneider, A., group, K.O.-S., 2018. C-reactive protein (CRP) and long-term air pollution with a focus on ultrafine particles. Int. J. Hyg Environ. Health 221, 510–518.
Pope 3rd, C.A., Bhatnagar, A., McCracken, J.P., Abplanalp, W., Conklin, D.J., O'Toole, T., 2016. Exposure to fine particulate air pollution is associated with endothelial injury and systemic inflammation. Circ. Res. 119, 1204–1214.
Risom, L., Moller, P., Loft, S., 2005. Oxidative stress-induced DNA damage by particulate air pollution. Mutat. Res. 592, 119–137.
Sallsten, G., Barregard, L., 2021. Variability of urinary creatinine in healthy individuals. Int. J. Environ. Res. Publ. Health 18, 3166.
Schnelle-Kreis, J., Sklorz, M., Orasche, J., Stolzel, M., Peters, A., Zimmermann, R., 2007. Semi volatile organic compounds in ambient PM2.5. Seasonal trends and daily resolved source contributions. Environ. Sci. Technol. 41, 3821–3828.
Siu, G.M., Draper, H.H., 1982. Metabolism of malonaldehyde in vivo and in vitro. Lipids 17, 349.
Suzuki, J., Inoue, Y., Suzuki, S., 1995. Changes in the urinary excretion level of 8-hydroxyguanine by exposure to reactive oxygen-generating substances. Free Radic. Biol. Med. 18, 431–436.
Tao, F., Gonzalez-Flecha, B., Kobzik, L., 2003. Reactive oxygen species in pulmonary inflammation by ambient particulates. Free Radic. Biol. Med. 35, 327–340.
Taverne, Y.J., Bogers, A.J., Duncker, D.J., Merkus, D., 2013. Reactive oxygen species and the cardiovascular system. Oxid. Med. Cell. Longev. 2013, 862423.
Traverso, N., Menini, S., Maineri, E.P., Patriarca, S., Odetti, P., Cottalasso, D., Marinari, U.M., Pronzato, M.A., 2004. Malondialdehyde, a lipoperoxidation-derived aldehyde, can bring about secondary oxidative damage to proteins. J. Gerontol. A Biol. Sci. Med. Sci. 59, B890–B895.
Trettin, A., Böhmer, A., Suchy, M.T., Probst, I., Staerk, U., Stichtenoth, D.O., Frölich, J.C., Tsikas, D., 2014. Effects of paracetamol on NOS, COX, and CYP activity and on oxidative stress in healthy male subjects, rat hepatocytes, and recombinant NOS. Oxid. Med. Cell. Longev. 2014.
Urbancova, K., Lankova, D., Rossner, P., Rossnerova, A., Svecova, V., Tomaniova, M., Veleminsky Jr., M., Sram, R.J., Hajslova, J., Pulkrabova, J., 2016. Evaluation of 11 polycyclic aromatic hydrocarbon metabolites in urine of Czech mothers and newborns. Sci. Total Environ. 577, 212–219.
Valavanidis, A., Vlachogianni, T., Fiotakis, C., 2009. 8-hydroxy-2' -deoxyguanosine (8-OHdG): a critical biomarker of oxidative stress and carcinogenesis. J. Environ. Sci. Health C Environ. Carcinog. Ecotoxicol. Rev. 27, 120–139.
VanRooij, J.G., De Roos, J.H., Bodelier-Bade, M.M., Jongeneelen, F.J., 1993. Absorption of polycyclic aromatic hydrocarbons through human skin: differences between anatomical sites and individuals. J. Toxicol. Environ. Health 38, 355–368.
Vattanasit, U., Navasumrit, P., Khadka, M.B., Kanitwithayanun, J., Promvijit, J., Autrup, H., Ruchirawat, M., 2014. Oxidative DNA damage and inflammatory responses in cultured human cells and in humans exposed to traffic-related particles. Int. J. Hyg Environ. Health 217, 23–33.
Wolf, K., Cyrys, J., Harcinikova, T., Gu, J., Kusch, T., Hampel, R., Schneider, A., Peters, A., 2017. Land use regression modeling of ultrafine particles, ozone, nitrogen oxides and markers of particulate matter pollution in Augsburg, Germany. Sci. Total Environ. 579, 1531–1540.
Wood, S.N., 2006. Low-rank scale-invariant tensor product smooths for generalized additive mixed models. Biometrics 62, 1025–1036.
Wu, X., Lintelmann, J., Klingbeil, S., Li, J., Wang, H., Kuhn, E., Ritter, S., Zimmermann, R., 2017. Determination of air pollution-related biomarkers of exposure in urine of travellers between Germany and China using liquid chromatographic and liquid chromatographic-mass spectrometric methods: a pilot study. Biomarkers 22, 525–536.
Yang, L., Wang, W.C., Lung, S.C., Sun, Z., Chen, C., Chen, J.K., Zou, Q., Lin, Y.H., Lin, C. H., 2017. Polycyclic aromatic hydrocarbons are associated with increased risk of

chronic obstructive pulmonary disease during haze events in China. Sci. Total Environ. 574, 1649–1658.
Yang, Q., Qiu, X., Li, R., Ma, J., Li, K., Li, G., 2015. Polycyclic aromatic hydrocarbon (PAH) exposure and oxidative stress for a rural population from the North China Plain. Environ. Sci. Pollut. Res. Int. 22, 1760–1769.
Yoon, H.-S., Lee, K.-M., Lee, K.-H., Kim, S., Choi, K., Kang, D., 2012. Polycyclic aromatic hydrocarbon (1-OHPG and 2-naphthol) and oxidative stress (malondialdehyde) biomarkers in urine among Korean adults and children. Int. J. Hyg Environ. Health 215, 458–464.
Zhang, H., Han, Y., Qiu, X., Wang, Y., Li, W., Liu, J., Chen, X., Li, R., Xu, F., Chen, W., Yang, Q., Fang, Y., Fan, Y., Wang, J., Zhang, H., Zhu, T., 2020. Association of internal exposure to polycyclic aromatic hydrocarbons with inflammation and oxidative stress in prediabetic and healthy individuals. Chemosphere 253, 126748.
Zhu, H., Martinez-Moral, M.P., Kannan, K., 2021. Variability in urinary biomarkers of human exposure to polycyclic aromatic hydrocarbons and its association with oxidative stress. Environ. Int. 156, 106720.

Received: 21 July 2017 | Revised: 10 November 2017 | Accepted: 15 December 2017

DOI: 10.1002/bmc.4183

RESEARCH ARTICLE

WILEY Biomedical Chromatography

Detection of monohydroxylated polycyclic aromatic hydrocarbons in urine and particulate matter using LC separations coupled with integrated SPE and fluorescence detection or coupled with high-resolution time-of-flight mass spectrometry

Jutta Lintelmann[1] | Xiao Wu[1] | Evelyn Kuhn[1] | Sebastian Ritter[1] | Claudia Schmidt[2] | Ralf Zimmermann[1,3]

[1] Joint Mass Spectrometry Centre, Cooperation Group 'Comprehensive Molecular Analytics', Helmholtz Zentrum München GmbH, Neuherberg, Germany

[2] Institute of Epidemiology II, Helmholtz Zentrum München GmbH, Neuherberg, Germany

[3] Joint Mass Spectrometry Centre, Institute of Chemistry, Chair of Analytical Chemistry, University of Rostock, Rostock, Germany

Correspondence
Jutta Lintelmann, Joint Mass Spectrometry Centre, Cooperation Group 'Comprehensive Molecular Analytics', Helmholtz Zentrum München, Neuherberg, Germany.
Email: lintelmann@helmholtz-muenchen.de

Abstract

A high-performance liquid chromatographic (HPLC) method with integrated solid-phase extraction for the determination of 1-hydroxypyrene and 1-, 2-, 3-, 4- and 9-hydroxyphenanthrene in urine was developed and validated. After enzymatic treatment and centrifugation of 500 µL urine, 100 µL of the sample was directly injected into the HPLC system. Integrated solid-phase extraction was performed on a selective, copper phthalocyanine modified packing material. Subsequent chromatographic separation was achieved on a pentafluorophenyl core–shell column using a methanol gradient. For quantification, time-programmed fluorescence detection was used. Matrix-dependent recoveries were between 94.8 and 102.4%, repeatability and reproducibility ranged from 2.2 to 17.9% and detection limits lay between 2.6 and 13.6 ng/L urine. A set of 16 samples from normally exposed adults was analyzed using this HPLC-fluorescence detection method. Results were comparable with those reported in other studies. The chromatographic separation of the method was transferred to an ultra-high-performance liquid chromatography pentafluorophenyl core–shell column and coupled to a high-resolution time-of-flight mass spectrometer (HR-TOF-MS). The resulting method was used to demonstrate the applicability of LC-HR-TOF-MS for simultaneous target and suspect screening of monohydroxylated polycyclic aromatic hydrocarbons in extracts of urine and particulate matter.

KEYWORDS

HPLC-integrated SPE, LC-HR-TOF-MS, OH-PAH, $PM_{2.5}$, urine

1 | INTRODUCTION

Polycyclic aromatic hydrocarbons (PAH), ubiquitous hazardous pollutants, enter the body mainly through inhalation and ingestion. Part of these hydrophobic substances is oxidized and finally excreted in the urine as glucuronide- or sulfate conjugates of monohydroxylated PAH (OH-PAH; Jacob & Seidel, 2002).

The renal excretion of monohydroxylated-PAH makes them suitable for the use as biomarkers of exposure. In the 1980s, the first methods for the determination of 1-hydroxypyrene, a highly accepted biomarker of exposure to PAH, were introduced (Grimmer, Dettbarn, & Jacob, 1993; Jongeneelen, Anzion, & Henderson, 1987). Since then the number of studies covering occupational and environmental exposure has risen immensely (e.g. Li et al., 2008; Li et al., 2012; Lin et al., 2016; Motorykin, Santiago-Delgado et al., 2015; Nilsson et al., 2013; Polanska et al., 2014). Simultaneously, the number of quantifiable

Abbreviations: 1-OH-Phe, 1-hydroxyphenanthrene; 1-OH-Pyr, 1-hydroxypyrene; 2-OH-Phe, 2-hydroxyphenanthrene; 3-OH-Phe, 3-hydroxyphenanthrene; 4-OH-Phe, 4-hydroxyphenanthrene; 9-OH-Phe, 9-hydroxyphenanthrene; FLD, fluorescence detection; HR-TOF-MS, high-resolution time-of-flight mass spectrometry; OH-PAH, monohydroxylated PAH; PAH, polycyclic aromatic hydrocarbons; PFP, pentafluorophenyl; SPE, solid-phase extraction.

OH-PAH has increased, and it differs depending on the analytical method applied and the study performed (Lankova, Urbancova, Sram, Hajslova, & Pulkrabova, 2016; Li et al., 2006; Polanska et al., 2014; Urbancova et al., 2017). Monohydroxylated PAH are not only formed in mammalian organisms but can also be generated by combustion of organic materials and during transformation processes of PAH in ambient air (Avagyan, Nyström, Lindgren, Boman, & Westerholm, 2016; Keyte, Harrison, & Lammel, 2013; Lin et al., 2015; Ma et al., 2016). In contrast to the determination of PAH in aerosols, the quantification of OH-PAH is not yet common. Their concentrations on particulate matter are approximately a factor of 2–30 lower than the concentrations of the respective parent PAH (Barrado, García, Barrado, & Pérez, 2012; Barrado, García, Castrillejo, & Barrado, 2013; Hayakawa, Tang, & Toriba, 2016). Compared with PAH, OH-PAH show significantly lower ozone-related stabilities. This can be an important issue for the sampling of particulate matter because degradation of OH-PAH and artifact formation have to be considered (Miet, Le Menach, Flaud, Budzinski, & Villenave, 2009). Nevertheless, the determination of OH-PAH can provide important information regarding the health effects and risk assessment of exposure to particulate matter (Hayakawa et al., 2016).

For a reliable determination of low concentrations of OH-PAH in complex matrices, sample processing, chromatographic separation and detection must be optimally matched. Conventional sample processing procedures for urine start with the enzymatic hydrolysis of sulfate and glucuronide conjugates of the OH-PAH. Subsequent extraction, enrichment and clean-up of the OH-PAH are performed by liquid–liquid extraction with nonpolar solvents (Lankova et al., 2016; Li et al., 2006; Seidel et al., 2008) or solid-phase extraction on different materials (Chauhan et al., 2015; Chetiyanukornkul, Toriba, Kameda, Tang, & Hayakawa, 2006; Fan, Wang, Ramage, & She, 2012; Liu, Luo, Bi, Li, & Lin, 2015; Motorykin, Scherlau et al., 2015; Onyemauwa et al., 2009; Ramsauer et al., 2011; Romanoff et al., 2006; Zhou, Hu, & Li, 2016). Typical sample volumes needed for sample processing are in the range of 2–10 mL urine before enzymatic hydrolysis.

Extraction of OH-PAH in particulate matter is achieved with ultrasonic extraction, Soxhlet extraction or pressurized solvent extraction using solvents like dichloromethane and methanol. The resulting extracts are evaporated and the residue is dissolved in suitable solvents and either pre-fractionated by SPE or directly analyzed (Avagyan, Nyström, Boman, & Westerholm, 2015; Barrado et al., 2012, 2013; Hayakawa et al., 2016; Miet et al., 2009).

Mainly two chromatographic methods and two detection methods are used for separation and quantification of OH-PAH: gas chromatography–mass spectrometry (GC-MS) and high-performance liquid chromatography coupled to mass spectrometry or fluorescence detection (LC-MS, HPLC-FLD; e.g. Avagyan et al., 2015; Barrado et al., 2012; Fan et al., 2012; Lankova et al., 2016; Li et al., 2006; Motorykin, Scherlau, et al., 2015; Onyemauwa et al., 2009; Seidel et al., 2008). GC-methods are advantageous owing to their high resolution power allowing the separation of isomeric OH-PAH. However, a clear demerit of GC-methods is the derivatization procedure which is necessary for OH-PAH prior to analysis. Thus, the number of time-consuming sample processing steps increases, involving the risk of a decrease in practicability and reliability. In contrast, HPLC-based methods work well for the analysis of polar compounds but conventional HPLC systems do not allow the separation of isomeric hydroxyphenanthrenes. At least two of the five compounds are co-eluting. In 2016 Lankova and co-workers demonstrated the ultra high-performance LC separation of the five isomeric hydroxyphenanthrenes on a PFP column with 1.7 μm particles. Even if a baseline separation was not achieved for all isomers, a reliable integration and quantification was possible (Lankova et al., 2016).

An HPLC set-up offers the possibility to integrate the SPE of enzymatically hydrolyzed urine into the system, leading to increased practicability and thus to higher throughput and reliability of the analyses (Bourgogne, Grivet, Varesio, & Hopfgartner, 2015). In spite of the obvious benefits, this principle is rarely applied. Recent examples were presented by Leroyer et al. (2010), You et al. (2014) and Wang et al. (2017). Constraints of the methods presented so far are the selection of target OH-PAH (Leroyer et al., 2010) or the need for expensive state-of-the-art technology (Wang et al., 2017). None of the methods enables the chromatographic separation and thus the quantification of all isomeric hydroxyphenanthrenes. An early HPLC-FLD method with system-integrated sample processing for the determination of 1-hydroxypyrene and three hydroxyphenanthrenes in urine was described by Boos and his group (Boos, Lintelmann, & Kettrup, 1992; Lintelmann, Hellemann, & Kettrup, 1994). SPE was performed on a laboratory-made material consisting of silica particles that were chemically modified with a copper phthalocyanine derivate. The method allowed a fast, selective and highly reliable determination of OH-PAH in small sample volumes of urine after enzymatic hydrolysis. It was optimized, validated and published as a recommended method of the German Research Foundation (Lintelmann & Angerer, 1999). However, the separation of the isomeric compounds 2-, and 3-hydroxyphenanthrene was not possible by applying this set-up.

The detection methods coupled to HPLC are usually fluorescence and tandem mass spectrometry (MS/MS). Fluorescence detection is sensitive, selective, robust and cost-efficient but tandem mass spectrometry is more selective owing to the detection of specific mass losses (transitions). MS/MS methods do not enable a *post hoc* evaluation of mass spectra or isotopic patterns originating from further, nontargeted analytes. For *post hoc* analysis and for substance identification, high-resolution mass spectrometric methods like Orbitrap mass spectrometry or time-of-flight mass spectrometry can be applied. Recently, Avagyan and Westerholm (2017) described a strategy for target and suspect screening of OH-PAH in air particulates using liquid chromatography–Orbitrap high-resolution mass spectrometry. The coupling between highly efficient chromatographic separation and high-resolution mass spectrometry can be an important tool for the investigation of matrices containing OH-PAH.

With the aim of utilizing the advantages of HPLC-integrated SPE and high-resolution mass spectrometric detection, LC-based methods for the determination or detection of 1-hydroxypyrene and 1-, 2-, 3-, 4- and 9-hydroxyphenanthrene were developed in this study. An HPLC-FLD method with integrated SPE on a copper phthalocyanine solid-phase material allows the direct injection of enzymatically hydrolyzed urine and the subsequent chromatographic separation of all isomers of hydroxyphenanthrenes on a core–shell analytical column within a conventional HPLC system. The amount of urine needed for

quantification is <0.5 mL, and the sensitivity of the method allows the reliable determination of low and high OH-PAH concentrations in urine of individuals exposed to normal, ambient PAH-concentrations. The HPLC-FLD method was validated and successfully applied for the analysis of 16 urine samples from adults.

The chromatographic separation of the HPLC-FLD method was transferred to an UHPLC-system and coupled to a high-resolution time-of-flight mass spectrometer (HR-TOF-MS) with folded flight path technology. The LC-HR-TOF-MS method was used to demonstrate the feasibility of target and suspect screening of selected OH-PAH in extracts of urine and particulate matter.

2 | EXPERIMENTAL

2.1 | Chemicals and reagents

Acetic acid Optima® LC/MS was from Fisher Scientific (Geel, Belgium). Methanol gradient-grade, dichloromethane emsure® and sodium acetate emsure® were obtained from VWR International (Darmstadt, Germany). Water for HPLC was generated by a Milli-Q Ultra Plus Water System, Millipore GmbH (Schwabach, Germany). Acetonitrile for HPLC, LC-MS-grade water and LC-MS-grade methanol were purchased from Th. Geyer (Renningen, Germany). β-Glucuronidase/arylsulfatase solution (from *Helix pomatia*) was from Roche Diagnostics (Mannheim, Germany) and SPE-cartridges Bond Elut Focus (60 mg, 3 mL) were from Agilent Technologies (Santa Clara, USA). The colorimetric assay kit used for method comparison of creatinine determination was purchased from Cayman (Ann Arbor, MI, USA). The ESI Tuning Mix G2421-60001 was a product of Agilent Technologies (Santa Clara, CA, USA). Nitrogen for the mass spectrometer and for sample processing was taken from a central gas supply which is provided by a liquid nitrogen tank or from gas bottles (5.0 purity; Linde, Germany).

2.2 | Standard substances

1-Hydroxyphenanthrene (1-OH-Phe) and 9-hydroxyphenanthrene (9-OH-Phe) came from Santa Cruz Biotechnology Inc. (Santa Cruz, CA, USA). 2-Hydroxyphenanthrene (2-OH-Phe), 3-hydroxyphenanthrene (3-OH-Phe), 4-hydroxyphenanthrene (4-OH-Phe) and 1-hydroxypyrene (1-OH-Pyr) were from the PAH Research Institute Dr Schmidt (Greifenberg, Germany). Creatinine was purchased from Acros Organics (Morris Plains, NJ, USA). The purity of all standards was >98%.

Stock solutions of the substances were prepared in methanol at a concentration of ~100 µg/mL and stored at −20°C. From these stock solutions single standard solutions were obtained by dilution with methanol. For HPLC-FLD these single standard solutions were combined and further diluted with distilled water or enzymatically treated urine, and sonicated for 30 s. The solutions were put into the autosampler directly before start of the sequence. For LC-MS analyses only methanolic standards were used.

2.3 | Urine samples

A set of urine samples was obtained from excess material of the urine preparation (midstream urine was immediately centrifuged at 2450 g_{max} for 10 min, aliquoted and stored at −80°C) within the KORA FF4 study (Kowall et al., 2017). The investigations were carried out in accordance with the Declaration of Helsinki, including written informed consent of all participants. The KORA FF4 study was approved by the ethics committee of the Bavarian Chamber of Physicians, Munich (EC no. 06068). The samples provided were used for the method set-up and comparison of creatinine determination, the validation of the HPLC-FLD method, the LC-HR-TOF-MS analyses and the exemplary HPLC-FLD analysis of real samples.

2.4 | Particulate matter

Samples of particulate matter ($PM_{2.5}$) were collected during a monitoring campaign which was performed between 2006 and 2012 in Munich. Filter samples were obtained using a high-volume sampler HVS (Anderson, USA), that was operated for 24 h at a flow rate of ca. 800 L/min every 3 days. After sampling the filters were wrapped in aluminum foil and stored in a desiccator at 4°C until sample processing.

2.5 | Sample processing

2.5.1 | Urine

Urine samples (0.5 or 3 mL) were filled into glass vials and mixed with the same volume of sodium acetate buffer (1 M, pH 5.5). For enzymatic hydrolysis of the conjugates 5 µL (for 0.5 mL sample) or 20µL (for 3 mL sample) of *β*-glucuronidase/arylsulfatase solution was added and the mixture was incubated for 3 h at 37°C in an incubator INNOVA 44R from Eppendorf (Hamburg, Germany).

Further steps after enzymatic hydrolysis depended on the analysis method used: for HPLC-FLD with system-integrated sample processing the samples were centrifuged for 10 min at 4000 rpm in a Hettich EBA 20 centrifuge (Hettich, Bäch, Switzerland), and the supernatant was transferred to an autosampler vial. For all sample processing steps glass vessels were used to avoid loss of analytes owing to irreversible adsorption to hydrophobic surfaces of plastic materials.

For the LC-HR-TOF-MS detection of OH-PAH in urine an SPE on Focus cartridges (polymeric sorbent) was performed according to a modified procedure described by Romanoff et al. (2006). Cartridges were preconditioned with methanol and water (1 mL in each case, ca. 10 mL/min). A 4 mL aliquot of the enzymatically hydrolyzed urine samples was added to the SPE cartridge (ca. 1 mL/min) and rinsed with 1 mL water and 3 mL methanol/water, 3:7, v/v (ca. 10 mL/min). The sorbent was dried by drawing a constant flow of nitrogen for 3 min through the column bead. Finally the analytes were eluted with 4 mL dichloromethane (ca. 0.5 mL/min). SPE was carried out on a Visiprep™ 24 vacuum manifold equipped with a KNF Laboport vacuum pump (both from Sigma, St Louis, MO, USA). The extract was carefully evaporated to dryness in a Barkey vapotherm mobil S from Barkey GmbH (Leopoldshöhe, Germany) under a gentle stream of nitrogen at 40°C. The residue was dissolved in 50 µL methanol and filled into an autosampler vial.

2.5.2 | Creatinine determination

For the quantification of creatinine, which is necessary to control highly variable urine dilutions in real samples, a fast HPLC method

was developed. On a Phenomenex Luna NH_2-column (3 µm, 150 × 2 mm i.d. with SecurityGuard™ NH_2, 2 mm i.d.; Phenomenex, Aschaffenburg, Germany) creatinine was separated from matrix components using acetonitrile–water, 80:20, v/v at 0.55 mL/min and 15°C. Detection and quantification were carried out at 235 nm. To verify identification, UV spectra were recorded and compared with the standard spectrum regularly. A 10 µL aliquot of a diluted and vortexed urine sample (1:20 with water, 0.5 min on a vortex from Neolab; Heidelberg, Germany) was injected. Analysis was carried out on an HP 1100 system from Agilent (St Clara, CA, USA).

To investigate the performance of this method, a set of 12 urine samples was analyzed applying the HPLC method described above as well as the colorimetric assay kit for creatinine. For the determination using the assay, samples were treated and photometrically investigated as described in the product manual. A short statistic evaluation resulted in a Spearman's Rank correlation > 0.92. A Wilcoxon Rank test showed no significant differences between the two datasets.

2.5.3 | Particulate matter

Samples of particulate matter ($PM_{2.5}$) were extracted according to a protocol described in detail in a previous publication (Lintelmann, Heil-França, Hübner, & Matuschek, 2010). In brief, filter samples were extracted by accelerated solvent extraction with dichloromethane/methanol (50:50, v/v), and the extract was evaporated. The residue was dissolved in acetonitrile, filtered and used for analyses.

2.6 | Instrumentation

2.6.1 | HPLC-FLD

The HPLC-FLD system used for the determination of OH-PAH with system-integrated sample processing was an Ultimate 3000 (Thermo Fisher Scientific, Dreieich, Germany) instrument, consisting of a dual gradient pump (DGP 3600 M), an autosampler (WPS-3000 TSL analytical), a column compartment (TCC-3200) equipped with two 10-port switching valves from Valco, a photodiode array detector (PDA 3000) and a fluorescence detector (RF 2000). For HPLC-integrated SPE a guard cartridge (5 × 2.1 mm) from MZ Analysentechnik (Mainz, Germany) was depleted, cleaned and filled with solid-phase material (copper phthalocyanine modified silica, 25–40 µm). The material was a gift from Professor Boos (until 2014, Research group BioSeparation, Institute of Clinical Chemistry, LMU Munich, Germany) and can now be obtained from Recipe (Clin Tox® Human Biomonitoring, 1-Hydroxyppyren im Urin; Recipe®, Munich, Germany). The column was put into a cartridge holder (MZ-Analysentechnik, Mainz, Germany) and integrated into the HPLC system via a 10-port switching valve. A Kinetex PFP column (2.6 µm, 100 × 3 mm i.d., with SecurityGuard™ PFP, 2.1 mm i.d.; Phenomenex, Aschaffenburg, Germany) was used for the separation of OH-PAH. An in-line filter with 0.2 µm porosity (IDEX Health & Science, Oak Harbour, WA, USA) was installed in front of the analytical column to avoid irreversible blockages of the analytical column. Time programmed fluorescence detection was applied. Hydroxyphenanthrenes were measured at 249/364 nm (excitation/emission) and 1-hydroxypyrene was detected at 343/385 nm (excitation/emission). The instrumental set-up is shown in Figure 1.

2.6.2 | LC-HR-TOF-MS

The MS-HR-TOF (Citius™ HRT, Leco Corporation, St Joseph, MI, USA, with folded flight path technology) was equipped with an electrospray interface and coupled to an Agilent 1290 Infinity Binary UHPLC-system (G1316C column oven, G4226A autosampler with thermostat G1330B, and a G4220A binary pump, Agilent Technologies; Waldbronn, Germany). As analytical column a Kinetex PFP (1.7 µm, 100 × 2.1 mm i.d. with SecurityGuard™ PFP, 2.1.mm i.d.; Phenomenex, Aschaffenburg, Germany) was used. Instrument control, data acquisition and analysis were performed with ChromaTOF software Version 1.74 (Leco Corporation, St Joseph, MI, USA). Optimized MS conditions in negative ion mode were as follows: nitrogen desolvation flow, 7.0 L/min; nitrogen nebulizer pressure, 45 psi; desolvation temperature, 700°C; nozzle temperature, 120°C; spray voltage, −2800 V; nozzle potential, −70 V; mass range, 100–1700 mu at 0.75 spectra/s.

Mass calibration was achieved by periodic co-infusion of the ESI-L low concentration tuning mix at 5 µL/min at the end of each chromatographic run. Mass accuracies of tuning compounds were in the range of 0.01–0.34 ppm and mass resolutions were between 30,000 and 60,000 (mass/full-width at half peak height).

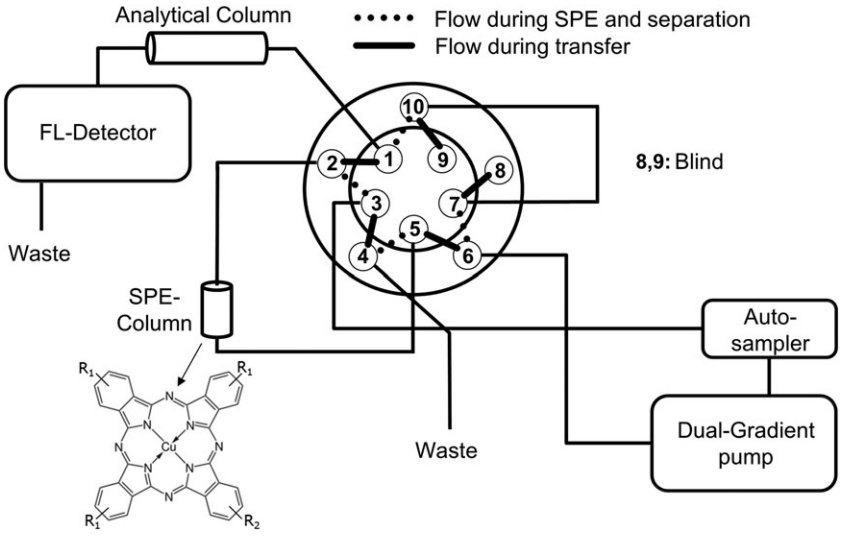

FIGURE 1 Instrumental set-up of the HPLC-FLD system with integrated solid-phase extraction

2.7 | Chromatographic conditions

Different LC-separation programs for HPLC-FLD and LC-HR-TOF-MS analyses were applied to meet the individual instrumental conditions. The programs are listed in Tables 1 and 2.

3 | RESULTS AND DISCUSSION

3.1 | HPLC-FLD

3.1.1 | Analysis cycle

The application of a core–shell material with 2.6 µm allows the separation of the isomeric hydroxyphenanthrenes using a conventional HPLC, which still is more widespread in analytical laboratories than state-of-the-art UHPLC systems. In addition, lower operating pressure and higher tolerable extra-column volumes of core–shell columns compared with UHPLC columns facilitate the integration of SPE columns into the HPLC system. For HPLC-integrated SPE, copper phthalocyanine modified silica was used. This material selectively adsorbs planar, polyaromatic compounds (ring number ≥ 3) from aqueous solutions. The interactions are reversible and can be interrupted by organic solvents (Boos et al., 1992). The specific mechanism and its integration into the HPLC system allow a fast, selective and highly reliable determination of OH-PAH in urine. The direct injection of variable volumes of enzymatically treated urine enable the analysis of very low sample volumes (<0.5) of urine. An analysis cycle for the determination of OH-PAH in urine consists of three steps: (1) clean-up and enrichment of the target analytes on the HPLC-integrated SPE-column and simultaneous equilibration of the analytical column; and (2) on-line connection of SPE-column and analytical column by valve-switching – the OH-PAH are transferred from the SPE column to the analytical column; and (3) disconnection of the columns by an additional valve switching followed by chromatographic separation and detection of the analytes. At the same time, the SPE column is cleaned and re-equilibrated for the next analysis cycle.

The robustness of the extraction cartridge allowed the injection of >600 samples without any loss of extraction or clean-up capacities until now.

TABLE 1 Time programs for the HPLC-separation of hydroxyphenanthrenes and 1-hydroxypyrene

HPLC Method I[a]			HPLC Method II[a,b]			HPLC Method II[c]		
Time (min)	A	B	Time (min)	A	B	Time (min)	A	B
0	55	45	0	55	45	0	10	90
12	62	38	8	55	45	10	10	90
19	62	38	8.1	100	0	12	10	90
23	69.5	30.5	10.0	100	0	12.1	100	0
34	90	10	10.1	60	40	17	100	0
36	100	0	14.0	60	40	19	10	90
41	100	0	21.7	62	62	62	10	90
42	55	45	28.7	62	62			
52	55	45	32.7	69.5	30.5			
			43.7	90	10			
			45.0	100	0			
			50.0	100	0			
			51.0	55	45			
			62.0	55	45			

A, Methanol; B, water. [a]Gradient for analytical column; flow, 300 µL/min; temperature, 20°C. [b]At program time 10 min the switching valve is switched connecting the SPE column to the analytical column and allowing transfer of the analytes to the analytical column. At program time 12 min the switching valve is moved back. Injection volume: 5 µL for HPLC analysis without integrated SPE, 100 µL for HPLC analysis with integrated SPE. [c]Gradient for integrated SPE-column, flow: 400 µL/min, temperature: 20°C.

TABLE 2 Time programs for the UHPLC-separation of hydroxyphenanthrenes and 1-hydroxypyrene

UHPLC[a] Method III			UHPLC[b] Method IV		
Time (min)	A	B	Time (min)	A	B
0	55	45	0	55	45
12	62	38	12	62	38
19	62	38	13	62	38
24	90	10	14	90	10
30	90	10	16	90	10
32	100	0	17	100	0
34	55	45	18	100	0
40	55	45	19	55	45
			22	55	45

A, Methanol; B, 0.1% acetic acid. [a]Flow 150 µL/min; [b]Flow 300 µL/min. Injection volume: 2.5 µL.

3.1.2 | Validation

The validation of the HPLC-FLD method for the determination of five hydroxyphenanthrenes and 1-hydroxypyrene was carried out by investigating and calculating matrix-independent recoveries, matrix-dependent recoveries, repeatability, reproducibility, calibration functions, limit of detection (LOD) and limit of quantification (LOQ) for the biological matrix urine.

Recoveries

For matrix-independent recoveries, 5 µL of methanol standards (0.45–12.06 pg/µL) was analyzed twice by HPLC-FLD without system-integrated SPE (Table 1, HPLC-method I). Subsequently these standards were diluted 1:20 with ultrapure water. Aliquots of 100 µL of these aqueous standards were analyzed twice by HPLC-FLD with system-integrated SPE (Table 1, HPLC-method II). Peak areas of the respective signals were compared. Acceptable recoveries with good coefficients of variation were obtained (cf. Table 3).

For the matrix-dependent recovery 10 urine samples from adult individuals were pooled, enzymatically hydrolyzed and analyzed five times. Aliquots of this urine pool as well as ultrapure water were spiked with different concentrations of the metabolites and analyzed twice in the SPE-integrated mode (Table 1, HPLC-method II, concentration range 23–603 ng/L in water and enzymatically hydrolyzed urine; for detailed information see Table S1 in the Supporting Information). Peak areas were compared taking into account the mean of the nonspiked urine. The results presented in Table 3 indicate that recoveries were very good with low

TABLE 3 Matrix-independent and matrix-dependent recoveries for the HPLC-FLD determination of monohydroxylated polycyclic aromatic hydrocarbons (OH-PAH) in urine

Compound	Recovery A (%) (n = 6)	CV (%)	Recovery B (%) (n = 6)	CV (%)
2-OH-Phe	92.4	4.9	97.8	3.3
3-OH-Phe	103.6	6.1	102.4	8.1
1-OH-Phe	113.0	4.1	103.0	10.5
9-OH-Phe	123.3	7.6	99.0	15.1
4-OH-Phe	101.6	8.6	94.9	6.9
1-OH-Pyr	63.8	6.0	102.2	4.2

A, Recoveries of aqueous standards analyzed with integrated SPE (HPLC-method II) compared with methanol standards analyzed after direct injection, without integrated SPE (HPLC-method I). B, Recoveries of spiked urine samples compared with aqueous standards. Analyses were performed with integrated SPE (HPLC-method II). OH-PAH concentrations of the pooled, nonspiked sample were between 26.4 and 169.2 ng/L.

coefficients of variation. Only 9-OH-Phe has a coefficient of variation >10%. Li and co-workers found that 9-OH-Phe shows fluctuating stabilities especially during enzymatic hydrolysis (Li et al., 2006). Therefore we tried to keep all steps of sample storage, sample processing and analysis highly reproducible to minimize degradation effects. Nevertheless the results for this analyte have to be considered with respect to its assumed instability.

All further HPLC-FLD analyses during the validation process and the investigation of real samples were carried out applying HPLC with integrated SPE, HPLC-method II.

Repeatability and reproducibility

For the examination of method repeatability, the pooled urine sample described above was injected and analyzed five times within one sequence. Additionally, two further urine samples were enzymatically treated and analyzed within one sequence for nine and five times, respectively. The reproducibility was investigated combining three urine samples and dividing this pool into five parts. The subsamples were enzymatically hydrolyzed and analyzed on five different days. Coefficients of variation for repeatability and reproducibility are good with values between 1.0 and 17.9%. (Table 4). As expected, 9-OH-Phe shows the highest variation.

Linearity, sensitivity, limit of detection and limit of quantification

A six-point calibration was performed by analyzing the aqueous standards twice in every sequence. The standards were freshly prepared for every sequence. Representative calibration results are shown in Table 5. The correlation coefficients generally meet the requirements with values >0.995. The only exception is again 9-hydroxyphenanthrene. The broad linear working ranges in combination with the low limits of detection and quantification (LOD = x_{blank} + 3 × s_{blank}, LOQ = x_{blank} + 10 × s_{blank}, with s = standard deviation of blind values and x_{blank} = concentration of blanks) allow the reliable quantification of low and high metabolite concentrations in urine without additional dilution or enrichment steps. Figure 2 shows a representative chromatogram of a urine sample containing details of a typical analysis cycle.

3.1.3 | Real samples

The HPLC-FLD method with integrated SPE for the determination of OH-PAH was developed with the goal of being able to analyze small volumes (≤0.5 mL, respectively) of 400 urine samples originating from a selected cohort exposed to normal, ambient PAH-levels. Before its routine use, the applicability of the method was demonstrated by analyzing a set of 16 urine samples. The donors were male and female adults living in the Augsburg area in Bavaria, Germany. Exceptional exposure to PAH (e.g. occupational exposure) was not expected. The set should represent a random sampling of adults living in a semi-urban environment.

Creatinine was determined as described in Section 2.5.2 and the concentrations were used to calculate the ratio µg OH-PAH/g creatinine. This step was performed to preserve comparability with published data, and all comparisons were conducted on basis of µg OH-PAH/g creatinine.

Graphical investigations (boxplot, histogram, Q-Q-plot) as well as a Shapiro–Wilks test showed that a normal distribution was not given for µg/g creatinine but can be achieved for log(µg/g creatinine). Therefore Spearman's rank correlations for µg/g creatinine and Pearson correlations for log(µg/g creatinine) were calculated. As shown in Tables S2 and S3, the coefficients are very similar. Highest correlations are observed for the hydroxyphenanthrenes among themselves. In contrast to the other hydroxyphenanthrenes, Pearson correlation coefficients for 9-OH-Phe are <0.82, probably owing to its instability

TABLE 4 Repeatability, reproducibility, limits of detection and limits of quantification for the HPLC-FLD determination of OH-PAH in urine

OH-PAH	Repeatability, CV (%)			Reproducibility, CV (%)	LOD (ng/L urine)	LOQ (ng/L urine)
	n = 9	n = 5	n = 5	n = 5		
2-OH-Phe	2.9	4.2	4.0	2.2	3.8	9.9
3-OH-Phe	1.0	3.4	1.5	5.2	2.6	6.7
1-OH-Phe	2.1	2.0	2.4	5.3	4.8	12.3
9-OH-Phe	8.8	n.d.	7.2	17.9	13.6	34.6
4-OH-Phe	2.9	3.9	2.4	5.9	5.1	12.9
1-OH-Pyr	15.6	3.3	2.1	12.4	3.3	8.7

HPLC-method II was applied. n.d., Not detected in this sample. Concentrations of OH-PAH in the urine samples were between 26.4 and 413.5 ng/L.

TABLE 5 Calibration curves and linear ranges for the determination of OH-PAH in urine using HPLC-FLD

OH-PAH	Calibration function	Correlation coefficient	Linear range (ng/L urine)
2-OH-Phe	$y = 791.2x - 2.27$	0.998	10–637
3-OH-Phe	$y = 1235.1x - 12.21$	0.995	7–360
1-OH-Phe	$y = 558.0x - 8.84$	0.998	12–816
9-OH-Phe	$y = 179.4x - 5.05$	0.985	35–990
4-OH-Phe	$y = 588.4x - 2.95$	0.998	13–536
1-OH-Pyr	$y = 161.9x - 7.71$	0.998	19–1200

HPLC-method II was applied.

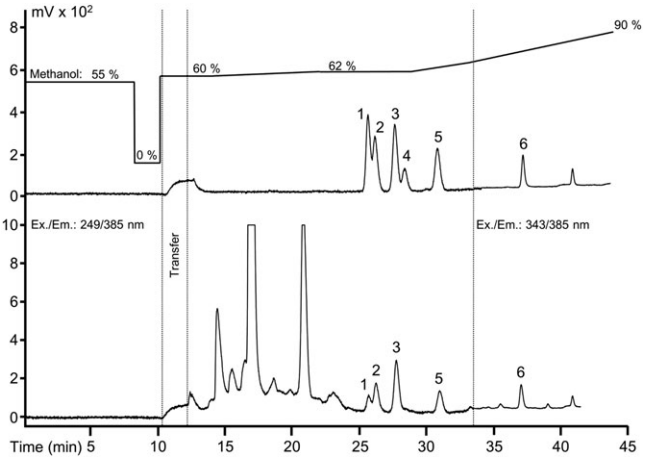

FIGURE 2 HPLC-FLD-chromatogram of a standard solution of OH-PAH (on top) and an enzymatically treated urine sample (at the bottom). 1, 2-OH-Phe; 2, 3-OH-Phe; 3, 1-OH-Phe; 4, 9-OH-Phe; 5, 4-OH-Phe; 6, 1-OH-Pyr. Concentrations of the OH-PAH determined were between 50 urine and 170 ng/L urine. HPLC-method II was applied

during enzymatic cleavage. This demonstrates yet again that values for 9-OH-Phe should be considered carefully. High correlations for hydroxyphenanthrenes were also observed by Polanska et al. (2014), who analyzed the urine of nonsmoking Polish pregnant women. We also found significant correlations between 1-hydroxypyrene and the hydroxyphenanthrenes, with Pearson correlation coefficients between 0.62 and 0.76. Polanska et al. found lower correlations with coefficients in the range from 0.35 to 0.59. These slightly different findings underline the necessity of studies investigating the validity of 1-OH-Pyr as a biomarker of internal PAH burden.

To set benchmarks for future epidemiological and biomonitoring studies the Centers for Disease Control and Prevention's National Health and Nutrition Examination Survey measured OH-PAH in urine specimen from almost 3000 participants (Li et al., 2008). The geometric mean calculated for adults (≥20 years) ranged from 0.034 µg/g creatinine for 9-OH-Phe to 0.137 µg/g creatinine for 1-OH-Phe. The geometric means measured in our study are in a similar range [0.033 µg/g creatinine (4-OH-Phen) to 0.214 µg/g creatinine (1-OH-Pyr)] with a tendency to higher values (see Table 6). Li et al. published a table in which concentrations of 1-OH-Pyr in urine collected in various countries were compared. It appears that German adults excreted higher amounts than adults in USA or Korea, which supports our findings. In contrast, Polanska et al. (2014) found mean values

TABLE 6 Descriptive statistics of OH-PAH in urine of 16 individuals (µg/g creatinine)

	Mean	± SD	Geometric mean	95th percentile
2-OH-Phe	0.162	0.177	0.085	0.464
3-OH-Phe	0.293	0.288	0.173	0.767
1-OH-Phe	0.304	0.266	0.191	0.744
9-OH-Phe	0.090	0.112	0.053	0.275
4-OH-Phe	0.066	0.089	0.033	0.249
1-OH-Pyr	0.289	0.242	0.214	0.714
∑-OH-Phe	0.908	0.817	0.574	2.173

between 0.17 µg/g creatinine for 4-OH-Phe and 1.50 µg/g creatinine for 1-OH-Phe in urine of Polish pregnant women. The mean values in our study are lower, ranging from 0.066 µg/g creatinine for 4-OH-Phe to 0.304 µg/g creatinine for 1-OH-Phe. The group of Urbancova et al. (2017) recently analyzed 531 urine samples of newborns and their mothers in the Czech Republic. They documented mean values between 0.098 µg/g creatinine for 3-OH-Phe and 0.540 µg/g creatinine for 1-OH-Phen. These concentrations are also in the same range as discussed before. The different findings for population groups in different countries are probably caused by influencing factors like ambient PAH concentrations and nutrition habits.

All studies mentioned above distinguish between the isomeric hydroxyphenanthrenes, allowing a consideration of their concentration patterns in urine. Considering the concentration patterns of the hydroxyphenanthrenes, the highest (geometric) mean concentrations are found for 1-OH-Phe in all studies. Lowest values are found for 9-OH-Phe or 4-OH-Phe in the studies of Li and Polanska as well as in the presented study (Li et al., 2008; Polanska et al., 2014). The values of 2-OH-Phe and 3-OH-Phe are in between them. Urbancova documented another order with 3-OH-PAH having the lowest mean, followed by 2-OH-Phe, 4-OH-Phe, 9-OH-Phe and 1-OH-Phe (Urbancova et al., 2017). The (geometric) mean for 1-OH-Pyr is mostly in the range of the values for 2- or 3-OH-Phe for all studies. It is important to note that Urbancova et al. investigated adults and newborns. Differences of exposure and metabolism probably influence concentrations and patterns of OH-PAH.

In all it can be concluded that the concentration levels of the OH-PAH determined in our study are consistent with the concentration levels reported in other studies for European and international populations. Concentration patterns of the target analytes are also very similar. Therefore the results underline the applicability of the

HPLC-FLD method with integrated SPE extraction for the reliable determination of 1-hydroxypyrene and 1- 2- 3- 4-, and 9-hydroxyphenanthrene in urine of normally exposed individuals.

3.2 | LC-HR-TOF-MS

In addition to the HPLC-FLD method, an LC-HR-TOF-MS (Citius™ HR-TOF, Leco Corporation, St Joseph, MI, USA) method was developed and investigated. To the best of our knowledge the hyphenation between UHPLC and HR-TOF-MS for the analysis of OH-PAH has not previously been described, and we expect that this method can essentially contribute to the following issues:

- identification of the target OH-PAH in the matrices urine and particulate matter; and
- feasibility of simultaneous target and suspect screening of OH-PAH in extracts of urine and $PM_{2.5}$.

The mass spectrometer was equipped with a UHPLC-instrument, and an appropriate PFP-column with 1.7 µm particles was used. Differences between the HPLC-FLD system and the LC-HR-TOF-MS system required adjustments of the UHPLC gradient considering column dimensions and different extra-column conditions (capillary connections, ion source parameters). The mobile phase was added with 0.1% acetic acid to increase ionization and thus sensitivity for the analytes. All measurements were done in negative ionization mode. Owing to the high-pressure conditions of UHPLC, a stable and reliable integration of the SPE-column into the LC-HR-TOF-MS-system could not be achieved. The selective copper phthalocyanine material cannot be used for an SPE procedure using cartridges. Thus, we decided to use an SPE method for sample processing of urine, as described by Romanoff et al. (2006; see Section 2.5.1.).

It rapidly became clear that the LC-HR-TOF-MS method was not sensitive enough to quantify OH-PAH in low volumes of urine samples or in extracts of $PM_{2.5}$ with low concentrations of OH-PAH. Therefore, this method was not validated, but some key parameters were determined to allow an assessment of its performance concerning the analysis of OH-PAH.

3.2.1 | Linearity, sensitivity and instrument detection limit

For the calculation of calibration curves, standards at four concentration levels from 5 to 500 pg/µL of the OH-phenanthrenes and 1-OH-pyrene were analyzed twice. Linearity was good with correlation coefficients >0.998. With increasing mass resolution the application of signal-to-noise ratios for the calculation of instrument detection limits loses its validity. The approach using the standard deviation of signals obtained after repeated injections of one standard concentration is more reliable (Vergeynst, Langenhove, Joos, & Demeestere, 2013). For this purpose one standard with a concentration of 5 ng/mL was injected four times. Instrument detection limits between 2.2 and 13.3 pg (on column) were calculated. With these detection limits the investigation of real samples (urine volume ≥ 3 mL, highly concentrated $PM_{2.5}$ extracts) should be possible. Calibration functions were determined applying UHPLC methods III and IV; the instrument detection limit was only determined for UHPLC method III. More information can be found in Table S4.

3.2.2 | Real samples

Three extracts of pooled urine samples were injected and analyzed by LC-HR-TOF-MS. Hydroxyphenanthrenes and 1-hydroxypyrene were successfully identified by matching retention times, isotopic patterns and accurate masses (mass accuracy threshold < 3 ppm) of standards and detected targets (cf. Tables 7 and 8). Concentrations of OH-PAH

TABLE 7 Parameters of target and suspect analytes detected in an extract of $PM_{2.5}$

Chemical formula $[M - H]^-$	Exact mass, *m/z*, (Da) $[M - H]^-$	Accurate mass, *m/z* (Da) $[M - H]^-$	Mass delta *m/z* (ppm)	RT (min)	(Suggested) compound identity
$C_{10}H_7O$	143.05024	143.05027	−0.21	3.92	Hydroxynaphthalene
$C_{10}H_7O$	143.05024	143.05033	−0.63	4.54	Hydroxynaphthalene
$C_{13}H_7O_2$	195.04515	195.04528	−0.67	5.78	Hydroxyfluorenone
$C_{13}H_7O_2$	195.04515	195.04511	0.21	6.31	Hydroxyfluorenone
$C_{13}H_7O_2$	195.04515	195.04523	−0.41	8.86	Hydroxyfluorenone
$C_{13}H_9O$	181.06589	181.06562	1.49	7.11	Hydroxyfluorene
$C_{13}H_9O$	181.06589	181.06564	1.38	7.58	Hydroxyfluorene
$C_{13}H_9O$	181.06589	181.06572	0.94	8.40	Hydroxyfluorene
$C_{14}H_9O$	193.06589	193.06600	−0.57	9.39	2-Hydroxyphenanthrene[a]
$C_{14}H_9O$	193.06589	193.06583	0.31	9.72	3-Hydroxyphenanthrene[a]
$C_{14}H_9O$	193.06589	193.06576	0.67	10.56	1-Hydroxyphenanthrene[a]
$C_{14}H_9O$	193.06589	193.06588	0.05	12.35	4-Hydroxyphenanthrene[a]
$C_{16}H_9O$	217.06589	217.06570	0.88	13.24	Hydroxyfluoranthene
$C_{16}H_9O$	217.06589	217.06608	−0.88	14.24	Hydroxyfluoranthene
$C_{16}H_9O$	217.06589	217.06582	0.32	14.69	Hydroxyfluoranthene
$C_{16}H_9O$	217.06589	217.06578	0.51	15.01	1-Hydroxypyrene[a]
$C_{20}H_{11}O$	267.08154	267.08112	1.57	15.77	Hydroxybenzo[a]pyrene

[a]Target analytes, identified by comparing with standard substances. UHPLC-method IV was applied.

TABLE 8 Parameters of target and suspect analytes detected in an extract of urine

Chemical formula $[M-H]^-$	Exact mass, *m/z* (Da) $[M-H]^-$	Accurate mass, *m/z* (Da) $[M-H]^-$	Mass delta *m/z* (ppm)	RT (min)	(Suggested) compound identity
$C_{10}H_7O$	143.05024	143.05000	1.68	7.88	Hydroxynaphthalene
$C_{14}H_9O$	193.06589	193.06537	2.70	15.47	2-Hydroxyphenanthrene[a]
$C_{14}H_9O$	193.06589	193.06566	1.19	16.00	3-Hydroxyphenanthrene[a]
$C_{14}H_9O$	193.06589	193.06570	0.98	17.40	1-Hydroxyphenanthrene[a]
$C_{14}H_9O$	193.06589	193.06573	0.83	18.27	9-Hydroxyphenanthrene[a]
$C_{14}H_9O$	193.06589	193.06593	−0.21	20.87	4-Hydroxyphenanthrene[a]
$C_{16}H_9O$	217.06589	217.06574	0.69	24.82	1-Hydroxypyrene[a]

[a]Target analytes, identified by comparing with standard substances.

UHPLC-method III was applied.

were calculated based on the calibration curves of the LC-HR-TOF-MS method. For urine samples, concentrations were between ~80 and ~850 ng/L, the OH-PAH concentrations in $PM_{2.5}$ ranged from ~5 to ~147 pg/m^3. It is to be noted that the values were obtained applying a nonvalidated method, therefore the results have to be considered as semi-quantitative. However, it can be seen that the values are of a similar magnitude to those found in other studies (Barrado et al., 2012; Lankova et al., 2016). Representative mass traces are shown in Figure 3.

To investigate the feasibility of simultaneous target and suspect screening using the LC-HR-TOF-MS method, we followed a shortened strategy compared with that published by Avagyan and Westerholm (2017). In this publication the detection and (suspect) identification of different OH-PAH in particulate matter of wood smoke and ambient air is described. The OH-PAH listed in in this work and in Avagyan et al. (2015), Avagyan, Aberg, & Westerholm, 2016) were used as a starting point to perform a *post hoc* evaluation of the chromatographic and especially the mass spectrometric data obtained during LC-HR-TOF-MS-analyses of extracts of $PM_{2.5}$ and urine. Exact masses for the molecular formulae suggested by Avagyan et al. were calculated and used for suspect screening. Elemental composition assignments (mass tolerance 5 ppm), isotopic pattern calculations and mass calculations were done using the ChromaTOF software (version 1.74, Leco Corporation, St Joseph, MI, USA). Furthermore a manual comparison of isotopic patterns with theoretical isotopic patterns was performed. The $PM_{2.5}$-samples analyzed were collected in February 2012 in the inner city of Munich, Germany. In winter, the site is dominated by emissions of traffic and heating. Preceding measurements of the $PM_{2.5}$ extract showed high concentrations of azaarenes (9.6–624.0 pg/m^3, unpublished, own results) therefore detectable OH-PAH concentrations were expected. Table 7 gives an overview of suspect analytes detected, and related chromatographic and mass spectrometric data. It can be seen that, in addition to the target analytes mentioned above, the existence of further OH-PAH, namely hydroxynaphthalenes, hydroxyfluorenone, hydroxyfluorene, hydroxyfluoranthene and hydroxybenzo[a]pyrene – or isomers of these compounds – can be assumed. Compared with the findings of Avagyan and Westerholm (2017), we did not find exact masses or respective isotopic patterns for hydroxyacenaphthylene, dihydroxyanthraquinone, hydroxybenzo[ghi]fluoranthene and hydroxydibenzo[ah]fluorene. For most exact masses two or more peaks with retention times within 1–3 min were detected, indicating the existence of isomeric compounds (see also Figure S1).

The search parameters used for the $PM_{2.5}$ extract were also applied for a *post hoc* evaluation of the data acquired during LC-HR-TOF-MS analysis of urine extracts. Compared with the results for $PM_{2.5}$, significantly less exact masses of OH-PAH were detected. As well as the target analytes, only the *m/z* and isotopic pattern characteristic for hydroxynaphthalenes were found. Hydroxyfluorenes were not detected (see Table 8, Figure S2). Explanations for these results could be the low concentrations in combination with an insufficient sensitivity of the HR-TOF-MS. Alternatively, the SPE-procedure was not optimized and validated, and losses of low-molecular-weight, low-hydrophobic analytes were possible. A thorough implementation of the strategy proposed by Avagyan et al. (mass-selected collision-induced fragmentation, verification with standards) lies far beyond the scope of our work. Nevertheless the results obtained for extracts of urine and $PM_{2.5}$ demonstrate the feasibility of simultaneous target and suspect screening of OH-PAH in different matrices using LC-HR-

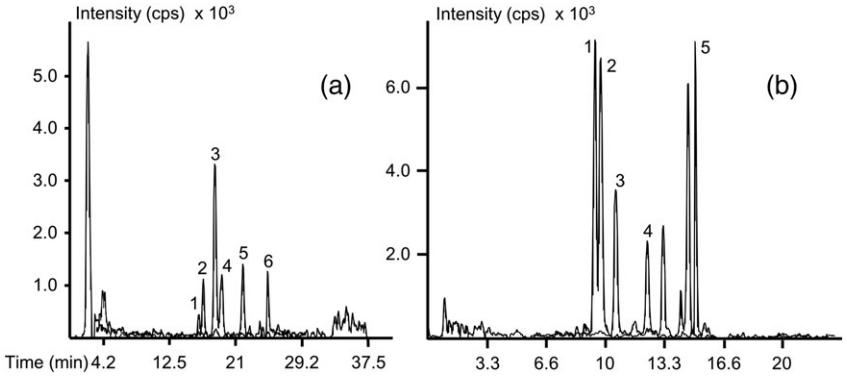

FIGURE 3 Extracted ion chromatograms of exact masses of hydroxyphenanthrenes (XIC, 193.0659 ± 0.0005) and 1-hydroxypyrene (XIC, 217 ± 0.0005) in extracts of urine (a) and $PM_{2.5}$ (b). Identified OH-PAH: 1, 2-OH-Phe; 2, 3-OH-Phe; 3, 1-OH-Phe; 4, 4-OH-Phe; 5, 1-OH-Pyr. Urine extract was analyzed using UHPLC-method III; $PM_{2.5}$ extract was measured applying UHPLC-method IV

TOF-MS. Moreover they support the existence of various OH-PAH in urban particulate matter, and the approach is very interesting for target analytical applications in complex environmental matrices.

4 | CONCLUSIONS

An HPLC-FLD method for the determination of hydroxyphenanthrenes and 1-hydroxypyprene in small volumes (<0.5 mL) of urine samples was developed and validated. The method describes for the first time the chromatographic separation of five isomeric hydroxyphenanthrenes coupled to HPLC-system-integrated sample processing. Using a selective material for system-integrated SPE, detection limits between 2.6 and 13.6 ng/L urine were achieved. To demonstrate and check the applicability of the method, a set of 16 urine samples was analyzed. Concentration levels and patterns of OH-PAH were similar to those reported in national and international studies. These findings underline the validity of the HPLC-FLD method for the reliable, routine determination of 1-hydroxypyrene and 1-, 2-, 3-, 4-, and 9-hydroxyphenanthrene in urine samples of individuals exposed to low and increased PAH-levels. The performance characteristics and the ability to use conventional instrumentation make the method attractive for applications analyzing high sample numbers using a simple, conventional HPLC-FLD system.

The successful transfer of the chromatographic separation to a UHPLC system and its coupling to HR-TOF-MS showed that LC-HR-TOF-MS is a valuable tool for target and suspect screening of different matrices containing OH-PAH. The LC-based methods described in this work cover diverse analytical aspects of OH-PAH ranging from low-level quantification in urine over suspect screening to tentative or reliable identification in urine and aerosol samples.

ACKNOWLEDGMENTS

This work was supported by intramural funding for Environmental Health projects of Helmholtz Zentrum München – German Research Center for Environmental Health and by funding from the Helmholtz association via the Helmholtz Virtual Institute HICE-Aerosol and Health (www.hice-vi.eu). We gratefully acknowledge Juergen Wendt from Leco Instrumente GmbH, Germany and Kevin Siek from from Leco Corp, USA for fruitful scientific discussions and indispensable support of the practical work with the Leco Citius® HRTOF instrument.

ORCID

Jutta Lintelmann http://orcid.org/0000-0002-0113-5746

REFERENCES

Avagyan, R., Aberg, M., & Westerholm, R. (2016). Suspect screening of OH-PAHs and non-target screening of other organic compounds in wood smoke particles using HR-Orbitrap-MS. *Chemosphere*, *163*, 313–321.

Avagyan, R., Nyström, R., Boman, C., & Westerholm, R. (2015). Determination of hydroxylated polycyclic aromatic hydrocarbons by HPLC-photoionization tandem mass spectrometry in wood smoke particles and soil samples. *Analytical and Bioanalytical Chemistry*, *407*, 4523–4534.

Avagyan, R., Nyström, R., Lindgren, R., Boman, C., & Westerholm, R. (2016). Particulate hydroxy-PAH emissions from a residential wood log stove using different fuels and burning conditions. *Atmospheric Environment*, *140*, 1–9.

Avagyan, R., & Westerholm, R. (2017). Target and suspect screening of OH-PAHs in air particulates using liquid chromatography–orbitrap high resolution mass spectrometry. *Talanta*, *165*, 702–708.

Barrado, A. I., García, S., Barrado, E., & Pérez, R. M. (2012). $PM_{2.5}$-bound PAHs and hydroxy-PAHs in atmospheric aerosol samples: Correlations with season and with physical and chemical factors. *Atmospheric Environment*, *49*, 224–232.

Barrado, A. I., García, S., Castrillejo, Y., & Barrado, E. (2013). Exploratory data analysis of PAH, nitro-PAH and hydroxy-PAH concentrations in atmospheric PM_{10}-bound aerosol particles. Correlations with physical and chemical factors. *Atmospheric Environment*, *67*, 385–393.

Boos, K.-S., Lintelmann, J., & Kettrup, A. (1992). Coupled-column high-performance liquid chromatographic method for the determination of 1-hydroxypyrene in urine of subjects exposed to polycyclic aromatic hydrocarbons. *Journal of Chromatography A*, *600*, 189–194.

Bourgogne, E., Grivet, C., Varesio, E., & Hopfgartner, G. (2015). Generic on-line solid phase extraction sample preparation strategies for the analysis of drugs in biological matrices by LC-MS/MS. *Journal of Pharmaceutical and Biomedical Analysis*, *102*, 290–298.

Chauhan, A., Bhatia, T., Singh, A., Saxena, P. N., Kesavchandran, C., & Mudiam, M. K. R. (2015). Application of nano-sized multi-template imprinted polymer for simultaneous extraction of polycyclic aromatic hydrocarbon metabolites in urine samples followed by ultra-high performance liquid chromatographic analysis. *Journal of Chromatography. B, Biomedical Sciences and Applications*, *985*, 110–118.

Chetiyanukornkul, T., Toriba, A., Kameda, T., Tang, N., & Hayakawa, K. (2006). Simultaneous determination of urinary hydroxylated metabolites of naphthalene, fluorene, phenanthrene, fluoranthene and pyrene as multiple biomarkers of exposure to polycyclic aromatic haydrocarbons. *Analytical and Bioanalytical Chemistry*, *386*, 712–718.

Fan, R., Wang, D., Ramage, R., & She, J. (2012). Fast and simultaneous determination of urinary 8-hydroxy-2′-deoxyguanosine and ten monohydroxylated polycyclic aromatic hydrocarbons by liquid chromatography/tandem mass spectrometry. *Chemical Research in Toxicology*, *25*, 491–499.

Grimmer, G., Dettbarn, G., & Jacob, J. (1993). Biomonitoring of polycyclic aromatic hydrocarbons in highly exposed coke plant workers by measurement of urinary monohydroxy metabolites. *Environmental Research*, *100*, 394–423.

Hayakawa, K., Tang, N., & Toriba, A. (2016). Recent analytical methods for atmospheric polycyclic aromatic hydrocarbons and their derivatives. *Biomedical Chromatography*, *31*, e3862.

Jacob, J., & Seidel, A. (2002). Biomonitoring of polycyclic aromatic hydrocarbons in human urine. *Journal of Chromatography. B, Analytical Technologies in the Biomedical and Life Sciences*, *778*, 31–47.

Jongeneelen, F. J., Anzion, R. B. M., & Henderson, P. T. (1987). Determination of hydroxylated metabolites of polycyclic aromatic hydrocarbons in urine. *Journal of Chromatography A*, *413*, 227–232.

Keyte, I. J., Harrison, R. M., & Lammel, G. (2013). Chemical reactivity and long-range transport potential of polycyclic aromatic hydrocarbons – A review. *Chemical Society Reviews*, *42*, 9333–9391.

Kowall, B., Rathmann, W., Stang, A., Bongaerts, B., Kuss, O., Herder, C., … Meisinger, C. (2017). Perceived risk of diabetes seriously underestimates actual diabetes risk: The KORA FF4 study. *PLoS One*, *12*(1), 1–13.

Lankova, D., Urbancova, K., Sram, R. J., Hajslova, J., & Pulkrabova, J. (2016). A novel strategy for the determination of polycyclic aromatic hydrocarbon monohydroxylated metabolites in urine using ultra-high-performance liquid chromatography with tandem mass spectrometry. *Analytical and Bioanalytical Chemistry*, *408*, 2515–2525.

Leroyer, A., Jeandel, F., Maitre, A., Howsam, M., Deplanque, D., Mazzuca, M., & Nisse, C. (2010). 1-Hydroxypyrene and 3-hydroxybenzo[a]pyrene

as biomarkers of exposure to PAH in various environmental exposure situations. *Science of the Total Environment*, *408*, 1166–1173.

Li, Z., Romanoff, L. C., Bartell, S., Pittman, E. N., Trinidad, D. A., McClean, M., … Sjödin, A. (2012). Excretion profiles and half-lives of ten urinary polycyclic aromatic hydrocarbon metabolites after dietary exposure. *Chemical Research in Toxicology*, *25*, 1452–1461.

Li, Z., Romanoff, L. C., Trinidad, D. A., Hussain, N., Jones, R. S., Porter, E. N., … Sjödin, A. (2006). Measurement of urinary monohydroxy polycyclic aromatic hydrocarbons using automated liquid–liquid extraction and gas chromatography/isotope dilution high-resolution mass spectrometry. *Analytical Chemistry*, *78*, 5744–5751.

Li, Z., Sandau, C. D., Romanoff, L. C., Caudill, S. P., Sjödin, A., Needham, L. L., & Patterson, D. G. Jr. (2008). Concentration and profile of 22 urinary polycyclic aromatic hydrocarbon metabolites in the US population. *Environmental Research*, *107*, 320–331.

Lin, Y., Ma, Y., Qiu, X., Li, R., Fang, Y., Wang, J., … Di Hu, D. (2015). Sources, transformation, and health implications of PAHs and their nitrated, hydroxylated, and oxygenated derivatives in $PM_{2.5}$ in Bejing. *Journal of Geophysical Research: Atmospheres*, *120*, 7219–7228.

Lin, Y., Qiu, X., Yu, N., Yang, Q., Araujo, J. A., & Zhu, Y. (2016). Urinary metabolites of polycyclic aromatic hydrocarbons and the association with lipid peroxidation: A biomarker-based study between Los Angeles and Beijing. *Environmental Science and Technology*, *50*, 3738–3745.

Lintelmann, J., & Angerer, J. (1999). PAH-metabolites. In J. Angerer, & K. H. Schaller (Eds.), *Analysis of hazardous substances in biological materials*, *Vol. 6* (pp. 163–187). Weinheim: Wiley.

Lintelmann, J., Heil-França, M., Hübner, E., & Matuschek, G. (2010). A liquid chromatography–atmospheric pressure photoionization tandem mass spectrometric method for the determination of azaarenes in atmospheric particulate matter. *Journal of Chromatography A*, *1217*, 1636–1646.

Lintelmann, J., Hellemann, C., & Kettrup, A. (1994). Coupled-column high-performance liquid chromatographic method for the determination of four metabolites of polycyclic aromatic hydrocarbons, 1-, 4-, and 9-hydroxyphenanthrene and 1-hydroxypyrene, in urine. *Journal of Chromatography. B, Analytical Technologies in the Biomedical and Life Sciences*, *660*, 67–73.

Liu, L., Luo, Y., Bi, J., Li, H., & Lin, J.-M. (2015). Quantification of selected monohydroxy metabolites of polycyclic aromatic hydrocarbons in human urine. *Science China Chemistry*, *58*, 1579–1584. https://doi.org/10.1007/s11426-015-5357-2

Ma, Y., Cheng, Y., Qiu, X., Lin, Y., Cao, J., & Hu, D. (2016). A quantitative assessment of source contributions to fine particulate matter ($PM_{2.5}$)-bound polycyclic aromatic hydrocarbons (PAHs) and their nitrated and hydroxylated derivatives in Hong Kong. *Environmental Pollution*, *219*, 742–749.

Miet, K., Le Menach, K., Flaud, P. M., Budzinski, H., & Villenave, E. (2009). Heterogeneous reactions of ozone with pyrene, 1-hydroxypyrene and 1-nitropyrene adsorbed on particles. *Atmospheric Environment*, *43*, 3699–3707.

Motorykin, O., Santiago-Delgado, L., Rohlman, D., Scherlau, J. E., Harper, B., Harris, S., … Simonich, S. L. M. (2015). Metabolism and excretion rates of parent and hydroxy-PAHs in urine collected after consumption of traditionally smoked salmon for Native American volunteers. *Science of the Total Environment*, *514*, 170–177.

Motorykin, O., Scherlau, J. E., Jia, Y., Harper, B., Harris, S., Harding, A., … Simonich, S. L. M. (2015). Determination of parent and hydroxy PAHs in personal $PM_{2.5}$ and urine samples collected during Native American fish smoking activities. *Science of the Total Environment*, *505*, 694–703.

Nilsson, R., Antic, R., Berni, A., Dallner, G., Dettbarn, G., Gromadzinska, J., … Seidel, A. (2013). Exposure to polycyclic aromatic hydrocarbons in women from Poland, Serbia and Italy–Relation between PAH, metabolite excretion, DNA damage, diet and genotype (the EU DIEPHY project). *Biomarkers*, *18*, 165–173.

Onyemauwa, F., Rappaport, S. M., Sobus, J. R., Gajdošová, D., Wu, R., & Waidyanatha, S. (2009). Using liquid chromatography–tandem mass spectrometry to quantifiy monohydroxylated metabolites of polycyclic aromatic hydocarbons in urine. *Journal of Chromatography. B, Analytical Technologies in the Biomedical and Life Sciences*, *877*, 1117–1125.

Polanska, K., Hanke, W., Dettbarn, G., Sobala, W., Gromadzinska, J., Magnus, P., & Seidel, A. (2014). The determination of polycyclic aromatic hydrocarbons in the urine of non-smoking Polish pregnant women. *Science of the Total Environment*, *487*, 102–109.

Ramsauer, B., Sterz, K., Hagedorn, H.-W., Engl, J., Scherer, G., McEwan, M., … Cheung, F. (2011). A liquid chromatography/tandem mass spectrometry (LC-MS/MS) method for the determination of phenolic polycyclic aromatic hydrocarbons (OH-PAH) in urine of non-smokers and smokers. *Analytical and Bioanalytical Chemistry*, *399*, 877–889.

Romanoff, L. C., Li, Z., Young, K. J., Blakely, N. C. III, Patterson, D. G. Jr., & Sandau, C. D. (2006). Automated solid-phase extraction method for measuring urinary polycyclic aromatic hydrocarbon metabolites in human biomonitoring using isotope–dilution gas chromatography high-resolution mass spectrometry. *Journal of Chromatography, B. Analytical Technologies in the Biomedical and Life Sciences*, *835*, 47–54.

Seidel, A., Spickenheuer, A., Straif, K., Rihs, H.-P., Marczynski, B., Scherenberg, M., … Pesch, B. (2008). New biomarkers of occupational exposure to polycyclic aromatic hydrocarbons. *Journal of Toxicology and Environmental Health A*, *71*, 734–745.

Urbancova, K., Lankova, D., Rossner, P., Rossnerova, A., Svecova, V., Tomaniova, M., … Pulkrabova, J. (2017). Evaluation of 11 polycyclic aromatic hydrocarbon metabolites in urine of Czech mothers and newborns. *Science of the Total Environment*, *577*, 212–219.

Vergeynst, L., Langenhove, H., Joos, P., & Demeestere, K. (2013). Accurate mass determination, quantification and determination of detection limits in liquid chromatography–high-resolution time-of-flight mass spectrometry: Challenges and practical solutions. *Analytica Chimica Acta*, *789*, 74–82.

Wang, Y., Meng, L., Pittman, E. N., Etheredge, A., Hubbard, K., Trinidad, D. A., … Calafat, A. M. (2017). Quantification of urinary mono-hydroxylated metabolites of polycyclic aromatic hydrocarbons by on-line solid phase extraction–high performance liquid chromatography–tandem mass spectrometry. *Analytical Bioanalytical Chemistry*, *409*, 931–937.

You, F., Zhu, L., He, L., Ran, L.-J., Jin, Y., & Sun, C.-J. (2014). Simultaneous determination of seven metabolites of polycyclic aromatic hydrocarbons in human urine by online solid phase extraction-high performance liquid chromatography. *Chinese Journal of Analytical Chemistry*, *42*, 1723–1728.

Zhou, L., Hu, Y., & Li, G. (2016). Conjugated microporous polymers with built-in magnetic nanoparticles for excellent enrichment of trace hydroxylated polycyclic aromatic hydrocarbons in human urine. *Analytical Chemistry*, *88*, 6930–6938.

SUPPORTING INFORMATION

Additional Supporting Information may be found online in the supporting information tab for this article.

How to cite this article: Lintelmann J, Wu X, Kuhn E, Ritter S, Schmidt C, Zimmermann R. Detection of monohydroxylated polycyclic aromatic hydrocarbons in urine and particulate matter using LC separations coupled with integrated SPE and fluorescence detection or coupled with high-resolution time-of-flight mass spectrometry. *Biomedical Chromatography*. 2018;32:e4183. https://doi.org/10.1002/bmc.4183

Research Article

TRANSPARENT PROCESS OPEN ACCESS

EMBO Molecular Medicine

Cholesterol metabolism promotes B-cell positioning during immune pathogenesis of chronic obstructive pulmonary disease

Jie Jia[1,2,†], Thomas M Conlon[1,2,†], Rim SJ Sarker[1,2], Demet Taşdemir[3], Natalia F Smirnova[1,2], Barkha Srivastava[1,2], Stijn E Verleden[4], Gizem Güneş[1,2], Xiao Wu[5], Cornelia Prehn[6,7], Jiaqi Gao[1,2], Katharina Heinzelmann[1,2], Jutta Lintelmann[5], Martin Irmler[8], Stefan Pfeiffer[9], Michael Schloter[9], Ralf Zimmermann[5,10], Martin Hrabé de Angelis[7,8,11], Johannes Beckers[7,8,11], Jerzy Adamski[6,7,11], Hasan Bayram[3,12], Oliver Eickelberg[1,2,13,*] & Ali Önder Yildirim[1,2,**]

Abstract

The development of chronic obstructive pulmonary disease (COPD) pathogenesis remains unclear, but emerging evidence supports a crucial role for inducible bronchus-associated lymphoid tissue (iBALT) in disease progression. Mechanisms underlying iBALT generation, particularly during chronic CS exposure, remain to be defined. Oxysterol metabolism of cholesterol is crucial to immune cell localization in secondary lymphoid tissue. Here, we demonstrate that oxysterols also critically regulate iBALT generation and the immune pathogenesis of COPD. In both COPD patients and cigarette smoke (CS)-exposed mice, we identified significantly upregulated CH25H and CYP7B1 expression in airway epithelial cells, regulating CS-induced B-cell migration and iBALT formation. Mice deficient in CH25H or the oxysterol receptor EBI2 exhibited decreased iBALT and subsequent CS-induced emphysema. Further, inhibition of the oxysterol pathway using clotrimazole resolved iBALT formation and attenuated CS-induced emphysema *in vivo* therapeutically. Collectively, our studies are the first to mechanistically interrogate oxysterol-dependent iBALT formation in the pathogenesis of COPD, and identify a novel therapeutic target for the treatment of COPD and potentially other diseases driven by the generation of tertiary lymphoid organs.

Keywords B cell; chronic obstructive pulmonary disease; inducible bronchus-associated lymphoid tissue; oxysterol; tertiary lymphoid organ

Subject Categories Immunology; Respiratory System

DOI 10.15252/emmm.201708349 | Received 31 July 2017 | Revised 8 March 2018 | Accepted 14 March 2018 | Published online 19 April 2018

EMBO Mol Med (2018) 10: e8349

Introduction

Chronic obstructive pulmonary disease (COPD) is a leading cause of chronic mortality and morbidity worldwide with limited therapeutic options, characterized by progressive and largely irreversible airflow limitation resulting from long-term exposure to toxic gases and particles, in particular cigarette smoke (CS; Berndt *et al*, 2012; Vogelmeier *et al*, 2017). This induces chronic bronchitis, small airway remodeling, and emphysema (loss of septal tissue; Tuder & Petrache, 2012). Growing evidence supports a crucial role for inducible bronchus-associated lymphoid tissue (iBALT) in the development of COPD (Hogg *et al*, 2004; Gosman *et al*, 2006; van der Strate *et al*, 2006; Polverino *et al*, 2015; Faner *et al*, 2016). Furthermore, we and others have recently shown that an absence of

1 Comprehensive Pneumology Center (CPC), Institute of Lung Biology and Disease, Helmholtz Zentrum München, Munich, Germany
2 Member of the German Center for Lung Research (DZL), Munich, Germany
3 Department of Chest Diseases, School of Medicine, University of Gaziantep, Gaziantep, Turkey
4 Division of Pneumology, KU Leuven, Leuven, Belgium
5 Joint Mass Spectrometry Centre, Comprehensive Molecular Analytics, Helmholtz Zentrum München, Munich, Germany
6 Institute of Experimental Genetics, Genome Analysis Center, Helmholtz Zentrum München, Munich, Germany
7 German Center for Diabetes Research (DZD), Munich, Germany
8 Institute of Experimental Genetics, Helmholtz Zentrum München, Munich, Germany
9 Research Unit Comparative Microbiome Analysis, Helmholtz Zentrum München, Munich, Germany
10 University of Rostock, Rostock, Germany
11 Chair of Experimental Genetics, Technische Universität München, Freising-Weihenstephan, Germany
12 School of Medicine, Koç University, Istanbul, Turkey
13 Division of Pulmonary Sciences and Critical Care Medicine, University of Colorado, Denver, CO, USA
*Corresponding author. Tel: +1 303 724 4075; E-mail: oliver.eickelberg@ucdenver.edu
**Corresponding author. Tel: +49 89 3187 4037; E-mail: oender.yildirim@helmholtz-muenchen.de
†These authors contributed equally to this work

iBALT, either through the use of B cell-deficient mice or administration of anti-CXCL13 antibody or BAFF-receptor fusion protein, prevented CS-induced emphysema in animal models of COPD (Bracke *et al*, 2013; John-Schuster *et al*, 2014; Seys *et al*, 2015).

Inducible bronchus-associated lymphoid tissue is a tertiary lymphoid organ that develops in the lungs during infection, autoimmunity, or chronic inflammation (Rangel-Moreno *et al*, 2011; Hwang *et al*, 2016). Interestingly, iBALT is located predominantly alongside the bronchial epithelium (Gregson *et al*, 1979). It is organized into regions of B-cell follicles surrounded by T-cell zones reminiscent of conventional secondary lymphoid organs (Randall, 2010). Follicular dendritic cells and high endothelial venules are located in the B- and T-cell zones, respectively (Moyron-Quiroz *et al*, 2004; Rangel-Moreno *et al*, 2007). A protective role for iBALT has been described due to their ability to fight viral infection (Moyron-Quiroz *et al*, 2004; Chiu & Openshaw, 2015), and however, they can have a detrimental impact on the outcome of chronic inflammatory conditions such as COPD (Hwang *et al*, 2016). Their causative role against COPD development and the mechanism underlying iBALT positioning upon the bronchus, however, remains to be defined.

The oxysterol metabolism of cholesterol has recently emerged as a central pathway that regulates the structure and function of secondary lymphoid tissue (Hannedouche *et al*, 2011; Liu *et al*, 2011; Gatto *et al*, 2013; Li *et al*, 2016). The sequential action of two enzymes cholesterol 25-hydroxylase (CH25H) and 25-hydroxycholesterol 7-alpha-hydroxylase (CYP7B1) synthesizes 7α,25-dihydroxycholesterol (7α,25-OHC) from cholesterol, the main ligand of Epstein–Barr virus-induced gene 2 (EBI2; also known as GPR183; Hannedouche *et al*, 2011; Liu *et al*, 2011). EBI2 is a G protein-coupled receptor expressed on lymphocytes and dendritic cells (DCs), which plays a key role in their positioning within secondary lymphoid tissue. EBI2 on B cells (Gatto *et al*, 2009; Pereira *et al*, 2009) and 7α,25-OHC generated by lymphoid stromal cells (Yi *et al*, 2012) guides activated B-cell movement during humoral responses.

In this study, we hypothesize that oxysterols are critically involved in the immune pathogenesis of COPD by guiding B-cell positioning within iBALT structures. We demonstrate, in both COPD patients and CS-exposed mice, upregulated CH25H and CYP7B1 expression in airway epithelial cells. Moreover, mice deficient in CH25H or EBI2 exhibited decreased iBALT formation and subsequent CS-induced emphysema. Further, activated B cells through BCR cross-linking failed to migrate toward CS-stimulated airways *ex vivo* following genetic or pharmacological inhibition of the oxysterol pathway, establishing a role for oxysterol metabolism in guiding iBALT generation to the airways during COPD immunopathogenesis. Finally, inhibition of the oxysterol pathway, using the CYP7B1 inhibitor clotrimazole, resolved B cell-driven iBALT formation and attenuated CS-induced emphysema *in vivo* in a therapeutic approach. Collectively, our studies are the first to mechanistically interrogate oxysterol-dependent iBALT formation in the pathogenesis of COPD, and identify a novel therapeutic target for the treatment of COPD in particular, as well as other chronic diseases driven by the generation of tertiary lymphoid organs.

Results

Oxysterol metabolism increases in airway epithelial cells of COPD patients and mouse

Airway epithelial cells secrete a plethora of immune mediators (Benam *et al*, 2016), yet immunological factors that orchestrate iBALT positioning remain to be defined. We analyzed transcriptomics data from publically available datasets of small airway epithelial cells from COPD patients (Tilley *et al*, 2011) combined with our data derived from chronic CS-exposed mice lungs (John-Schuster *et al*, 2014), revealing a conserved interspecies signature for the expression of key genes related to the Gene Ontology terms (Wang *et al*, 2013) of "Inflammatory Response", "Macrophage Activation", and "Leukocyte Migration" (Fig EV1A). Gene expression patterns were also similar within the Gene Ontology term "Metabolic Process", and in particular, *CH25H* and *CYP7B1* were upregulated following both CS exposure in mice and in COPD patients (Fig 1A). Similarly, RNAseq analysis of lung homogenates from an independent COPD patient cohort confirmed higher *CH25H* expression in the lungs of COPD patients compared to non-smoking control individuals (Fig 1B), supporting a previous study (Sugiura *et al*, 2012). To demonstrate an association with emphysema, lung core samples from a third independent cohort composed of emphysematous and non-emphysematous tissue from the same COPD patients were analyzed (Fig 1C). mRNA expression of *CH25H* and the pro-inflammatory chemokine *CXCL8* were significantly upregulated in emphysematous regions rather than non-emphysematous regions of COPD patient lungs, while in contrast to recent findings (Faner *et al*, 2016), *CXCL13* expression did not differ (Fig 1D). Staining of airway sections revealed that CH25H was localized to the airway epithelial cells in both human and mice (Fig 1E), suggesting that the initiating lesion in both patients and mice following chronic CS exposure emanates from the airways. *CH25H* mRNA expression was elevated in isolated airway epithelial cells from COPD patients compared to healthy smoking controls (fourth independent cohort; Fig 1F), as well as in isolated mouse airways after CS exposure, and remained elevated for at least 16 weeks (Fig 1G). Bronchoalveolar lavage fluid obtained from mice exposed to 6 months chronic CS revealed a higher concentration of 25-hydroxycholesterol as assessed by liquid chromatography–high-resolution mass spectrometry (Fig 1H).

To address the mechanism underlying the regional upregulation of CH25H predominantly localized to the airways in COPD patients and in particular that associated with emphysematous tissue, we first undertook gene set enrichment analysis (GSEA; Mootha *et al*, 2003; Subramanian *et al*, 2005) on the publically available transcriptomics dataset of small airway epithelial cells from COPD patients described above (Tilley *et al*, 2011). CH25H upregulation is driven by TLR4 Myd88-independent signaling (Diczfalusy *et al*, 2009), and indeed, GSEA revealed a strong enrichment of both total TLR- and TLR4-dependent signaling in small airway epithelial cells taken from the lungs of COPD patients compared to smoking controls (Fig EV1B). Supporting a recent observation that *TLR4* expression is increased in the airways of COPD patients (Haw *et al*, 2017). Furthermore, staining of airway sections revealed a strong increase in TLR4 expression localized to the airways of emphysematous COPD patients rather than non-emphysematous or healthy

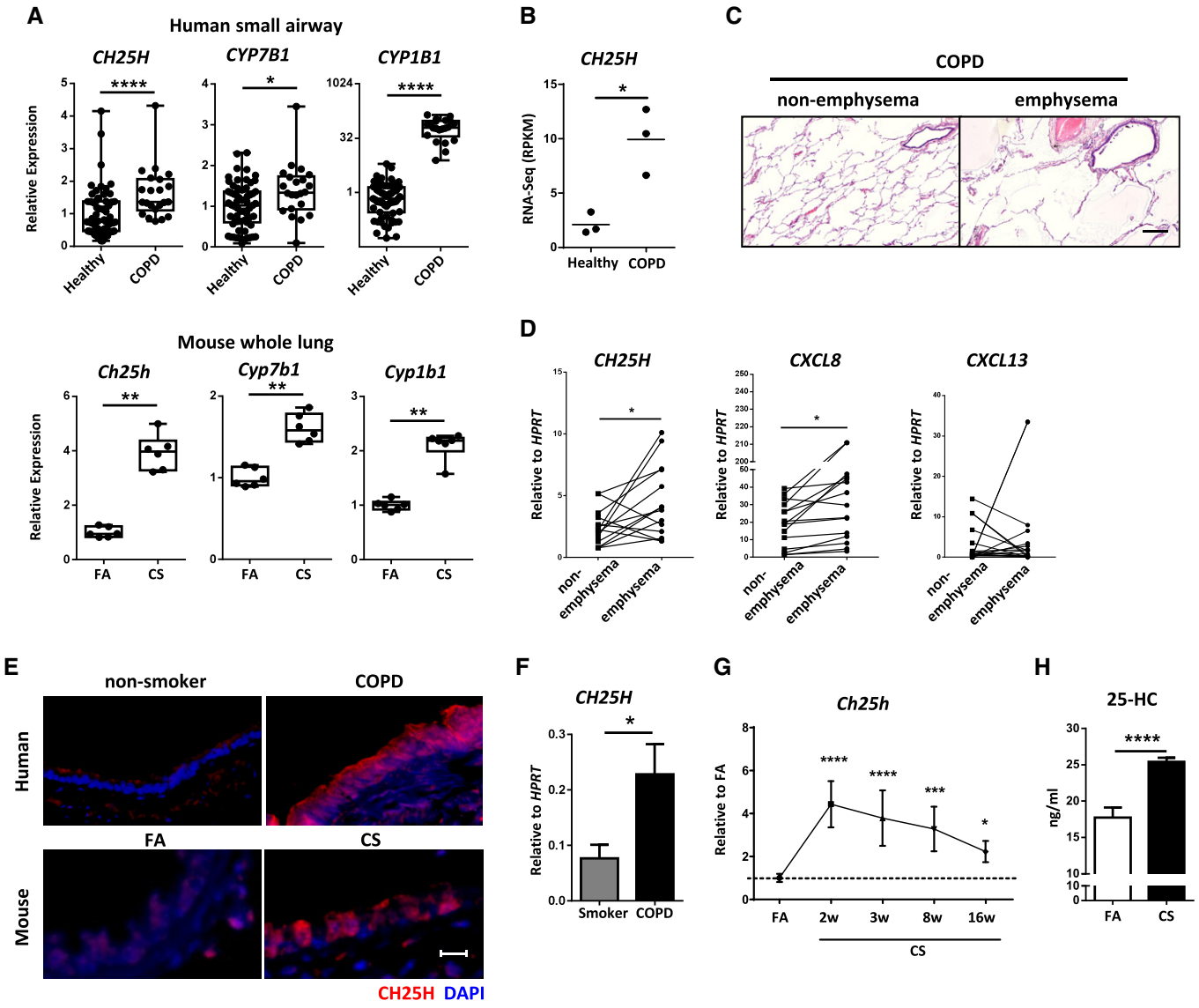

Figure 1. Increased expression of the oxysterol metabolizing enzyme CH25H in airway epithelial cells of COPD patients.

A Box and whisker plots of mouse lung and human small airway epithelial cell microarray data of the relative expression of the genes from NCBI GEO data series. The box extends from the 25th to 75th percentiles with the central line indicating the median and the whiskers the minimum and maximum values. Each dot represents an individual. FA, filtered air; CS, cigarette smoke. *P = 0.0119, **P = 0.0022 (*Ch25h*, *Cyp7b1*, and *Cyp1b1*) and ****$P < 0.0001$.

B RNAseq data of *CH25H* expression in an independent COPD cohort, three patients per group. *P = 0.0136.

C Representative H&E-stained lung cores from non-emphysematous and emphysematous regions of the same COPD patient lung (fourteen patients). Scale bar, 500 μm.

D *CH25H*, *CXCL8*, and *CXCL13* mRNA abundance from lung core samples described in (C). Individual patients shown. *P = 0.0261 (*CH25H*) and 0.0482 (*CXCL8*).

E Representative immunofluorescence analysis of airway from lungs of human non-smokers or COPD patients and from mice exposed to filtered air (FA) or cigarette smoke (CS) for 6 months, stained to detect CH25H (red) and DAPI (blue). Four to eight patients per group, and eight mice per group. Scale bar, 50 μm.

F *CH25H* mRNA abundance in isolated airway epithelial cells from smokers (n = 10) and COPD patients (n = 11). *P = 0.0236.

G *Ch25h* mRNA abundance in isolated airways from C57BL/6 mice exposed to cigarette smoke (CS) for the duration indicated, shown relative to filtered air (FA), one experiment with five mice per group. *P = 0.0377, ***P = 0.0002, and ****$P < 0.0001$.

H Levels of 25-hydroxycholesterol in the bronchoalveolar lavage fluid of C57BL/6 mice exposed to FA or CS for 6 months as determined by liquid chromatography–high-resolution TOF mass spectrometry, one experiment with four mice per group. ****$P < 0.0001$.

Data information: Data are mean ± SD (F, G, H). Mann–Whitney test (A, F), two-tailed unpaired t-test (B, H), two-tailed paired t-test (D) or one-way ANOVA, and uncorrected Fisher's LSD (G).

control airways (Fig EV1C). Additionally, treating human bronchial epithelial cell lines with the TLR4 agonist LPS induced expression of *CH25H* similar to that observed with cigarette smoke (Fig EV1D and E). Interestingly, the pro-inflammatory cytokine TNF-α alone was also able to induce enhanced *CH25H* expression in airway epithelial cells, suggesting that the pro-inflammatory environment in addition

to direct effects of CS exposure upon the airway epithelial cells is capable of enhancing *CH25H* expression. These translational results lead us to hypothesize that CS-activated CH25H signaling in the airway epithelium may confer iBALT formation.

Diminished oxysterol pathways impaired iBALT formation and attenuated cigarette smoke-induced COPD

To determine the role of CH25H in iBALT formation *in vivo*, we exposed CH25H-deficient mice to CS for 4 and 6 months to induce emphysema development (John-Schuster *et al*, 2014; Cloonan *et al*, 2016; Baarsma *et al*, 2017). Importantly, the lungs of these mice showed no general metabolic differences, even after CS exposure, compared to the wild-type animals (Fig EV2A). Wild-type mice developed clear evidence of emphysema accompanied by iBALT formation from 4 months onwards (Fig 2A–C), that specifically associated with the airways further with vessels and septal tissue (Fig 2D), whereas in *Ch25h*$^{-/-}$ mice formation of iBALT and the hallmarks of emphysema failed to develop (Fig 2A–D). Flow cytometric analysis of whole lung cells showed that both T and B cells were activated after CS exposure similarly in both *Ch25h*$^{-/-}$ and wild-type mice (Fig 2E), suggesting that CH25H is important for cellular positioning within the iBALT and not recruitment and activation of T and B cells to the lung. In support, cellular recruitment into the BAL as well as mRNA expression of *Cxcl13*, *Cxcl9*, *Ccl19*, *Ccl21*, *Cxcl1,* and *Mcp1* was equivalently increased in both wild-type and *Ch25h*$^{-/-}$ mice following CS exposure (Fig EV2B and C).

We have previously shown that B cell-deficient mice do not generate iBALT and that this prevented CS-induced emphysema by impairing the activation of macrophages and MMP12 upregulation (John-Schuster *et al*, 2014). To address the mechanisms underlying the protection against emphysema in *Ch25h*$^{-/-}$ mice, flow cytometric analysis was undertaken on the lavaged lungs to address the recruitment of macrophages into the lung tissue following CS exposure. In contrast to the BAL, total F4/80^{+} macrophages and CD11c^{-} CD11b^{+} recruited macrophages were significantly reduced in the lungs of *Ch25h*$^{-/-}$ mice compared to wild-type animals following chronic CS exposure (Fig EV2D–F). In support, immunohistochemically stained galectin-3-positive macrophages (Fig EV2G), mRNA expression of *Adgre1* the gene for F4/80 (Fig EV2H), and the *Mmp12:Timp1* ratio (Fig EV2I) were significantly reduced in the lungs of *Ch25h*$^{-/-}$ mice compared to wild type, following exposure to CS. Furthermore, flow cytometric analysis revealed reduced Ly6g-positive neutrophils in the lungs of *Ch25h*$^{-/-}$ mice compared to wild-type animals following chronic CS exposure (Fig EV2J–K).

To confirm the importance of local oxysterol production in iBALT generation and COPD pathogenesis, we next exposed mice lacking EBI2, the receptor for 7α,25-OHC, to chronic cigarette smoke for 4 months. Similar to *Ch25h*$^{-/-}$ mice, these *Ebi2*$^{-/-}$ animals also failed to generate iBALT or any features of emphysema (Fig 3A–C). Leukocyte recruitment to the bronchoalveolar lavage fluid following CS exposure was similar in both wild-type and *Ebi2*$^{-/-}$ mice (Fig EV3A), with cytokine and chemokine expression profiles similar to that observed for *Ch25h*$^{-/-}$ and wild-type mice (Fig EV3B). Flow cytometric analysis of whole lung cells revealed that both T and B cells were recruited to the lungs of *Ebi2*$^{-/-}$ mice in similar numbers to wild-type animals following CS exposure (Fig 3D and E), but interestingly less B cells were activated in the *Ebi2*$^{-/-}$ mice (Fig 3D), suggesting a further role for EBI2 beyond B-cell positioning (Benned-Jensen *et al*, 2011). To address this, splenic B cells were isolated from *Ebi2*$^{-/-}$ and wild-type mice and activated *ex vivo* by IgM cross-linking. Similar to the *in vivo* situation flow cytometric analysis revealed reduced activation of *Ebi2*$^{-/-}$ B cells as demonstrated by less upregulation of the surface activation marker CD69 (Fig EV3C), which was accompanied by reduced MHC II expression (Fig EV3D). CD69 expression in B cells is regulated by Egr1 (Richards *et al*, 2001; Vazquez *et al*, 2009), a primary response gene rapidly induced in B cells following BCR cross-linking (Seyfert *et al*, 1989; McMahon & Monroe, 1995). Interestingly, *Ebi2*$^{-/-}$ B cells 6 h post-BCR cross-linking upregulated *Egr1* less than wild-type B cells (Fig EV3E), proposing that the impaired activation of *Ebi2*$^{-/-}$ B cells may stem from an inability to fully induce expression of the early response gene *Egr1*. Future work should determine further the role of Ebi2 in *Egr1* transcriptional regulation.

To exclude a role for 25-hydroxycholesterol in emphysema development beyond iBALT formation, we examined B cell-deficient mice (μMT) that are resistant to CS-induced iBALT formation and emphysema (John-Schuster *et al*, 2014). Consistent with wild type, these animals demonstrated increased expression of *Ch25h* and *Cyp7b1* (Fig EV4A and B) in their lungs with CH25H expression localizing to the airway epithelial cells (Fig EV4C) following acute and chronic CS exposure. Collectively, these data demonstrated that oxysterol-induced signaling pathways guide iBALT generation during CS-induced COPD.

Figure 2. Impaired iBALT formation and attenuated cigarette smoke-induced COPD in CH25H-deficient mice.

A Representative H&E-stained lung from wild-type (WT) and CH25H-deficient (*Ch25h*$^{-/-}$) mice exposed to filtered air (FA) or cigarette smoke (CS) for 4 and 6 months. Scale bar, 200 μm.

B, C Mean chord length (MCL) and iBALT quantification of lung sections from the mice described in (A), following 4 months (B) or 6 months (C) of CS exposure. (B) $^{**}P = 0.0002$ and $^{****}P < 0.0001$ (emphysema quantification) and $^{**}P = 0.0095$ (iBALT quantification). (C) $^{**}P = 0.0022$ (emphysema quantification), $^{*}P = 0.0207$ (FA vs. CS, WT mice, iBALT quantification), and $^{*}P = 0.0373$ (CS WT vs. CS *Ch25h*$^{-/-}$ mice, iBALT quantification).

D Left: Representative immunofluorescence images of the three regions quantified, stained to detect CD45R (B cells, red), CD3 (T cells, green), and DAPI (blue). A, airway; V, vessel. Scale bar, 50 μm. Right: Quantification of iBALT localized on the airway, vessels, and septal area from the mice described in (A). Airway: $^{***}P = 0.0007$ (FA vs. 6 m CS, WT mice) and $^{***}P = 0.0008$ (6 m CS WT vs. 6 m CS *Ch25h*$^{-/-}$ mice). Vessel: $^{*}P = 0.0446$ (FA vs. 6 m CS, WT mice) and $^{*}P = 0.0356$ (6 m CS WT vs. 6 m CS *Ch25h*$^{-/-}$ mice). Septum: $^{*}P = 0.0194$ (FA vs. 6 m CS, WT mice).

E Flow cytometric analysis of whole lung single-cell suspensions from mice in (A), to detect CD69-positive CD19 and CD3 cells. Left: Example dot plots of FA- and CS-exposed mice. Right: Frequency of CD69-positive cells. CD69^{+} CD19^{+} cells: $^{**}P = 0.0062$ and $^{****}P < 0.0001$. CD69^{+} CD3^{+} cells: $^{*}P = 0.0230$ and $^{****}P < 0.0001$.

Data information: Data are mean ± SD. *P*-values determined by one-way ANOVA and Tukey's multiple comparisons test. Data are representative of two independent experiments (A–D) or one experiment (E) with four mice per FA group or six mice per CS group.

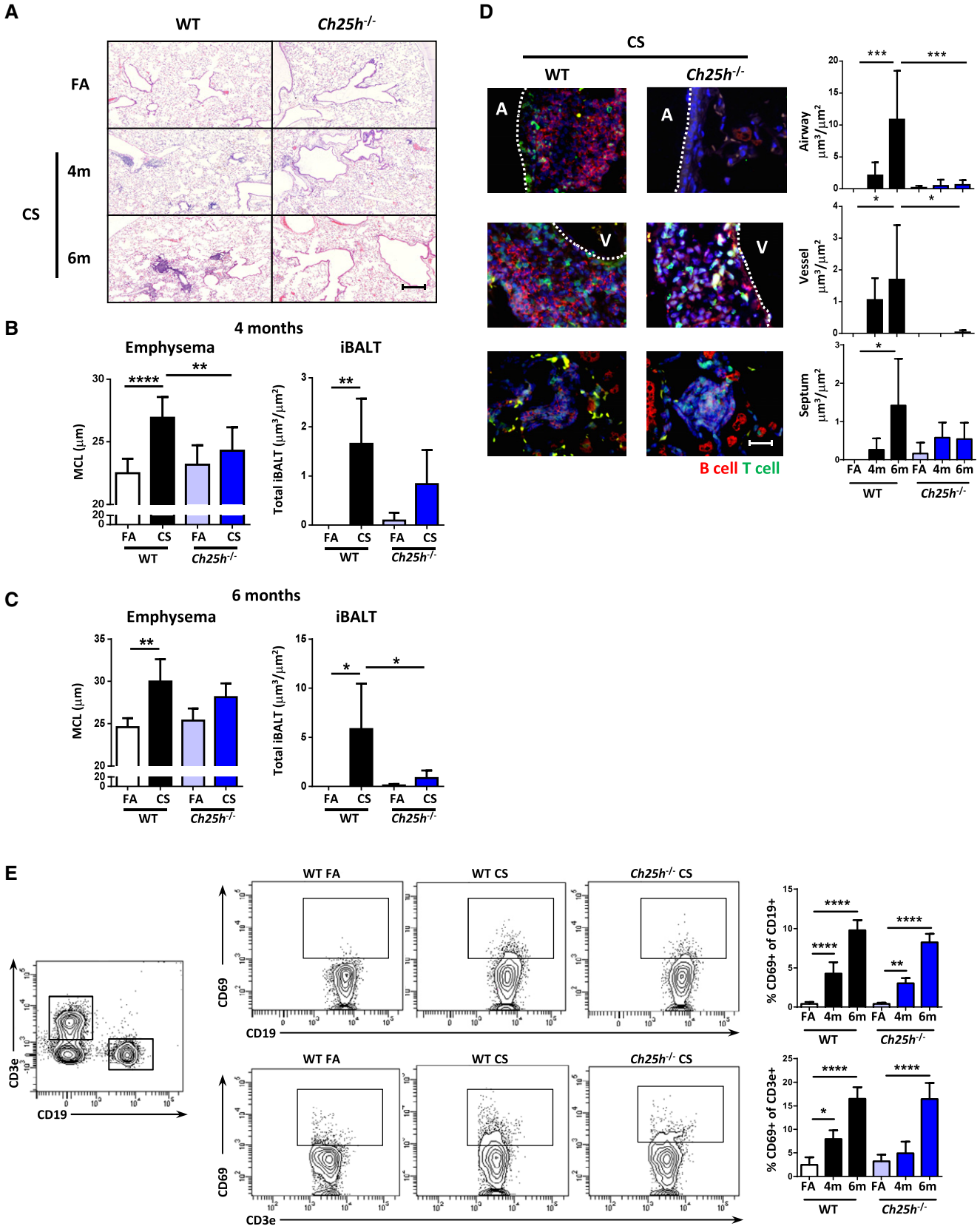
A
WT
Ch25h-/-
FA
4m
CS
6m
B
4 months
Emphysema
iBALT
MCL (μm)
Total iBALT (μm³/μm²)
FA CS FA CS
WT
Ch25h-/-
C
6 months
Emphysema
iBALT
D
CS
WT
Ch25h-/-
A
V
B cell T cell
Airway μm³/μm²
Vessel μm³/μm²
Septum μm³/μm²
FA 4m 6m FA 4m 6m
WT
Ch25h-/-
E
CD3e
CD19
WT FA
WT CS
Ch25h-/- CS
CD69
% CD69+ of CD19+
% CD69+ of CD3e+

Figure 2.

CH25H deficiency does not protect against iBALT-independent emphysema

Previous data demonstrate that professional APCs can express CH25H under inflammatory conditions (Park & Scott, 2010; Liu *et al*, 2013). These findings led us to interrogate whether differential cytokine secretion by resident alveolar or bone marrow-recruited macrophages (BMDM) deficient in CH25H were involved in emphysema development. Isolated alveolar macrophages significantly increased expression of *Ch25h* under both polarizing conditions (Fig EV5A), while BMDM from wild-type mice significantly increased expression of *Ch25h* only under M1-polarizing conditions (Fig EV5B). Importantly, both alveolar and bone marrow macrophages from wild-type and *Ch25h*$^{-/-}$ mice induced strong expression of *Tnfa* and *Il1b* under M1-polarizing conditions as well as *Irf4* and *Fizz1* as key transcription factors regulating M2 polarization (Satoh *et al*, 2010) after culturing with IL-4 (Fig EV5A and B). To extend these findings, we cultured bone marrow-derived DCs isolated from wild-type and *Ch25h*$^{-/-}$ mice with LPS and found similarly increased expression of *Il12a*, *Tnfa*, and *Nos2* from both mice (Fig EV5C). In combination, this suggests that impaired cytokine secretion by professional APCs is not a contributing factor in CH25H-deficient mice. Furthermore, recent evidence revealed that depletion of alveolar macrophages ameliorated elastase-induced

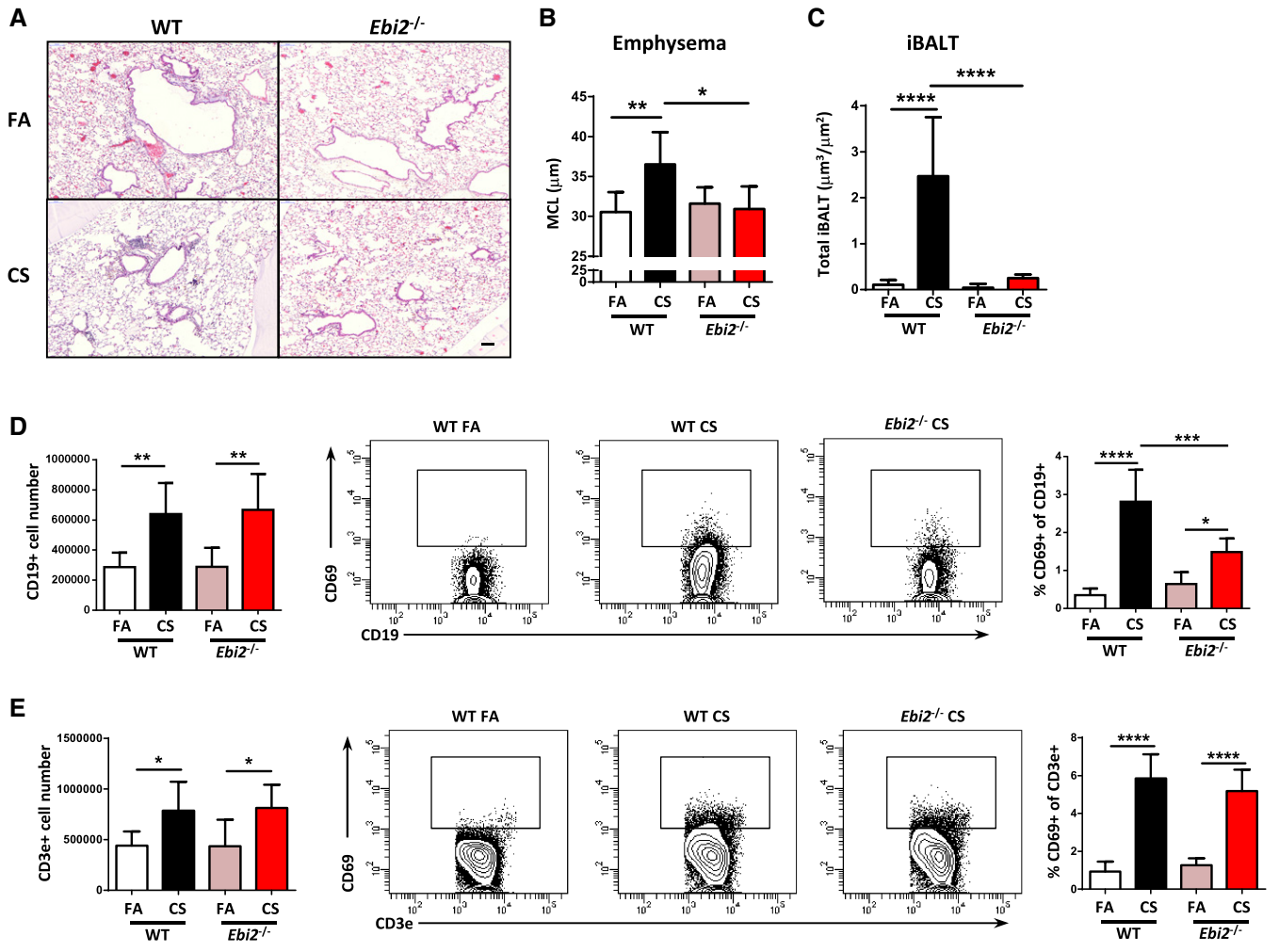

Figure 3. EBI2-deficient mice are protected against iBALT formation and cigarette smoke-induced COPD.

A Representative H&E-stained lung from wild-type (WT) and EBI2-deficient (*Ebi2*$^{-/-}$) mice exposed to filtered air (FA) or cigarette smoke (CS) for 4 months. Scale bar, 100 μm.

B Mean chord length (MCL) quantification of lung sections from the mice described in (A). **P* = 0.0155 and ***P* = 0.0064.

C Quantification of total lung iBALT from the mice in (A). *****P* < 0.0001.

D, E Flow cytometric analysis of whole lung single-cell suspensions from mice in (A), to detect CD19$^+$ and CD69$^+$ CD19$^+$ cells (D) and CD3$^+$ and CD69$^+$ CD3$^+$ cells (E). CD19$^+$ cells: ***P* = 0.0027 (FA vs. CS, WT mice) and ***P* = 0.0028 (FA vs. CS, *Ebi2*$^{-/-}$ mice). CD69$^+$ CD19$^+$ cells: **P* = 0.0232, ****P* = 0.0003, and *****P* < 0.0001. CD3$^+$ cells: **P* = 0.0319 (FA vs. CS, WT mice) and **P* = 0.0368 (FA vs. CS, *Ebi2*$^{-/-}$ mice). CD69$^+$ CD3$^+$ cells: *****P* < 0.0001.

Data information: Data are mean ± SD. *P*-values determined by one-way ANOVA and Tukey's multiple comparisons test. Data are from one experiment six mice per group (*Ebi2*$^{-/-}$ CS), seven mice per group (WT CS or *Ebi2*$^{-/-}$ FA), or eight mice per group (WT FA).

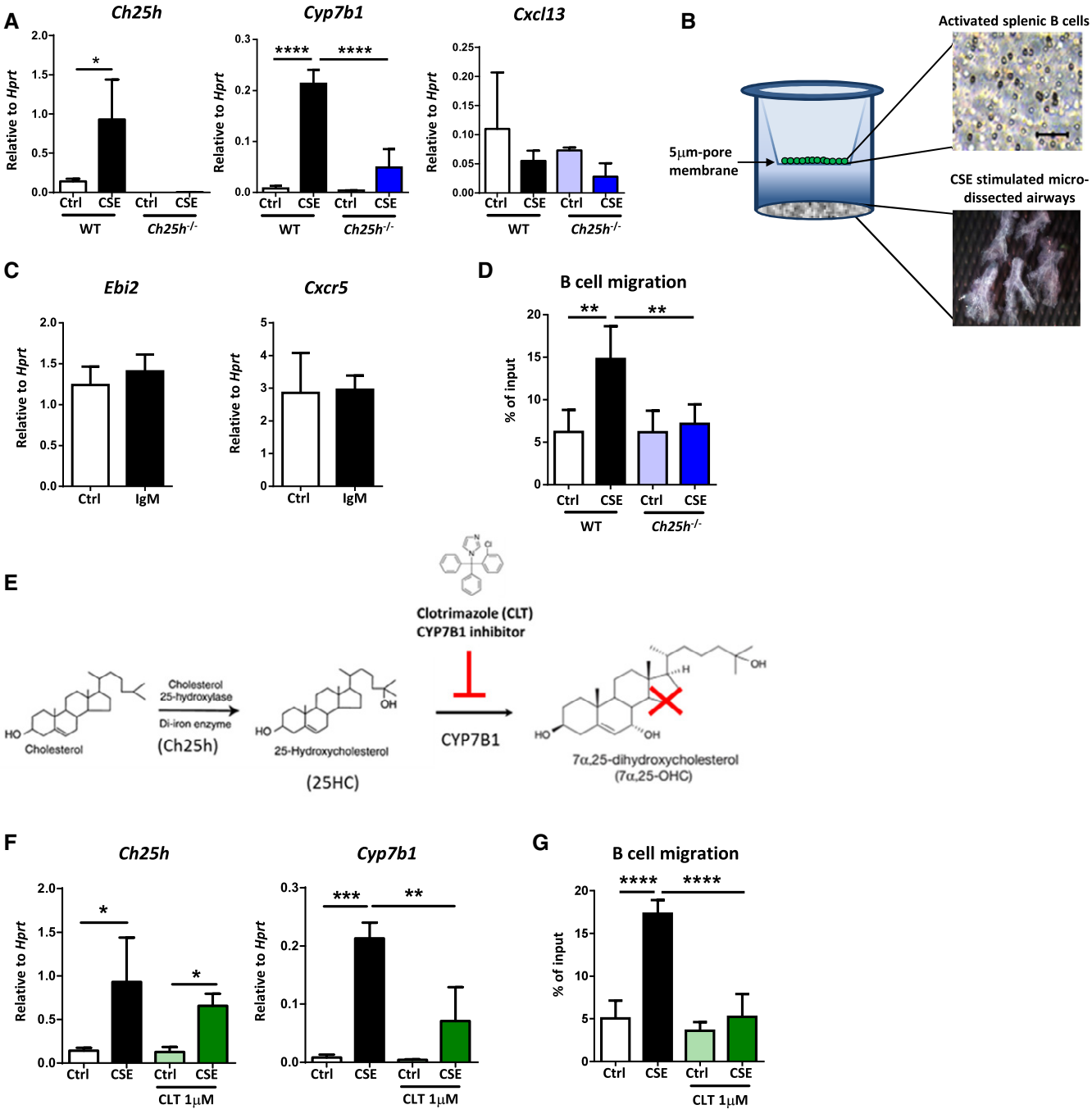

Figure 4. CH25H deficiency or attenuation of CYP7B1 activity with clotrimazole impairs B-cell migration toward CSE-treated airways *ex vivo*.

A *Ch25h*, *Cyp7b1*, and *Cxcl13* mRNA abundance from CSE-treated airways dissected from wild-type (WT) or CH25H-deficient (*Ch25h*$^{-/-}$) mice. *P = 0.0400 and ****P < 0.0001.

B Schematic representation of *ex vivo* B-cell migration assay.

C *Ebi2* and *Cxcr5* mRNA abundance from IgM cross-linked B cells isolated from the spleen of C57BL/6 mice.

D Frequency of IgM cross-linked splenic B cells migrating toward medium from CSE-treated airways dissected from WT or *Ch25h*$^{-/-}$ mice. **P = 0.0012 (Ctrl vs. CSE, WT airways) and **P = 0.0035 (CSE WT vs. CSE *Ch25h*$^{-/-}$ airways).

E Schematic representation of the metabolism of 7α,25-OHC from cholesterol.

F *Ch25h* and *Cyp7b1* mRNA abundance from CSE-treated airways, in the absence or presence of 1 μM clotrimazole, dissected from C57BL/6 mice. *Ch25h*: *P = 0.0297 (Ctrl vs. CSE, untreated airways) and *P = 0.0112 (Ctrl vs. CSE, clotrimazole treated airways). *Cyp7b1*: **P = 0.0056 and ***P = 0.0008.

G Frequency of IgM cross-linked splenic B cells migrating toward medium from CSE-treated airways, in the absence or presence of 1 μM clotrimazole, dissected from C57BL/6 mice. ****P < 0.0001.

Data information: Data are mean ± SD. P-values determined by one-way ANOVA and Tukey's multiple comparisons test. All experiments repeated twice with three mice per group.

emphysema (Ueno *et al*, 2015), an iBALT-independent emphysema mouse model (Dau *et al*, 2015; Sarker *et al*, 2015). Therefore, we utilized this model to demonstrate that loss of CH25H in macrophages did not impact upon emphysema development. Both wild-type and *Ch25h*$^{-/-}$ mice developed a severe emphysema following elastase treatment, with no evidence of iBALT formation in either mice (Fig EV5D–H). These data further demonstrate that CH25H-deficient macrophages are not protective against elastase-induced emphysema, implying the role of CH25H in iBALT-mediated COPD pathogenesis.

Oxysterols guide B-cell migration to the airways

7α,25-OHC guides B-cell positioning in secondary lymphoid tissue (Yi *et al*, 2012). To address the role of airway-specific CH25H in guiding B cells, we used microdissected airway trees (Yildirim *et al*, 2008) stimulated with cigarette smoke extract (CSE) *ex vivo*, which demonstrated increased expression of *Ch25h and Cyp7b1* in airways from wild-type mice, whereas *Ch25h*$^{-/-}$ mice did not express *Ch25h* and failed to increase the expression of *Cyp7b1* (Fig 4A). Isolated airways from both mice showed no differences in *Cxcl13* expression (Fig 4A). To further corroborate these findings, we utilized a novel *ex vivo* assay in which IgM cross-linked activated splenic B cells were tested for their ability to migrate toward the CSE-stimulated airway trees (Fig 4B). mRNA analysis of IgM cross-linked B cells revealed no change in the expression levels of the 7α,25-OHC receptor *Ebi2* (Hannedouche *et al*, 2011; Liu *et al*, 2011) and the CXCL13 receptor *Cxcr5* (Gunn *et al*, 1998; Legler *et al*, 1998; Fig 4C). Consistent with increased *Ch25h* and *Cyp7b1*, we observed a strong increase in the number of activated B cells migrating toward wild-type CSE-activated airways (Fig 4D).

To demonstrate that increased expression of CH25H- and CYP7B1-mediated oxysterol 7α,25-OHC guided B-cell migration, we cultured dissected wild-type airways in the presence of clotrimazole, a CYP7B1 inhibitor (Liu *et al*, 2011; Fig 4E). As expected, this treatment did not affect *Ch25h* levels, but was sufficient to reduce *Cyp7b1* mRNA expression (Fig 4F) and significantly impaired the ability of activated B cells to migrate toward CSE-treated airways (Fig 4G). These data suggested that 7α,25-OHC is guiding B-cell movement toward the airways. These results strongly indicate that the CS-induced airway epithelial oxysterols are capable of driving B-cell migration, which contribute to iBALT generation on the airways in experimental COPD.

Oxysterol inhibitor as a novel therapeutic target for COPD

As there are currently no clinical regimes to reverse the progression of emphysema (Vogelmeier *et al*, 2017), we evaluated whether inhibiting the generation of 7α,25-OHC could alleviate established experimental COPD when clotrimazole was administrated as a therapeutic dosing strategy (Fig 5A). Wild-type mice with pulmonary inflammation following two months chronic CS exposure (comparable with human COPD GOLD stages 0–1) were treated with clotrimazole during months two to four, leading to significantly reduced iBALT formation (Fig 5B and D) and lack of emphysema development (Fig 5C). At the cellular level, we observed reduced macrophage and lymphocyte cell numbers in BAL fluid of these clotrimazole-treated CS-exposed mice (Fig 5E). Importantly, wild-type mice exposed to CS for 4 months (comparable with human COPD GOLD stages 1–2), presenting clear signs of iBALT formation and COPD (Fig 2A–D and 5B–D), then treated with clotrimazole, showed attenuated iBALT and emphysema (Fig 5F–H). There was also reduced macrophage cell numbers in the BAL fluid of late clotrimazole-treated CS-exposed mice (Fig 5I). Taken together, these data suggest that inhibiting the generation of 7α,25-OHC with clotrimazole not only prevents iBALT formation, but is able to disrupt established iBALT and attenuate experimental CS-induced COPD.

Discussion

This study reveals a role for oxysterol metabolism in guiding iBALT generation to the airways during COPD pathogenesis. Mice deficient in CH25H, an enzyme crucial for the metabolism of cholesterol toward the oxysterol 7α,25-OHC, or EBI2, the main receptor of 7α,25-OHC, did not generate iBALT in their lungs following exposure to chronic CS and were protected against the development of COPD. We also demonstrated that COPD patients and CS-exposed mice significantly upregulated CH25H and CYP7B1 expression in airway epithelial cells, and this was sufficient to promote B-cell

Figure 5. Clotrimazole protects against and reverses cigarette smoke-induced COPD.

A Schematic representation of clotrimazole therapeutic strategies.

B Representative H&E-stained lung from C57BL/6 mice exposed to filtered air (FA) or cigarette smoke (CS) for 4 months and treated with clotrimazole (i.p. 80 mg/kg 3 times per week) from months 2 to 4 or oil controls (Early therapeutic group). Scale bar, 200 μm.

C Mean chord length (MCL) quantification of lung sections from mice in (B). *P = 0.0242 and ****P < 0.0001.

D Quantification of iBALT localized on the airway, vessels, and septal area from mice described in (B). *P = 0.0249 (FA vs. CS, oil-treated mice) and *P = 0.0116 (CS oil vs. CS clotrimazole-treated mice).

E Bronchoalveolar lavage fluid (BALF) total and differential cell counts from mice in (B). Total cells: ***P = 0.0003 and ****P < 0.0001. Macrophages: **P = 0.0033, ***P = 0.0009 and ****P < 0.0001. Neutrophils: ****P < 0.0001. Lymphocytes: **P = 0.0011 and ****P < 0.0001.

F Representative H&E-stained lung from C57BL/6 mice exposed to filtered air (FA) or cigarette smoke (CS) for 6 months and treated with clotrimazole (i.p. 80 mg/kg 3 times per week) from months 4 to 6 or oil controls (Late therapeutic group). Scale bar, 200 μm.

G Mean chord length (MCL) quantification of lung sections from mice in (F). **P = 0.0039.

H Quantification of iBALT localized on the airway, vessels, and septal area from mice described in (F). Airway: *P = 0.0101. Vessel: *P = 0.0236. Septal: *P = 0.0238.

I BALF total and differential cell counts from mice in (F). Total cells: **P = 0.0011 and ***P = 0.0007. Macrophages: **P = 0.0047. Neutrophils: **P = 0.0012 and ***P = 0.0004.

Data information: Data are mean ± SD. P-values determined by one-way ANOVA and Tukey's multiple comparisons test. Data are representative of two independent experiments with four mice per FA group, six mice per CS group (B–E), or five mice per CS group (F–I).

migration. Furthermore, activated B cells failed to migrate *ex vivo* toward CS-stimulated airways from *Ch25h*$^{-/-}$ or wild-type mice where oxysterol synthesis had been blocked. Finally, inhibition of the oxysterol pathway, using the CYP7B1 inhibitor clotrimazole, resolved iBALT formation and attenuated CS-induced emphysema *in vivo* in a therapeutic approach.

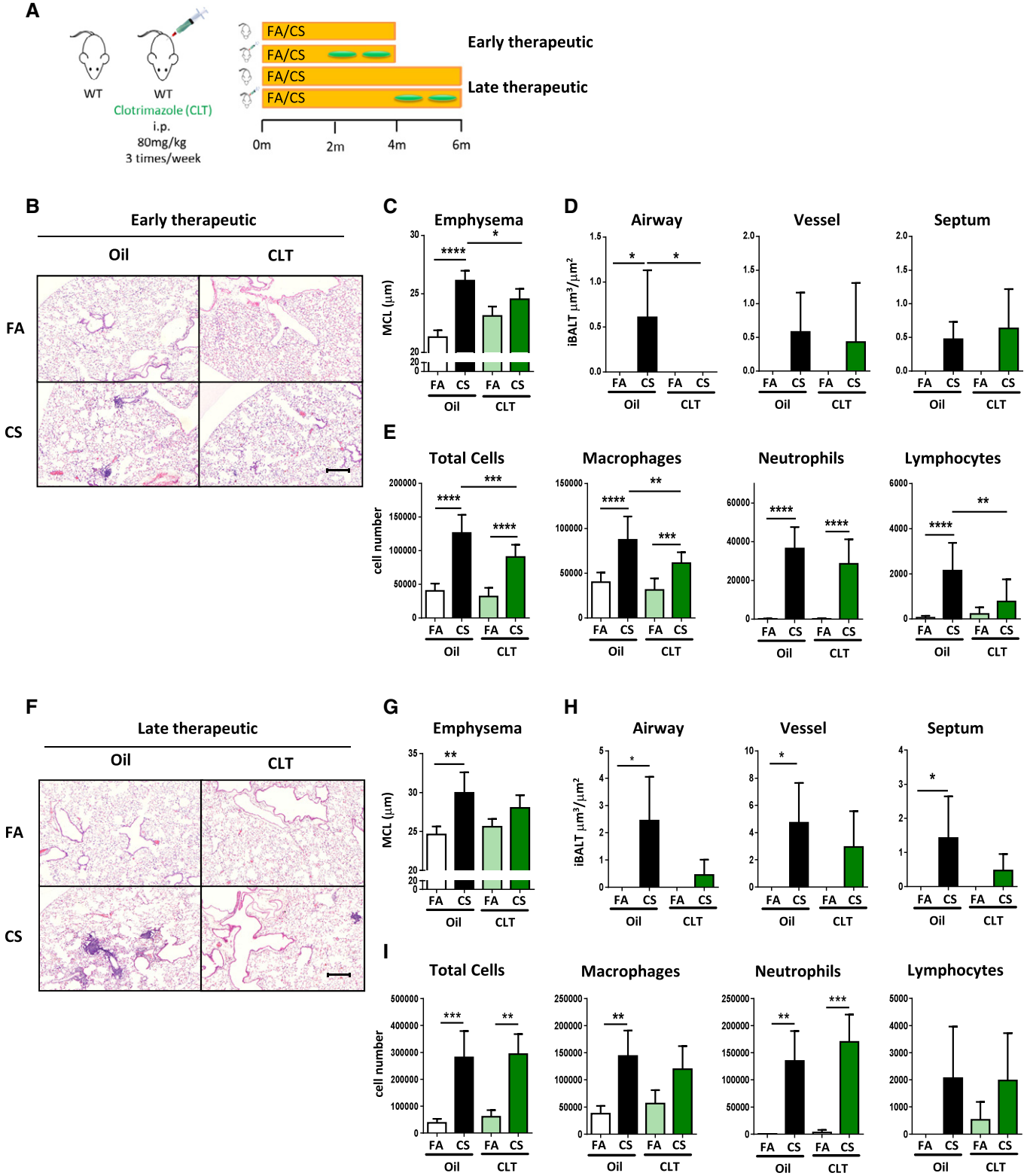

Figure 5.

Our data suggest that B cells are organized into iBALT structures upon the bronchus because of local secretion of 7α,25-OHC by the airway epithelial cells, akin to 7α,25-OHC generated by lymphoid stromal cells guiding activated B-cell movement during humoral responses (Yi *et al*, 2012). We do not exclude the possibility that T-cell migration is also disrupted, especially since EBI2 is expressed by CD4 T cells and activated T-cell positioning in the outer T zone of lymphoid follicles is directed by 7α,25-OHC (Li *et al*, 2016). However, we recently demonstrated that B cell-deficient mice were protected from CS-induced COPD despite normal function of CD4 T cells (John-Schuster *et al*, 2014). Notably, lymphocytes are recruited to the lung equivalently in wild-type mice and in mice where the oxysterol axis had been disturbed (*Ch25h*$^{-/-}$ and *Ebi2*$^{-/-}$ mice). Levels of *Cxcl13*, *Cxcl9*, *Ccl19,* and *Ccl21* were increased in these mice following CS exposure equivalent to their wild-type counterparts, supporting our hypothesis.

The pro-inflammatory oxysterol 27-hydroxycholesterol (27-OHC) has also been demonstrated in the airways of COPD patients (Kikuchi *et al*, 2012) and recently described to be involved in splenic DC positioning and homeostasis (Lu *et al*, 2017). 27-OHC is synthesized by CYP7B1-driven metabolism of 27-hydroxycholesterol (Lu *et al*, 2017), and its synthesis will therefore be blocked by clotrimazole treatment. 27-OHC is, however, a poor chemokine for B cells (Liu *et al*, 2011), and as iBALT failed to form in *Ch25h*$^{-/-}$ mice following chronic CS exposure, this would suggest that 7α,25-OHC is the major EBI2 ligand for iBALT generation. It has also been reported that 27-OHC is able to accelerate senescence of both fibroblasts and airway epithelial cells (Hashimoto *et al*, 2016) and that 25-hydroxycholesterol may promote fibroblast-mediated tissue remodeling through NF-κB signaling (Ichikawa *et al*, 2013), suggesting that impairing oxysterol metabolism may have additional direct effects on lung tissue regeneration. However, we show here that *Ch25h*$^{-/-}$ mice are not protected against iBALT-independent emphysema development and that B cell-deficient mice upregulate oxysterol synthesizing enzymes after chronic CS exposure similar to their wild-type counterparts, yet are still protected against COPD development (John-Schuster *et al*, 2014).

Inducible bronchus-associated lymphoid tissue size and number correlates with the severity of COPD in patients (Hogg *et al*, 2004; Polverino *et al*, 2015), suggesting a therapeutic opportunity, especially considering current therapeutic regimes against COPD do not reverse the progression of emphysema (Tanaka *et al*, 2013; Vogelmeier *et al*, 2017). We clearly show that mice treated with the CYP7B1 inhibitor clotrimazole, resolved iBALT formation, and attenuated CS-induced emphysema *in vivo*. Based on our findings, we speculate that disruption of iBALT generation through the targeting of oxysterols, rather than complete B-cell depletion, particularly as a recent rituximab trial in COPD patients failed because of increased risk of infectious complications (Brusselle *et al*, 2009), opens new therapeutic strategies on a broader perspective for other diseases associated with tertiary lymphoid organs beyond COPD, such as pulmonary hypertension, cancer, transplant rejection, and autoimmunity (Pitzalis *et al*, 2014).

Materials and Methods

Transcriptomic data analysis

Microarray data were obtained from data series held at the NCBI Gene Expression Omnibus (GEO) database (Barrett *et al*, 2013). Mouse whole lung data of filtered air versus chronic CS-exposed animals were obtained from accession GSE52509 (John-Schuster *et al*, 2014), and human data comparing gene expression in the small airway epithelial cells of COPD patients with healthy non-smoking controls from accession GSE11784 (Tilley *et al*, 2011). Data were analyzed using the GEO web tool GEO2R (Barrett *et al*, 2013) with default settings, whose back end uses Bioconductor (Gentleman *et al*, 2004) R packages to transform and analyze the data, to generate the $\log_2$ transformed expression values for each gene relative to filtered air or healthy controls. Gene Ontology pathway analysis was undertaken on GEO2R gene expression data with a $P < 0.05$ using the web-based gene set analysis toolkit WebGestalt (Wang *et al*, 2013). A heat map of selected genes ($\log_2$ transformed expression values, with a $P < 0.05$, as calculated by GEO2R) taken from the Gene Ontology pathway analysis was generated by Genesis software (Sturn *et al*, 2002; Release 1.7.7, Institute for Genomics and Bioinformatics, Graz University of Technology).

Gene set enrichment analysis (GSEA) software from the Broad Institute (http://www.gsea-msigdb.org/gsea/index.jsp; Mootha *et al*, 2003; Subramanian *et al*, 2005) was used to determine the enrichment of Reactome gene lists obtained from the GSEA-Molecular Signatures Database for total TLR- and TLR4-specific signaling. Data from the series matrix file comparing gene expression in the small airway epithelial cells of COPD patients with healthy smoking controls (accession GSE11784) were downloaded from the NCBI GEO database.

Human lung tissue

Lung core samples of emphysematous and healthy regions from the same explanted lungs of COPD patients undergoing lung transplantation were provided by Dr. Stijn Verleden (University of Leuven, Belgium) following ethical approval of the University of Leuven Institutional Review Board (ML6385). All participants provided written consent and experiments conformed to the principles set out in the Declaration of Helsinki. Patient demographics are highlighted in Table 1. Immediately following transplant, lungs were air-inflated at

Table 1. Demographics and clinical characteristics of COPD transplant patients (mean ± SEM). Lung core samples were histologically separated into non-emphysematous and emphysematous tissue.

	COPD
Subjects (*n*)	16
Mean age years	57.06 ± 1.23
Sex	
Male	7
Female	9
Height (m)	1.65 ± 0.02
Weight (kg)	59.44 ± 3.18
Smoking (packs/year)	39.00 ± 7.55
FEV1 (%)	34.38 ± 5.55
FVC (%)	82.73 ± 5.84
FEV1/FVC (%)	31.01 ± 5.07

FEV1, Forced expiratory volume in the first second; FVC, Forced vital capacity.

10 cm H_2O pressure and fixed using constant pressure in the fumes of liquid nitrogen. Afterward lungs were sliced using a band saw and sampled using a core bore. Upon receipt, lung cores were portioned for fixation in 4% paraformaldehyde followed by paraffin embedding and total RNA isolation (peqGOLD Total RNA Kit, Peqlab).

Primary bronchial epithelial cell culture

Primary bronchial epithelial cell cultures were obtained from smokers with and without COPD, who had lobectomy or pneumonectomy for lung cancer or other reasons at Gaziantep University Hospital (Turkey), using an explant cell culture technique (Devalia *et al*, 1990; Bayram *et al*, 1998). The demographic characteristics of patients are given in Table 2. The study was approved by The Ethics Committee of Gaziantep University, informed written consents were taken from study volunteers, and experiments conformed to the principles set out in the Declaration of Helsinki. Total cellular RNA was isolated using commercially available kits (QIAcube, Qiagen).

RNAseq analysis

Total RNA of human lung derived from COPD explants or healthy donor controls was sequenced using the Illumina system (HiSeq 2000) by the company GATC Biotech.AG (Konstanz, Germany). Raw data analysis was performed by Genomatix Software GmbH. Expression values were calculated as RPKM (Reads per kilobase million per mapped reads) for all loci available from reads uniquely aligned to the human genome. In this study, we only present the expression of *CH25H*.

Mice

B6.129S6-*Ch25h*^{tm1Rus}/J (*Ch25h*$^{-/-}$) mice were obtained from The Jackson Laboratory and B6N(Cg)-*Gpr183*$^{tm1.1(KOMP)Vlcg}$/J (*Ebi2*$^{-/-}$) from the KOMP Repository, University of California Davis. Age-matched female C57BL/6J mice and B cell-deficient B6.129S2-*Igh-6*^{tm1Cgn} (μMT) mice were obtained from Charles River Laboratories. Mice were housed under specific pathogen-free conditions at a constant temperature and humidity with a 12-hour light cycle and allowed food and water *ad libitum*. All animal experiments were performed according to strict governmental and international guidelines and were approved by the local government for the administrative region of Upper Bavaria, Germany.

Table 2. Demographics and clinical characteristics of study subjects for the primary bronchial epithelial cell cultures (mean ± SEM).

	Smokers	COPD
Subjects (*n*)	10	11
Mean age years	61.10 ± 12.75	65.82 ± 8.49
Smoking (packs/year)	32.00 ± 11.83	49.55 ± 26.12**
FEV1 (%)	92.80 ± 8.50	75.64 ± 15.58*
FVC (%)	98.30 ± 12.07	92.91 ± 14.41
FEV1/FVC (%)	76.00 ± 3.68	63.36 ± 6.32**
GOLD (mean, min-max)	NA	1.73 (1,3)

FEV1: Forced expiratory volume in the first second; FVC: Forced vital capacity. *$P < 0.01$, **$P < 0.001$ COPD versus smokers (Mann–Whitney test).

Mouse COPD models and treatment

Eight- to 12-week-old female mice were used in all experiments. For the CS-induced COPD model, mice were exposed to 100% mainstream CS (John *et al*, 2014) at a particle concentration of 500 mg/m^3, generated from 3R4F research cigarettes (Filter removed, Tobacco Research Institute, University of Kentucky), for 50 min twice/day, 5 days/week for 4 or 6 months. Mice exposed to filtered air were used as controls. For the elastase-induced iBALT-independent COPD model, mice were instilled oropharyngeally with a single application of 80 U/kg body weight porcine pancreatic elastase (PPE; Sigma-Aldrich) in 80 μl PBS. Mice treated with 80 μl PBS were included as controls. For CYP7B1 inhibition, clotrimazole (Sigma-Aldrich) 10 mM in DMSO was further diluted in corn oil (Mazola, Unilever) and applied i.p. at a dose of 80 mg/kg body weight 3 times/week for 2 months. Mice were treated after 2 or 4 months of CS exposure and smoked for a further 2 months in parallel with the clotrimazole treatment.

Lung function analysis

Mice were anaesthetized with ketamine–xylazine, tracheostomized, cannulated, and the diffusing capacity for carbon monoxide (DFCO) calculated (Fallica *et al*, 2011). Briefly, 0.8 ml mixed gas (0.5% Ne, 21% O_2, 0.5% CO and 78% N_2) was instilled into the mice lungs and withdrawn 2 s later for analysis on a 3000 Micro GC Gas Analyzer (Infinicon). DFCO was calculated as $1\text{-}(CO_1/CO_0)/(Ne_1/Ne_0)$ where 0 and 1 refer to the gas concentration before and after instillation, respectively. Respiratory function was analyzed using a forced pulmonary maneuver system (Vanoirbeek *et al*, 2010; Buxco Research Company, Data Sciences International) running FinePointe Software (version 6, Data Sciences International) and the quasistatic PV maneuver protocol.

Bronchoalveolar lavage

After lung function analysis, lungs were lavaged with 3 × 500 μl aliquots of sterile PBS (Gibco, Life Technologies) supplemented with Complete Protease Inhibitor Cocktail tablets (Roche Diagnostics). Cells were pelleted at 400 *g* for 20 min and resuspended in 500 μl RPMI-1640 medium (Gibco, Life Technologies) for the total cell count using a Neubauer Chamber. Cytospins of the cell suspension were then prepared and stained using May-Grünwald-Giemsa for differential cell counting (200 cells/sample) using morphological criteria. Bronchoalveolar lavage fluid was retained for mass spectrometry analysis.

Mouse lung processing

The two right lower lung lobes were snap-frozen in liquid nitrogen, homogenized and total RNA isolated (peqGOLD Total RNA Kit, Peqlab). The right upper two lobes were dissociated into single-cell suspensions in PBS supplemented with 0.1% FCS and 2 mM EDTA

using the lung dissociation kit and gentleMACS Dissociator from Miltenyi Biotec for flow cytometry analysis. The left lung was inflation fixed with 6% paraformaldehyde under a constant pressure of 20 cm and then embedded into paraffin.

Quantitative real-time RT–PCR

1 μg RNA was reverse transcribed using Random Hexamers and MuLV Reverse Transcriptase (Applied Biosystems) or by the Precision Reverse Transcription Kit (Qiagen). Gene expression was analyzed using SensiFAST SYBR Hi-ROX Kit (Bioline) on a StepOnePlus 96-well Real-Time PCR System (Applied Biosystems) or a RG-600 model RT–PCR machine (Corbett Research). Primer sequences can be found in Table 3. Expression of each gene was calculated relative to the housekeeping gene *HPRT1* or *Hprt1* as $2^{-\Delta C_t}$.

Immunofluorescence staining

3-μm sections from mouse left lung or human core samples were stained as described (John-Schuster *et al*, 2016). Briefly, sections were deparaffinized, rehydrated, and heat-induced epitope retrieval undertaken using HIER Citrate Buffer (pH 6.0, Zytomed Systems). Sections were blocked using 5% BSA in PBS and then incubated

Table 3. Primer sequences used for the quantitative real-time RT–PCR.

Gene	Forward primer	Reverse Primer
CH25H	CTC TAC CAG CAT GTG ATG TTT GT	CAT GTC GAA GAG TAG CAG GCA
CXCL8	GGC TCT CTT GGC AGC CTT C	GGT TTG GAG TAT GTC TTT ATG CAC
CXCL13	CAA GTC AAT TGT GTG TGT GGA	GGG AAT CTT TCT CTT AAA CAC TGG
HPRT1	AGG AAA GCA AAG TCT GCA TTG TT	GGT GGA GAT GAT CTC TCA ACT TTA A
TLR4	AGA CCT GTC CCT GAA CCC TAT	CGA TGG ACT TCT AAA CCA GCC A
Adgre1	CTC TGT GGT CCC ACC TTC AT	GAT GGC CAA GGA TCT GAA AA
Arg1	GGA ACC CAG AGA GAG CAT GA	TTT TTC CAG CAG ACC AGC TT
Ccl19	TGG GAA CAT CGT GAA AGC CT	GTG GTG AAC ACA ACA GCA GG
Ccl21	CGG CTG TCC ATC TCA CCT AC	AGG GAA TTT TCT TCT GGC TGT
Ch25h	GAC CTT CTT CGA CGT GCT GA	CCA CCG ACA GCC AGA TGT TA
Cxcl1	CCG AAG TCA TAG CCA CAC	GTG CCA TCA GAG CAG TCT
Cxcl13	TCT CTC CAG GCC ACG GTA TTC T	ACC ATT TGG CAC GAG GAT TCA C
Cxcl9	CGA GGC ACG ATC CAC TAC AA	AGG CAG GTT TGA TCT CCG TT
Cxcr5	TGG ATG ACC TGT ACA AGG AAC TG	CGG TGC CTC TCC AGG ATT AC
Cyp27a1	GGA GGG CAA GTA CCC AAT AA	TTC AGC AGC CTC TGT TTC AA
Cyp7b1	GGA GCC ACG ACC CTA GAT G	GCC ATG CCA AGA TAA GGA AGC
Ebi2	ATG GCT AAC AAT TTC ACT ACC CC	ACC AGC CCA ATG ATG AAG ACC
Fizz1	TGC CAA TCC AGC TAA CTA TCC C	ACG AGT AAG CAC AGG CAG TT
Gmcsf	ATG CCT GTC ACG TTG AAT GA	CCG TAG ACC CTG CTC GAA TA
Hprt1	AGC TAC TGT AAT GAT CAG TCA ACG	AGA GGT CCT TTT CAC CAG CA
Hsd3b7	AGT GGT GGG GCC TAA CAT CA	CTG CTC AGC AAG GGC TTT AC
Il12p35	ACT AGA GAG ACT TCT TCC ACA ACA AGA G	GCA CAG GGT CAT CAT CAA AGA C
Il1a	AGC GCT CAA GGA GAA GAC	CTG TCA TAG AGG GCA GTC C
Il1b	CAA CCA ACA AGT GAT ATT CTC CAT G	GAT CCA CAC TCT CCA GCT GCA
Il6	GTT CTC TGG GAA ATC GTG GA	TGT ACT CCA GGT AGC TAT GG
Irf4	AAA GGC AAG TTC CGA GAA GGG	CTC GAC CAA TTC CTC AAA GTC A
Lta	TCC ACT CCC TCA GAA GCA CT	AGA GAA GCC ATG TCG GAG AA
Ltb	TAC ACC AGA TCC AGG GGT TC	ACT CAT CCA AGC GCC TAT GA
Ltbr	AAG CCG AGG TCA CAG ATG AAA	CGA GGG GAG GAA GTG TTC TG
Mcp1	CTT CTG GGC CTG CTG TTC A	CCA GCC TAC TCA TTG GGA TCA
Mmp12	TGT ACC CCA CCT ACA GAT ACC TTA	CCA TAG AGG GAC TGA ATG TTA CGT
Nos2	CGG CAA ACA TGA CTT CAG GC	GCA CAT CAA AGC GGC CAT AG
Timp1	CAC TGA TAG CTT CCA GTA AGG CC	CTT ATG ACC AGG TCC GAG TTG C
Tnfa	CAC CAC GCT CTT CTG TCT	GGC TAC AGG CTT GTC ACT C

overnight at 4°C with primary antibody, followed by 1 h with secondary antibody and counterstained with DAPI (1:4,000, Sigma-Aldrich), mounted in fluorescent mounting medium (Dako), and imaged with a fluorescent Olympus BX51 microscope running cellSens software (Version 1.14, Build 14116, Olympus). Primary antibodies: rat IgG2a anti-mouse CD45r (1:50, clone: RA3-6B2, BD Biosciences), rabbit IgG1 anti-mouse CD3 (1:300, Cat. No. C7930, Sigma-Aldrich), mouse IgG2b anti-human/mouse CH25H (1:500, Cat. No. ab76478, Abcam). Secondary antibodies: Alexa Fluor 488 conjugated goat anti-mouse IgG antibody (1:300, Cat. No. A11001, ThermoFisher Scientific), Alexa Fluor 488 conjugated goat anti-rabbit IgG antibody (1:300, Cat. No. A11008, ThermoFisher Scientific), Alexa Fluor 568 conjugated goat anti-rat IgG antibody (1:300, Cat. No. A11077, ThermoFisher Scientific).

Immunohistochemical staining

3-μm sections from human core samples or mouse lung were deparaffinized, rehydrated, and then treated with 1.8% (v/v) H_2O_2 solution (Sigma-Aldrich) to block endogenous peroxidase. Heat-induced epitope retrieval was performed in HIER citrate buffer (pH 6.0, Zytomed Systems) in a decloaking chamber (Biocare Medical). To inhibit non-specific binding of antibodies, sections were treated with a blocking antibody (Biocare Medical). Human sections were incubated at 4°C overnight with a rabbit anti-TLR4 primary antibody (1:50, Cat. No. ab13556, Abcam), followed by 1 h with an anti-rabbit HRP-conjugated secondary antibody (Biocare Medical). Signals were amplified by adding chromogen substrate 3,3′-diaminobenzidine (DAB; Biocare Medical). Mouse sections were incubated at 4°C overnight with a rabbit anti-galectin-3 primary antibody (1:100, Cat. No. sc-20157, Santa Cruz Biotechnology), followed by 1 h with a Rabbit-on-Rodent AP-Polymer (Biocare Medical). Signals were amplified by adding chromogen substrate Vulcan fast red (Biocare Medical). All sections were counterstained with hematoxylin (Sigma-Aldrich), dehydrated, and mounted.

Quantitative morphometry

H&E-stained tissue sections were analyzed by design-based stereology using an Olympus BX51 light microscope equipped with the new Computer Assisted Stereological Toolbox (newCAST, Visiopharm) as described (John-Schuster *et al*, 2014), by readers blinded to the study groups. Briefly, for mean chord length (MCL) measurements, 20 frames were selected randomly across multiple sections by the software, using the ×20 objective, and superimposed by a line grid and points. The intercepts of lines on alveolar wall (I_{septa}) and points localized on air space (P_{air}) were counted and calculated as $MCL = \sum P_{air} \times L(p)/\sum I_{septa} \times 0.5$, where L(p) is the line length per point. The volume of inflammation (V) was quantified in 50 frames, using the ×40 objective, by counting points hitting inflammatory cell zones (P_{inflam}). For calculation, the P_{inflam} were referenced to intercepts of lines with both airways and vessels ($I_{airway/vessel}$): $V = \sum P_{inflam} \times L(p)/\sum I_{airway/vessel}$. Further, airway-, vessel-, or septum-associated inflammation quantification was classified by the location of the inflammation and was calculated referring to intercept of lines with airway, vessel, or both, respectively.

Flow cytometry

10^6 cells from filtered single-cell lung suspensions were blocked with purified anti-mouse CD16/CD32 (Clone: 93, eBioscience) before incubating for 30 min on ice with antibody cocktails. After washing and re-suspending in MACS buffer, cells were analyzed on a BD FACSCanto II flow cytometer (BD Biosciences) and BD FACSDiva software. B-cell and T-cell staining was performed with: APC-conjugated anti-CD19 (clone: 6D5, Miltenyi Biotec), APC-Vio770-conjugated anti-CD3e (clone: 17A2, Miltenyi Biotec), PE-Vio770-conjugated anti-CD22 (clone: Cy34.1, Miltenyi Biotec), PE-conjugated anti-CD80 (clone: 16-10A1, Miltenyi Biotec), PerCP-Vio700-conjugated anti-MHCII (clone: M5/114.15.2, Miltenyi Biotec), VioGreen-conjugated anti-CD69 (clone: H1.2F3, Miltenyi Biotec), FITC-conjugated anti-IgG (Biolegend), VioBlue-conjugated anti-GL7 (Biolegend). For the macrophage profile: VioGreen-conjugated anti-CD45 (clone: 30F11, Miltenyi Biotec), APC-Vio770-conjugated anti-Ly6C (clone: 1G7.G10, Miltenyi Biotec), VioBlue-conjugated anti-Ly6G (clone: 1A8, Miltenyi Biotec), FITC-conjugated anti-MHCII (clone: M5/114.15.2, Miltenyi Biotec), PerCP-Vio700-conjugated anti-F4/80 (clone: REA126, Miltenyi Biotec), PE-conjugated anti-CD11b (clone: M1/70.15.11.5, Miltenyi Biotec), APC-conjugated anti-CD11c (clone: N418, Miltenyi Biotec), PE-Vio770-conjugated anti-CD64 (clone: REA286, Miltenyi Biotec).

Microdissection of airways

Middle and distal airways from C57BL/6J and *Ch25h*$^{-/-}$ mice were isolated and incubated *ex vivo* as described (Yildirim *et al*, 2008). Briefly, after sacrifice by a ketamine–xylazine over dose, the trachea was cannulated, the lungs removed from the thorax and infused with 1% low-melting agarose dissolved in 1:1 Ham's F12 nutrient medium (Sigma-Aldrich) and distilled water (Gibco, Life Technologies). Airways were dissected under a microscope (Zeiss) from the left lung after the agarose had solidified on ice for 30 min. The isolated airways were washed and cultured in airway epithelial cell medium (PromoCell) at 37°C, 5% CO_2.

B-cell isolation and migration assay

B cells were purified from the spleens of C57BL/6J mice by negative selection (B cell Isolation Kit, mouse, Miltenyi Biotec). For the migration assay, primary mouse airways were isolated 1 day prior and treated with 10% CSE in airway epithelial cell culture medium (PromoCell) or culture medium alone for 24 h. To inhibit CYP7B1, clotrimazole in DMSO was diluted with culture medium or combined with 10% CSE to a final concentration of 1 μM. The supernatants were transferred as conditioned medium to the lower well of 24-well transwell plates (Permeable Polycarbonate Membrane Inserts, Corning, Fisher Scientific), for inducing B-cell migration, while the airway samples were snap-frozen in liquid nitrogen for RNA isolation. Freshly isolated B cells at 2.5×10^6/ml in 100 μl were activated by unconjugated AffiniPure $F(ab')_2$ Fragment Goat anti-mouse IgM, μchain-specific antibody (1.3 μg/ml, 115-006-020, Jackson Immunoresearch Laboratories) for 1 h at 37°C in 5.0 μm pore-sized transwell inserts (Permeable Polycarbonate Membrane Inserts, Corning, Fisher Scientific). Transwell inserts were then placed into the wells of conditioned medium and

incubated for 3 h at 37°C. Migrated B cells were collected and counted by Neubauer Chamber and reported as percentage of input.

Cigarette smoke extract preparation

Cigarette smoke extract was generated by bubbling smoke from three research cigarettes (3R4F, Tobacco Research Institute, University of Kentucky) through 30 ml of airway epithelial cell culture medium (PromoCell) at a puffing speed equating to one cigarette every 5 min, in a closed environment with limited air flow. This solution was taken as 100% CSE.

Isolation and stimulation of professional APCs

Primary alveolar macrophages were isolated from the lungs of C57BL/6J and *Ch25h*$^{-/-}$ mice by BAL with 10 washes of 1 ml PBS (Gibco, Life Technologies). Cells were pelleted at 400 *g* for 20 min and resuspended in complete RPMI-1640 medium supplemented with 10% fetal bovine serum, 50 μM β-mercaptoethanol, and 100 U/ml penicillin and streptomycin (all from Gibco, Life Technologies). 5×10^4 cells in 1 ml were seeded in 24-well plates and allowed to adhere for 1 h. Non-adherent cells were removed by washing twice with PBS. To generate bone marrow-derived macrophages (BMDM) and DCs (BMDC), bone marrow was flushed from femurs and tibias of C57BL/6J and *Ch25h*$^{-/-}$ mice with RPMI-1640 medium. Cells were disaggregated by passing through a 40-μm mesh and cultured in complete RPMI-1640 medium supplemented with 5% fetal bovine serum, 50 μM β-mercaptoethanol, and 100 U/ml penicillin and streptomycin at a concentration of 1×10^6 cells/ml in 24-well plates. For BMDMs, the medium was supplemented with 20 ng/ml murine recombinant M-CSF (ImmunoTools), and for BMDCs, the medium was supplemented with 20 ng/ml murine recombinant GM-CSF (ImmunoTools) and cultured at 37°C, 5% CO_2. Cells were maintained by replacing the medium with fresh medium on alternate days ensuring removal of non-adherent cells. On day 6, adherent BMDMs were collected. For BMDCs, on day 7–8 adherent cells were harvested and resuspended at 1×10^6 cells/ml in 10 ml complete RPMI-1640 medium in 100-mm petri dishes and cultured for a further 24–48 h. The non-adherent, non-proliferating, maturing DCs were collected as they were released. Primary alveolar macrophages and BMDMs were polarized toward M1 by culturing with complete RPMI-1640 medium containing 1 μg/ml LPS (from *Escherichia coli* 0111:B4, Sigma-Aldrich) and 20 ng/ml recombinant murine IFNγ (ImmunoTools) for 24 h or an M2 phenotype with 20 ng/ml recombinant murine IL-4 (ImmunoTools) for 24 h. BMDCs were stimulated with 1 μg/ml LPS for 24 h.

Bronchial epithelial cell lines

The human bronchial epithelial cell lines BEAS-2B (ATCC CRL-9609) and 16-HBE (Cozens *et al*, 1994) were maintained in airway epithelial cell medium (PromoCell) supplemented with 10% fetal bovine serum and 100 U/ml penicillin and streptomycin (all from Gibco, Life Technologies) at 37°C, 5% CO_2. Cells were seeded and grown to confluence over 48 h in 24-well plates before stimulation with LPS (from *E. coli* 0111:B4, Sigma-Aldrich), CSE or recombinant human TNF-α (PeproTech), at the concentrations described in the figure legends.

The paper explained

Problem
Long-term environmental exposure to toxic gases and particles, in particular cigarette smoke, can result in chronic obstructive pulmonary disease (COPD), currently the third leading cause of death worldwide. It manifests as chronic bronchitis, small airway remodeling, and emphysema, resulting in progressive and largely irreversible airflow limitation and impaired gaseous exchange. Currently, the only available therapies aim at symptom management and do not reverse disease progression. There is strong evidence that advanced stages of COPD are driven by the generation of inducible bronchus-associated lymphoid tissue (iBALT). Yet, we do not know how iBALT gets organized upon the bronchi and if its disruption can reverse COPD progression.

Results
We have demonstrated that oxysterols, metabolites of cholesterol, are critically involved in iBALT generation and the immune pathogenesis of COPD. In both, COPD patients and mouse models of the disease, we identified upregulated oxysterol enzymes in airway epithelial cells. Furthermore, mice genetically or pharmacologically deficient in the oxysterol pathway were protected from cigarette smoke-induced emphysema and iBALT formation.

Impact
This study provides valuable new insights into the mechanism of iBALT-driven COPD pathogenesis and highlights the oxysterol pathway as a potential therapeutic approach for COPD disease progression, and conceivably, the many other chronic diseases associated with tertiary lymphoid organ development.

Analysis of 25-hydroxycholesterol

Determination of 25-hydroxycholesterol in cell culture supernatant and BALF was performed based on mass spectrometric methods previously described for different instrumentation (Honda *et al*, 2009; Huang *et al*, 2014). 25-hydroxycholesterol was derivatized, and the product was analyzed using ultra-high pressure liquid chromatography (UHPLC) coupled with high-resolution time-of-flight mass spectrometry (LC-HRTOF-MS). UHPLC separation was performed on a 1290 Infinity Binary LC-System using an Eclipse C-18, 1.8 μm, 50 × 2.1 mm I.D. analytical column (both from Agilent Technologies). Mass spectrometric detection was accomplished on a Citius™ High Resolution multi-reflection time-of-flight mass spectrometer (LC-HRT, Leco).

Metabolomics analysis

The targeted metabolomics approach was based on LC-ESI-MS/MS and FIA-ESI-MS/MS measurements by Absolute*IDQ*™ p180 Kit (BIOCRATES Life Sciences AG) which has been described in detail (Zukunft *et al*, 2013). Frozen lung tissue was homogenized and extracted as described previously (Conlon *et al*, 2016; Zukunft *et al*, 2018). Mass spectrometric analyses were done on an API 4000 triple quadrupole system (Sciex Deutschland GmbH) equipped with a 1200 Series HPLC (Agilent Technologies) and a HTC PAL auto sampler (CTC Analytics) controlled by the software Analyst 1.5.1. Data evaluation for quantification of metabolite concentrations and quality assessment was performed with the MetIDQ™ software

package, which is an integral part of the AbsoluteIDQ™ Kit. Individual metabolite concentrations for each sample can be found in Dataset EV1, with a more detailed description of the methods found in Appendix Supplementary Methods.

Statistical analysis

No statistical methods were used to predetermine sample size. GraphPad Prism (Version 6, GraphPad Software) was used for all statistical analysis. Data are presented as mean ± SD with sample size and number of repeats indicated in the figure legends. For comparison between two groups, statistical significance was analyzed with Student's *t*-test. For multiple comparisons, one-way ANOVA and Tukey's multiple comparisons test were used. $P < 0.05$ were considered significant.

Expanded View for this article is available online.

Acknowledgements
The authors acknowledge the help of Christine Hollauer, Heike Bollig, and Maximilian Pankla. We thank Julia Scarpa, Werner Römisch-Margl, and Katharina Faschinger for metabolomics measurements performed at the Helmholtz Zentrum München, Genome Analysis Center, Metabolomics Core Facility. RZ, JL, XW, and AÖY thank the HGF for supporting the virtual Institute HICE.

Author contributions
TMC, JJ, OE, and AÖY conceived the study and experimental design. TMC, JJ, RSJS, NFS, BS, GG, DT, XW, JG, KH, and MI performed experiments. SEV prepared patient lung core samples. DT and HB generated primary human bronchial epithelial cell cultures and undertook analysis. XW, RZ, and JL designed and analyzed oxysterol mass spectrometry measurements. CP and JA designed and analyzed targeted metabolomics. MI, JB, and MHA contributed to microarray analysis. SP and MS contributed to lung mycobiome analysis. TMC, JJ, RSJS, NFS, and AÖY analyzed and interpreted the data. TMC, JJ, OE, and AÖY wrote the manuscript. All authors read and edited the manuscript.

Conflict of interest
The authors declare that they have no conflict of interest.

References

Baarsma HA, Skronska-Wasek W, Mutze K, Ciolek F, Wagner DE, John-Schuster G, Heinzelmann K, Gunther A, Bracke KR, Dagouassat M *et al* (2017) Noncanonical WNT-5A signaling impairs endogenous lung repair in COPD. *J Exp Med* 214: 143 – 163

Barrett T, Wilhite SE, Ledoux P, Evangelista C, Kim IF, Tomashevsky M, Marshall KA, Phillippy KH, Sherman PM, Holko M *et al* (2013) NCBI GEO: archive for functional genomics data sets–update. *Nucleic Acids Res* 41: D991 – D995

Bayram H, Devalia JL, Sapsford RJ, Ohtoshi T, Miyabara Y, Sagai M, Davies RJ (1998) The effect of diesel exhaust particles on cell function and release of inflammatory mediators from human bronchial epithelial cells in vitro. *Am J Respir Cell Mol Biol* 18: 441 – 448

Benam KH, Villenave R, Lucchesi C, Varone A, Hubeau C, Lee HH, Alves SE, Salmon M, Ferrante TC, Weaver JC *et al* (2016) Small airway-on-a-chip enables analysis of human lung inflammation and drug responses in vitro. *Nat Methods* 13: 151 – 157

Benned-Jensen T, Smethurst C, Holst PJ, Page KR, Sauls H, Sivertsen B, Schwartz TW, Blanchard A, Jepras R, Rosenkilde MM (2011) Ligand modulation of the Epstein-Barr virus-induced seven-transmembrane receptor EBI2: identification of a potent and efficacious inverse agonist. *J Biol Chem* 286: 29292 – 29302

Berndt A, Leme AS, Shapiro SD (2012) Emerging genetics of COPD. *EMBO Mol Med* 4: 1144 – 1155

Bracke KR, Verhamme FM, Seys LJ, Bantsimba-Malanda C, Cunoosamy DM, Herbst R, Hammad H, Lambrecht BN, Joos GF, Brusselle GG (2013) Role of CXCL13 in cigarette smoke-induced lymphoid follicle formation and chronic obstructive pulmonary disease. *Am J Respir Crit Care Med* 188: 343 – 355

Brusselle GG, Demoor T, Bracke KR, Brandsma CA, Timens W (2009) Lymphoid follicles in (very) severe COPD: beneficial or harmful? *Eur Respir J* 34: 219 – 230

Chiu C, Openshaw PJ (2015) Antiviral B cell and T cell immunity in the lungs. *Nat Immunol* 16: 18 – 26

Cloonan SM, Glass K, Laucho-Contreras ME, Bhashyam AR, Cervo M, Pabon MA, Konrad C, Polverino F, Siempos II, Perez E *et al* (2016) Mitochondrial iron chelation ameliorates cigarette smoke-induced bronchitis and emphysema in mice. *Nat Med* 22: 163 – 174

Conlon TM, Bartel J, Ballweg K, Gunter S, Prehn C, Krumsiek J, Meiners S, Theis FJ, Adamski J, Eickelberg O *et al* (2016) Metabolomics screening identifies reduced L-carnitine to be associated with progressive emphysema. *Clin Sci (Lond)* 130: 273 – 287

Cozens AL, Yezzi MJ, Kunzelmann K, Ohrui T, Chin L, Eng K, Finkbeiner WE, Widdicombe JH, Gruenert DC (1994) CFTR expression and chloride secretion in polarized immortal human bronchial epithelial cells. *Am J Respir Cell Mol Biol* 10: 38 – 47

Dau T, Sarker RS, Yildirim AO, Eickelberg O, Jenne DE (2015) Autoprocessing of neutrophil elastase near its active site reduces the efficiency of natural and synthetic elastase inhibitors. *Nat Commun* 6: 6722

Devalia JL, Sapsford RJ, Wells CW, Richman P, Davies RJ (1990) Culture and comparison of human bronchial and nasal epithelial cells in vitro. *Respir Med* 84: 303 – 312

Diczfalusy U, Olofsson KE, Carlsson AM, Gong M, Golenbock DT, Rooyackers O, Flaring U, Bjorkbacka H (2009) Marked upregulation of cholesterol 25-hydroxylase expression by lipopolysaccharide. *J Lipid Res* 50: 2258 – 2264

Fallica J, Das S, Horton M, Mitzner W (2011) Application of carbon monoxide diffusing capacity in the mouse lung. *J Appl Physiol (1985)* 110: 1455 – 1459

Faner R, Cruz T, Casserras T, Lopez-Giraldo A, Noell G, Coca I, Tal-Singer R, Miller B, Rodriguez-Roisin R, Spira A *et al* (2016) Network analysis of lung transcriptomics reveals a distinct B-cell signature in emphysema. *Am J Respir Crit Care Med* 193: 1242 – 1253

Gatto D, Paus D, Basten A, Mackay CR, Brink R (2009) Guidance of B cells by the orphan G protein-coupled receptor EBI2 shapes humoral immune responses. *Immunity* 31: 259 – 269

Gatto D, Wood K, Caminschi I, Murphy-Durland D, Schofield P, Christ D, Karupiah G, Brink R (2013) The chemotactic receptor EBI2 regulates the homeostasis, localization and immunological function of splenic dendritic cells. *Nat Immunol* 14: 446 – 453

Gentleman RC, Carey VJ, Bates DM, Bolstad B, Dettling M, Dudoit S, Ellis B, Gautier L, Ge Y, Gentry J *et al* (2004) Bioconductor: open software development for computational biology and bioinformatics. *Genome Biol* 5: R80

Gosman MM, Willemse BW, Jansen DF, Lapperre TS, van Schadewijk A, Hiemstra PS, Postma DS, Timens W, Kerstjens HA, Groningen, Leiden Universities Corticosteroids in Obstructive Lung Disease Study G (2006) Increased number of B-cells in bronchial biopsies in COPD. *Eur Respir J* 27: 60 – 64

Gregson RL, Davey MJ, Prentice DE (1979) The response of rat bronchus-associated lymphoid tissue to local antigenic challenge. *Br J Exp Pathol* 60: 471 – 482

Gunn MD, Ngo VN, Ansel KM, Ekland EH, Cyster JG, Williams LT (1998) A B-cell-homing chemokine made in lymphoid follicles activates Burkitt's lymphoma receptor-1. *Nature* 391: 799 – 803

Hannedouche S, Zhang J, Yi T, Shen W, Nguyen D, Pereira JP, Guerini D, Baumgarten BU, Roggo S, Wen B *et al* (2011) Oxysterols direct immune cell migration via EBI2. *Nature* 475: 524 – 527

Hashimoto Y, Sugiura H, Togo S, Koarai A, Abe K, Yamada M, Ichikawa T, Kikuchi T, Numakura T, Onodera K *et al* (2016) 27-Hydroxycholesterol accelerates cellular senescence in human lung resident cells. *Am J Physiol Lung Cell Mol Physiol* 310: L1028 – L1041

Haw TJ, Starkey MR, Pavlidis S, Fricker M, Arthurs AL, Mono Nair P, Liu G, Hanish I, Kim RY, Foster PS *et al* (2017) Toll-like receptor 2 and 4 have opposing roles in the pathogenesis of cigarette smoke-induced chronic obstructive pulmonary disease. *Am J Physiol Lung Cell Mol Physiol* 314: L298 – L317

Hogg JC, Chu F, Utokaparch S, Woods R, Elliott WM, Buzatu L, Cherniack RM, Rogers RM, Sciurba FC, Coxson HO *et al* (2004) The nature of small-airway obstruction in chronic obstructive pulmonary disease. *N Engl J Med* 350: 2645 – 2653

Honda A, Yamashita K, Hara T, Ikegami T, Miyazaki T, Shirai M, Xu G, Numazawa M, Matsuzaki Y (2009) Highly sensitive quantification of key regulatory oxysterols in biological samples by LC-ESI-MS/MS. *J Lipid Res* 50: 350 – 357

Huang MQ, Lin W, Wang W, Zhang W, Lin ZJ, Weng N (2014) Quantitation of P450 3A4 endogenous biomarker - 4beta-hydroxycholesterol - in human plasma using LC/ESI-MS/MS. *Biomed Chromatogr* 28: 794 – 801

Hwang JY, Randall TD, Silva-Sanchez A (2016) Inducible bronchus-associated lymphoid tissue: taming inflammation in the lung. *Front Immunol* 7: 258

Ichikawa T, Sugiura H, Koarai A, Kikuchi T, Hiramatsu M, Kawabata H, Akamatsu K, Hirano T, Nakanishi M, Matsunaga K *et al* (2013) 25-hydroxycholesterol promotes fibroblast-mediated tissue remodeling through NF-kappaB dependent pathway. *Exp Cell Res* 319: 1176 – 1186

John G, Kohse K, Orasche J, Reda A, Schnelle-Kreis J, Zimmermann R, Schmid O, Eickelberg O, Yildirim AO (2014) The composition of cigarette smoke determines inflammatory cell recruitment to the lung in COPD mouse models. *Clin Sci (Lond)* 126: 207 – 221

John-Schuster G, Hager K, Conlon TM, Irmler M, Beckers J, Eickelberg O, Yildirim AO (2014) Cigarette smoke-induced iBALT mediates macrophage activation in a B cell-dependent manner in COPD. *Am J Physiol Lung Cell Mol Physiol* 307: L692 – L706

John-Schuster G, Gunter S, Hager K, Conlon TM, Eickelberg O, Yildirim AO (2016) Inflammaging increases susceptibility to cigarette smoke-induced COPD. *Oncotarget* 7: 30068 – 30083

Kikuchi T, Sugiura H, Koarai A, Ichikawa T, Minakata Y, Matsunaga K, Nakanishi M, Hirano T, Akamatsu K, Yanagisawa S *et al* (2012) Increase of 27-hydroxycholesterol in the airways of patients with COPD: possible role of 27-hydroxycholesterol in tissue fibrosis. *Chest* 142: 329 – 337

Legler DF, Loetscher M, Roos RS, Clark-Lewis I, Baggiolini M, Moser B (1998) B cell-attracting chemokine 1, a human CXC chemokine expressed in lymphoid tissues, selectively attracts B lymphocytes via BLR1/CXCR5. *J Exp Med* 187: 655 – 660

Li J, Lu E, Yi T, Cyster JG (2016) EBI2 augments Tfh cell fate by promoting interaction with IL-2-quenching dendritic cells. *Nature* 533: 110 – 114

Liu C, Yang XV, Wu J, Kuei C, Mani NS, Zhang L, Yu J, Sutton SW, Qin N, Banie H *et al* (2011) Oxysterols direct B-cell migration through EBI2. *Nature* 475: 519 – 523

Liu SY, Aliyari R, Chikere K, Li G, Marsden MD, Smith JK, Pernet O, Guo H, Nusbaum R, Zack JA *et al* (2013) Interferon-inducible cholesterol-25-hydroxylase broadly inhibits viral entry by production of 25-hydroxycholesterol. *Immunity* 38: 92 – 105

Lu E, Dang EV, McDonald JG, Cyster JG (2017) Distinct oxysterol requirements for positioning naive and activated dendritic cells in the spleen. *Sci Immunol* 2: eaal5237

McMahon SB, Monroe JG (1995) Activation of the p21ras pathway couples antigen receptor stimulation to induction of the primary response gene egr-1 in B lymphocytes. *J Exp Med* 181: 417 – 422

Mootha VK, Lindgren CM, Eriksson KF, Subramanian A, Sihag S, Lehar J, Puigserver P, Carlsson E, Ridderstrale M, Laurila E *et al* (2003) PGC-1alpha-responsive genes involved in oxidative phosphorylation are coordinately downregulated in human diabetes. *Nat Genet* 34: 267 – 273

Moyron-Quiroz JE, Rangel-Moreno J, Kusser K, Hartson L, Sprague F, Goodrich S, Woodland DL, Lund FE, Randall TD (2004) Role of inducible bronchus associated lymphoid tissue (iBALT) in respiratory immunity. *Nat Med* 10: 927 – 934

Park K, Scott AL (2010) Cholesterol 25-hydroxylase production by dendritic cells and macrophages is regulated by type I interferons. *J Leukoc Biol* 88: 1081 – 1087

Pereira JP, Kelly LM, Xu Y, Cyster JG (2009) EBI2 mediates B cell segregation between the outer and centre follicle. *Nature* 460: 1122 – 1126

Pitzalis C, Jones GW, Bombardieri M, Jones SA (2014) Ectopic lymphoid-like structures in infection, cancer and autoimmunity. *Nat Rev Immunol* 14: 447 – 462

Polverino F, Cosio BG, Pons J, Laucho-Contreras M, Tejera P, Iglesias A, Rios A, Jahn A, Sauleda J, Divo M *et al* (2015) B Cell-Activating Factor. An Orchestrator of Lymphoid Follicles in Severe Chronic Obstructive Pulmonary Disease. *Am J Respir Crit Care Med* 192: 695 – 705

Randall TD (2010) Bronchus-associated lymphoid tissue (BALT) structure and function. *Adv Immunol* 107: 187 – 241

Rangel-Moreno J, Moyron-Quiroz JE, Hartson L, Kusser K, Randall TD (2007) Pulmonary expression of CXC chemokine ligand 13, CC chemokine ligand 19, and CC chemokine ligand 21 is essential for local immunity to influenza. *Proc Natl Acad Sci USA* 104: 10577 – 10582

Rangel-Moreno J, Carragher DM, de la Luz Garcia-Hernandez M, Hwang JY, Kusser K, Hartson L, Kolls JK, Khader SA, Randall TD (2011) The development of inducible bronchus-associated lymphoid tissue depends on IL-17. *Nat Immunol* 12: 639 – 646

Richards JD, Dave SH, Chou CH, Mamchak AA, DeFranco AL (2001) Inhibition of the MEK/ERK signaling pathway blocks a subset of B cell responses to antigen. *J Immunol* 166: 3855 – 3864

Sarker RS, John-Schuster G, Bohla A, Mutze K, Burgstaller G, Bedford MT, Konigshoff M, Eickelberg O, Yildirim AO (2015) Coactivator-associated arginine methyltransferase-1 function in alveolar epithelial senescence and elastase-induced emphysema susceptibility. *Am J Respir Cell Mol Biol* 53: 769 – 781

Satoh T, Takeuchi O, Vandenbon A, Yasuda K, Tanaka Y, Kumagai Y, Miyake T, Matsushita K, Okazaki T, Saitoh T *et al* (2010) The Jmjd3-Irf4 axis

regulates M2 macrophage polarization and host responses against helminth infection. *Nat Immunol* 11: 936 – 944

Seyfert VL, Sukhatme VP, Monroe JG (1989) Differential expression of a zinc finger-encoding gene in response to positive versus negative signaling through receptor immunoglobulin in murine B lymphocytes. *Mol Cell Biol* 9: 2083 – 2088

Seys LJ, Verhamme FM, Schinwald A, Hammad H, Cunoosamy DM, Bantsimba-Malanda C, Sabirsh A, McCall E, Flavell L, Herbst R *et al* (2015) Role of B cell-activating factor in chronic obstructive pulmonary disease. *Am J Respir Crit Care Med* 192: 706 – 718

van der Strate BW, Postma DS, Brandsma CA, Melgert BN, Luinge MA, Geerlings M, Hylkema MN, van den Berg A, Timens W, Kerstjens HA (2006) Cigarette smoke-induced emphysema: a role for the B cell? *Am J Respir Crit Care Med* 173: 751 – 758

Sturn A, Quackenbush J, Trajanoski Z (2002) Genesis: cluster analysis of microarray data. *Bioinformatics* 18: 207 – 208

Subramanian A, Tamayo P, Mootha VK, Mukherjee S, Ebert BL, Gillette MA, Paulovich A, Pomeroy SL, Golub TR, Lander ES *et al* (2005) Gene set enrichment analysis: a knowledge-based approach for interpreting genome-wide expression profiles. *Proc Natl Acad Sci USA* 102: 15545 – 15550

Sugiura H, Koarai A, Ichikawa T, Minakata Y, Matsunaga K, Hirano T, Akamatsu K, Yanagisawa S, Furusawa M, Uno Y *et al* (2012) Increased 25-hydroxycholesterol concentrations in the lungs of patients with chronic obstructive pulmonary disease. *Respirology* 17: 533 – 540

Tanaka K, Ishihara T, Sugizaki T, Kobayashi D, Yamashita Y, Tahara K, Yamakawa N, Iijima K, Mogushi K, Tanaka H *et al* (2013) Mepenzolate bromide displays beneficial effects in a mouse model of chronic obstructive pulmonary disease. *Nat Commun* 4: 2686

Tilley AE, O'Connor TP, Hackett NR, Strulovici-Barel Y, Salit J, Amoroso N, Zhou XK, Raman T, Omberg L, Clark A *et al* (2011) Biologic phenotyping of the human small airway epithelial response to cigarette smoking. *PLoS ONE* 6: e22798

Tuder RM, Petrache I (2012) Pathogenesis of chronic obstructive pulmonary disease. *J Clin Invest* 122: 2749 – 2755

Ueno M, Maeno T, Nishimura S, Ogata F, Masubuchi H, Hara K, Yamaguchi K, Aoki F, Suga T, Nagai R *et al* (2015) Alendronate inhalation ameliorates elastase-induced pulmonary emphysema in mice by induction of apoptosis of alveolar macrophages. *Nat Commun* 6: 6332

Vanoirbeek JA, Rinaldi M, De Vooght V, Haenen S, Bobic S, Gayan-Ramirez G, Hoet PH, Verbeken E, Decramer M, Nemery B *et al* (2010) Noninvasive and invasive pulmonary function in mouse models of obstructive and restrictive respiratory diseases. *Am J Respir Cell Mol Biol* 42: 96 – 104

Vazquez BN, Laguna T, Carabana J, Krangel MS, Lauzurica P (2009) CD69 gene is differentially regulated in T and B cells by evolutionarily conserved promoter-distal elements. *J Immunol* 183: 6513 – 6521

Vogelmeier CF, Criner GJ, Martinez FJ, Anzueto A, Barnes PJ, Bourbeau J, Celli BR, Chen R, Decramer M, Fabbri LM *et al* (2017) Global strategy for the diagnosis, management, and prevention of chronic obstructive lung disease 2017 report. GOLD executive summary. *Am J Respir Crit Care Med* 195: 557 – 582

Wang J, Duncan D, Shi Z, Zhang B (2013) WEB-based GEne SeT analysis toolkit (WebGestalt): update 2013. *Nucleic Acids Res* 41: W77 – W83

Yi T, Wang X, Kelly LM, An J, Xu Y, Sailer AW, Gustafsson JA, Russell DW, Cyster JG (2012) Oxysterol gradient generation by lymphoid stromal cells guides activated B cell movement during humoral responses. *Immunity* 37: 535 – 548

Yildirim AO, Veith M, Rausch T, Muller B, Kilb P, Van Winkle LS, Fehrenbach H (2008) Keratinocyte growth factor protects against Clara cell injury induced by naphthalene. *Eur Respir J* 32: 694 – 704

Zukunft S, Sorgenfrei M, Prehn C, Moller G, Adamski J (2013) Targeted metabolomics of dried blood spot extracts. *Chromatographia* 76: 1295 – 1305

Zukunft S, Prehn C, Rohring C, Moller G, Hrabe de Angelis M, Adamski J, Tokarz J (2018) High-throughput extraction and quantification method for targeted metabolomics in murine tissues. *Metabolomics* 14: 18